Study of new chemical derivatization techniques for lignin analysis by size exclusion chromatography

Esakkiammal Sudha Esakkimuthu

THÈSE

Pour obtenir le grade de

DOCTEUR DE L'UNIVERSITE GRENOBLE ALPES

Spécialité : **2MGE : Matériaux, Mécanique, Génie civil, Electrochimie**

Arrêté ministériel : 25 mai 2016

Présentée par

Esakkiammal Sudha ESAKKIMUTHU

Thèse dirigée par **Gérard MORTHA,** Professeur**,** Grenoble INP et Co-encadrée par **Nathalie MARLIN,** Maître de Conférences, Grenoble INP
préparée au sein du **Laboratoire Génie des Procédés Papetiers (LGP2)** dans **l'École Doctorale I-MEP2 - Ingénierie - Matériaux, Mécanique, Environnement, Energétique, Procédés, Production**

Étude de nouvelles techniques de derivation chimique de la lignine en vue de l'analyse par chromatographie d'exclusion stérique

Thèse soutenue publiquement le **30 janvier 2020**,
devant le jury composé de :

Monsieur Nicolas BROSSE
Professeur des Universités, Université de Lorraine, Rapporteur
Monsieur Christophe GEANTET
Directeur de Recherche, CNRS, Université Lyon 1, Rapporteur
Monsieur Sami HALILA
Chargé de Recherche, CNRS, Université Grenoble Alpes, Examinateur
Monsieur Gérard MORTHA
Professeur des Universités, Grenoble INP, Directeur de thèse
Madame Nathalie MARLIN
Maître de Conférences, Grenoble INP, Co-encadrante
Madame Marie-Christine BROCHIER-SALON
Ingénieur de Recherche, Grenoble INP, Invitée
Monsieur Dominique LACHENAL
Professeur des Universités, Émérite, Grenoble INP, Invité

I would like to dedicate my thesis to

my beloved mother

"Mrs. Parvathi"

Acknowledgements

First of all, I am very grateful to my supervisors Prof. Gérard Mortha and Dr. Nathalie Marlin for providing me this opportunity to pursue my research career. I would like to thank Prof. Gerard for his wonderful guidance in analytical chemistry techniques, his guidance encourages and enlarges my research knowledge and become an independent. I would like to express my sincere gratitude to Dr. Nathalie for her constant guidance and motivation throughout my thesis. During my critical situation, my supervisors understood and came forward to bring me out and move on. I am so lucky to have them as my thesis supervisors. Without their support, I would not accomplish this thesis. I like to thank Dr. Marie-Christine Brochier-Salon for part of my thesis work and I learnt a lot about NMR techniques from her. I also thank, for her kindness and support.

I would like to thank jury members: Prof. Nicolas Brosse and Dr. Christophe Geantet and Dr. Sami Halila for accepting the invitation. Thanks to Prof. Dominique Lachenal, Dr. Marie-Christine Brochier-Salon for being part of my thesis jury.

Thanks to Dr. Luis Serrano, post doc for the collaborative work under the Qualin project, and thanks to Dr. Fanny Bardot for the discussions on the lignin chemistry during my post-master program.

I would like to thank Prof. Christine Chirat and Prof. Dominique Lachenal for their support before and during my PhD work. Thanks to all professors in Grenoble INP-Pagora, Prof. Naceur Belgacem, Prof. Alain dufresne and Prof. Julien Bras.

Thanks to the Biochip technicians, David and Karine helped me a lot to learn new instruments and to have hands-on experience with all analytical instruments. Thanks to Jessie, a technician, for helping me during final stage of my thesis.

My special thanks to French ministry and the doctoral school ED-IMEP2 for funding and providing me the great opportunity to perform my thesis. Thanks to Mme. Augustine Alessio for her great support from the school.

I express my thanks to Elsa, who helped me in various aspects, motivated me to apply teaching assistant, conferences etc. and also for her love and friendship.

Also, I like to thank my senior colleague Jennifer, Claire and Chamseddine. Thanks to Lakshmanan anna and Seema for introducing about the post-master course and internship.

Thanks to my friends Axelle, Amina, Helene, Jahan, Camille, Gabrielle, Hugo, Johanna, Manon, Fleur, Hippolyte and Flavien. They were all in my side during the hard situations to step-out of it.

I would also like to thank the administrative unit and Mme. Sylvie and HR department Mme. Anne Marie, M. Stephane Vernac, Mme. Laurence Platel for their help in sorting-out administrative things. Thanks to IT service M. Franck and Mme. Lydia for their good service and friendly nature.

Once again thanks to Dr. Nathalie for giving the opportunity to work as a teaching assistant and also to Mme. Sandrine.

I like to express my sincere thanks to Sridevi Akka and Raja Anna, for motivating me to continue my career and pursue the PhD, It is ever long memory for me. Thanks to Manikandan Anna and Kabila Akka, you are always with us during our hard time.

My particular thanks to my parents Parvathi-Esakkimuthu and my uncle Selvaraj and aunty Ammachi. Without them, I would not establish my career.

I wish to thank my family members, my sisters Shenbaga Devi and Indra, brother in-laws, Prabhakaran and Nagarajan, aththai-mama Sakthi-Ramar, father-in-law Ponnuchamy, mother-in-law Muthumariammal and sister-in-law Sangeetha and kutties Harini and Siddarth.

My special thanks go to my beloved husband Veerapandian. Without his endless love and support, I would not succeed and thanks to my lovable boy Esakki Parthiban for his cooperation (not crying a lot) to complete my thesis.

Introduction

Lignocellulosic biomass is considered as the main renewable source for conversion into wide range of value-added applications and products, which could immensely replace fossil fuel dependency. The biomass macromolecular components are mainly cellulose, hemicelluloses and lignin. Lignin is the second most abundant biopolymer on earth after cellulose and it possesses a highly-branched, three-dimensional aromatic structure with a variety of functional groups and chemical linkages. In particular, lignin is bearing hydroxyl, methoxyl, carbonyl and carboxyl groups.

In the last few decades, researchers have made great efforts to characterize lignin for establishing the synthesis formulation of various materials. Lignin is extensively used as a precursor for different applications such as phenolic resins, surfactants, polyurethanes, epoxides, acrylics, and many other products. The characterization of lignin in terms of chemical linkages, structural features, functional groups and polymer chain length is of primary importance to evaluate the possible lignin applications.

Numerous analytical methods and techniques have been employed for lignin structural characterization and reactivity study. Amongst, functional groups quantification (phenolic and alcoholic hydroxyls, carbonyls and carboxyls) after lignin derivatization by various analytical techniques, including wet chemical methods, and molar mass distribution (MMD) by size exclusion chromatography (SEC), are the most prominent methods. However, MMD analysis for lignin is more complex than for many other polymers due to the irregular, polar and partially branched structure of lignin, leading to low solubility and partial aggregation in most SEC solvents. As a consequence, SEC provides rather inaccurate results, which limits the possibilities for lignin valorisation and new applications.

Most studies focused on the possible chemical modifications of lignin hydroxyl groups to decrease lignin polarity and to improve its dissolution in different solvents. Till date, acetylation is the most widely used derivatization method prior to SEC analysis. However, it exhibits several drawbacks; typically, incomplete solubility, association effect between the molecules and aggregation inside the column, etc. A majority of the lignin MMD studies have applied conventional SEC analysis using polystyrene as standard polymer column calibration, due to the lack of lignin calibrants, and UV and DRI (Differential Refractive Index) as in-line detectors. One important factor that mainly affects the MMD results is the type of calibration standard used; polystyrene in most studies. Indeed, lignin structural conformation is totally different from polystyrene, which leads to unreliable molar mass data.

The main objective of this PhD work was thus to improve the SEC performance in the case of lignin, by enhancing its solubility in various solvents using derivatization. Three different

derivatization methods were compared: acetylation, fluorobenzylation and fluorobenzoylation. The two latter methods have been developed by Prof. M. Barrelle and collaborators about twenty years ago, but never tested extensively for SEC application.

In this study, lignin reactivity during the derivatization reactions has been assessed using various analytical methods (UV, IR, GC, ^{1}H NMR, ^{13}C NMR, ^{19}F NMR) and the numbers and types of hydroxyl groups present in the studied lignin samples have been quantified. Then the derivatized lignins have been studied by SEC analysis for MMD determination. In addition to the investigation of the lignin fluorobenzylation reaction for improving lignin behaviour in a SEC system, the MMD analysis itself has been upgraded by the application of the universal calibration principle. Indeed, the presence of an in-line viscometer in the LGP2 chromatographic system enabled to measure the intrinsic viscosity of each eluted polymer fraction. Different polymer standards (polystyrene, polymethylmethacrylate and cellulose acetate) have been tested and it was proven that *universal calibration* provided better results than standard conventional calibration using polystyrene.

The present PhD manuscript is designed and organized as follows:

- CHAPTER 1 provides an overview of the importance of lignocellulosic biomass in recent decades for sustainable applications, and its components. In this section, the lignin structure and the different chemical treatments employed for lignin isolation from lignocellulosic biomass are discussed. Despite of various types of functional groups present in lignins, the possible derivatization methods have been extensively analysed and followed by the review of some relevant applications of lignin. Moreover, classical techniques used for the quantification of different lignin functional groups are presented.
- CHAPTER 2 describes the materials and methods used, in particular the different technical lignin samples selected (Protobind 1000, Indulin, Organosolv, Kraft and Eucalyptus Kraft). The analytical methods, operating conditions and protocols used are also described in this section.

Results and discussions are presented in three CHAPTERS which are divided as follows:

- Since lignin reactivity is mainly based on the free phenolic hydroxyl groups available in the molecule, CHAPTER 3 investigates the acetylation as a proven method for lignin phenolic hydroxyl groups derivatization. For that purpose, all the selected lignin samples have been acetylated and then subjected to the aminolysis reaction, followed by a GC analysis. Hence, the number of hydroxyl groups have been quantified and compared with values obtained via other analytical techniques such as differential UV, ^{1}H NMR, ^{13}C NMR, ^{31}P NMR, IR, conductometric and potentiometric methods.

- CHAPTER 4 is devoted to the investigation of the fluorobenzylation as a new derivatization method to improve lignin analysis, by (1) decreasing lignin polarity thus increasing its solubility in the SEC solvent, and by (2) giving access to structural information after ^{19}F NMR analysis. First the lignin functional groups reactivity towards the fluorobenzylation reaction has been examined and the ^{19}F NMR chemical shifts have been verified. Fluorobenzylation has been primarily tested on lignin model compounds (vanillin, vanillyl alcohol, Veratryl alcohol, acetovanillone and cellobiose) containing phenolic and aliphatic hydroxyl groups. The reactivity and selectivity of fluoro-derivatizations have been studied using ^{19}F and ^{13}C NMR spectroscopies. Based on the results obtained on model compounds, commercial lignins have been characterized.
- In CHAPTER 5, lignin fluorobenzylation and fluorobenzoylation have been applied for SEC analysis improvement and compared to classical acetylation. Lignin derivatization is necessary to favour the solubility and SEC behaviour of the polymer. Another new input in this chapter is the use of universal calibration and the comparison with standard conventional calibration. Two solvent systems have been tested and compared for SEC: DMAc/LiCl and THF.

The main findings of this thesis work have been summarized in the CONCLUSION part, which also contains a discussion of the future perspectives of this thesis work.

Contents

Abbreviations

CA	Cellulose acetate
CF3PH	Trifluoromethylphenylhydrazine
DMAc/LiCl	Dimethylacetamide/Lithiumchloride
DMF	Dimethylformamide
DMAP	Dimethylaminopyridine
DMSO	Dimethylsulphoxide
DP	Degree of polymerization
DRI	Differential refractive index
DV	Differential viscosity
EtOAc	Ethylacetate
EU-KR	Eucalyptus-Kraft lignin
FB	Fluorobenzylation
FBC	4-fluorobenzylchloride
FBO	Fluorobenzoylation
FT-IR	Fourier transform-Infrared
GC	Gas chromatography
GC-FID	Gas chromatography – Flame ionization detector
GPC	Gel permeation chromatography
HPSEC	High performance size exclusion chromatography
H_3PO_4	Ortho-phosphoric acid
HPLC	High performance liquid chromatography
IND	Indulin lignin
KR	Kraft lignin
LS	Light scattering
MALS	Multi-angle static light scattering
Mn	Number average molecular weight
MMD	Molar mass distribution
Mw	Weight Average molecular weight
MPTF	4-methylbenzotrifluoride
NBu	N- tetrabutylammoniumhydroxide
ORG	Organosolv lignin
NMR	Nuclear magnetic resonance

PB	Protobind 1000
PD	Polydispersity
PMMA	Polymethylmethacrylate
PS	Polystyrene
RT	Retention volume
SEC	Size exclusion chromatography
THF	Tetrahydrofuran
Tg	Glass transition temperature
UV	Ultra-violet
Vh	Hydrodynamic volume
Vr	Elusion volume
η	Intrinsic viscosity

List of Figures

List of Tables

CHAPTER 1

1 Bibliographic Study

In this chapter, a general overview of lignocellulosic biomass and its typical components are illustrated. In addition, a focus on lignin is made, including the description of lignin structure with different linkages and functional groups, and a review on chemical modifications and lignin characterizations. Finally, motivations and outlines of this thesis work are provided.

1.1 Introduction

For decades, fossil resources are used for the production of fuels and chemical feed stocks, contributing for more than 80% of the energy consumed in the world. Globally, the energy demand has been tremendously increasing whereas fossil resources drop rapidly which affects the countries that solely depend on petroleum. Increasing oil price, greenhouse gas emission and environmental impacts are also the driven forces to search for alternative sources. Recently, a research activity associated to energy sector shows that the energy demand would remarkably increase, over 60% by 2030 (Jacobson and Delucchi, 2009). From the statistical review of world energy in 2016, fossil fuel is involved in around 85% of global energy consumption (Figure 1.1).

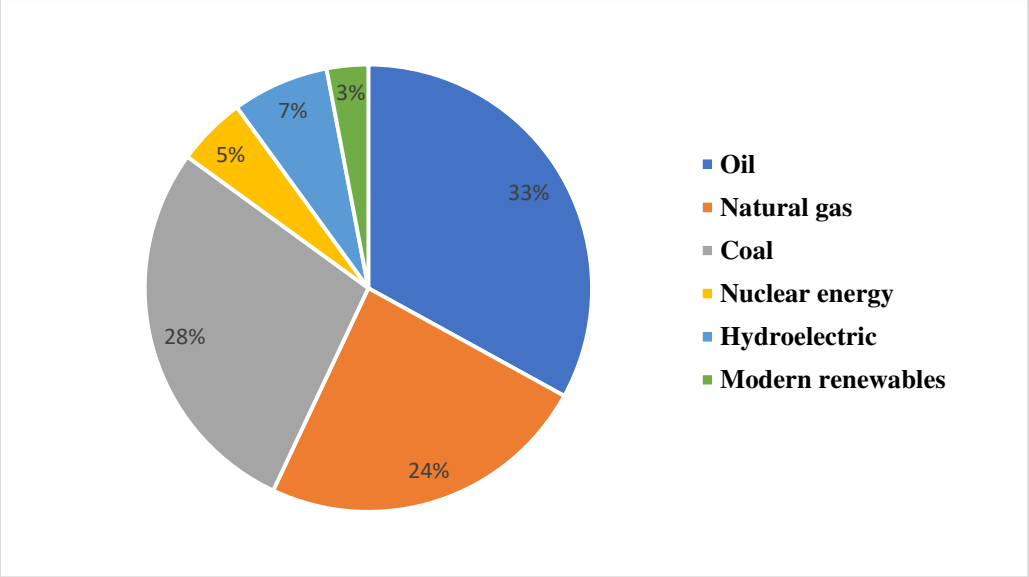

Figure 1.1. Share of global primary energy consumption in the world in 2016[1]

Last few years, renewable energy field is overwhelming and renewable resources are thought to be ideal candidates to replace fossil resources (Carlos Serrano-Ruiz et al., 2011). The renewable energies comprised wind and solar-energies, and hydro-electricity. These new alternatives can partly substitute natural gas and coal for the production of heat and electricity. However, they strongly depend on natural processes such as the weather, geographical location etc and therefore they appear limited as bioenergy sources.

Biomass, the main sustainable organic source on earth, including forestry and wood processing residues, crop residues and animal wastes may be a better alternative. In particular, lignocellulosic biomass is an interesting bioresource for the replacement of petroleum based fuels, chemicals and carbon based materials (Ragauskas et al., 2006a) as it contains a large amount of carbon. It is also renewable and readily available on earth and most importantly non-edible. Therefore, without affecting food chain and land use, lignocellulosic biomass should allow sustainable production of fuels and chemicals (Carlos Serrano-Ruiz et al., 2011).

The different steps for the production of fuels and chemicals from petroleum and biomass sources are illustrated in Figure 1.2. This picture clearly shows that the conversion of biomass into fuels and chemicals requires deep chemical changes along with multistep chemical processing and therefore it is cumbersome comparing to petroleum where separation used fractional distillation.

[1] https://www.financialsense.com/robert-rapier/renewable-gains-offset-coals-decline-in-2016

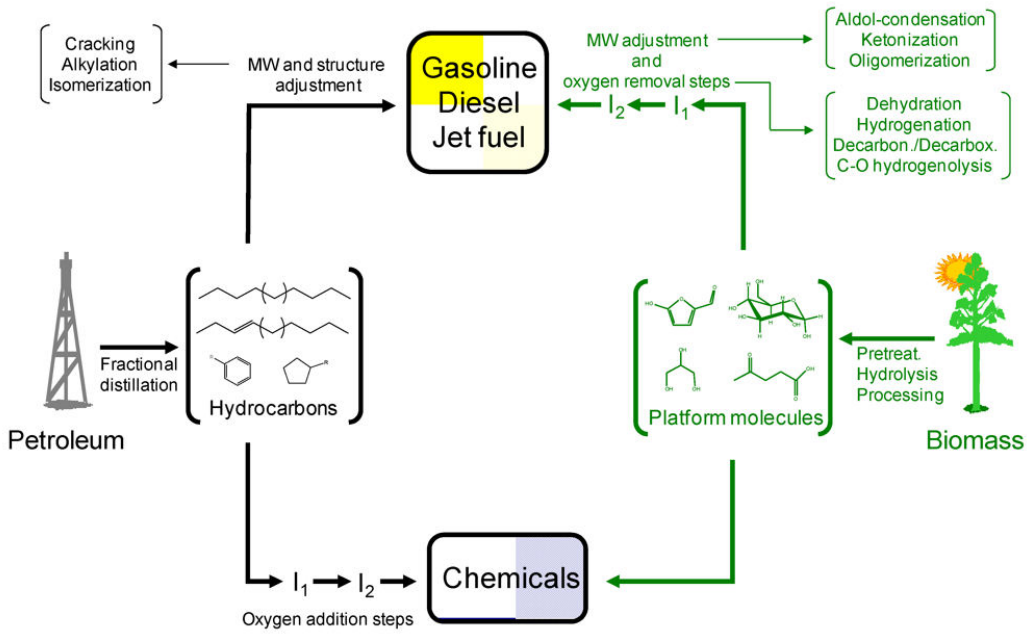

Figure 1.2. Petroleum processing vs biomass to produce fuels and chemicals (Carlos Serrano-Ruiz et al., 2011)

Many recent studies have been focused on the investigation of lignocellulosic biomass feed stock conversion in to biofuels, power, heat and value added chemicals, and this concept is known as biorefinery (Ragauskas et al., 2006a). In this biorefinery process, first generation biofuel-bioethanol has been produced from sugar cane and sugar beet in order to reduce energy demand. However, the major limitation is that the energy crops occupy the agricultural land which led for food demand. To overcome this constraint, forestry and agricultural wastes (wheat straw and other residues), industrial process residues, house hold wastes and aquaculture (algae and seaweeds) were investigated to make second generation biofuels and chemicals through thermochemical or biochemical pathway (Cherubini, 2010). Therefore, lignocellulosic biomass plays a vital role in the modern society for the replacement of fossil fuel to overcome the energy demand and to decrease the most dangerous greenhouse gas emission. In the following sections, detailed information about lignocellulosic biomass is established.

1.2 Lignocellulosic Biomass

The typical cell wall of plant is made up of by a composite material called lignocellulosic biomass. It is naturally composed of carbohydrate polymers, cellulose (35-83 % dry weight basis) and hemicelluloses (0-30% dry weight basis) and of an aromatic amorphous polymer, lignin (1-43%). Some other components such as extractives and minerals are also present but in minor quantities (Dence and Lin, 1992). The composition of the lignocellulosic biomass varies with plant species and

environmental conditions (Cen et al., 2001). This composition and interactions between lignocellulosic biomass components significantly affect the plant cell wall physicochemical properties, therefore understanding each component percentage is important in every plant source to further utilize for wide range of biorefinery applications.

Lignocellulosic biomass consists of crystalline cellulose fibrils bound by non-crystalline and a matrix of hemicelluloses along with lignin (Wyman, 1994; Ramos, 2003). The typical structure of lignocellulosic biomass is shown in Figure 1.3

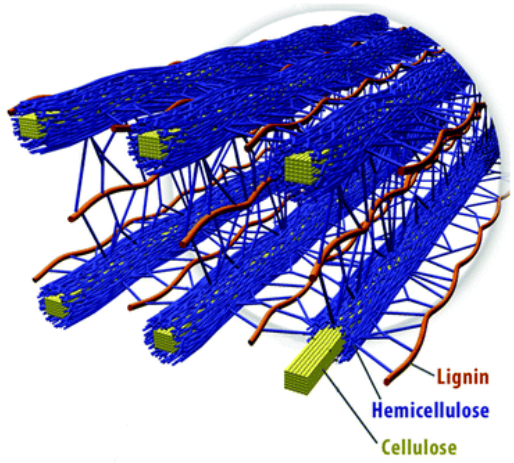

Figure 1.3. Structural arrangement of cellulose, hemicelluloses and lignin in lignocellulosic biomass (Brandt et al., 2013)

Lignocellulosic biomass is already widely exploited by the pulp and paper industry to convert it into cellulosic fibres for paper and chemical applications. Today, pulp and paper mills investigate the biorefinery concept to add, in the fibre line, new processes to extract added value products. The biorefinery concept starts with pre-treatment processes such as conventional soda, kraft, organosolv and sulphite pulping processes (a detailed explanation is given in the following section), with the final objective to separate individual components for further valorisation into different potential applications (Figure 1.4).

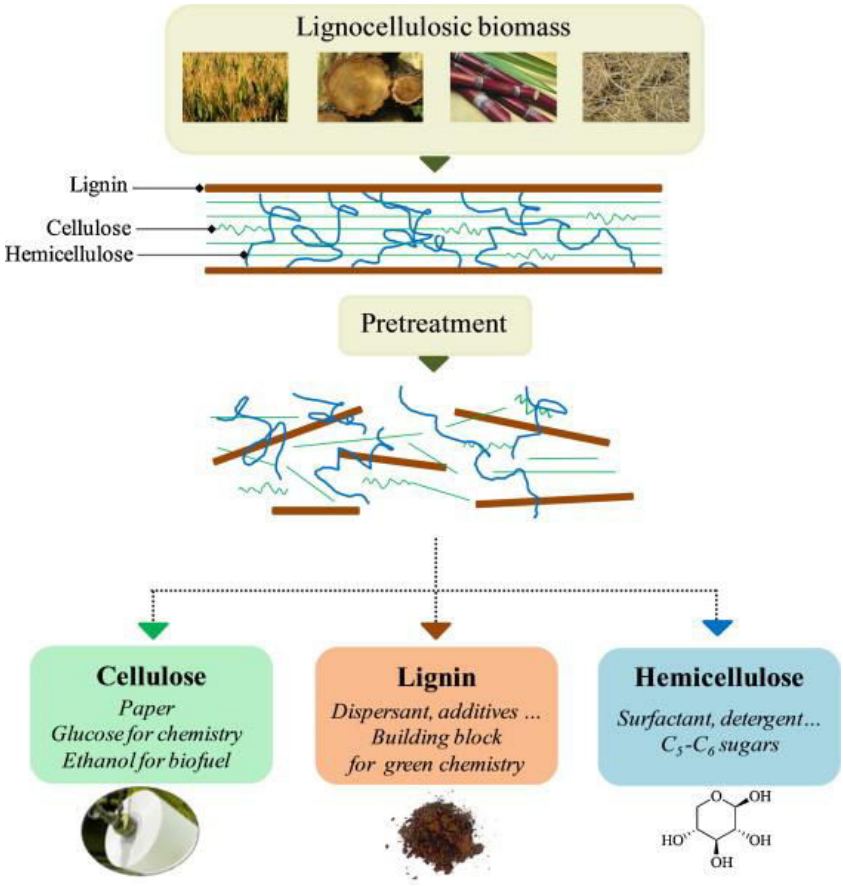

Figure 1.4. Lignocellulosic biomass to biorefinery applications (Laurichesse and Avérous, 2014)

1.2.1 Cellulose

Cellulose is the most abundant biopolymer and a main wood components; the worldwide estimated amount is around $2x10^9$ tons $year^{-1}$ (Sasaki et al., 2003). Cellulose is a linear homopolymer, comprising linear glucan chains linked through repeating (1→4) glycoside bonds, β-D-glucopyranose units, as shown in Figure 1.5.

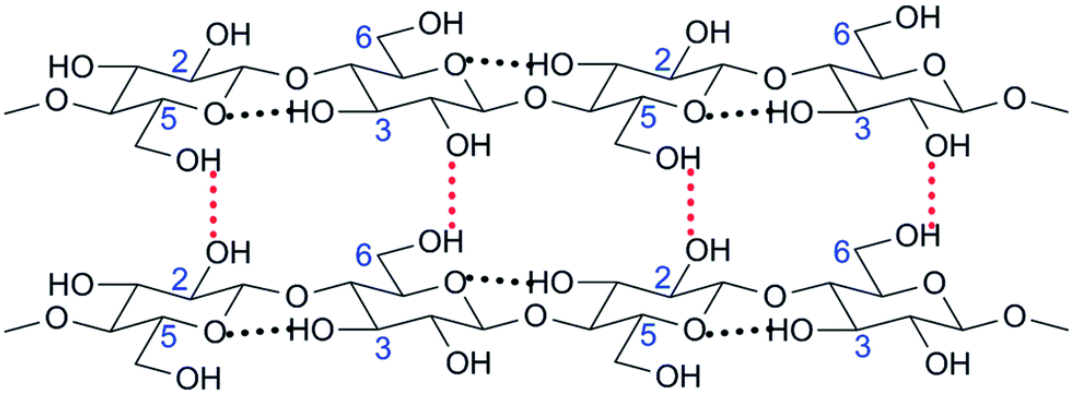

Figure 1.5. Chemical structure of Cellulose polymer (Credou and Berthelot, 2014)

The dimer of cellulose is called cellobiose. The size of the cellulose polymer mainly described by the degree of polymerisation (DP) varies depending on the plant species and environmental conditions. The DP is determined through the number of anhydroglucose units present in the cellulose. The average DP of cellulose ranges from 3000 to 15000 depending upon the source, with an average DP of around 10 000 in wood (Jones et al., 2017). During cellulose extraction from wood, the DP decreases till an average of 600 to 1200 (Lynd et al., 2002). Cellulose chains are arranged in parallel and stabilised through strong lateral intramolecular and intermolecular hydrogen bonds. Cellulose contains both crystalline and amorphous domains, forming rope like structures called microfibrils (Milton, 1995). The cellulose possesses two ends, a reducing functional group in one end and a non-reducing group in the other end (Habibi et al., 2010). In general, cellulose mostly exists in crystalline phase in living plants and it has two allomorphs such as I_{α} and I_{β}, (O'Sullivan, 1997) whose differ in their hydrogen bond arrangements. It has been reported that crystalline cellulose becomes amorphous when it is heated at 20˚C with a pressure of 25 MPa (Deguchi et al., 2006).

Dissolution of cellulose is non-trivial in either polar or non-polar solvents due to three hydroxyl groups such as OH-C2, OH-C3 and OH-C6, which form a network of strong hydrogen bonds. Hydrogen bonds are quite polar and the solvents are incapable of breaking these bonds to make cellulose soluble. Interestingly, cellulose contains both hydrophilic (OH groups) and hydrophobic part (CH_2 groups), however the latter is dominant due to large amount of C-H groups in cellulose (Glasser et al., 2012).

During the kraft pulping process, the cellulose fraction with low degree of polymerisation can be dissolved directly in the liquor. In such alkaline conditions, cellulose depolymerisation is greatly enhanced (Sjöholm et al., 1997). Cellulose is also affected in acidic environments. Organic acid-catalysed reaction using oxalic and maleic acid for example and heterogeneous catalysts reactions are also employed for cellulose depolymerisation yielding oligomers and glucose (Shrotri et al., 2018; Stein et al., 2010).

Besides, various chemical reactions can be performed on cellulose hydroxyl groups to increase its added value for chemical applications like oxidation, sulphonation and esterification (Sjostrom, 1993; Gu et al., 2013). Furthermore, the reducing end or hemiacetal exists as aldehyde under equilibrium. Therefore, the existence of aldehyde group in cellulose can undergo chemical derivatisation like hydrazinolysis and the resulting product can used as adsorbent for efficient removal of Cd (II) and Pb (II) ions from aqueous solution (Jia et al., 2017; Naven and Harvey, 1996).

Due to the large abundance of cellulose in nature, it is the most thoroughly exploited natural polymer and it is valorised into many applications, the major one being in the pulp and paper industry. In recent year, nanocellulose and microfibrillated cellulose have also gained considerable attention

due to interesting specific properties (low weight, biodegradability, high strength and stiffness etc). In the future, they will be used in a wide range of applications, including bio-nanocomposite production, paints, cosmetics, foods and pharmaceutical products (Siró and Plackett, 2010).

1.2.2 Hemicelluloses

Hemicelluloses are carbohydrate type branched biopolymers present in the secondary cell wall of vegetal biomass. They are bound to cellulose through strong hydrogen bonds leading to a matrix network with cellulose micro fibrils, that provides a strong structural backbone for the cell wall (Mosier et al., 2005). Hemicelluloses are divided into four main groups: mannans, xylans and mixed-linkage of xyloglucans and β-glucans (Ebringerová et al., 2005). It consists of mainly C-6 sugars such as D-glucose, D-mannose, galactose and C-5 or pentoses sugars namely, L-arabinose and D-xylose. The typical DP of hemicelluloses in wood is around 80-200 (Sjostrom, 1993), lower than cellulose (Milton, 1995). Moreover, hemicelluloses occupy up to 50% of the vegetal biomass, and their composition can vary in different plant or wood species and also within the parts of the lignocellulosic substrate (for instance leaves, roots and stems). Xylans and glucomannans are the predominant components in hemicelluloses (Figure 1.6).

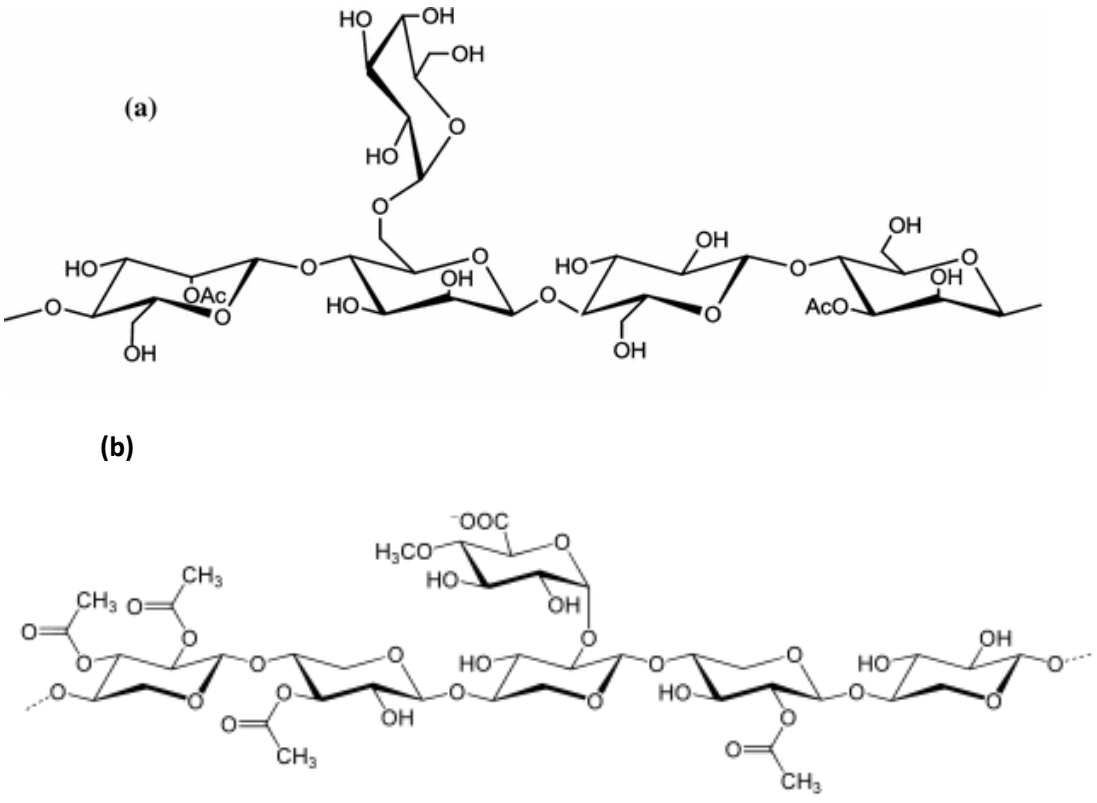

Figure 1.6. Chemical structure of main hemicellulose compounds, (a) glucomannan (Prakobna et al., 2015) (b) xylan (Horst et al., 2005)

Xylans are the major hemicelluloses type in hardwoods and herbaceous plants, constituting around 20-30% of the secondary cell wall (Gírio et al., 2010). Linear and slightly shorter branched polymers called galactoglucomannan are the main components of softwood hemicelluloses (Sjostrom, 1993), while in the cases of straw and grass hemicelluloses, glucurono-arabinoxylans, arabinoxylans and arabino-glucuronoxylans are the dominant components (Gírio et al., 2010). In contrast to cellulose, hemicelluloses are amorphous and shorter polymer and often more branched macromolecules, leading to different properties. As an example, it is partly soluble in water (Albertsson et al., 2011).

During pulping processes, hemicelluloses are generally conserved for paper applications due to their tendency of increasing the paper strength in particular, tensile, fold, and tear resistance properties. (Anjos et al., 2004; Bajpai, 2018). Hemicelluloses also influence the pulp yield. In the case of dissolving pulp applications, hemicelluloses are known to be undesirable impurities since they affect the production and the reactivity of high purity cellulose. Various processes are employed for removing hemicelluloses selectively, including alkaline, nitrine and cuen extraction and ionic liquids extraction. (Froschauer et al., 2013; Puls et al., 2006; Sixta, 2008).

Hemicelluloses can be hydrolysed with the help of acids to break the macromolecule into oligomers, and, after further reaction, to the formation of sugar monomers. Less severe conditions than for cellulose may be employed for this conversion, because of the amorphous nature of hemicelluloses. Hemicelluloses can be pyrolysed and decomposed into various products including the formation of furfural, methylglyoxal, glycolaldehyde, acetaldehyde and C6 products etc (Zhou et al., 2018).

Hemicelluloses could be valorised in various potential applications, such as protective colloids, emulsifiers, plant gum for thickeners, stabilizers and adhesives (Kamm and Kamm, 2004; Zhang, 2008). In recent years, xylitol (Walther et al., 2001; Buhner and Agblevor, 2004) (from fermented xylose) is used as a sweetener for the replacement of sucrose sugars for diabetic patients. Furthermore, furfurals, produced from the chemical degradation of hemicelluloses, are used as a solvent for lubricants, adhesives, coatings and furan resins etc (Kamm et al., 2008; Zhang, 2008).

1.2.3 Lignin

This section gives general introduction on lignin, structures of lignin, linkages present in lignin and lignin isolation from the vegetal biomass via different pulping processes.

1.2.3.1 Introduction

Lignin research has been started more than a century ago. The name “lignin” is derived from the Latin word *lignum* meaning wood, as reported in the Sarkanen work (Sarkanen and Ludwig, 1971).

During the year of 1838, Anselme Payen, first, recognised the composite behaviour of wood and named the fibrous material as cellulose and the carbon rich substance as an encrusting material in lignified cell walls. Later in 1865, Schulze introduced the term “lignin” and subsequently in 1957, Adler proposed the first lignin model (Adler, 1957).

Lignin is the second most abundant aromatic biopolymer in plant, distinctly different from other bio-polymers (cellulose and hemicelluloses) and covers the space inside the cell wall through cross linkages with polysaccharides. It is covalently bonded to hemicelluloses and cellulose as well as with cell wall glycoproteins. These interactions provide a strong structural support to the plant. Polysaccharides in the plant cell wall are highly hydrophilic and more susceptible to water absorption, however, crosslinked and hydrophobic character of lignin prevents the water absorption in to cell wall.

The complex poly aromatic and highly branched structure of softwood and hardwood lignins is shown in Figure 1.7 and Figure 1.8.

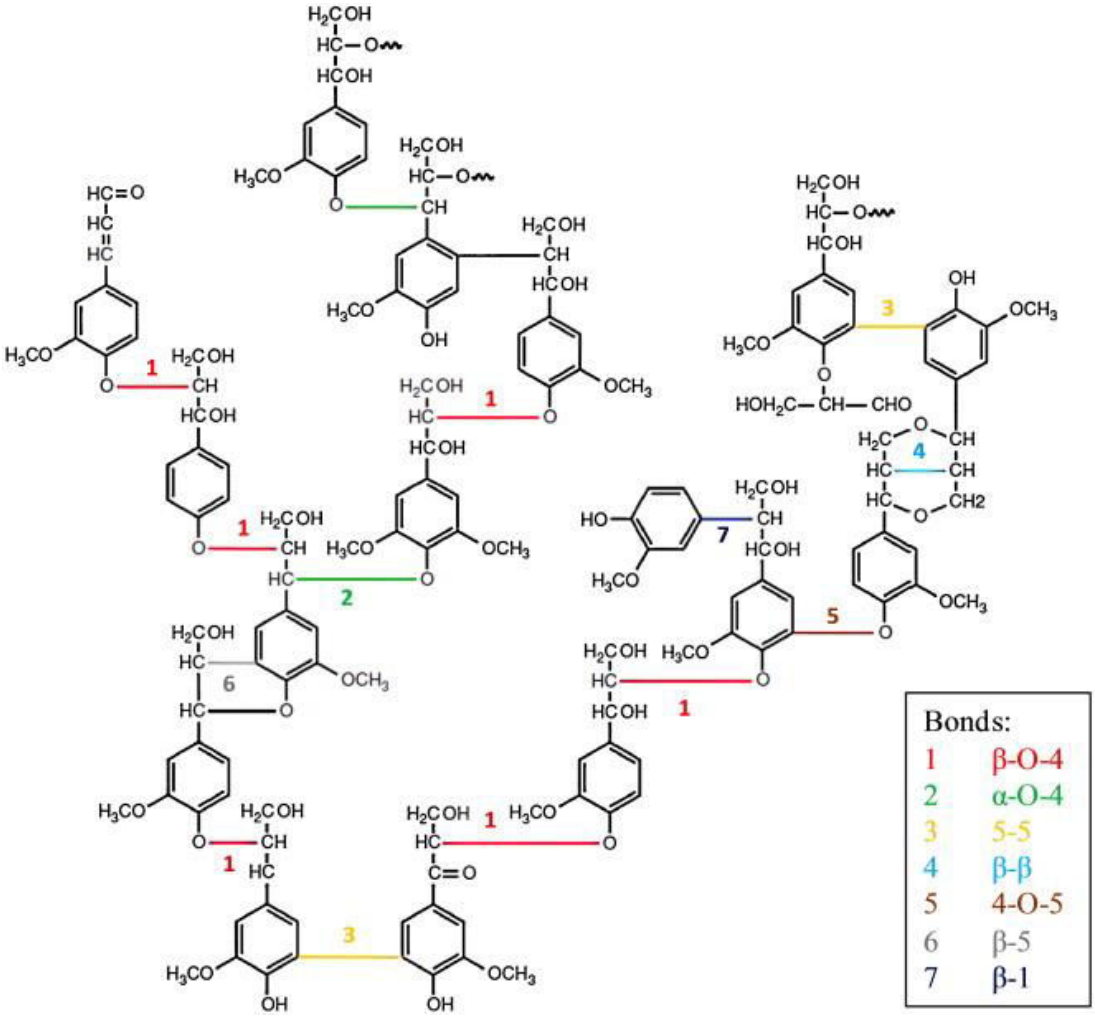

Figure 1.7. Softwood lignin structure and main linkages (Windeisen and Wegener, 2012)

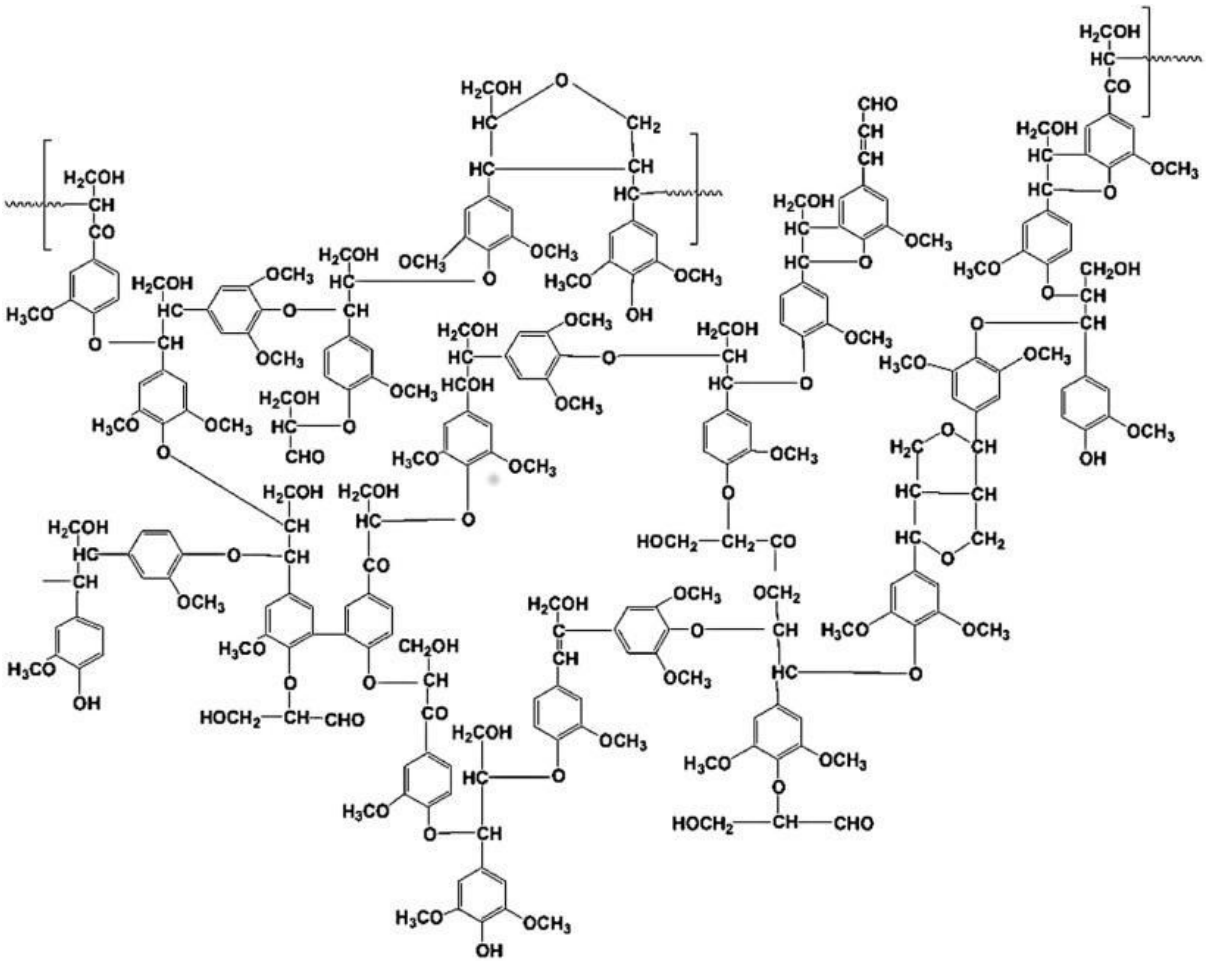

Figure 1.8. Partial structure of a hardwood lignin molecule from European beech (Le Floch et al., 2015)

The lignin content in wood exhibits large variations. For instance, softwood contains around 25 to 30 weight/percentage whereas it makes up 9 to 23 wt % in hardwoods (Sixta, 2008). Like softwood, grasses also contain lignin from 10 to 30 wt %. It is interesting to note that tissues of some plants such as nut shells present high amount of lignin, ranging from 30 to 40 wt % whereas in some soft tissues like cotton seed hairs and leaves, no lignin is present (Sun and Cheng, 2002). Furthermore, similar to the cellulose and hemicelluloses, lignin composition and proportion heavily vary with respect to cell types in the plant species.

Lignin mainly consists of three major phenyl propane units: p-hydroxyphenyl (**H**), guaiacyl (4-hydroxy-3-methoxyphenyl) (**G**) and syringyl (4-hydroxy-3,5-dimethoxyphenyl) (**S**) propane units. These units originally come from the main precursors namely coumaryl, coniferyl and sinapyl aromatic alcohols (Figure 1.9).

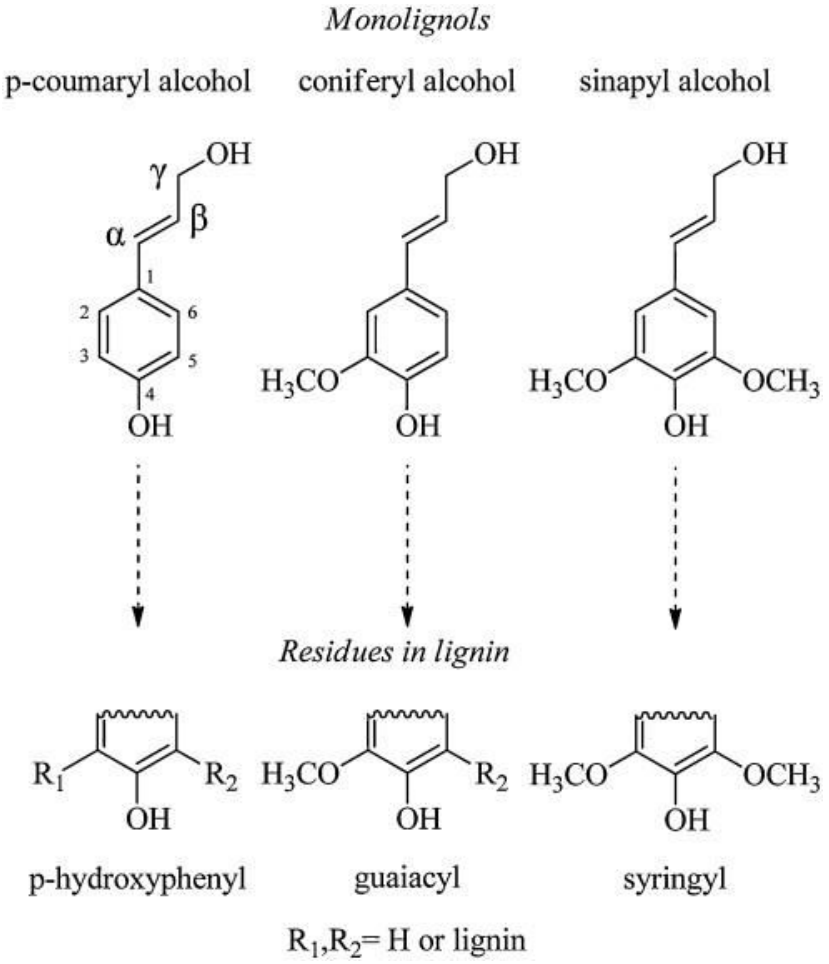

Figure 1.9. The three main precursors of lignin (monolignols) and their corresponding structures in lignin

Straw and grass plants are made up of all three **H**, **G** and **S** units. **G** unit is the main unit in softwood lignins, whereas in hardwood lignins, **G** and **S** units are dominant. Due to this diverse nature of lignin, the exact lignin structure cannot be resolved completely (Hon, 1996) (Dorrestijn et al., 2000).

There are various mechanisms explaining the formation of lignin macromolecule in plants through different processes such as biological, chemical and biochemical ways. One theory believes that lignin formation is totally controlled biochemically at proteinaceous level (Davin and Lewis, 2005). Another important theory states that lignification starts with radical production through the oxidation by various enzymes like peroxidases, phenol oxidases, and laccases etc, leading to dehydrogenated monolignols (e.g., coniferyl alcohol) (Gang et al., 1999; Ralph et al., 2004; Vanholme et al., 2010). The resulting radicals are significantly stabilised due to delocalisation of an unpaired electron and consequently, these radicals randomly couple each other into macro polymer (Achyuthan et al., 2010). For instance, the active radical intermediates are generated from the monolignol (coniferyl alcohol) by

oxidation of the phenol unit. The phenoxy radicals couple each other to the formation of lignin polymer yielding units with different interunit linkages (Zhang et al., 2012). A schematic reaction of the formation of lignin with different linkages is shown in Figure 1.10.

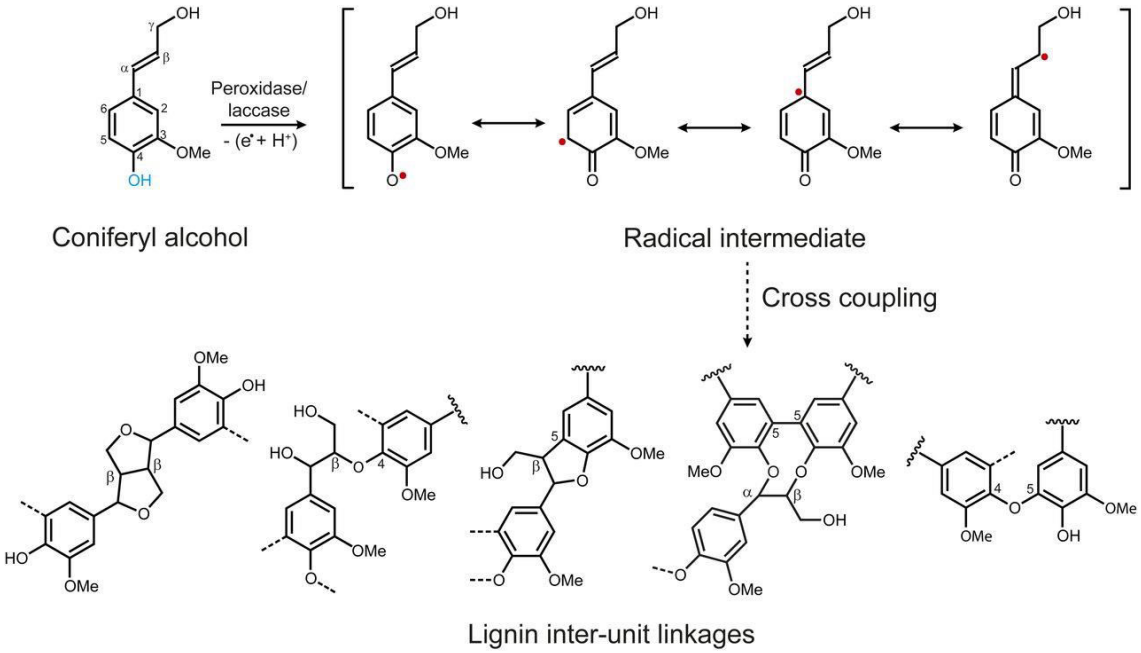

Figure 1.10. Lignin formation reaction (Zhang et al., 2012)

Lignin is hydrophobic compared with carbohydrate polymers such as cellulose and hemicellulose. However, the number of hydroxyl groups present in the lignin is sufficient to play a crucial role as a reactive site to form hydrogen bonds with water molecules. (Hatakeyama et al., 1983).

Due to its highly complex chemical structure, the precise structure of lignin is still unknown. The lignin macromolecule is amorphous and presents conjugated systems leading to colour: native lignin in wood is yellow and residual lignin in paper pulp is brown. Besides, almost all lignins in plants are insoluble in inert solvents. Lignin is made of highly rigid molecules cross-linked each other, restricting the molecular motion and therefore increasing the glass transition temperature (Tg). Tg of kraft lignins and lignosulphonates is observed at 100 ºC, and Tg of hydrolysed lignin samples from different industrial lignin plants are found in a temperature range of 70-85 ºC (Hatakeyama and Hatakeyama, 2010).

Thermal decomposition of lignin has been investigated with the help of thermogravimetry (TG) techniques. The results suggested that a slight mass variation occurred in the temperature range of 0 – 150 ºC which can be attributed to vaporization of residual water in the sample. Thermal decomposition starts around 200 ºC and the extrapolated temperature for kraft lignin and

lignosulphonate are around 321 and 324 ºC, respectively. At 500 ºC, the residual mass of lignin was found to be ca. 45% (Hatakeyama and Hatakeyama, 2010).

The calorific values of oven-dried hardwood and softwood are predicted to be 19.7 MJ/kg and 20.9 MJ/kg, respectively. The difference in heat values is due to the lignin content, higher in softwood in comparison with hardwood. The estimated calorific value of cellulose, hemicelluloses and lignin are 17 MJ/kg, 16.63 MJ/kg and 21.13 MJ/kg, respectively. It has been known that moisture wood produces low heat (15 MJ/kg) due the presence of water that consumes some energy for evaporation during combustion process (Ince, 1979; Demirbaş, 2001; Spellman, 2011; Kim et al., 2017).

1.2.3.2 Linkages in Lignin

As seen in Figure 1.7, lignin exhibits a complex and irregular structure, because it is formed through a random polymerisation process. The lignin linkages have been examined during delignification processes or after breaking the lignin polymer units into monomers. The most widely used techniques are oxidation (Hedges and Mann, 1979), pyrolysis (Faix et al., 1990), biodegradation (Tien and Kirk, 1983) and acidolysis (Lapierre et al., 1991). Lignin structural elucidation has also been investigated by various laboratory chemical methods, numerous NMR (Faix et al., 1994) techniques, gas chromatography – mass spectrometry (GC-MS) (Faix et al., 1990), electron microscopies (Fromm et al., 2003) and spectroscopic techniques (Faix, 1991; Atalla and Agarwal, 1985). The reported studies have found that the most typical linkages are β-O-4, β-5, α-O-4, 4-O-5, 5-5, β- β and β-1 (Zakzeski et al., 2010; Syrjänen and Brunow, 2000; Chakar and Ragauskas, 2004) (Figure 1.11).

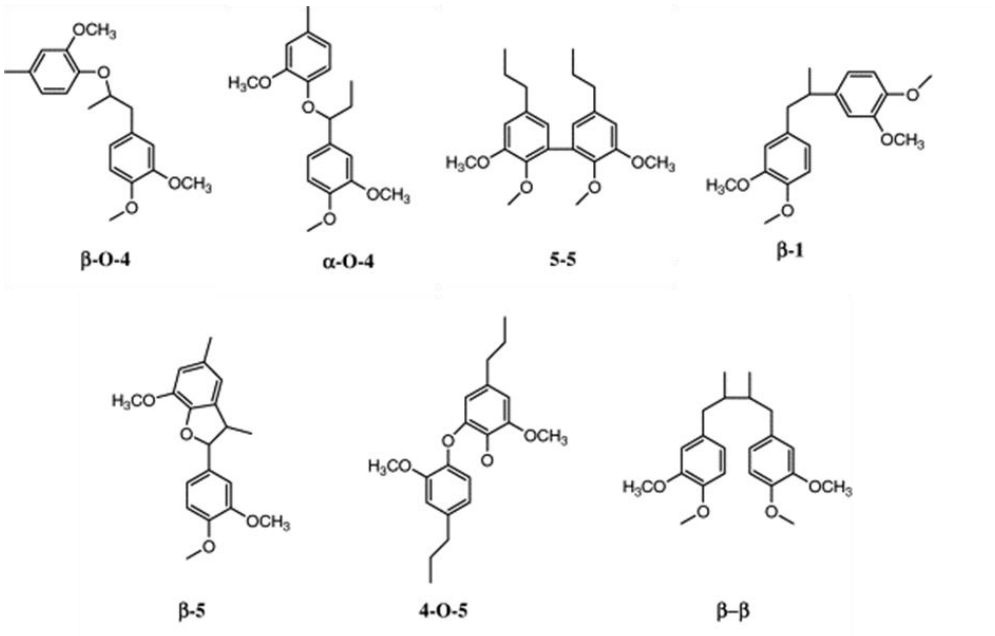

Figure 1.11. The most common unit linkages in lignin (Chakar and Ragauskas, 2004)

Among them the β-O-4 linkage is the predominant. The hardwood lignin consists of around 60% of β-O-4 linkages whereas it makes up to 40% in softwood lignin. The remaining 40% linkages in hardwood lignin are rather evenly distributed among other linkages such as β-5, 5-5 and β-β etc. However, in the case of softwood lignin, around 15% linkage goes for β-5 and 12% for 5-5 linkage (Dorrestijn et al., 2000). The percentages of different linkages are illustrated in Table 1.1. Among all linkages, the higher linkage content is obtained via position 5 of the aromatic ring which explains that guaiacyl units are readily available whereas position 5 in syringly unit is preoccupied and blocked.

Table 1.1. Approximate lignin inter-unit linkage percentages found in softwood and hardwood (Adler, 1977)

Linkage type	Percentage (%)	
	Softwood	**Hardwood**
β-O-4	45-55	60
5-5	19-22	9
β-5	9-12	6
4-O-5	4-7	6.5
β-1	7-9	1
β- β	2-4	3

As seen in the Figure 1.7 and Figure 1.8, it is clearly demonstrated that lignin contains numerous functional groups and the most abundance of functional groups are illustrated in Table 1.2. Some characteristic groups such as methoxyl, aliphatic, phenolic hydroxyl groups and carbonyl groups are common and thus responsible for the chemical reactivity of lignin. However, it should be noted that these functional groups can vary depending on the wood species and also differ within the cell walls (Capanema et al., 2005; Javaid et al., 2019; Sjostrom, 1993).

Table 1.2. Various functional groups present in softwood and hardwood lignin of different types (abundance per 100 C-9 units)

Functional groups	Softwood lignin	Hardwood lignin
Methoxyl	90 – 95	139 –158
Phenolic hydroxyl	20 – 30	10 – 15
Benzyl alcohol	30 – 45	40 – 50
Carbonyl	10 – 15	17 – 24
Aliphatic hydroxyl	115 – 120	88 – 166

1.2.3.3 Isolation of lignin

Due to its three-dimensional branched structure and the strong linkages between lignin units and carbohydrates, lignin isolation is a tedious process. In the pulp and paper industry, lignin is partially depolymerised to extract cellulose fibres. Lignin is a by-product of the cellulose fibre extraction, still under-valorised.

Various extraction and isolation methods are used to recover lignin from the lignocellulosic feedstock, which normally alter the structure, in particular the lignin functional groups and the lignin physical and chemical properties so that the resulting extracted lignin is highly heterogeneous (Lora and Glasser, 2002). The most common extraction techniques in pulp and paper industry are the Kraft, Sulphite, Soda and Organosolv processes. The goal of these processes is to extract cellulose fibres from lignocellulosic biomass: it is achieved by depolymerising lignin and making it soluble in the liquid phase medium. Thus around 40-50 million tons per year of lignin are isolated worldwide (Strassberger et al., 2014; Zoia et al., 2014), mainly through the Kraft process, the dominating pulping process. Today extracted lignin is mainly burnt in the recovery boiler of the pulp mill to produce energy, only a small fraction (2%) is commercially available for value added applications (Chakar and Ragauskas, 2004).

Extracted lignin structure strongly depends on the pulping process from which lignin derives. Moreover, isolation techniques can be categorised according to the chemical method used for extracting lignin. Thus, the pulping processes and the impact on lignin structure are described in the following sections.

1.2.3.3.1 Kraft Pulping

Kraft pulping is the most dominant cooking process, producing around 85% (about $43x10^6$ tons per year) of lignin worldwide (Ragauskas et al., 2006b; Suib, 2013). This process provides high quality paper pulp with a yield between 45 to 50%, using various wood chips materials. This is the most popular process because it produces resistant fibres and all the dissolved material is burnt in a recovery boiler to harvest the energy required to run the mill. In this process, the wood chips are mixed with an aqueous solution of sodium hydroxide (NaOH) and sodium sulfide (Na_2S), also named white liquor, in a large pressurized vessel called digester. The wood and white liquor mixture is heated from 70˚C to 170˚C for about 2 hours or more. During the reaction, lignin is extensively degraded and dissolved due to the breaking of ether linkages between lignin units. After the reaction, two distinct phases are formed: small alkali soluble lignin fragments are in the liquid phase which turns brown (black liquor), and the solid phase contains insoluble lignocellulosic fibres with residual lignin. In parallel, a small portion of hemicelluloses and cellulose is also degraded and dissolved (Gierer, 1980). For paper application, last lignin traces are eliminated by bleaching. During Kraft pulping process, around 85-93 % lignin and 56-71 % hemicelluloses are removed (Patil et al., 2011). Cellulose is conserved but it is partially depolymerised (DP in the range of 1000-1500). Soluble Kraft lignin is recovered from the black liquor by acidification. Its number average molar mass (Mn) is ranged from 1000 to 3000 Da (Polydispersity (PD) = 2.5–3.5) (Glasser et al., 1993). During the Kraft process, reactions lead to structural changes in the isolated lignin. In particular, the most important reaction is excessive cleavage of β-O-4 linkages that is responsible for connecting different phenylpropane units in lignin. For instance, the sulphide ion accelerates the cleavage of the ether linkages in phenolic units. Furthermore, the cleavage of oxygen-carbon is more feasible and predominant than carbon-carbon bond in alkaline environment during cooking process and possible reaction scheme is shown in Figure 1.12 (Gellerstedt, 2009).

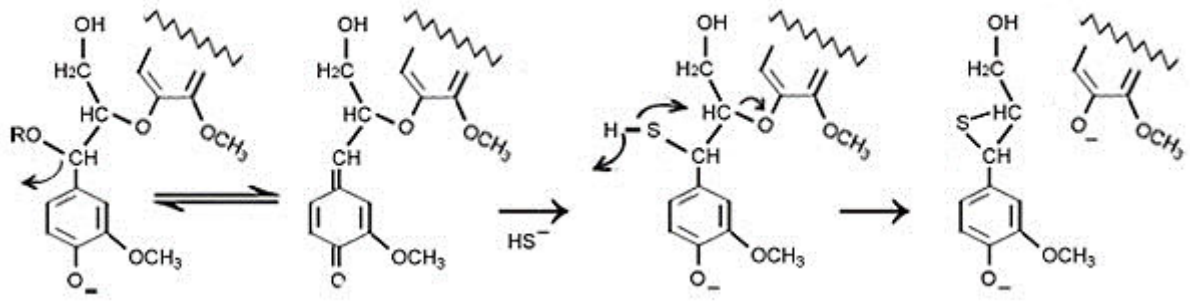

Figure 1.12. Cleavage of β-O-4 linkage during kraft process

1.2.3.3.2 Sulphite Pulping

Globally, sulphite pulps hold the production of less than 4% compared to Kraft pulps. During 1866-1867, the scientist B. C. Tilgman initially developed the sulphite pulping process to manufacture pulp from wood, using calcium as base (Sixta, 2006). Sulphite process is devoted to the production of specialty pulps with high reactivity for chemical applications (Sixta, 2006). Sulphite pulping is performed using aqueous solution of sulphite (SO_3^{2-}) or hydrogensuphite (HSO_3^-) on wood chips with heating (Saake and Lehnen, 1990).

The reaction may be carried out in a wide pH range, but the most important processes are acid sulphite and bisulphite processes. In acid sulphite cooking, the pulping liquor contains high amount of free SO_2 whereas bisulphite cooking liquors contain equal proportion of free SO_2 and HSO_3^- (Biermann, 1996). Acid cooking time is between 4 to 14 hours and to avoid lignin condensation, temperature is maintained between 130 to 145°C. The main advantage of acid cooking is that it uses all bases such as calcium, magnesium and sodium, calcium being the cheapest one. However, long cooking time is a drawback. In contrast, bisulphite pulping is performed on a larger pH range, at higher temperatures from 150 to 170 °C. This process provides different pulp grades and is able to cook all wood species, even high resinous woods. The degradation of lignin during sulphite processes is comparatively less than during Kraft process with the same extent of time (Lvova et al., 2014). Sulphite process produces pulps with high brightness, therefore bleaching chemicals requirement are very less in comparison with Kraft process. In addition, lignin is sulfonated by the action of HS^- ions, which favours lignin dissolution in the cooking liquor. The recovered lignin is called lignosulphonate due to the presence of sulphur (Marques et al., 2009; Magina et al., 2014). During sulphite process, the delignification through Sulphonation reaction is mainly occurred at α-position of the lignin whereas β-aryl ethers remained stable. The acid sulphite reaction is described in the Figure 1.15. In the presence of acid, the ether bond at the α position is more liable to break and eventually sulphonation group is introduced. The achieved number average molar mass (Mn) of the lignosulphonates from sulphite process ranges from 1000 Da to 50000 Da (PD = 4.2 to 7). In addition, lignosulphonates consist of around 30 wt% of sugars or carbohydrate, ash and other impurities. It is important to note that cooking chemicals after sulphite process cannot be recycled and reused and thus lead to high pollution of the water reservoirs (Casey, 1960). Kraft lignins are mainly burnt to produce energy in pulp mill and it has a poor added value whereas lignosulphonates are already marketed for many applications(Cements).

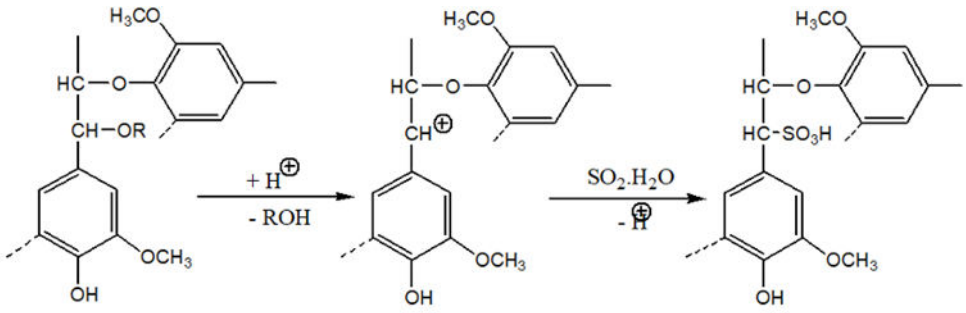

Figure 1.13. Reaction on lignin during acid sulphite cooking

1.2.3.3.3 Soda pulping

Soda pulping process represents 5% of the pulp production. It is particularly used to treat annual plants because they require less severe conditions compared to wood cooking (Suib, 2013). The lignocellulosic raw material is cooked in a liquor containing sodium hydroxide or a mix of soda and anthraquinone (Gierer et al., 1979). The produced lignins are sulphur free, they are called soda lignins and they are recovered based on acid precipitation of black liquor and liquid/solid separation. Soda lignins exhibit lower ash and sugar content compared to lignosulphonates (Nadif et al., 2002). The number average molar mass (Mn) is comparatively lower than the weight of lignin coming from other pulping processes due to multiple delignification reactions taking place during soda pulping. An example reaction is shown in Figure 1.17 where the most frequent delignification reaction is the cleavage reaction of non-phenolic β-O-4 bonds at alkaline conditions and the formation of phenolic lignin and epoxide (Heitner et al., 2016). They vary from 800 to 3000 Da (PD = 2.5 to 3.5).

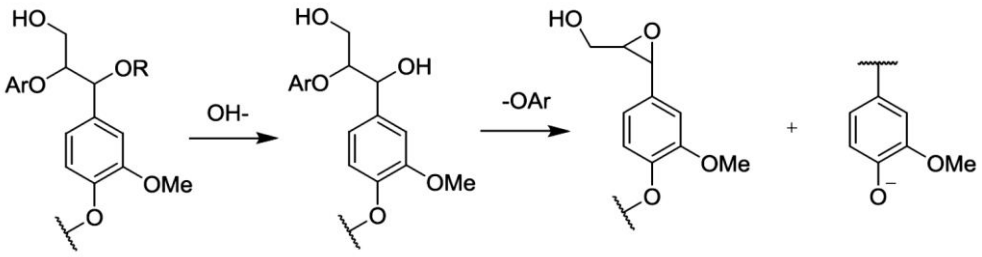

Figure 1.14. Reaction of cleavage of non-phenolic β-O-4 structures in lignin (Heitner et al., 2016).

1.2.3.3.4 Organosolv pulping

Organosolv pulping was mainly developed as an alternative for Kraft and sulphite pulping (Muurinen, 2000). During the process, the temperature ranges from 180 to 200 °C (Balogh et al., 1992; Sannigrahi and Ragauskas, 2013). Organic solvents are used as delignification agents in association with water and acid as catalyst. The process leads to two distinct phases: the cellulose

enriched solid phase and the liquor phase containing hemicelluloses and lignin products (Xu et al., 2006). Organosolv lignins are mostly produced through a strong treatment of biomass using various solvents such as methanol, ethanol, acetic acid, peroxyformic acid, ketones and phenols at different experimental conditions with different catalysts and reaction times. Various organosolv pulping can be applied based the employing organic solvents: Organocell (methanol), Alcell (ethanol), Avidel (formic and acetic acids), Acetosolv (acetic acid) and Milox (peroxyformic acid) (Gosselink, 2011; Muurinen, 2000; Sridach, 2010). The most common processes are ethanol/water mixture for Alcell and acetic acid with a small amount of HCl or H_2SO_4 for the production of Acetosolv lignin. The cleavage of α-O-4 lignin linkages is the most dominant reaction whereas cleavage of β-O-4 linkages is unlikely to occur, contrary to what happens in Kraft process (McDonough, 1993; S. Aziz and G.C. Goyal, 1993; Sannigrahi and Ragauskas, 2013). The typical number average molar mass (Mn) of organosolv lignins is 500 to 5000 Da (PD = 1.5 to 2.5).

All types of lignin are compared in the Table 1.3.

Table 1.3. Properties of technical lignins according to the extraction process (Laurichesse and Avérous, 2014)

Lignin Type	**Sulphur containing lignins**		**Sulphur free lignins**	
	Kraft	**Lignosulfonate**	**Soda**	**Organosolv**
Raw materials	Softwood Hardwood	Softwood Hardwood	Annual plants	Softwood Hardwood Annual plants
Solubility	Alkali Organic solvents	Water	Alkali	Wide range of organic solvents
Number average Molar mass (Mn = g/mol)	1 000-3 000	15 000-50 000	800-3 000	500-5 000
Polydispersity (PD)	2.5-3.5	6-8	2.5-3.5	1.5-2.5
Glass transition temperature (T_g)	140-150	130	140	90-110

1.3 Chemical Modification of Lignin

Lignin's high polarity due to variety of functional groups, poor thermal stability from amorphous nature and difficult melt processing prohibit the direct use in numerous applications. As seen from the

above sections, lignin contains various types of functional groups such as hydroxyl (aliphatic and phenolic), methoxyl, carbonyl and carboxylic groups. These functional groups foster the research and development of lignin into value added applications. Therefore, a series of modifications can be carried out on lignin functional groups to improve lignin chemical reactivity, solubility in organic solvents and to reduce the brittleness of lignin derived polymers. Among various functional groups present in lignin, hydroxyl groups are the primary choice for researchers: they can be modified using simple reaction conditions and after reaction, new chemical reactive sites may be formed. Several chemical modifications can be performed on lignin including methylation, amination, halogenation, nitration, etherification, esterification, silylation and phenolation etc. These reactions can be performed through either modification of hydroxyl groups or carbonyl groups or breaking linkages into corresponding derivatized lignin products. They may also decrease the hydrophilicity of lignin significantly and increase its compatibility with apolar polymers and dispersion into polymer matrix. Possible chemical modifications are listed in Figure 1.15.

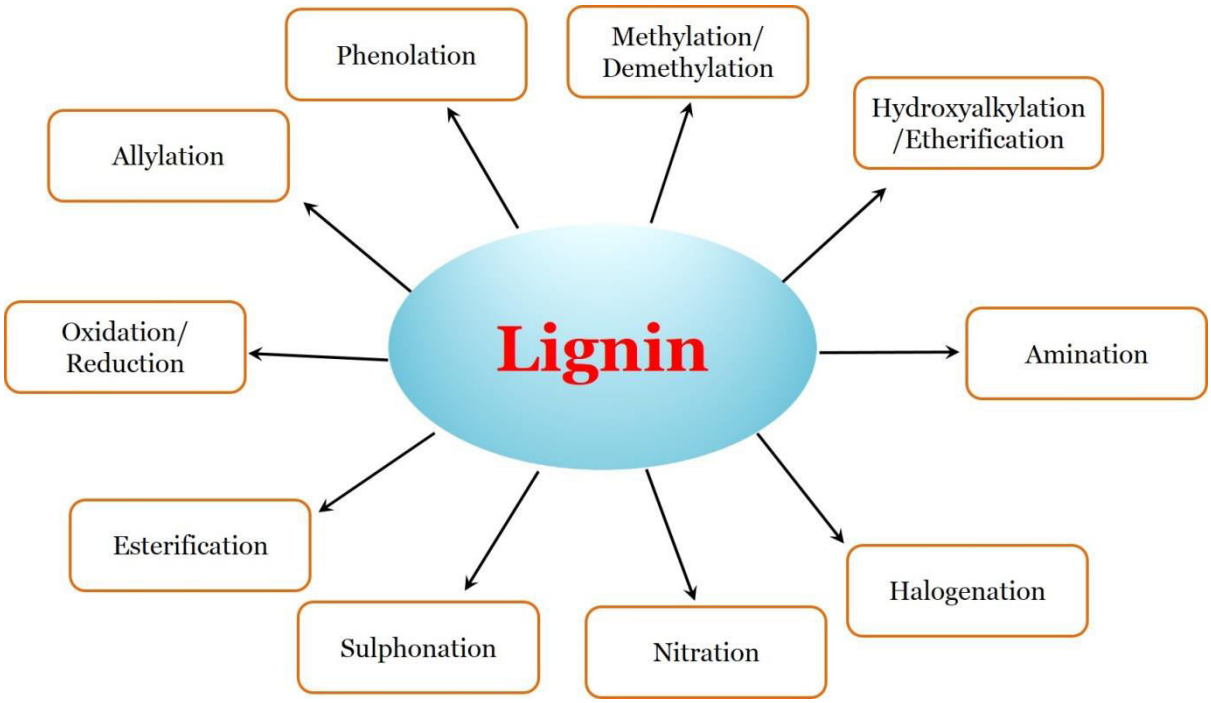

Figure 1.15. A schematic overview of various reactions for the synthesis of new chemical compounds from lignin

Chemical modifications of lignin into new chemical lignin derivatives via a series of different reactions are explained in the following sections.

1.3.1 Methylation

Methylation and/or demethylation are used in various synthetic applications. For instance, a major part of the alkylated lignin is mixed with synthetic polymers (poly(ethylene oxide) (PEO), poly(ethylene terephthalate) (PET), and poly(vinyl alcohol) (PVA)) to prepare polymers blends (Kadla and Kubo, 2004; Sen et al., 2015). Methylation is carried out on phenolic hydroxyl groups. Lignin methylated derivatives are produced using dimethyl sulphate $(CH_3)_2SO_4$ (Lewis et al., 1930) in aqueous NaOH without any side reaction; whereas, methylation with methyliodide CH_3I in presence of an excess of K_2CO_3 and N,N dimethylformamide HCO-N$(CH_3)_2$ has been reported as an ineffective and unselective reaction (Sadeghifar et al., 2012). After methylation, the glass transition temperature (Tg) was significantly reduced (153 to 128º C for the case of Kraft lignin) (Sadeghifar et al., 2012). These typical reactions are shown in Figure 1.16.

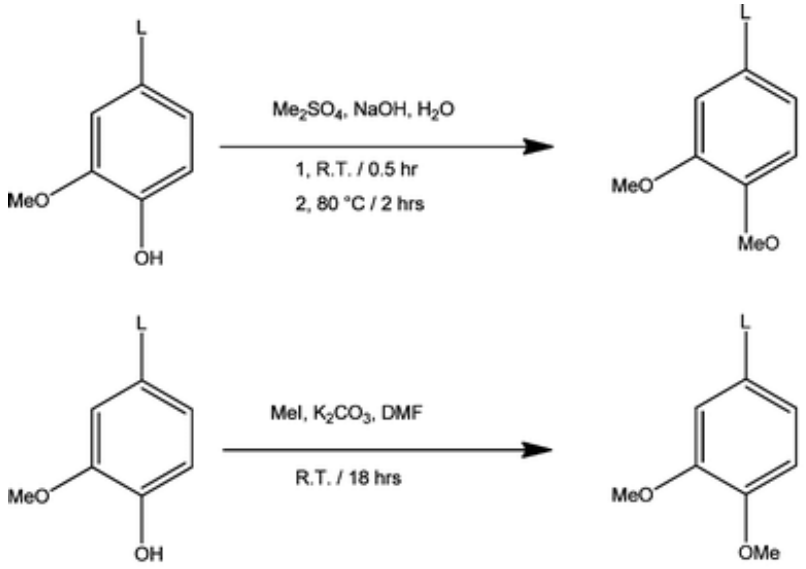

Figure 1.16. Methylation of lignin using various reaction conditions (Sadeghifar et al., 2012)

The selective methylation of hydroxyl groups, especially phenolic –OH groups in lignin, leads to less reactive phenyl methyl ether. Thus lignin reactivity is significantly reduced and used in polymer formulations (Argyropoulos, 2013).

1.3.2 Hydroxyalkylation/Etherification

Hydroxyalkylation of lignin hydroxyl groups is applied to develop biodegradable plastic composites. An example is the hydroxypropyl lignin homogeneously dispersed in a polymer matrix (for example, soy protein plastic isolate) to improve the mechanical properties of the composite (Chen et al., 2006). In particular, chemical modification by oxyalkylation was established to reduce the brittleness of lignin-derived polymers and also to enhance visco-elastic properties for various

applications (Wu and Glasser, 1984). Several studies suggested that hydroxyalkylation can be accomplished on different types of lignins with reagents such as 1,2 oxides, 1,2 carbonates and 1,2 sulphites with catalyst (alkali metal and alkali earth metal carbonate or hydroxide) or without catalyst at temperatures varying from 20˚C to 250˚C. The weight ratio of lignin and oxyalkylating agent used for this conversion is maintained at 3:1 (Allan, 1969; Christian et al., 1972). Wu et al. studied the hydroxypropylation of lignin using propylene oxide under alkaline condition at 180˚C (Wu and Glasser, 1984). Later Behzad Ahvazi et al. performed lignin based polyol synthesis from wheat straw soda lignin using propylene oxide. This study particularly investigated the direct oxyalkylation of lignin under acidic and alkaline conditions (Wu and Glasser, 1984; Pizzi and Walton, 1992; Lammers et al., 1993; Aniceto et al., 2012). Another study examined a two-step reaction with maleic anhydride and lignin followed by propylene oxide treatment (Thielemans and Wool, 2005). These results concluded that the direct oxyalkylation under alkaline condition is more efficient in alkaline conditions and leads to higher aliphatic hydroxyl group substitution (Ahvazi et al., 2011). Due to the considerable risks associated with propylene oxide such as flammability, toxicity and carcinogenicity characteristics, later, Kühnel et al. studied the oxyalkylation reaction by substituting propylene oxide by "green" propylene carbonate as a reagent (Kühnel et al., 2015). The typical reaction is illustrated in Figure 1.17. During the reaction lignin OH and PC, the ring opening process and two different reaction products were obtained with respect to different nucleophilicity and steric hindrance of OH_{aliph} and OH_{phen}. However, the formation of ether through OH_{phen} attack is predominant because of the catalyst K_2CO_3.

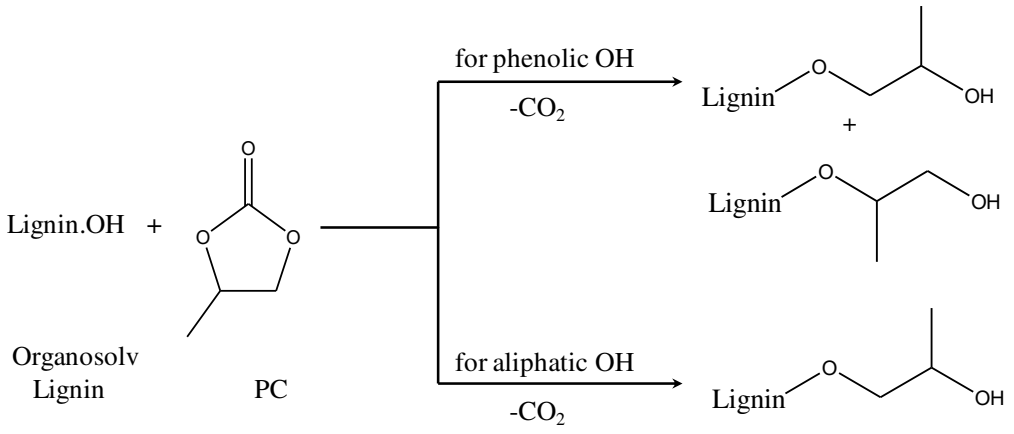

Figure 1.17. Organosolv lignin oxyalkylation reaction using propylene carbonate (Kühnel et al., 2015)

Additionally, Sevillano et al., proposed a new derivatisation method to diminish the lignin polarity in order to quantify the number of hydroxyl groups as well as use lignin as precursor for various polymer applications. In this reaction, phenolic and primary aliphatic hydroxyl groups form into

corresponding fluoro-ether derivatives using 4-fluorobenzylchloride. This reaction is known as fluorobenzylation (see Figure 1.18).

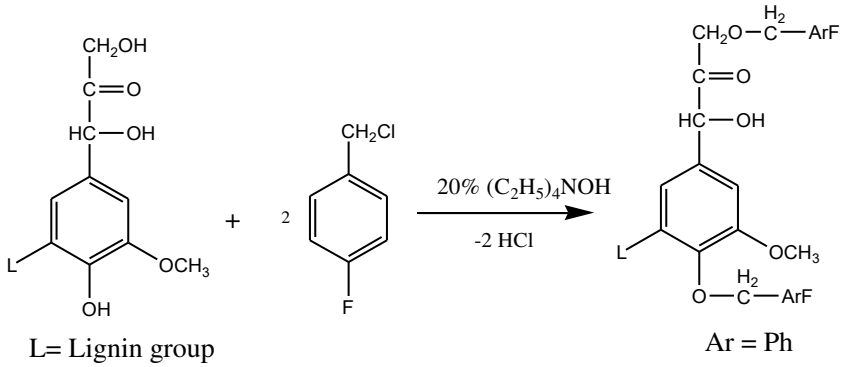

Figure 1.18. Etherification of lignin using 4-Fluorobenzylchloride (Sevillano et al., 2001)

1.3.3 Amination

Lignin amines have been synthesised through the Mannich reaction. For example, low molecular weight soda lignin fractions could react with amine and formaldehyde to get lignin amine. The product may be recovered by precipitation using isopropanol (Figure 1.19).

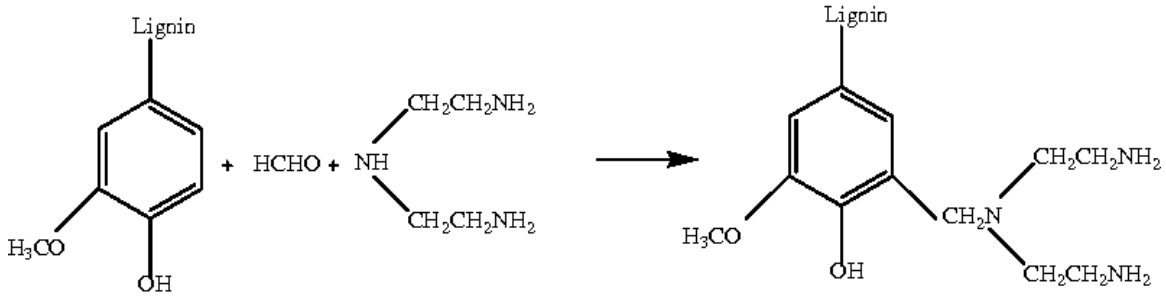

Figure 1.19. Synthesis of lignin amine product via the Mannich reaction(Wang et al., 2016)

Lignin amines contain both amine and hydroxyl functional groups which increases the interfacial bonding properties between polyvinyl chloride /wood-flour composites (act as a coupling agent) and enhances mechanical performance of composites (Yue et al., 2011). Lignin amine is significantly used as an additive in dye dispersant (Dilling and Samaranayake, 1999), asphalt emulsifier (Lin, 1985) and flocculant (Hoftiezer et al., 1984).

1.3.4 Halogenation

Halogenation of lignin can carried out on aromatic moiety or on the side chains (Calvo-Flores et al., 2015). The chlorination of lignin was first introduced by Cross and Bevan in 1882 (Cross and Bevan, 1882) and halogenated lignins have been used in building materials and in consumer goods as a fire retardant (Meister, 2000). Later, in 1913 Heuser et al. (Heuser and Sieber, 1913) investigated

the chlorination on spruce wood and the results showed that wood absorbed around 31% of its weight of chlorine after 2h. Polčín (Polčín, 1954) investigated the reaction of alkali sulphite lignin with chlorine gas and concluded that methoxy groups undergone oxidation and split from aromatic ring in aqueous media leading to *o*-quinones formation. However, due to environmental issues, halogenated lignin compounds, also called "*halolignin*" are not widely used. The corresponding reaction is given in Figure 1.20. The chlorine molecule turns into radicals which attack the aromatic ring and replace the hydrogen into chlorine substituted lignin compound.

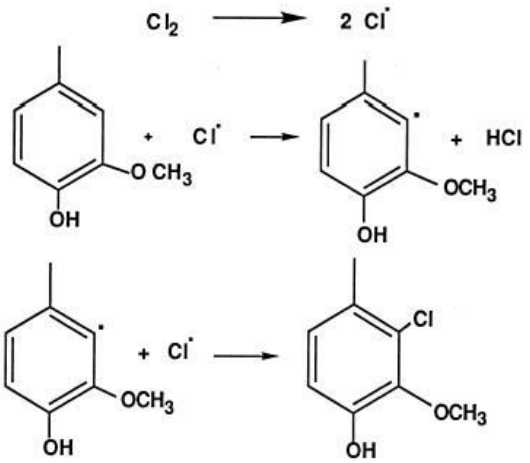

Figure 1.20. Halogenation of lignin into halolignin (Meister, 2002)

1.3.5 Nitration

Nitration can be readily carried out with nitric acid HNO_3 or with gaseous nitrogen dioxide NO_2 as nitrating agents. Nitrolignins are synthesised by the reaction of alkali lignin with a mixture of fuming nitric acid and acidic anhydride with a molar ratio of 4:1 at a temperature below 0˚C, under ice bath. After the reaction, the solid precipitate is recovered by ultra-centrifugation. Nitro group is introduced in the aromatic ring and solubility of nitrolignins is similar to that of halolignins. The schematic representation of lignin nitration is shown in Figure 1.21. The main application of this reaction is the formation of interpenetrating polymer networks (IPN) which can be obtained by treating polyurethane and nitrolignin.

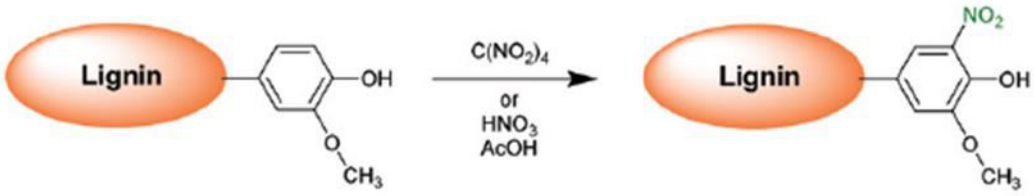

Figure 1.21. Formation of nitrolignin using different reagents (Kai et al., 2016)

1.3.6 Sulphonation

Sulphite and Kraft pulping processes provide sulphur containing lignin. Lignin sulphonation occurs during extraction processes as already shown in Figure 1.13. Klason used calcium chloride to precipitate the ligninsulphonic acids (Klason, 1920) from sulphite pulping process. During this process, the authors named the precipitated product "α-ligninsulphonic acid" and the remaining lignin in the solution "β-lignosulphonic acid" (Lindsey and Tollens, 1892). In general, lignosulphonates from the sulphite process contain more sulphur groups, i.e. a higher degree of sulphonation, than Kraft Lignins. The presence of sulphonated groups enhances the polarity of lignosulphonates and thus they are water soluble. The molecular weight of lignosulphonates is higher than that of Kraft lignin. It is used in numerous applications, for instance, (i) as dispersants in cement admixtures and dye solutions, (ii) in composites to enhance the hydrophilicity and (iii) as flocculants (to decrease the settling time of solution or suspensions) in which sulfonated lignin-based products need to be cross-linked with other compounds such as polyethylene glycol, tosylchloride, and formaldehyde (Aro and Fatehi, 2017).

1.3.7 Esterification

Synthetic polymers are used in many applications including textile and packaging industries. They can be obtained through condensation of typical monomers such as alcohol and dicarboxylic acid originating from petroleum resources. For instance, polyethylene terephthalate is obtained by treating two monomers such as diol and dicarboxylic acid. As already know, the lignin macromolecule possesses variety of functional groups, therefore it can substitute both monomers and/or either one monomer in order to make processes and products sustainable and greener.

Several authors reported that lignin-based polyesters such as lignin-sobacoyl ester (Binh et al., 2009), lignin – acetic/propionic/butyric anhydride esters (Fox and McDonald, 2010) and lignin-telechelic polybutadiene esters (Saito et al., 2012) acquire thermal stability and the resulting polymers exhibit large molecular weight with comparatively higher Tg (glass transition temperature). A typical example of lignin esterification is shown in Figure 1.22. Lignin compound is treated with polyene containing carboxylic acid groups at both ends in the presence of strong base into the formation of polyester.

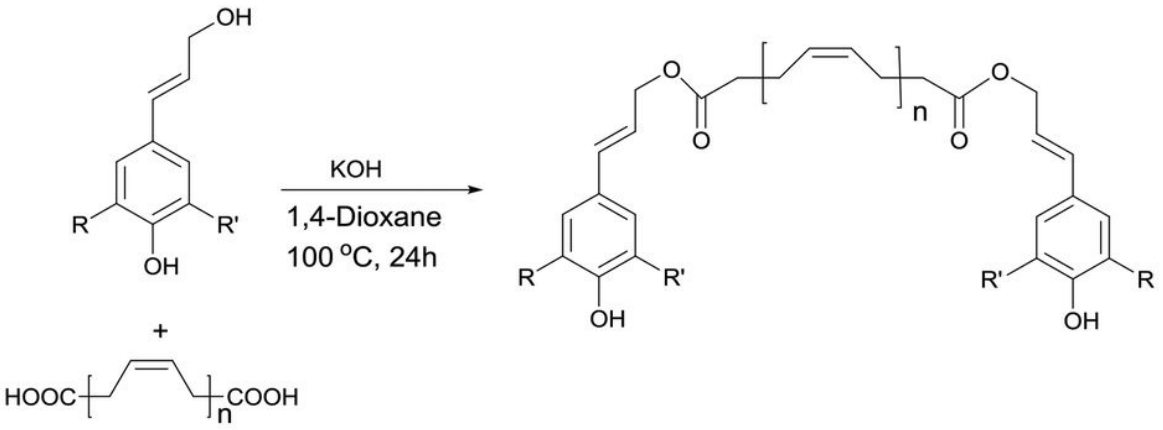

Figure 1.22. Synthesis of polyester from lignin and dicarboxylic acid (Saito et al., 2012)

Another esterification reaction has been reported in the literature, the fluorobenzoylation. It was carried out with 4-fluorobenzoic acid anhydride (Sevillano et al., 2001) to convert lignin secondary hydroxyl groups into corresponding fluoro-esters derivative (illustrated in Figure 1.23) for analytical issues.

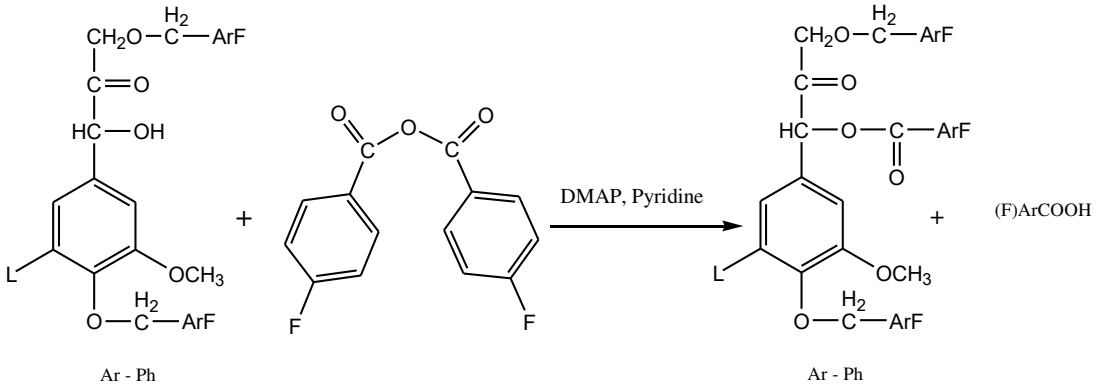

Figure 1.23. Esterification of lignin using the 4-fluorobenzoic anhydride chemical (Sevillano et al., 2001)

Acetylation is another esterification reaction. Acetylation of lignin is performed with the combination of acetic acid and acetic acid anhydride for the synthesis of lignin-acetyl esters (Faix, 1992; Buono et al., 2016). Acetylation was reported to enhance the photo-stability of jute fibres and milled wood lignin and also it helps to brighten the ground wood pulps and thermomechanical pulps by prohibit the photooxidation (Paulsson and Simonson, 2002). Acetylation of lignin reaction is given in Figure 1.24, the lignin is treated with acetic anhydride. The lignin OH nucleophile attacks acetyl group to the formation of acetylated lignin and acetic acid by-product.

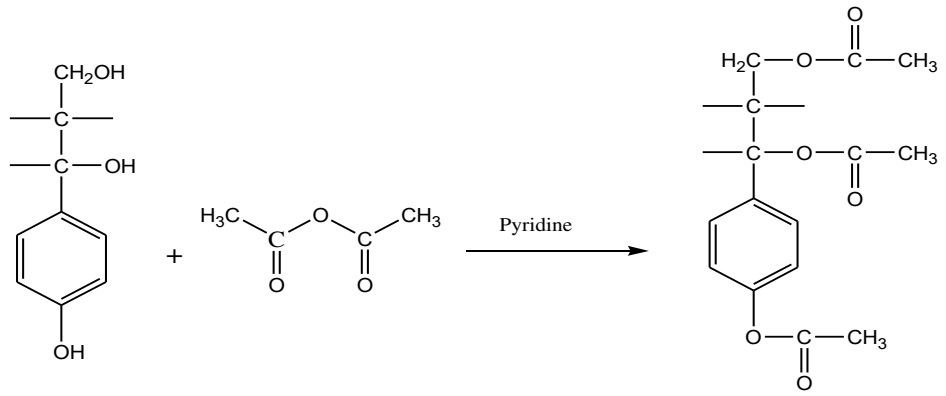

Figure 1.24. Acetylation of lignin using acetic anhydride and pyridine

1.3.8 Silylation

In recent years, silylation is becoming one of the most popular methods to elucidate the structure of lignin using ^{29}Si NMR. The silylation reaction scheme is shown in Figure 1.25 for soda lignin. Lignin hydroxyl groups in soda lignin have been silylated using tert-butyldimethyl silyl chloride (TDMSCl). It should be noted that all hydroxyl groups present in the lignin were silylated. The obtained silylated product enhanced the thermal stability and lowered the Tg of the lignin product compared to acetylation (Buono et al., 2016).

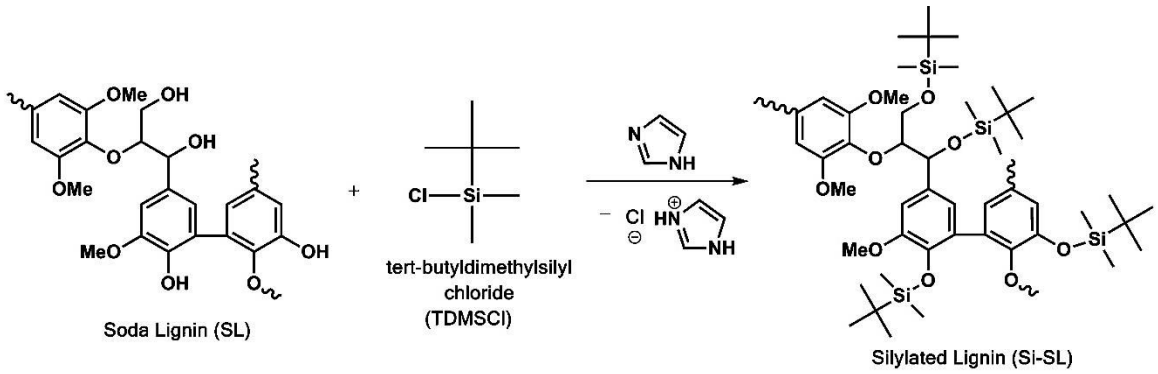

Figure 1.25. Synthesis of silylated lignin from soda lignin and tert-butyldimethyl silyl chloride (Buono et al., 2016)

1.3.9 Oxidation/Reduction

Lignin is sensitive to strong catalytic processes which cleave the linkages and turn lignin into small fragments. This can be achieved by different treatments: oxidation, reduction and cracking oxidation and cracking reduction reactions. They are detailed below.

Oxidation: C-O bonds and in particular ether bonds are the most predominant linkages in lignin. Therefore, lignin fragmentation particularly focuses on the cleavage of ether linkages. This can be

done by the oxidative treatment of lignin using potassium permanganate/sodium periodate and/or nitrobenzene oxidation (Wu and Glasser, 1979). Lignin fragmentation is additionally useful to determine the initial structure of lignin (Gellerstedt and Lindfors, 1984; Harman-Ware et al., 2013; Masingale et al., 2009). After full oxidation, products from lignin oxidation are a mixture of aromatic compounds such as ketones, aldehydes, acid allylic alcohols and ethers etc, which may be eventually used as precursors for various chemical syntheses (Zhang et al., 2009). Several researchers reported that lignin oxidation can be done using various metal based catalysts, Schiff base catalysts and porphyrin catalysts (Evtuguin et al., 1998; Gupta et al., 2009; Harris et al., 1938; Kuwahara et al., 1984; Parpot et al., 2000).

Reduction or Hydrogenation: As stated above for C-O bonds, catalytic hydrogenation reaction produces low oxygen content compounds, bio-oils and phenols. Harries et al. demonstrated that the hydrogenation of hardwood lignin gives carbon rich compounds (Harris et al., 1938). Till date, numerous homogeneous and heterogeneous catalysts have been reported for successful hydrogenation of lignin (Pepper and Supathna, 1978; Pepper et al., 1966). In particular, heterogeneous catalyst (copper-metal oxide) effectively produces lignin monomeric compounds that can be used for fuel additives (Barta et al., 2010). Other catalysts such as Ni-Pd, phase transfer catalyst (chloro-1,5-hexadiene)-rhodium) and $RhCl_3$/trioctylamine generate phenols and aromatic ring compounds (Cyr et al., 2000; Januszkiewicz and Alper, 1983; Nasar et al., 1994). Although, hydrogenation process possesses some advantages (synthesis of high carbon containing compounds and fuel additives) the main drawbacks remain that the reaction should be performed using high H_2 pressure with strong temperature and the reuse of catalyst after the reaction is difficult.

1.3.10 Allylation

Recently, Llevot et al., has developed a new catalytic highly efficient approach called Tsuji-Trost allylation (Llevot et al., 2017) for converting hydroxyl groups in lignin with allyl methyl carbonate. Various dialkyl carbonates are used as alkylation agent for hydroxyl groups including aliphatic and aromatic hydroxyls. The resulting products contain new functional groups introduced into the lignin structure. The authors found that phenolic –OH groups (shown in Figure 1.26) in lignin are selectively converted into allyl derivatives with high yield. This particular method can be used to improve lignin reactivity.

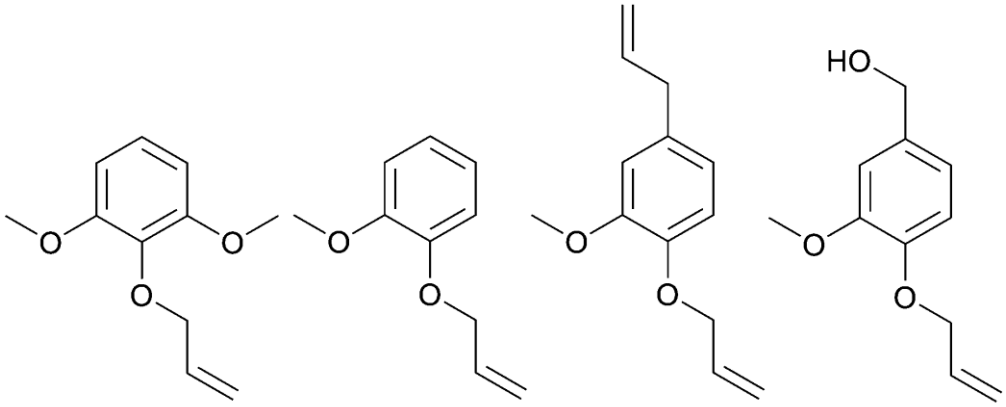

Figure 1.26. Allylated products from different bioderived phenols by Tsuji–Trost reaction with allyl methyl carbonate

1.3.11 Phenolation

Phenolation reaction of lignin is used for phenol formaldehyde resin synthesis. Prior to the use of lignin for resin synthesis, lignin molecules are activated by introducing phenol groups via phenolation. Highest phenolation is achieved with hardwood organosolv and softwood sulphite lignins whereas a weak activation is obtained for soda and softwood Kraft lignin (Podschun et al., 2015). A recent study from Jiang et al., reported an effective phenolation of lignin with a minimal amount of sulphuric acid and phenol as a solvent (Jiang et al., 2018). The results also demonstrated that during phenolation, most of the ether linkages were cleaved. A scheme is provided in Figure 1.27.

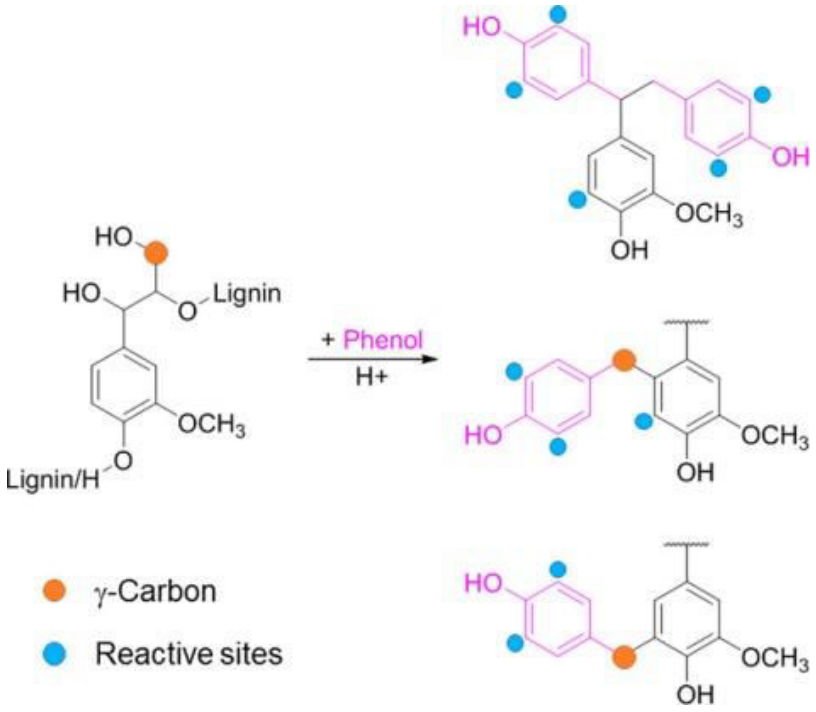

Figure 1.27. Phenolation of lignin

1.4 Lignin applications

Lignin is a potential source of renewable material for the production of phenolic compounds (Dorrestijn et al., 1999). Its derivatives are widely used in many applications like binders, adhesives, antioxidants, disinfectants, resins, fibers, drugs and wood preservatives etc.

Lignin amines are used as additives, emulsifier, flocculants, dye dispersants and in polymer synthesis namely polyurethanes, phenolic resins and epoxy resins etc (Yue et al., 2011).

Self-finding high density fibreboards were manufactured from industrial softwood Kraft lignin, soda wheat straw lignin and hydrolysed wheat straw lignin (Tupciauskas et al., 2017).

Lignin antioxidant properties in polypropylene have been studied with different lignins extracted from various botanical origins (addition of 1% lignin weight). The conclusion is that the solubility of the lignin in polypropylene is a key parameter, more important than lignin phenolic content and lignin intrinsic viscosity. Low molecular weight lignin and low phenolic content lead to increase lignin solubility and gives better antioxidant property (Pouteau et al., 2003).

Activated Kraft and soda lignins are used as a binder and wood adhesive. Prior to the introduction in various applications, lignins are activated through periodate oxidation to improve the reactivity. Gosselink et al., developed fully renewable binders from lignin with poly furfural alcohol and partially renewable lignin based phenol formaldehyde binder (Gosselink et al., 2011).

Organosolv lignins are used as a filler in ink, varnishes, paints and also used to increase the viscosity of the polyether polyol and to improve the rheological properties (Belgacem et al., 2003).

Lignin acts as a macro-monomer in the synthesis of phenol formaldehyde resins and the modified oxypropylated polyols are used in different polyurethane formulation (adhesive and foams) (Krässig, 1993).

1.5 Lignin analysis: literature review

Lignin phenolic hydroxyl group quantification and molar mass distribution are essential for lignin valorisation. It provides useful information about the lignin structure and its degradation mechanism (Dence and Lin, 1992). As seen in the above sections, due to high polarity and poor solubility of lignin, lignin analysis is complex and there is no singular method to elucidate its chemical and physical structure. Till date, many derivatization methods (acetylation, fluorobenzylation, fluorobenzoylation and phosphorylation) are employed to replace lignin functional groups, followed by their detection using different characterization techniques (UV, FT-IR, GC, NMR and GPC).

All classical methods are presented in the next paragraph as well their limitations.

1.5.1 Lignin functional group analysis

1.5.1.1 By ultraviolet spectroscopy (UV)

UV spectroscopy is a convenient and useful technique for quantitative and qualitative analysis of the lignin in wood or black liquor. Lignin aromatic structure absorbs and exhibits maxima in the ultraviolet region. The position and the intensity of the maxima depends on the type of lignin, modification and solvent used for the analysis (Lin, 1992). Tiainen et al. used UV spectroscopy to quantify phenolic hydroxyl groups in milled wood lignin, Kraft lignin and model compounds carrying one aromatic hydroxyl group. This method uses the absorbance difference in the maxima close to 300 nm and 350 nm of the sample dissolved in alkali (lignin ionized form) and neutral (lignin non-ionized form) medium, respectively. The authors found that the UV spectroscopic method results are consistent with ^{1}H NMR results for the case of milled wood lignin and Kraft lignin. However, UV method gives too low phenolic values for modified lignins and model compounds bearing more than one hydroxyl groups in the aromatic ring (Tiainen et al., 1999). Similarly, several authors conducted UV analysis to quantify the phenolic hydroxyl group in alkaline solution by measuring the absorbance before and after ionization using the maxima at 300 nm. At this region, phenolic hydroxyl group conjugated with carbonyl group leads to erroneous phenolic hydroxyl group determination. Indeed, the obtained absorbance from analysis is directly proportional to the purity of the lignin and sometime low absorbance occurred due to the co-precipitation of other materials such as sugars and wax etc (Tamminen and Hortling, 1999; Zakis, 1994). Although the UV method is a rapid method for phenolic group measurements, limitations exists: the quantification of phenolic structures bearing more than one phenolic hydroxyl groups is not reliable and the full solubility of lignin samples in the medium is a prerequisite which is not always satisfied, depending on the lignin type (Serrano Cantador et al., 2018; Tiainen et al., 1999).

1.5.1.2 Fourier Transform Infrared (FT-IR)

FT-IR is a rapid and widespread spectroscopic technique to analyse the lignin functional groups. The advantages are the short analysis time, high sensitivity, easy use, direct analysis on solid samples like wood, paper and pulp (Stenius, 2000) and convenient data handling (Faix, 1991). Lignin bands are found at various ranges, from 1500 to 1600 cm^{-1} and also between 1470 and 1460 cm^{-1} (Wegener et al., 2009). FT-IR is mainly used to qualitatively analyse different types of lignin along with various functional groups including carbonyl, methoxyl, hydroxyl and carboxyl groups (Faix, 1991; Hortling et al., 1997) and to follow the efficiency of derivatization reactions.

Examples of the use of FT-IR for lignin analysis are numerous. For instance, Ibrahim et al. conducted a graft copolymerization of Kraft lignin with acrylamide. The authors found that lignin shows absorption at 3417 cm^{-1} for phenolic or hydroxyl groups, 1638 cm^{-1} for aromatic ring and the 1462 cm^{-1} band has been attributed to C-H stretching (M.N. Mohamad et al., 2006). Similarly, Ghatak carried out the experiment with wheat straw soda black liquor and reported a series of IR absorbance bands. For lignin, the main bands are assigned as following: 3437 cm^{-1} to O-H stretching of hydroxyl, 2928 cm^{-1} to C-H stretching in methyl and methylene groups, 1637, 1604, 1516 cm^{-1} to aromatic skeletons, 1331 cm^{-1} to syringyl ring C-O stretching and 1284 cm^{-1} to guaiacyl ring C-O. However, some bands are difficult to evaluate due signal overlapping and the assignment of some bands is thus complex (Ghatak, 2008). The major drawback of this method is that it is not quantitative.

1.5.1.3 Titration methods

1.5.1.3.1 Oximation

Lignin oximation is applied to determine the carbonyl group content. The reaction is performed with hydroxylamine hydrochloride. In this direct method, all types of carbonyl groups (α-carbonyl and *o*- and *p*-quinones) react, producing oxime and liberating HCl (Heuser, 1953). The liberated HCl is titrated and the obtained value reveals the amount of carbonyl groups in the sample (Gierer and Soderberg, 1959).

Zakis developed a modified oximation method (Zakis, 1994) because he stated that the previous oximation followed by HCl formation relies on equilibrium and the hindered α C=O are poorly reactive during the reaction. The author proposed to use DMSO as a solvent and triethanolamine (TEA) compound in excess. In this case, TEA neutralizes the acid released during the reaction and buffers the pH level. Moreover, the unreacted triethanol amine may also be titrated by potentiometric and conductometric methods. This modified oximation method leads to quantify all types of carbonyl groups in lignin (Zakis, 1994) (Figure 1.28).

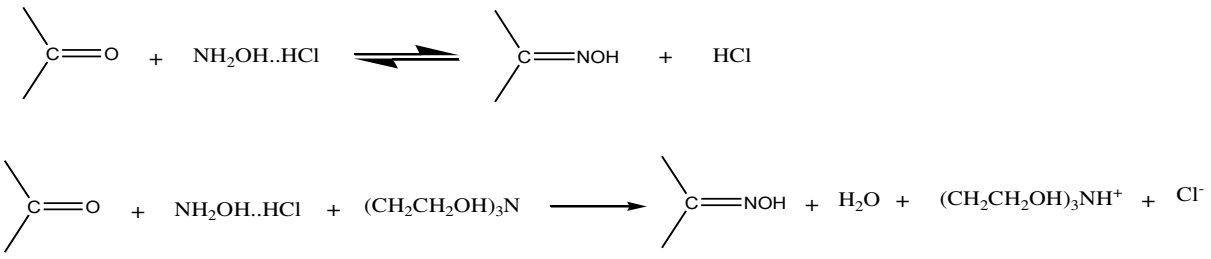

Figure 1.28. Oximation of carbonyl groups

1.5.1.3.2 Borohydride method

Total carbonyl content in lignin could be determined by sodium borohydride reduction ($NaBH_4$). During the reaction, lignin carbonyl groups are reduced by $NaBH_4$ and the excess amount of $NaBH_4$ is quenched by sulphuric acid, liberating hydrogen molecule. The liberated hydrogen molecule is estimated by volumetric titration, meanwhile the same procedure is repeated without lignin sample, called blank titration. The calculated difference value corresponds to the total number of carbonyl content (Gierer and Soderberg, 1959; Marton and Adler, 1961; Marton et al., 1961). The main drawback of this method is the accuracy that the obtained carbonyl content is about twice the values and error is approximately 3 % or higher.(Lin and Dence, 1992)

1.5.1.4 Gas Chromatography (GC)

1.5.1.4.1 Periodate oxidation

Adler developed the estimation of free phenolic hydroxyl groups in softwood lignin through periodate oxidation followed by GC analysis. The author treated guaiacol in aqueous solution with excess of sodium periodate at 4˚C in a dark room. The reaction leads to oxidative demethylation and subsequently methanol liberation and *o*-quinone formation. The formed methanol is stable (Adler et al., 1955, 1959) and therefore, quantified by GC with an internal standard. This particular analytical method provides the number of phenolic groups in the investigated guaiacol compound. However, periodate oxidation does not allow the estimation of catechols and p-hydroxy phenyl units due to the lack of methyl group adjacent to the phenolic position (Lai et al., 1990). This is a limitation for lignin analysis.

1.5.1.4.2 Aminolysis

Aminolysis is a traditionally established method to determine the phenolic hydroxyl group content in lignin. This method comprises the acetylation of the lignin sample, evaporation and drying, followed by the aminolysis reaction and gas chromatography (GC) analysis. This multi-step method was originally developed by Månsson and tested on acetylated lignin model compounds (Månsson, 1982) and also on milled wood lignin samples (Månsson, 1983). After acetylation, aromatic acetyl groups are selectively deacetylated by pyrrolidine reagent (detailed analysis can be found in Chapter 3). This reagent mainly favours the deacetylation of aromatic acetyl groups under mild conditions which is considerably much faster than the aliphatic acetyl groups. Then, the resulting 1-acetyl pyrrolidine can be easily quantified by GC. The value is proportional to the number of phenolic hydroxyl groups present in the lignin. However, there are some limitations in this method: (1) long preparation time requires for lignin acetylation (2) some inherent imprecision arises in the estimation of the phenolic groups due to the presence of lignin sugar residues.

Phenolic hydroxyl groups of spruce and aspen lignins were tested using aminolysis and periodate oxidation methods. According to aminolysis method, spruce and aspen lignin phenolic hydroxyl contents were reported as 0.649±0.029 and 0.445±0.031 mmol/lignin respectively, whereas periodate oxidation gives 0.702±0.005 and 0.493±0.008 mmol/g lignin. The results of periodate oxidation show higher phenolic content than aminolysis method. Moreover, the higher standard deviation obtained with the aminolysis method is due to the numerous steps involved in the analysis (Lai et al., 1990).

1.5.1.5 NMR techniques

NMR spectroscopy is a powerful tool and ^{1}H, ^{13}C, ^{31}P and ^{19}F NMR are the most commonly used NMR techniques for the structural characterization of lignin macromolecule.

1.5.1.5.1 ^{1}H NMR

The 100% natural abundance and high sensitivity of the proton nucleus significantly contribute to use it as one of the spectroscopic technique. Pioneering work has been carried out by Lundquist's research group to quantify carboxylic, formyl, aromatic and methoxyl groups in lignin using ^{1}H NMR (Lundquist et al., 1979a, 1979b, 1980; Li, 1994). Ludwig et al. developed the methodology to analyse the lignin as acetate derivatives using deuteriochloroform (Ludwig et al., 1964a, 1964b). During the time of 1970 and 1980s, modern high frequency Fourier transform instruments have been employed to get clear NMR spectra. Tiainen et al. quantified the phenolic hydroxyl groups in lignin by exchanging phenolic proton in D_2O (deuterated water or heavy water) without acetylation (Tiainen et al., 1999). The major limitation of this method is the short chemical shift ranges (i.e., δ 12-0 ppm) so that ^{1}H NMR significantly suffers from severe signal overlapping (Lundquist, 1992).

1.5.1.5.2 ^{13}C NMR

^{13}C NMR has broader spectral window and enhances signal resolution compared to ^{1}H NMR. It has been extensively used to study the complex lignin structure and it is an attractive technique for functional group determination. After acetylation of lignin hydroxyl groups, carbon of methyl and carboxyl groups gives signal respectively at 20.8 ppm and about 170 ppm without spectrum overlapping. This signal offers good signal/noise (S/N) ratios, and for this reason, acetylated lignins are usually used for the quantitative estimation of different hydroxyl groups. In the acetylated lignins, the resolution of the carboxyl carbon signal allows to separate primary (170.8 ppm), secondary (170 ppm) and phenolic hydroxyl groups (168.9 ppm) (Robert and Brunow, 1984). Barrelle et al. also quantified the ratio of aliphatic and phenolic hydroxyl groups of acetylated organosolv lignin using ^{13}C NMR and found the value of 0.79 (Barrelle, 1993). Limitations associated with the ^{13}C NMR technique are the following: ^{13}C nucleus is not sensitive enough (1/5800 compared to proton) and it exhibits a limited natural abundance (1.1% only). Thus, huge sample quantity, long acquisition times

and high purity lignins without impurity (carbohydrate residues, ashes and extractives) are required (Kaplan, 1998; Serrano Cantador et al., 2018).

1.5.1.5.3 ^{31}P NMR

The ^{31}P NMR spectroscopic method has been developed by Argyropoulos et al. (Argyropoulos, 1994; Argyropoulos and Zhang, 1998; Argyropoulos et al., 1992, 1993; Berlin and Balakshin, 2014; Hoareau et al., 2004; Zawadzki and Ragauskas, 2001). This technique rapidly became popular in recent decades. ^{31}P NMR spectroscopy enables the quantification of phenolic, aliphatic hydroxyl groups and carboxylic groups of lignin in a single analysis.

Using lignin like model compounds after derivatization with 1,3,2-dioxaphospholanyl chloride (I), spin lattice relaxation times and solvent effects in ^{31}P NMR have been studied. The result showed that spin lattice relaxation time (T1) of phosphorus nuclei attached to carboxylic acid is 5 s and phenol and alcohol derivatives were 9 s and 8 s respectively. The chemical shifts of primary hydroxyls in β-O-4 model compounds of lignin were more sensitive to solvent concentration, whereas alpha and guaiacyl hydroxyls were only slightly sensitive (Argyropoulos et al., 1993). The same author studied the chromophores and carboxylic acids in mechanical pulp lignin using trimethyl phosphite derivatization and quantified *o*-quinone groups using ^{31}P NMR. These derivatizations form trimethyl phosphite-carboxylic acid adduct along with *o*-quinone and coniferaldehyde adducts. The chemical shifts of these adducts appeared at the same spectral region. The adsorption intensity of the carboxylic acid adduct is highly dependent on the degree of ionization of the acid group. Thus, based on this information, *o*-quinone group content is quantified by preventing trimethyl phosphite-carboxylic acid adduct formation. Similar approach is used for semi-quantitative determination of quinonoid in isolated lignin (Argyropoulos et al., 1992; Argyropoulos and Zhang, 1998). Initially, 1,3,2-dioxaphospholanyl chloride (I) has been used as a phosphitylating agent (Argyropoulos, 1994; Argyropoulos et al., 1993) for the quantification. Later, 2-chloro-4,4,5,5-tetramethyl-1,3,2-dioxaphospholane (TMDP) has been used for a better signal separation, also with cyclohexanol as an internal standard. Accurate determination of uncondensed and condensed phenolic moieties in lignin have been determined (Granata and Argyropoulos, 1995).

Zawadzki and Ragauskas et al., found that TMDP/^{31}P NMR method occasionally overlaps the cyclohexanol-phosphite product with derivatized phenolic and aliphatic structures. Therefore, they employed a series of N-hydroxy compounds as alternative internal standards, namely N- hydroxy-phthalimide, 1-hydroxy-7-azabenzotriazole, endo-N-hydroxy-5-norbornene-2,3-dicarboximide and N-hydroxy-1,8-naphthalimide. The obtained results revealed that these compounds were suitable as internal standard and chemical shifts of phosphitylated N-hydroxy compounds are well separated from lignin-derived components (Zawadzki and Ragauskas, 2001).

Compared to acetylation, the phosphitylation reaction is faster, since the reagent is introduced directly in the NMR tube containing the lignin to be analysed. Although, a drawback of ^{31}P NMR is that the utilization of 2-chloro-4,4,5,5-tetramethyl-1,3,2-dioxaphospholane could slightly underestimate the hydroxyl group content due to incomplete derivatization compared to the data obtained by other analytical techniques applied to lignins (Berlin and Balakshin, 2014). Moreover, this *in-situ* reaction generates hydrochloric acid which could partly degrade lignin, and the resulting derivative is not stable so that the NMR acquisition should be done rapidly. Finally, the derivative may not be recovered for further studies.

1.5.1.5.4 ^{19}F NMR Spectroscopy

^{19}F NMR technique has been proposed to determine hydroxyl and carbonyl content. It has some peculiar properties such as the natural abundance of the ^{19}F nucleus which is 100% compared to 1.108% for ^{13}C, the high gyromagnetic ratio and a wide range of chemical shift. Sensitivity of ^{19}F nucleus is 59 times larger than ^{13}C. Moreover, ^{19}F nucleus exhibits low spin lattice relaxation time. Finally, the operating conditions are similar to that of ^{1}H NMR. All these factors sufficiently decrease the time and sample quantity needed for the analysis (Barrelle, 1993). The ^{19}F NMR spectroscopy has been applied for the quantitative determination of lignin phenolic and aliphatic hydroxyl groups (Barrelle, 1993), carbonyl (Sevillano et al., 2001) and carboxyl groups (Barrelle et al., 1992).

Hydroxyl group determination: Two decades ago Barrelle et al., developed lignin phenolic and aliphatic hydroxyl group determination by two main reactions such as fluorobenzylation and fluorobenzoylation, followed by ^{19}F NMR spectroscopy analysis (Barrelle, 1993). The authors synthesised a series of lignin model compounds and conducted fluoroderivatizations (esterification and etherification) along with guaiacol and p-hydroxyguaiacol. Phenolic hydroxyl groups were converted into fluorobenzyl ethers using fluorobenzylation. In the case of fluorobenzoylation, phenolic and aliphatic hydroxyl groups of model compounds were converted into fluorobenzoic acid esters. These reactions can be performed in several ways: i) with classical pyridine and 2- or 4-fluorobenzoic acid anhydride ii) fluoro-ester synthesis using phase transfer catalyst method (PTC) with 2- or 4- fluorobenzoyl chloride: a two-step reaction iii) fluoro-etherification of phenolic hydroxyl group through fluorobenzylation (4-fluorobenzyl chloride), followed by aliphatic hydroxyl group esterification using pyridine-carboxylic acid anhydride. The obtained fluoro containing derivatives were analysed by ^{19}F NMR spectroscopy. The ratio of (1) phenolic and aliphatic -OH groups content and (2) total number of hydroxyl groups have been calculated based on the quantitative internal standard.

The same fluoroderivatization procedure has been used on organosolv lignin and on exploded wood lignin (Barrelle et al., 1992). Phenolic hydroxyl groups in the organosolv lignin were etherified

using 4-fluorobenzyl chloride and the resulting derivative was treated with 4-fluorobenzoic acid anhydride. This reaction yields a combined 4-fluorobenzylated-4-fluorobenzoic acid alkyl derivative. The obtained ^{19}F NMR results were compared to ^{13}C NMR. Based on ^{19}F NMR, the author found the aliphatic-OH/ phenolic-OH groups ratio of organosolv lignin between 0.78 and 0.86. In addition, the total hydroxyl group content was 0.3 moles per 100 g lignin. It should be noted that this derivatization helps i) to distinguish the guaiacyl unit (G-lignin) from guaiacyl-syringyl (G-S) unit based on the difference in ^{19}F- chemical shift value of fluorobenzylated guaiacyl and fluorobenzylated syringyl; ii) to determine the ratio of syringyl/guaiacyl units; and iii) to approximate the determination of α-C=O content (Barrelle, 1995).

Carbonyl group determination: Glasser et al., reported the synthesis of lignin hydrazone derivatives using pentafluorophenylhydrazine as a reagent (Glasser et al., 1980). Later, the authors Lindner and Wegener applied this derivatization to quantify the amount of carbonyl group based on the nitrogen content of lignin pentafluorophenylhydrazone (Lindner and Wegener, 1988). Fernandes performed the carbonyl groups determination in several residual lignins from softwood unbleached and bleached pulps using fluorophenylhydrazine as derivatizing agent (Fernandes, 1992). Faix et al. has attempted to analyse pentafluorophenylhydrazone lignin derivative with the help of ^{19}F NMR, however this derivative shows rather complex ^{19}F NMR spectra due to non-equivalent fluorine atoms on the phenyl nucleus (Faix et al., 1998).

Ahvazi and Argyropoulos performed quantitative trifluoromethylation on lignin model compounds containing ketones, aldehydes and quinone carbonyl groups. The carbonyl groups were trifluoromethylated using (trifluoromethyl)trimethylsilane (TMS-CF_3) in the presence of tetramethylammonium fluoride (TMAF) followed by hydrolysis with aqueous HF (hydrogen fluoride). The obtained fluoroderivatives were analyzed using ^{19}F NMR and 3.3'-bis(trifluoromethyl)benzophenone used as an internal standard. ^{19}F NMR chemical shifts of trifluoromethyl groups vary significantly and consistently with different classes of carbonyl groups (Ahvazi and Argyropoulos, 1996a, 1996b; Ahvazi et al., 1999). Sevillano et al. performed the organosolv lignin carbonyl group quantification with different derivatization methods, called direct and indirect methods: i) lignin carbonyl groups were derivatized using trifluoromethylphenyl hydrazine – CF_3 method (direct method - Figure 1.29)

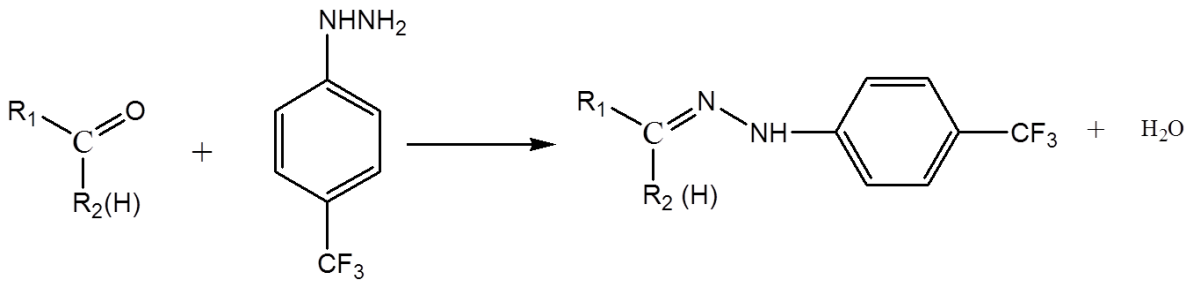

Figure 1.29. Reaction between carbonyl and trifluoromethyl phenyl hydrazine (CF_3 Method) for carbonyl group quantification in lignin

ii) in the case of indirect method, initially all lignin primary hydroxyl groups were fluorobenzylated using 4- fluorobenzyl chloride, then the part of the fluorobenzylated lignins were directly subjected to fluorobenzoylation by 4-fluorobenzoic anhydride. The carbonyl groups remain unchanged (non-reduced part) during the reaction, whereas the other part of the fluorobenzylated derivatives undergoes reduction with $NaBH_4$. This reaction converts carbonyl groups into secondary alcohol (reduced part) and is followed by fluorobenzoylation (Figure 1.30). The results showed that trifluoro compounds exhibit a better NMR sensitivity with no loss of spectral resolution compared to monofluoro compounds. Carbonyl content determination using CF_3 method followed by ^{19}F NMR has shown a good correlation with indirect methods and modified oximation method results (see Figure 1.28). CF_3 method produces reproducible results, it is easy to perform and it provides a clear and simple NMR spectra (Sevillano et al., 2001).

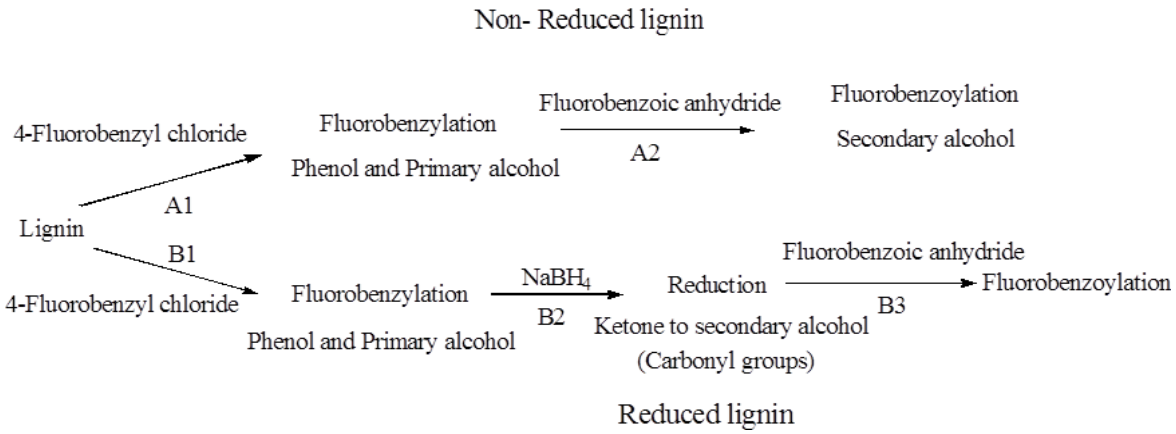

Figure 1.30. Reactions for carbonyl group determination using $NaBH_4$ reduction followed by fluorobenzoylation

More recently, Constant et al., studied the carbonyl group content in lignin and industrial humins using trifluoromethylphenylhydrazine derivatization. The reaction was performed directly in the NMR tube using ^{19}F NMR spectroscopy in a quantitative way. The results showed that the industrial humins, indulin Kraft lignin and Alcell lignin contain 6.6, 1.7 and 3.3 weight % of carbonyl functions, respectively. Aliphatic and conjugated carbonyl functions were also detected (Constant et al., 2017).

Table 1.4 summarizes various classical methods for phenolic hydroxyl group in lignin determination. It is clearly seen that numerous methods have been employed for lignin functional groups determination but each methods exhibit their own advantages and disadvantages (Faix et al., 1992).

Table 1.4. Summary of all known characterization methods to determine phenolic hydroxyl group of lignins, with the main advantages and disadvantages (Faix et al., 1992).

Method	Principle	Advantage	Disadvantage	References
periodate oxidation	MeOH arises from OMe in o-position to free phen. OH, GC of MeOH	requires only moderate number of analytical steps, reliable and simple performance	takes two days reaction time	Adler *et al.* (1958); Lai *et al.* (1990)
aminolysis of acetylated lignins	arom. AcO groups are more easily split in pyrrolidine than aliphatic; GC of Ac-pyrrolidine	reliable and reproducible results for lignins free of carbohydrates	laborious preparation and careful calibration work is necessary; time consuming; reducing end-groups of carbohydrates influence the results	Månsson (1983); Lai *et al.* (1990); Lindner (1989); Wegener & Strobel (1992)
diazomethane methylation	determination of OMe group increase after methylation	OMe determination is a very precise technique	diazomethane is poisonous; time consuming laborious technique; other groups than phen. OH can react with diazom.	Björkman & Persson (1957)
potentiometric or conductom. titration	titration with KOMe in DMF or LiOH in aceton	reproducible under similar conditions	carboxyl and enol groups also react with KOMe; unreliable for technical lignins; dependent from experimental conditions	Butler & Czepel (1956); Sarkanen & Schuerch (1955); Pobiner (1983)
UV spectrum in NaOH vs. the same sample in acidic solution	(1) at 250 nm (2) at 290 nm	UV spectrometer is a routine instrument everywhere available; a great body of literature	universal calibration not possible;solubility necessary; influence of C=O groups; results of (1) and (2) not congruent	Aulin-Erdtman (1954); Goldschmid (1954); Wexler (1964)
^{1}H-NMR of acetylated lignins	phen. OAc: 2.3 ppm aliph. OAc: 1.7 ppm	equipment is available in research institutes; gives additional information on aliph. OH groups	previous OMe determination required for internal calibration; solubility problems; limited accuracy due to overlapping signals	Lenz (1968); Ludwig (1971) Faix & Schweers (1974b)
^{13}C-NMR of acetylated lignins	aliph. OAc prim. OAc: 170.8 ppm sek. OAc: 170.0 ppm phen. OAc: 168.9 ppm	differentiation between prim. and sek. OH groups is possible, gives additional relevant information	see remarks about ^{1}H-NMR; time consuming; expensive research grade instruments are necessary; seldom used	Robert & Brunow (1984)
IR or FTIR of acetylated lignins	phen. OAc: 1765 cm^{-1} aliph. OAc: 1745 cm^{-1}	FTIR develops rapidly to a routine instrument; solubility is not required; rapid; low sample amount	heavily overlapping signals; difficult interlaboratory comparability because evaluation is not standardized	Hergert (1960, 1971); Faix (1987); Wegener & Strobel (1991)
DRIFT of non-acetylated lignins	multivariate calculation using the 1140, 1156, 1272 cm^{-1} bands	acetylation is not necessary	relation between the bands used and the phenolic OH group content is not obvious; interlaboratory comparison of DRIFT is difficult; results not yet confirmed by others	Schultz & Glasser (1986)
degradation of lignin, e.g.: – $KMnO_4$ oxid. – Thioacidolysis – Pyrolysis/GC	chem. or therm. degrad. to obtain low mol. products; then indirect conclusions to lignin		not a "real" phenolic OH group determination; can only be a rough estimation of the free and etherified arom. OH groups; time consuming	Gellerstedt & Gustafsson (1987); Gellerstedt *et al.* (1988); Lapierre & Rolando (1988); Whiting & Goring (1982)

1.5.2 Lignin molar mass distribution by Size Exclusion Chromatography (SEC)

Molar mass distribution of lignins (MMD) is a crucial characterization to understand fundamental properties of lignins such as their structure, physiochemical properties and reactivity for value-added applications (Pellinen and Salkinoja-Salonen, 1985a; Baumberger et al., 2007). For industrial

applications, substitution of petrochemical based aromatic compounds by lignin based compounds for polymer synthesis requires to know the exact molecular weight (El Mansouri and Salvadó, 2006). Size-exclusion chromatography (SEC – also referred as gel permeation chromatography, GPC, a variety of HPLC technique) is one of the preferred methods for MMD analysis of various polymers, also much referred for lignin analysis. SEC operates the separation of macromolecules by size at different elution time in a column filled with a nanoporous gel (stationary phase) and eluted with a solvent in which the polymer is totally dissolved. The solvent should be chosen carefully so that it fully swells and dissolves the polymer chains. Interactions between molecules, leading to molecular aggregates, and interactions between polymer and stationary phase, should be fully inhibited. If good conditions are attained, chromatographic separation occurs on the basis of the apparent hydrodynamic volume and shape of the molecules in the gel pores, which is linked to molecular diffusivities, rather than directly on the molecular masses (M). However hydrodynamic parameters and molar mass are well related when the density and shape of the dissolved macromolecules do not vary unpredictably with chain length, i.e. when the Mark-Houwink's law applies well and exhibits almost constant parameters (Chapter 5)

The classical SEC analysis uses the principle of standard calibration and requires the presence of only in-line concentration detectors, generally UV-visible spectrophotometer or differential refractometer (DRI). Dissolved monodisperse polymer standards are used to build a so-called "standard calibration curve" which relates linearly (log M) versus retention time (RT) – or elution volume (Vr) in the column. The unknown polymer sample mass is then calculated based on retention time. However, since no lignin standards are commercially available, other polymers like polystyrene standards are generally used, which makes quantification inaccurate. Another drawback of methods based on column retention time only is flow dispersion through columns and tubings, which enlarges the peaks. Mathematical corrections are possible to account for these phenomena, with again more or less accuracy.

To overcome these drawbacks, molar mass detectors have been added in-line, typically light-scattering (LS) detectors or viscometric detector (measure of the solution viscosity), developed during the last 40 years (illustrated in Figure 1.31).

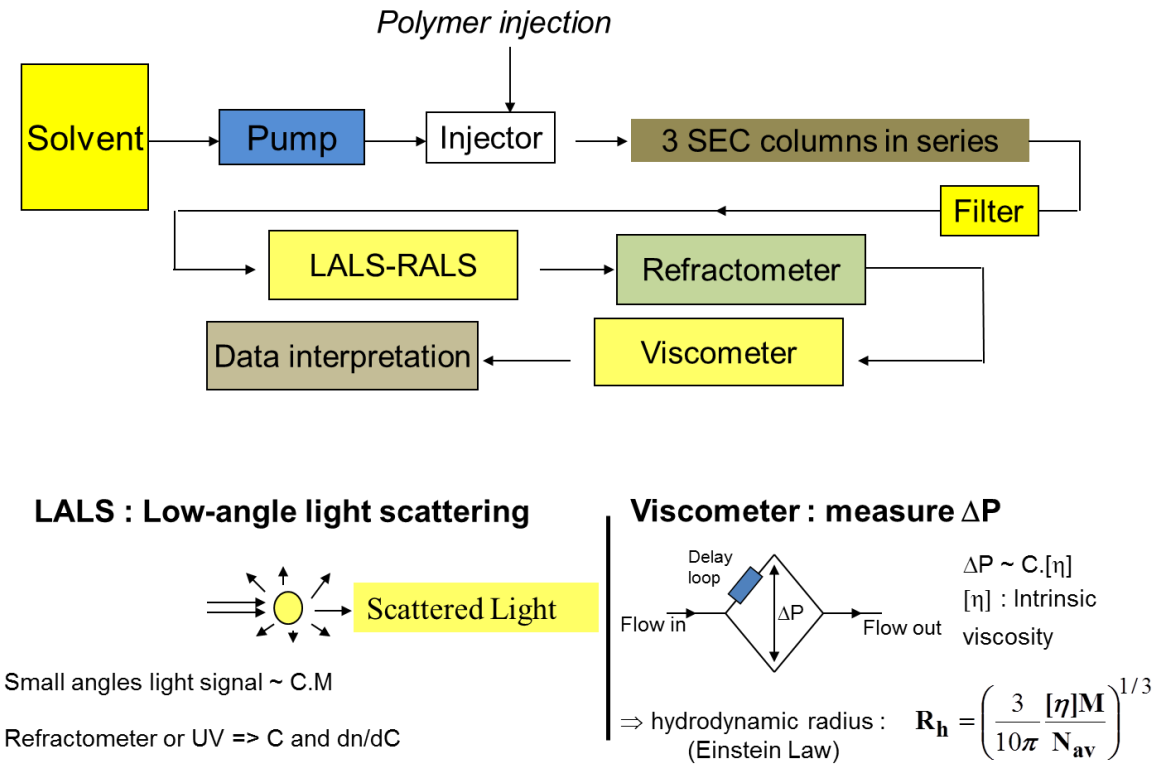

Figure 1.31. A schematic diagram of GPC setup for molar mass distribution study equipped with several detectors (equipment available at LGP2)

LS detectors, coupled to DRI, allow an exact quantification of the molar mass provided the refractive index (n) of the solvent and the refractive-index increment (dn/dC) of the polymer-solvent system are accurately known. This is generally not a difficulty, since the dn/dC can be easily determined by injecting a pure polymer sample (mono- or polydisperse) at known concentration and integrating the DRI signal. During this determination, the polymer should not be retained at all in the column.

Unfortunately, in the case of lignins, LS methods exhibit poor applicability in ordinary commercial SEC instruments, since they are restricted to non-light-absorbing, non-asymmetric and non-fluorescent molecules, which is not the case of lignin. However, recently, technical progress arose on classical instruments, with (1) the availability and easy placement of polarizers and fluorescent filters, and (2) the easy correction of light-absorption using the signal of one diode in a Multi-Angle Static Light Scattering (MALS) instrument (Wyatt Co.,).

Viscometry has also been proposed (Chum et al., 1987; Himmel et al., 1989) as another possible in-line detection for lignin analysis, using a differential viscosity detector (DV). Coupled to a concentration detector, it allows measuring the intrinsic viscosity of the polymer for the calculation of the molar mass by so-called “Universal Calibration” (Benoit et al., 1966). Universal Calibration is

based on the fact that the key parameter determining the retention time of macromolecules is the hydrodynamic volume (Vh) and not the molar mass. As Vh is proportional to the product of molar mass by the intrinsic viscosity, the measure of the viscosity by the in-line detector enables to get access accurately to the polymer molar mass. In this method, standard polymers of known mass M and intrinsic viscosity [η] (in fact the specific viscosity at low polymer concentration) are injected in the column, and the curve of Ln (M×[η]), i.e. Ln(Vh), versus RT is constructed, with the noticeable particularity that it should follow a unique straight line for different types of polymers. The straight line is called "universal calibration curve". This holds if the hydrodynamic principle of separation applies correctly. Then, measuring the RT and [η] value of an unknown polymer sample allows calculation of its molar mass. This will be investigated in this PhD work.

A frequent discrepancy occurring in SEC analysis is polymer association, which also occurs with lignin, due to polar interactions between the macromolecules and with the SEC system (Lindström, 1979, 1980; Sarkanen et al., 1981, 1982, 1984; Cathala et al., 2003; Connors et al., 1980; Norgren et al., 2002). Such behaviour increases LS and viscometric signals leading to the overestimation of the molar mass. Aggregate formation dominates in the case of underivatized lignins in a variety of solvents, including non-aqueous solvents (DMF, DMSO, THF) and water-NaOH. In non-aqueous solvents without the addition of electrolyte, the formation of association complex can exhibit as much as three order of magnitude higher molar mass than real values (Tolbert et al., 2014). In case of lignin-carbohydrate complexes, the elution properties of low molar mass carbohydrates in Sephadex G25/dioxane-water (1:1) and Sephadex LH 20/DMF were affected by the existence of aromatic groups in lignin-carbohydrate complexes, which causes retardation due to adsorption effects (Kristersson et al., 1983). Similarly, the adsorption forces between gel and lignin molecules, polarity and poor solubility issues leads to underestimation of molar masses (Chum et al., 1987). Lignin aggregates in DMSO or DMF can be avoided by improving solvation of the macromolecules and by forming H-bonds with electrolytes (Brown, 1967; Connors et al., 1980; Kristersson et al., 1983). The addition of LiCl to DMF decreases lignin aggregates and bimodal elution profile turned to a single peak (Connors et al., 2009). Similarly, Chum et al. (1987) used HPSEC because of its broad availability and capacity to provide a wide range of molar masses (200 to $3x10^6$ g mol^{-1}) in the case of acetylated alkali lignin, organosolv lignin and ball-milled lignin in styrene-divinyl benzene (SDVB) copolymer gels with DMF alone or DMF/LiBr as eluents. The result with DMF alone exhibited multimodal elution behaviour due to aggregation phenomena, whereas the addition of 0.1 M LiBr reduced lignin aggregates. Gosselink et al. studied the molar mass determination of Alcell™ Organosolv lignin using HPSEC with different organic solvents: DMF/LiCl 0.2 M, and THF. The obtained weight-average molar mass (Mw) was considerably lower in THF. It was concluded that HPSEC of lignin in organic solvents provides poorly comparable inter-laboratory results (Gosselink et

al., 2004). Previously, the same conclusion had been drawn by Milne et al. on different lignins analysed under identical standard conditions (Milne et al., 1992).

The early studies from Brown et al., and Faix et al., established that to decrease aggregates for SEC analysis due to the presence of polar hydroxyl groups, derivatization by various methods, typically acetylation, silylation and methylation was crucial (Brown, 1967; Faix et al., 1981).

Plant source, isolation method, functionality and molar mass distribution are determining factors for the solubility of lignin in chromatographic solvents. Moreover no universal GPC method is available for all types of lignins and in most cases, polystyrene gel with THF was used to calculate the more reliable molar mass distribution for different varieties of lignins (Faix, 1992)

The GPC columns are calibrated with narrow molar-mass distribution polystyrene standards and/or lignin model compounds in which the molar mass of these standards was determined by ultracentrifugation. In this method, the centrifugal field is used for measuring the sedimentation rate for the polymer. The molecular weight is calculated by Svedberg equation allowing for a sedimental coefficient and a diffusion coefficient (Umoren and Solomon, 2016). Siochi et al., performed hydroxypropylation of organosolv red oak lignin and determined the absolute molecular weight using GPC/LALLS and GPC/DV (differential viscosity detector). Using GPC/LALLS detector, organosolv red oak lignin Mw was found to be 11 500 g/mol whereas GPC/DV detector provides Mw value of 3 852g/mol. The obtained values with GPC/LALLS were three times higher than with GPC/DV. The authors proposed that the obtained results by GPC/LALLS were complicated because of the influence of sample absorbance and fluorescence, and the requirement of light polarisation correction. Thus the author proposed GPC/DV as more convenient and quite acceptable detector to study the absolute molar mass distribution of lignin (Siochi et al., 1990).

Glasser et al. also studied the absolute molecular weight distribution of hardwood, softwood and annual plant lignins produced through Kraft and Organosolv pulping processes using GPC with a differential viscosity detector and applying universal calibration with polystyrene standards. The results illustrated that the investigated lignins (Indulin AT, Indulin, Eucalin, ORG lignin, Alcell lignin, bagasse) exhibited Mw values between 3 000 and 20 000, polydispersity values between 2 and 12, Mark-Houwink exponential factors (α) value in the range of 0.17 and 0.35 and intrinsic viscosities between 37 and 8 $mL.g^{-1}$(Glasser et al., 1993).

Cathala et al. stated that DMF is known for lignin aggregation phenomena in SEC. To investigate this effect the author chose milled wood lignin (MWL) from spruce and guaiacyl lignin synthetic polymers (dehydrogenation polymers - DHP) as models for MMD study in SEC – DMF solvent using LS detector. The results showed that bimodal elution profile occurred due to association effects

between the macromolecules. To account for this, the authors fractionated lignin samples in THF and stated that THF-soluble fractions are responsible for low molar mass part and THF-insoluble fractions were responsible for higher molar mass corresponding to DMF elution profile. The different molar mass fractions were acetylated to break the association effect and characterized by SEC in THF and THF-LiBr, combined with online viscometric detection and universal calibration. The authors showed that Mark-Houwink plot of polymers exhibited low α values, which evidences that polymers matrixes are collapsed in THF and THF-LiBr. These results revealed that THF and THF-LiBr solvents are not suited for acetylated samples dissolution. Moreover, the authors concluded that MWL and DHP molar mass in DMF was overestimated, with values higher than 50 000-60 000, due to aggregation (Cathala et al., 2003).

Collaborative study of SEC analysis of technical lignins has been performed in the frame of the Eurolignin network to standardize the SEC chromatography methods. The authors performed acetylation using 1:2 v/v of pyridine/acetic anhydride stirring at room temperature for 6 days prior to the SEC analysis in THF system and styrene-divinylbenzene column was used for the analysis. The authors studied SEC of acetylated bagasse soda lignin without and with removal of insoluble fractions in the acetylation mixture. They reported that removal of insoluble fraction led to a lower proportion of higher molar mass fractions (Baumberger et al., 2007).

HPSEC is commonly operated using styrene-divinylbenzene columns and the results are referred to polystyrene calibration, although unprecise for lignin and lignin derivatives. Moreover, during the analysis, unclear association effects of non-polar lignin still exists even after derivatization. (Pellinen and Salkinoja-Salonen, 1985a). Incomplete lignin solubility in chromatographic solvents is also an important source of error to investigate lignin molar mass. Once again, derivatization partially overcomes such a difficulty and acetylation is most often used (Baumberger et al., 2007; Hatfield et al., 1999). The latter studies have shown that using long reaction time, over 6 days, more than 90% dissolution in THF can be achieved; although with same duration, Asikkala et al. reached only about 60% solubility in THF for Norway spruce milled-wood lignin (Asikkala et al., 2012). These authors developed a “universal derivatization” using acetylbromide in glacial acetic acid to obtain complete dissolution in 0.5 h in THF. However possible depolymerisation might occur since the derivatized sample degradation is apparent after one month of aging at room temperature.

As already cited, polystyrene is the most often used standard although its linear structure differs much from that of lignin. Lignin-like model compounds have been used for calibration and the obtained Mw values were 2 to 3 times higher than with polystyrene calibration (Faix and Beinhoff, 1992). DRI, LALS and RALS coupled detectors were used to measure the molar mass of acetylated lignin samples in THF, although with some difficulties linked to imperfect solubilization. In another

study, lignins fractions were separated by preparative GPC, reaching dispersity near to one, and such fractions were compared to polystyrene standards. Lignin fractions and polystyrene standards exhibited similar behavior over a wide range of molecular weight (Botaro and Curvelo, 2009).

Viscometry and other techniques, like MALDI-TOF-MS (matrix-assisted laser desorption ionization time-of-flight mass spectrometry) have been reported in several studies to measure absolute mass values. MMD by universal calibration was carried out on acetylated and hydroxypropylated lignins in THF (Himmel et al., 1989; Siochi et al., 1990; Cathala et al., 2003; Gosselink et al., 2004; Glasser et al., 1993). SEC with off-line MALDI-TOF-MS was originally proposed by Jacobs and Dahlman (Jacobs, 2000; Jacobs and Dahlman, 2001; Rönnols et al., 2016) and later also studied by Gosselink (Gosselink, 2011). However, MALTI-TOF is limited because the matrix plays a major role in desorption/ionization process. As an example, the analysis of pole(ethylene)glycol shows two different fragmentation pattern in 2,5-dihydroxybenzoicacid and dithranol matrixes (Wetzel et al., 2003).

To summarize, despite the number of studies and techniques investigated until now, there is still a certain level of uncertainty about real lignin molar mass values, and about the choice of which reliable method should be preferably used. There is still room for improvement, as illustrated by the very recent work of C. Crestini's group (Lange et al., 2016). The authors studied the molar mass distributions of different derivatized lignins (acetobromination, acetylation and benzoylation) with particular column setup and standard data treatment. The results showed that the effect of column setup and detector type significantly influenced the quality of GPC results.

1.6 Conclusion

Due to its complex nature, lignin analysis is difficult. However, to develop new ways of adding values, lignin characterization, i.e. functional groups and molar mass determination, is a key issue. Today lignin functional groups are classically quantified using tedious and costly methods, mainly NMR spectroscopy-based methods, which require lignin derivatization and an access to NMR equipment. As far as molar mass analysis is concerned, SEC is the reference method but it still suffers from limitations. Macromolecule association and aggregation in the SEC system are major concerns for polar chromatographic solvents (DMF), the presence of hydroxyl groups in lignin leads to poor solubility in the non-polar chromatographic solvent (THF) and polystyrene polymers used as calibrants do not provide accurate molecular weight. To overcome these issues, electrolyte in the polar solvent is often added and lignin derivatization (mainly acetylation) prior to non-polar solvents is carried out.

To further improve lignin analysis, this thesis work proposed:

(1) To develop a new fast method for lignin functional group analysis, the objective being to facilitate the lignin analysis for lignin suppliers, without the need of costly equipment.
(2) To investigate a new lignin derivatization reaction for lignin SEC analysis enhancement. The objectives are to increase lignin dissolution and reduce aggregation in the SEC system, and also to use the universal calibration instead of standard calibration with polystyrene polymers. For that purpose, lignin fluorobenzylation, previously developed for lignin functional groups quantification by ^{19}F NMR, has been studied.

Chapter 3 will present the new fast method developed for lignin functional groups determination, whereas chapter 4 and 5 are devoted to lignin fluorobenzylation study and SEC analysis.

Before presenting the result chapter, chapter 2 will detail all the materials and methods used in the PhD work.

CHAPTER 2

2 Materials and Methods

This chapter provides the detailed information on the materials and methods used in this thesis.

In the material section, different technical lignins and model compounds are presented. The model compounds are chosen according to the nature of functional groups and their position, to elucidate the reactivity toward different derivatization and to assign NMR signals for lignin samples characterization. After, the different derivatization methods (acetylation, fluorobenzylation and fluorobenzoylation) applied in the PhD work are described with main operating conditions. Then the different analytical methods, UV, FT-IR, GC, NMRs (^{1}H NMR, ^{13}C NMR, ^{19}F and ^{31}P NMR) and fast method (conductometric and potentiometric) used for quantifying the number of phenolic hydroxyl groups, carboxyl groups and carbonyl groups present in the lignin samples are presented. Finally, SEC methods (in DMAc/LiCl and THF) carried out for the study of lignin molar mass distribution, using conventional and universal calibration are explained.

2.1 Materials

2.1.1 Technical lignins

2.1.1.1 Commercial lignin samples

Four industrial lignin samples have been used in this study: (i) Soda lignin from wheat straw (Protobind 1000) (PB) was purchased from Green Value Enterprises LLC, (ii) Kraft lignin from pine (KL) was provided by the Centre Technique du Papier (CTP) (Grenoble, France), (iii) Organosolv lignin (ORG) (namely BioLignin® CIMV process using formic acid/acetic acid/water at 185-210ºC) from wheat straw was purchased from CIMV Company, and (iv) Kraft Indulin AT lignin (IND) was purchased from DKSH Switzerland Ltd (Serrano et al., 2018).

2.1.1.2 Eucalyptus Kraft lignin preparation at lab scale

A hardwood Kraft lignin from Eucalyptus has been also extracted at laboratory scale; the extraction operating conditions are described in the following paragraph. Eucalyptus chips were cooked using Kraft pulping process. 3 batches of 1200 g of wood chips were cooked using technical grade Na_2S and NaOH solutions. Effective and active alkalis were respectively 25 and 30% of NaOH on wood. Sulfidity was adjusted to 30% and the liquor on wood ratio was 8. Dry matter content of wood chips was measured as 87.4%. Cooking conditions used were heat up time of 40 min from 20˚C to 165˚C followed by plateau time of 80 min at 165˚C. After completion of cooking, 9.5 L of black liquor were extracted and transferred to the CTP (Centre Technique du Papier) Grenoble, France, where the lignin was recovered using CO_2 precipitation method followed by washing with diluted sulfuric acid. Around 100 g of Eucalyptus cooked Kraft lignin were obtained from 4 L of black liquor. Kappa number of the pulp was found to be 12.4% and the measured pulp yield was 50.0%.

2.1.2 Lignin like model compounds

2.1.2.1 Lignin-like model compounds for the study of hydroxyl group quantification

5 lignin model compounds, commercially available were used: Vanillin (CAS: 121-33-5), Acetovanillone (CAS: 498-02-2), Guaiacol (CAS: 90-05-1), Vanillyl alcohol (CAS: 498-00-0) and Veratryl alcohol (CAS: 93-03-8), as well as one model of cellulose: Cellobiose (CAS: 528-50-7). All model compounds were purchased from Sigma-Aldrich.

2.1.2.2 Lignin-like model compounds for the study of carbonyl group quantification

Lignin model compounds used for carbonyl group quantification are listed in Table 2.1, Table 2.2, and Table 2.3 below, and are referenced according to Figure 2.1, Figure 2.2 and Figure 2.3.

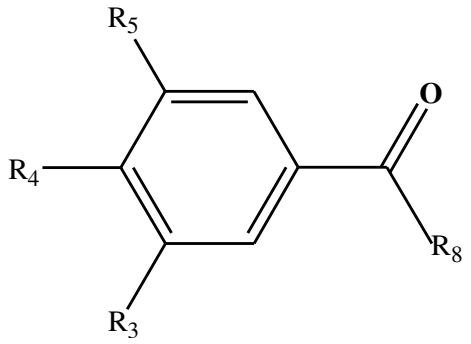

Figure 2.1. Lignin model compounds owing α-position carbonyl

Table 2.1. List of lignin model compounds containing α-position carbonyl group

Compound n°	R_3	R_4	R_5	R_8	Name	CAS No
1	OMe	OH	H	H-	4-Hydroxy-3-methoxy benzaldehyde	121-33-5
2	OMe	OH	OMe	H-	4-Hydroxy-3,5-dimethoxybenzaldehyde	134-96-3
3	OMe	OMe	OMe	H-	3,4,5-Trimethoxybenzaldehyde	86-81-7
4	H	OH	H	Me-	4-Hydroxyacetophenone	99-93-4
5	OMe	OH	OMe	Me-	4-Hydroxy-3,5-dimethoxyacetophenone	2478-38-8
6	H	H	H	Me(C=O)Et-	1-Phenyl-1,4-pentanedione	583-05-1
7	H	H	H	PhEt-	1,3-Diphenyl-1-propaneone	1083-30-3
8	H	OH	H	PhCH=CH-	Benzylidene-(4-Hydroxyacetophenone)	2657-25-2
9	H	OMe	H	PhCH=CH-	Benzylidene-(4-Methoxyacetophenone)	959-23-9
10	OMe	OMe	H	2-(OMe)PhOCH(CH_2OH)-	1-(3,4-Dimethoxy-phenyl)-3-hydroxyl-2-(2-methoxy-phenoxy)-propan-1-one	10548-77-3
11	OMe	OH	H	2-(OMe)PhOC(Me)(CH_2OH)-	3-hydroxy-1-(4-hydroxy-3-methoxyphenyl)-2-(2-methoxyphenoxy)propan-1-one	22317-34-6

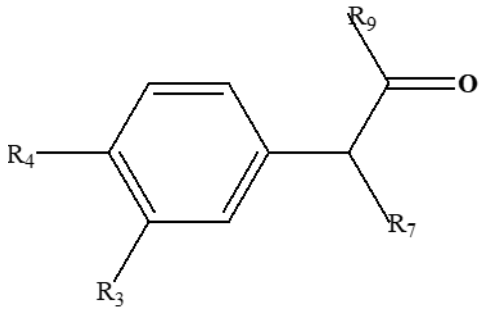

Figure 2.2. Lignin model compounds owing β-position carbonyl

Table 2.2. List of model compounds containing β-position carbonyl group

Compounds n°	R_3	R_4	R_7	R_9	Name	CAS No
12	H	H	H_2	H-	Phenylacetaldehyde	122-78-1
13	H	OMe	H_2	Me-	4-Methoxypheylacetone	122-84-9
14	H	H	Me	H-	2-Phenylpropionaldehyde	93-53-8
15	H	H	H_2	iPr-	3-Methyl-1-phenyl-2-butanone	2893-05-2
16	OCH_2O	OCH_2O	H_2	Et-	1-(3,4-Methylenedioxy)-phenyl-2-butanone	23023-13-4

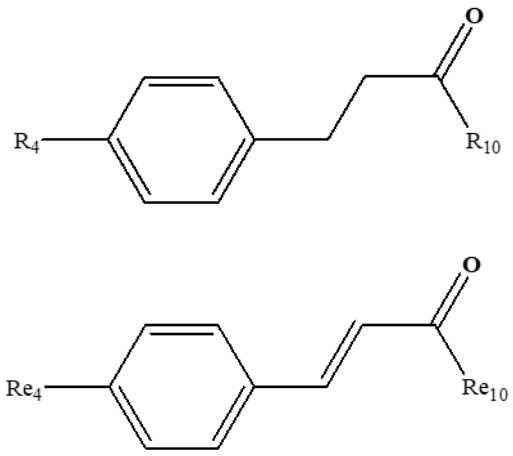

Figure 2.3. Lignin model compounds owing γ-position carbonyl

Table 2.3. List of lignin model compounds containing γ-position carbonyl group

Compounds n°	R_4	R_{e4}	R_{10}	R_{e10}	Name	CAS No
17	OMe		Me-		4-(4-Methoxyphenyl)-2-butanone	104-20-1
18	OH		Me-		Hydroxy-phenyl-2-butanone	5471-51-2
19	H		H		3-Phenylpropionaldehyde	104-53-0
20	OH		2,4,6-$(OH)_3$Ph-		2',4',6'-Trihydroxy-3-(4-hydroxyphenyl)propiophenone	60-82-2
21	OCH_2O		Me		3,4-Methylenedioxybenzylacetone	55418-52-5
22		OH		Me	4-Hydroxybenzylideneacetone	3160-35-8
23		OMe		H	4-Methoxycinnamaldehyde	1963-36-6
24		OCH_2O		Me	3,4-(Methylenedioxy)benzylideneacetone	3160-37-0
25		OMe		Ph-	4-Methoxybenzylideneacetophenone	959-23-9
26		OH		Ph-	4-Hydroxybenzylideneacetophenone	20426-12-4
27		OMe		4-(OMe)Ph-	4,4'-Dimethoxybenzylideneacetophenone	2373-89-9
28		OMe		Ph_2-	3-(4-Methoxyphenyl)-1-(2-Naphtyl)-prop-2-en-1-one	22359-67-7

2.1.3 Chemicals used

In reaction:

Tetrabutylammonium hydroxide $(CH_3CH_2CH_2CH_2)_4N(OH)$ (CAS: 2052-49-5), 1M in methanol, *noticed **NBu** in the discussion*, 4-fluorobenzyl chloride $FC_6H_4CH_2Cl$ (CAS: 352-11-4), *noticed **FBC** in the discussion*, lithium chloride LiCl (CAS: 7447-41-8), 4-Trifluoromethylphenylhydrazine CF3PH (CAS: 368-90-1), H3PO4 orthophophorinc acid(7664-38-2), 4-methylbenzotrifluoride (MBTF) (CAS: 6140-17-6) , 1-methyl naphthalene CAS (90-12-0), chromium (III) acetylacetonate, hydroxybenzoic acid (CAS: 21679-31-2), cholesterol (CAS: 57-88-5), 2-chloro-4,4,5,5-tetramethyl-1,3,2-dioxaphospholane (TMDP) (CAS: 14812-59-0) were purchased from Sigma-Aldrich.

Acetonitrile CH_3CN 99.95% (CAS: 75-05-8), ethyl acetate $CH_3COOC_2H_5$ 99.5%, (CAS: 141-78-6), *noticed **EtOA**c in the discussion,* sodium sulphate Na_2SO_4 99% (CAS: 7757-82-6) and diethyl ether 99.5% $(CH_3CH_2)_2O$ (CAS: 60-29-7), methanol CH_3OH (CAS: 67-56-1), Pyridine C_5H_5N (CAS:

110-86-1), acetic anhydride $(CH_3CO)_2O$ (CAS: 108-24-7) were purchased from Roth and sodium chloride NaCl (CAS: 7647-14-5) and HPLC grade tetrahydrofuran $(CH_2)_4O$ (CAS: 109-99-9), *noticed **THF** in the discussion*, was obtained from Acros.

Toluene C_7H_8 (CAS: 108-88-3) from Chimie-plus. 4-dimethyl –aminopyridine $C_7H_{10}N_2$ (CAS:1122-58-3) from Lancaster and 4-fluorobenzoic acid anhydride $C_{14}H_8F_2O_3$ (CAS: 25569-77-1) from Alfa-Aesar. Dimethylacetamide $CH_3C(O)N(CH_3)_2$ from HPLC grade (CAS: 129-19-5), *noticed **DMAc** in the discussion* and Dimethylsulfoxide DMSO purity ≥99.9% (CAS: 67-68-5) were purchased from Roth. Dimethylformamide DMF (CAS: 68-12-2) from Sigma-Aldrich.

For SEC calibration, narrow polymer standards were used: polymethyl methacrylates (PMMA: 1520, 6840, 13200, 31380, 73850, 135300, 342700, 525000, 1026000, 2095000) were purchased from Agilent and polystyrenes (PS: 1670, 4970, 10030, 28400, 64200) from Polymer Laboratories Ltd. A broad polymer standard was also used: cellulose acetate (CAS: 9004-35-7) from Aldrich.

2.2 Methods

2.2.1 Chemical Composition of technical lignins

All the lignin samples were analysed in terms of chemical composition

2.2.1.1 Dry matter content of lignin

Dry matter content was gravimetrically determined by drying samples at 105 °C to constant weight in an oven.

2.2.1.2 Ashes determination in lignin

The ashes content of all the lignin samples was obtained gravimetrically after in-furnace calcination for 4 h at 525 °C.

2.2.1.3 Sugar determination

The lignin sample is treated with sulfuric acid using the Klason method (TAPPI standard T-13). During the acid hydrolysis, all sugars pass into the liquid phase with the acid soluble lignin fraction which is measured by spectrophotometry at 205 nm (TAPPI UM250 um-83). Monosaccharides were quantified after the injection of 25 µL the Klason filtrate in high performance anion exchange chromatography (HPAEC) with pulsed amperometric detection (PAD) (HAUSALO, 1985). Sugars were eluted on a Dionex Carbopac PA1 column (4 mm x 250 mm) using a 2 mM of potassium hydroxide solution at a flow rate of 1 mL/min. Fucose was used as internal standard to calculate the sugars concentration (Cateto et al., 2008).

2.2.2 Lignin washing with solvents

The main motivation of solvent washing study is to find the suitable solvent for removing impurities from the crude lignin samples. In this case, the PB1000 lignin was chosen for this study. 1g of oven dried PB1000 lignin was washed using approximately 60 mL of different solvents (ethanol, ethyl acetate and hexane) (16.5g/L). The washing is carried out in two steps: initially, 30 mL of corresponding solvents were poured into the lignin sample and the mixture was stirred during about 1 hour, followed by vacuum filtrations through a 0.45 µm PTFE membrane. The recovered lignin sample was added again into 30 mL of pure solvent and stirred for 24 hours and second filtration was carried out. The filtered lignins were dried using vacuum-oven at 40°C. Based on the obtained results, ethylacetate (EtOAc) solvent removed impurities and preserve the lignin compare to other solvents and therefore it was selected for rest of the study.

2.2.3 Lignin and Model Compounds Derivatization

Prior to derivatization, all technical lignins are washed with EtOAc. The following paragraph give the operating conditions of the derivatization reactions applied on the washed lignin samples

2.2.3.1 Acetylation

100 mg of lignin sample (according to the dry matter content) were acetylated (Figure 2.4) with 5 ml of pyridine and acetic anhydride mixture (1/1: V/V) at room temperature for 15 h in a round bottom flask with continuous magnet stirring. After the reaction time, the mixture was quenched with 40 ml of 50% aqueous methanol and dried under vacuum. After methanol evaporation, the product was washed with toluene three times (3 x 40ml) to remove residual pyridine and once with 40 ml of 99.5% methanol. Finally, the samples were freeze dried to ensure total solvent removal. Acetylated lignin samples were used, first to develop the aminolysis reaction, and second, for quantitative ^{13}C-NMR analysis.

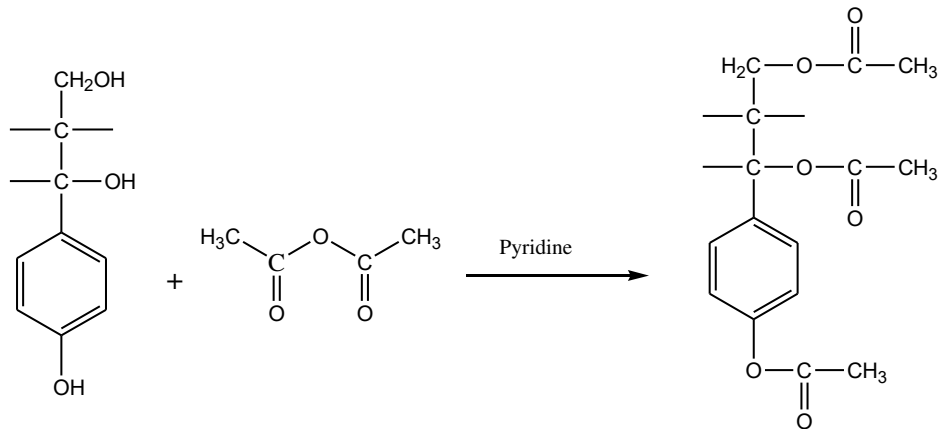

Figure 2.4. Lignin acetylation reaction

2.2.3.2 Fluorobenzylation and fluorobenzoylation

2.2.3.2.1 Fluorobenzylation of model compounds

100 mg of model compound were dissolved in 1 mL of NBu (tetra N-butylammonium hydroxide in 1M methanol) solution and stirred for 1h at 50°C. Then 10 mL of acetonitrile were added followed by 300 mg of 4-fluorobenzyl chloride (FBC), the derivatizing agent. The reaction mixture was stirred at 50°C for overnight. After, distilled water (30 mL) and EtOAc (30 mL) were finally added to the reaction mixture. The aqueous layer was separated and extracted with EtOAc (2×30mL). The combined EtOAc layer was washed with distilled water (2×30 mL) and with saturated sodium chloride solution (30 mL). The extracted EtOAc layer was dried with sodium sulfate, then filtered, evaporated and analyzed without any further purification.

2.2.3.2.2 Fluorobenzylation of the lignin

Lignin fluorobenzylation was performed using the same experimental conditions as for the model compounds and the reaction scheme is shown in Figure 2.5. Then the derivatized lignin recovery was performed by precipitation in diethyl ether. This organic part forms a viscous precipitate, precipitated again in ice cold distilled water. This precipitate was filtered through a 0.45 µm PTFE filter, washed with distilled water several times and oven dried at 50˚C (Barrelle et al., 1992; Barrelle, 1995).

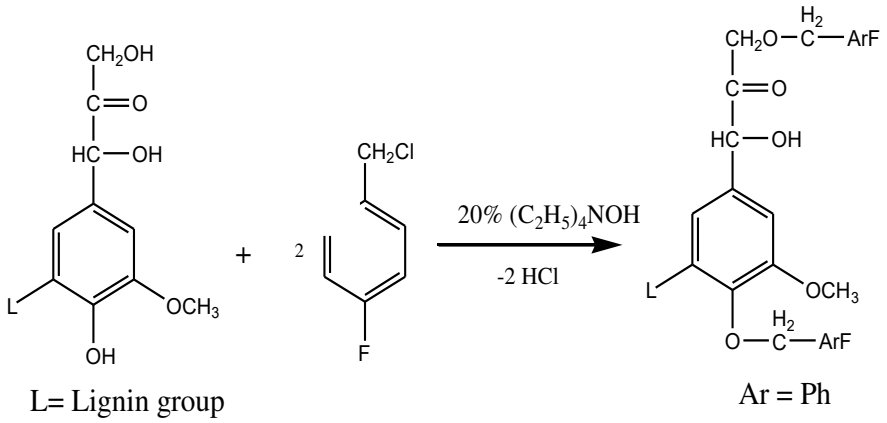

Figure 2.5. Fluorobenzylation of lignin using 4-benzylchloride

2.2.3.2.3 Fluorobenzoylation of the lignin

Fluorobenzylated lignins (100 mg) were dissolved in 2.5 mL of pyridine. After, 2.5 mg of 4-dimethyl-aminopyridine (DMAP) and 150 mg of 4-fluorobenzoic acid anhydride were progressively added into the reaction medium. The mixture was stirred for 48 h at 60˚C. Then derivatized lignins were poured into ice cold water. The obtained precipitate is washed with distilled water several times

and filtered through a 0.45µm PTFE filters and dried in the oven at 40°C. The reaction scheme is given in figure 2.5.

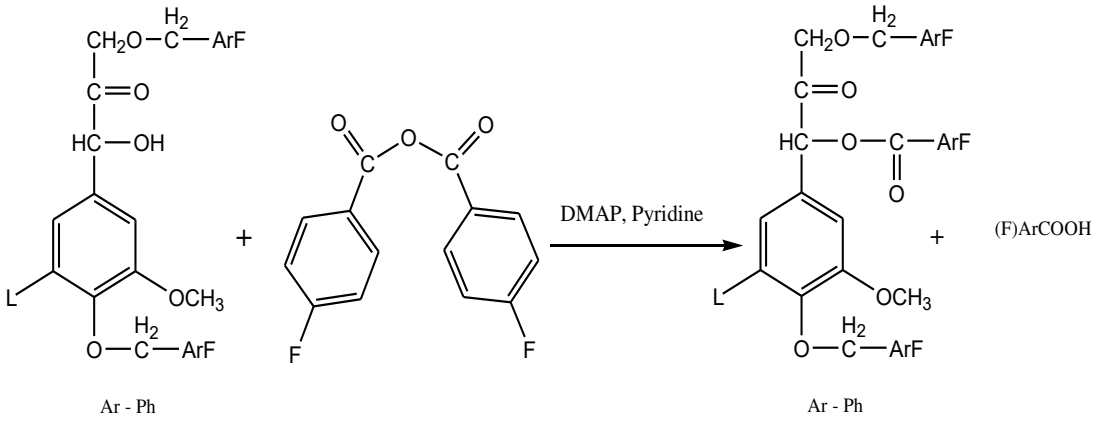

Figure 2.6. Fluorobenzoylation on fluorobenzylated lignin

2.2.3.3 Derivatization with trifluorometylphenylhydrazine

This reaction is applied for lignin carbonyl group quantification.

2.2.3.3.1 Model compounds derivatization

Lignin model compound's phenyl hydrazine derivatization reaction (Figure 2.7) was carried in the following conditions: carbonyl model compounds / CF_3PH ratio = 1M / 1M concentration. 50 mg of model compound was first solubilized in 1 mL DMSO-d6, followed by the addition of the CF_3PH (trifluoromethyl phenylhydrazine) reagent, and by 2 drops of phosphoric acid (for the kinetics study in acidic medium, see annexure A). For the kinetics study, after the acid addition, ^{19}F and ^{13}C NMR spectra were registered regularly to control the rate of hydrazone formation. When the derivatization has been completed, ^{1}H, ^{13}C and 2D NMR analyses have be performed to assign all signals belonging to the resulting hydrazones.

2.2.3.3.2 Lignin derivatization

Lignin carbonyl groups were quantified using a conventional method and the "in-situ NMR kinetics method". The operating conditions of both methods are described in the following paragraphs.

Conventional method: 100 mg of lignin (PB lignin in the presented work) were dissolved in 4 mL DMSO and 4 drops of orthophosphoric acid (H_3PO_4) were added, followed by 120 mg of 4-trifluoromethylphenylhydrazine (CF_3PH). The reactional mixture was stirred at room temperature for 48 hours. After the reaction time, reaction mixture was concentrated through solvent evaporation method and precipitated in a large quantity of cold distilled water. The precipitate was washed several

times with cold water to remove the excess of reagent, and then dried in an oven at 40˚C for 24 hours. The schematic derivatization reaction is presented in Figure 2.7.

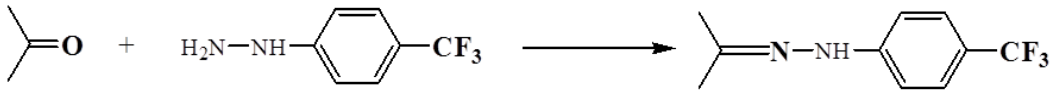

Figure 2.7. 4-trifluoromethylphenylhydrazine derivatization applied on carbonyl containing molécules

In-situ reaction kinetics: *In-situ* phenyl hydrazine derivatization kinetics of lignin (PB lignin in the presented work) has been studied inside the 5 mm NMR tube, based on the different conditions mentioned in the literature (Sevillano et al., 2001; Constant et al., 2017). Samples were prepared with reagents ratios indicated in Table 2.4. Initially, the lignin sample and the internal standard, the 4-methylbenzotrifluoride (MBTF), were dissolved in DMSO-d6 (0.7 mL). After dissolution, the reagents CF_3PH and H_3PO_4 (if necessary) were added and the reaction kinetics started to be recorded.

Table 2.4. Different kinetic conditions investigated for phenyl hydrazine derivatization

Conditions		**1** **This work**	**2** **Sevilano (2001)**	**3** **Constant (2017)**
Reagents	Lignin	100 mg	100 mg	100 mg
	reagent 4-trifluoromethylphenyl-hydrazine (CF_3PH)	120 mg	150 mg	93 mg
	internal standard 4-methylbenzotrifluoride (4-MBTF)	10 mg	10 mg	10 mg
	ortho phosphoric acid (H_3PO_4)	2 drops	-	-
Reaction temperature		25 ºC	25 ºC	40 ºC
Reaction duration (hours)		48	24	24

2.2.4 Analytical techniques for lignin phenolic hydroxyl group quantification

2.2.4.1 UV method

UV method works based on the wavelength shift between ionized and protonated phenolic hydroxyl groups in lignin. The absorbance intensities in the ionization differences is related to the phenolic hydroxyl groups content. In our case, the region of two maxima between 300 and 350 nm was chosen to calculate the ionization difference in UV spectrum (Tiainen et al., 1999).

20 mg of lignin sample were dissolved in a mixture of 10 mL dioxane and 10 mL 0.2 M aqueous NaOH solution. The solution was filtered through a 0.45 µm nylon filter to remove possible undissolved particles. 4 mL of the lignin solution were diluted to 50 mL in three different aqueous solutions (0.2 M NaOH solution, buffer pH 6 and buffer pH 12) to reach a final concentration in lignin of 0.08 g/L.

The UV measurements were carried out with a Shimadzu UV-1800 in the range 200-600 nm using the lignin solution in buffer pH 6 as reference. The absorbance of the maxima observed at 300 nm and 350 nm were used for the determination. The total phenolic hydroxyl group content per gram of lignin was calculated according to the Equation 2.1 (Tamminen and Hortling, 1999).

$$\text{Total OH phenolic content (mmol/g)} = \{0.425 \times A_{300nm}\,(NaOH) + 0.182 \times A_{350nm}\,(NaOH)\} \times a$$

Equation 2.1

where, A_{300nm} = absorbance at 300 nm, A_{350nm} = absorbance at 350 nm, a ($L \cdot g^{-1} \cdot cm^{-1}$) = correction term = $1/(c \cdot l) \cdot 10/17$, c (g/L) = lignin solution concentration and l (cm) = path length.

2.2.4.2 Aminolysis after lignin acetylation using gas chromatography

Internal standard calibration: To find the retention time of acetyl pyrrolidine and to make the calibration curve, commercially available acetyl pyrrolidine was purchased and injected with internal standard (1-methyl naphthalene). Internal standard and 1-acetyl pyrrolidine in dioxane were prepared at a concentration of 10 mg/mL. Three different mixtures such as 1:2, 1:1 and 2:1 in mL of internal standard and acetylpyrrolidine were prepared. 0.5 µL of these mixtures were injected into the GC to determine the calibration constant k value which is discussed in the following paragraph. The GC curve was calibrated with internal standard and the results were shown in Figure 2.8.

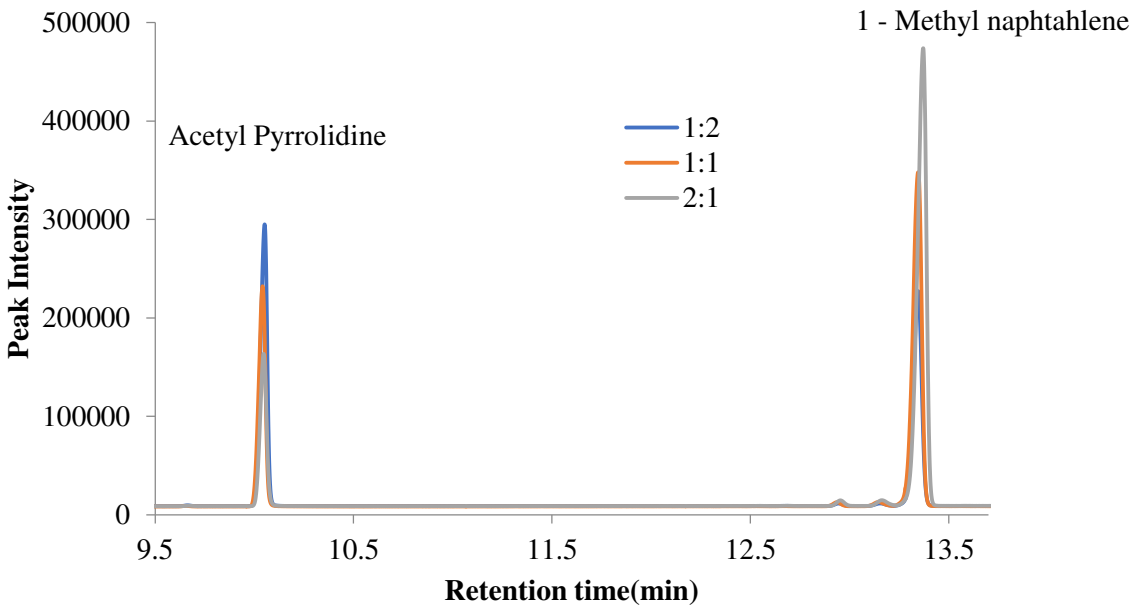

Figure 2.8. GC chromatogram obtained for acetyl pyrrolidine and internal standard (1-methyl naphthalene)

The calibration constant k was calculated according to the following equation,

$$k = \frac{A_a \times W_s}{A_s \times W_a} \qquad \text{Equation 2.2}$$

Where, Aa = chromatographic area of the product (1-acetyl pyrrolidine), As = chromatographic area of the internal standard, Wa = weight of product (mg), and Ws = weight of internal standard (mg).

From the above equation, the calibration constant k value was found to be 0.517787.

Aminolysis: Aminolysis consists of a two-step reaction, acetylation followed by aminolysis. 100 mg of acetylated lignin (acetylation described in Chapter 2) was dissolved in 5 mL dioxane containing 25 mg of internal standard (1-methyl naphthalene). To initiate the aminolysis reaction, 5mL of dioxane-pyrrolidine (1/1: v/v) reactant mixture was added at room temperature. The rate of 1-acetyl pyrrolidine formation was followed by periodically (for instances: 5, 10, 20, up to 60 minutes) injections of 0.5 µL reaction mixture into the gas chromatography equipment. 1-acetyl pyrrolidine formation is equivalent to the total phenolic-OH content. A GC-Trace (ThermoQuest) gas chromatograph was used with a flame ionization detector, helium as carrier gas, and a DB-5 capillary

column (30 m length, 320 µm internals diameter, 1 µm film thickness). The formation of 1-acetyl pyrrolidine content has been calculated according to the Equation 2.3.

$$\text{The formation of acetylpyrrolidine } (mmol/g \text{ lignin}) = \frac{A \times W_s \times 1000}{A_s \times W_L \times k \times 113} \quad \text{Equation 2.3}$$

where, A = chromatographic area corresponding to the 1-acetyl pyrrolidine signal, As = chromatographic area corresponding to the internal standard signal, W_L = weight of lignin (dry matter), W_S = weight of internal standard (1-methyl naphthalene) and k = calibration constant (obtained from a calibration curve). The obtained results have been plotted between the formation of acetylpyrrolidine Vs retention time. The content of phenolic hydroxyl groups was calculated by extrapolating the linear region to the zero time, as described by Dence and Lin, 1992 (Dence and Lin, 1992).

2.2.4.3 ^{13}C NMR analysis of acetylated lignin samples

350 mg of acetylated lignin was dissolved in 4 mL of DMSO-d6 with a further addition of 0.42 mL of relaxation agent, chromium (III) acetylacetonate in DMSO-d6 (50 mg/mL). The samples were stirred a long time to ensure complete dissolution and then transferred into a 10 mm NMR tube for spectrum recording. The NMR conditions are given in the paragraph devoted to NMR analysis conditions.

2.2.4.4 Conductometric and potentiometric titration – Fast method

A rapid method in aqueous medium based on simultaneous conductometric and acidic-base titration by pH was developed to determine the amount of phenolic hydroxyl groups in lignins. At the same time, this method is able to provide the carboxyl content. The operating conditions of the methods are described in the next section.

A solution made of 1 g of lignin, 500 mL of fresh deionized water, free of carbonates, and 8 mL of sodium hydroxide (NaOH) 1M (large excess) was prepared. After being stirred until total dissolution (around 15 min for most of the studied lignin samples), the solution was titrated back with 1M hydrochloric acid (HCl) using a Schott automatic burette. Simultaneous measurements of conductivity and pH were recorded with a Crison pH GLP 21 equipment. During titration, the titration vase was protected from air by a plastic film, to prevent sodium hydroxide carbonation by atmospheric CO_2.

2.2.5 Non-aqueous potentiometric titration method for carboxyl group determination

Carboxyl groups in lignin could be quantified using a non-aqueous potentiometric titration method with tetra-n-butylammonium hydroxide (TnBAH method) as titrating chemical (Lin and Dence,

1992). 175 mg of lignin and 25 mg of hydroxybenzoic acid are dissolved in 30 mL of DMF with constant agitation during 5 minutes. After lignin dissolution, the solution is titrated using TnBAH 0.05M in isopropanol under N_2 flow. Two inflection points appear during the titration, the first point corresponds to the carboxyl content and the second to the total weak acids, carboxyl and phenolic groups (COOH + ArOH).

2.2.6 NMR Analysis conditions

2.2.6.1 NMR analysis conditions for lignin phenolic hydroxyl groups quantification

NMR spectroscopic measurements were conducted on a Bruker AVANCE400 spectrometer equipped with a 5 mm BB/^{19}F-^{1}H/d Z-GRD probe and 10 mm probe for ^{13}C operating at 100.612 MHz, 161.982 MHz for ^{31}P and 400.130 MHz for ^{1}H. Acquisition and data treatment were done using the LINUX TopSpin 3.2 software. Different types of NMR analyses were applied for determining phenol group content. They are explained in the following sections.

2.2.6.1.1 ^{31}P-NMR

The experiments were conducted at 298 K, with 3.37 s acquisition time, 10 s relaxation delay and a 60° pulse using a 30 ppm spectral width. Proton broad band decoupling was applied only during acquisition time. 16k data points were used for data acquisition. Prior to Fourier transformation, zero-filling at 64k was applied, followed by apodization with a 1 Hz exponential. Chemical shifts are given relative to phosphoric acid (δ = 0 ppm). 30 mg of lignin was dissolved in 0.3 mL mixture of pyridine and deuterated chloroform (1.6/1, v/v). 0.5 mL of DMF was added with 0.1 mL of cholesterol solution (43 mg/mL) as internal standard and 0.1 mL of chromium (III) acetylacetonate solution (5 mg/mL) as relaxation reagent. Finally, 0.1 mL of 2-chloro-4,4,5,5-tetramethyl-1,3,2- dioxaphospholane (TMDP phosphitylation agent) is added to the mixture and vigorously stirred before the transfer into a 5 mm NMR tube for recording the spectrum. The used solvents were stored during several days over 4 Å molecular sieves.

2.2.6.1.2 ^{13}C-NMR

The experiments were conducted in deuterated solvent like DMSO-d6 at 323 K, with 1.1 s acquisition time, 2.0 s relaxation delay and a 60° pulse using a 25000 Hz spectral width. Proton broad band decoupling was applied only during acquisition time. 16k data points were used for data acquisition on a spectral width of 240 ppm for ^{13}C. Prior to Fourier transformation, zero-filling at 64k was applied, followed by apodization with a 10 Hz exponential. Chemical shifts are given relative to

TMS (tetramethylsilane, δ = 0 ppm). The positions of the peaks were referred to DMSO-d6 signal at 39.5 ppm.

2.2.6.1.3 ^{1}H-NMR

The experiments were conducted at 298 K, with 3.4 s acquisition time, 4.6 s relaxation delay and a 30° pulse using a 15 ppm spectral width. 32k data points were used for data acquisition. Prior to Fourier transformation, zero-filling at 64k was applied, followed by apodization with a 0.3 Hz exponential. Chemical shifts are given relative to TMS (tetramethylsilane, δ = 0 ppm). The positions of the peaks were referred with the two singlets for DMF as internal reference at 2.6 and 2.9 ppm. 10 mg of lignin was dissolved in 0.8 ml of deuterated solvent DMSO-d6 and 1 µL of DMF-d1. The samples were left overnight with the 4 Å molecular sieves. The sample was transferred into a 5 mm NMR tube and the spectrum was recorded. Thereafter 20% D_2O (by volume) was added and a new spectrum was recorded.

2.2.6.2 NMR analysis conditions for model compounds and sample preparation

2.2.6.2.1 ^{19}F NMR

The Bruker *invgate* sequence was used. The experiments were conducted with 1.25 s acquisition time, 8.76 s relaxation delay and a 30° pulse using a 65 ppm spectral width. 64k data points for model compounds were used for data acquisition. Prior to Fourier transformation, zero-filling at 64k was applied, followed by apodization with a 0.3 Hz exponential. Chemical shifts are given relative to $CFCl_3$ (δ = 0 ppm). The positions of the peaks were referred for C_6F_6 as internal reference at -164.90 ppm.

For OH quantification, the experiments were conducted at 298 K, with 4.35 s acquisition time, 8.76 s relaxation delay and a 30° pulse using a 20 ppm spectral width. 64k data points were used for data acquisition. Quantification and chemical shifts of peaks were referenced with 2-Fluoroacetophenone as internal reference at -112.86 ppm.

Lignin model compound derivatives were dissolved in deuterated solvent DMSO-d6 (40-50 mg/0.7 mL) using C_6F_6 as a reference (-164.90 ppm / $CFCl_3$). Lignin derivatives were dissolved in DMSO-d6 (15-20 mg/0.7 mL) and quantification was done using 2-Fluoroacetophenone (3 mg) as internal standard. The measurements were performed at 298 K. Chromium acetylacetonate was used as relaxation agent.

2.2.6.2.2 ^{13}C NMR

Analysis were performed on derivatized model compounds only (same tubes were used for ^{19}F and ^{13}C experiments), at 298K, using the Bruker *invgate* sequence. The experiments were conducted with 0.648 s acquisition time, 20 s relaxation delay and a 45° pulse using a 250 ppm spectral width. Proton broad band decoupling was applied only during acquisition time. 32 k data points were used for data acquisition. Prior to Fourier transformation, zero-filling at 64 k was applied, followed by apodization with a 2 Hz exponential. Chemical shifts are given relative to TMS (tetramethylsilane, $\delta = 0$ ppm). The positions of the peaks were referred to DMSO signal at 39.5 ppm.

2.2.6.2.3 ^{13}C DEPT

The Bruker *dept* sequence was used. The experiments were conducted with 0.648 s acquisition time, 3.0 s relaxation delay, a last pulse at 135° to select CH_2 carbons reversed compared to CH and CH_3, optimized for a 145 Hz coupling constant.

2.2.7 Lignin molar mass distribution analyses by Size Exclusion Chromatography (SEC)

SEC analysis is indispensable in order to predict the molar mass of lignin to valorize it in a wide range of applications. Due to their large variety of functional groups, lignins exhibit a high polarity character leading to solubility issues in the SEC analysis. The following sections present the SEC systems used (equipment, columns, operating conditions and solvents) in order to study the molar mass distribution of lignin, as well as the different calibration methods (conventional and universal) applied.

2.2.7.1 SEC in the DMAc/LiCl system

SEC analysis in DMAc was carried out using an OMNISEC system equipped with 2 polargel M column (30 cm x 7 mm) and one pre-column (Agilent Co). Columns were purchased from Agilent. 0.5% of DMAc/LiCl (5g of LiCl dissolved in 1L of DMAc) was used as eluent with a flow rate of 1 mL/min and the column temperature was set at 70°C. DRI (Differential Refractive Index) was used as detector. DMAc/LiCl system only standard conventional calibration curve was made using PS standard. 100 µL of all the PS standards and lignin samples were injected at a concentration of 2 mg in 1 mL of 0.5% DMAc/LiCl. The solutions are obtained as follows: 20 mg of underivatized lignin samples were dissolved in 10 mL of 0.5% DMAc/LiCl during 3 weeks under continuous agitation. For derivatized lignins, 10 mg of lignin samples were dissolved in 5 mL of 0.5% DMAc/LiCl during 5 days under continuous agitation. All stirred samples were filtrated (0.45 µm PTFE syringe filter) before analysis.

2.2.7.2 SEC in the THF system

SEC analysis in THF system was carried out using a Malvern TDA 302 system equipped with three 300×7.5mm Agilent PLGel mixed B (10 µm mixed B LS) columns and one pre-column (Agilent co). RALS-LALS and in-line viscometer detectors at 35°C were used. THF system universal calibration was made with the help of in line viscometric detector attached to the SEC and also the results were compared with individual conventional calibration. For the standard calibration of the columns, solutions of PS, PMMA and cellulose acetate polymer standards were prepared (0.4 mg/L to 1.6 mg/mL in THF). Lignin samples were prepared at the concentration of 10 mg/mL THF. 100µL of samples and standards were injected into the SEC equipment with a flow-rate of 1 mL/min. Before injection, sample dissolution was carried out in pure THF for 1 hour. The resulting solution was then filtered through a 0.45 µm PTFE syringe filter.

In parallel of standard calibration, universal calibration was investigated. It used polystyrene (PS), polymethylmethacrelate (PMMA) and cellulose acetate standards.

Universal calibration: A universal calibration curve was constructed with the concept of Mark-Houwink relationship. This concept was first tested on polystyrene polymers by Benoit et al. (Benoit et al., 1966) and stated that samples were eluted based on their hydrodynamic volume V_h, which determines the elution volume.

Mark- Houwink relationship

$$[\eta] = K'M^a$$

$[\eta]$ is the intrinsic viscosity of the polymer in dL/g

K' and *a* are Mark-Houwink constants, depending on the couple polymer/solvent

M is the molar mass of the polymer in g/mol

Based on the above equation, samples with same $[\eta]$ and same molar mass (M) possess same hydrodynamic volume. Thus, samples are eluted at same retention time. The obtained results were used to plot the universal calibration curve between log ([η].M) Vs retention time. In our case, to construct the universal calibration curve THF system equipped with in line viscometric detector was used, it provides the intrinsic viscosity of the polymer. The detailed calibration study is presented in the Chapter 5.

2.2.8 Lignin and lignin derivatives study by FT-IR

The Fourier Transform Infrared spectra for underivatized and derivatized lignin samples were recorded on a Perkin Elmer spectrometer with absorbance mode using KBr pellets. Spectra were recorded between 400 to 4000 cm^{-1} with 32 cumulative scans and 4 cm^{-1} resolution.

2.2.9 UV- Solubility study on lignin

To analyze the solubility of the fluorobenzylated and acetylated lignins in THF, UV spectrophotometry was used. The analysis was carried out on a UV-1800 SHIMADZU UV spectrophotometer between 190 nm to 750 nm. The maximum absorbance was observed at 280 nm. Un-derivatized and derivatized lignins were dissolved in THF (5mg/mL). After 1h of dissolution time, the solutions were filtered using a 0.45 µm PTFE filter to remove insoluble particles. Then the filtrate was diluted up to 25 mL using THF before UV analysis.

2.2.10 HPLC analysis of lignin model compound

Underivatized and derivatized lignin model compounds were analyzed by HPLC to verify the disappearance of the un-derivatized compound (original model compound) signal after the derivatization reaction. The measurements were performed on a HPLC system with a spectra physics 1500 Pump instrument using ALLTIMA C18 10U (250 mm × 4.6 mm) column and a UV-visible 6000 spectra detector at 280nm. A mixture of acidified water (0.1% acetic acid in water) and acetonitrile 90%/10% V/V was used as eluent with 0.6 mL/min flow rate and oven temperature set at 50˚C. 10µL of lignin model compounds and fluorobenzylated lignin model compounds solutions (0.5mg in 50mL of acetonitrile) were injected. Prior to the analysis, samples were filtered through a 0.45µm PTFE filter.

CHAPTER 3

3. Lignin Phenolic hydroxyl groups quantification using the aminolysis method and comparison with other methods

3.1. Introduction

Hydroxyl groups and in particular phenolic hydroxyls are the locus of many possible reactions. They are key functions for new lignin applications. Thus, this chapter is dedicated to quantifying the number of phenolic hydroxyl groups present in different technical lignins. This can be done using various quantification methods, directly on lignin or after lignin derivatization. The purpose of this chapter was to study the aminolysis method. In that case, the hydroxyl groups on lignin are acetylated and subsequent selective aminolysis is followed by GC-FID analysis. The obtained results are compared with those from other characterizations, using different techniques, done in the frame of another project (QUALIN project, Institut Carnot Polynat) carried out at LGP2 (Serrano et al., 2018).

3.2. Commercial lignin samples used for phenolic hydroxyl group quantification

Four industrial lignin samples were used in this study: (i) Soda lignin from wheat straw (Protobind 1000) (PB) was purchased from Green Value Enterprises LLC, (ii) Kraft lignin from pine (KL) was provided by the Centre Technique du Papier (CTP) (Grenoble, France), (iii) Organosolv lignin (ORG) (namely BioLignin® CIMV process using formic acid/acetic acid/water at 105-110ºC) from wheat straw was purchased from CIMV Company, and (iv) Kraft Indulin AT lignin (IND) was purchased from DKSH Switzerland Ltd.

3.3. Chemical composition of the lignin samples

The chemical composition of the different technical lignins is given in Table 3.1. Lignin purity was around 90% and ash and sugar contents were varying according to the lignin nature, in particular according to the extraction process. Organosolv lignin exhibited the highest sugar content due to the lighter extraction process using low temperature and weak acids. KF and IND, both from softwood Kraft cooking, exhibited the lowest xylose content and the highest galactose content. Indulin lignin showed highest ash content; it could be due to minerals used for its recovery and pine Kraft lignin extracted at CTP showed lighter ash content due to three successive washes using 2% sulfuric acid in order to remove the impurities.

Table 3.1. Chemical composition of the technical lignins, in %

Components (% w/w)	PB-Protobind lignin	ORG-Organosolv lignin	KF-Kraft lignin from pine	IND-Indulin lignin
Total lignin	92.4	89.2	93.7	95.7
Acid insoluble lignin	89.5 ± 1.2	87.8 ± 1.2	92.8 ± 0.3	94.7 ± 0.4
Acid soluble lignin	2.9 ± 0.2	1.4 ± 0.1	0.9 ± 0.2	1.0 ± 0.1
Total sugars	3.1 ± 0.2	7.2 ± 0.3	2.5 ± 0.1	2.6 ± 0.2
Glucose	1.0	4.3	0.2	0.3
Galactose	0.2	0.8	1.6	1.3
Xylose	1.5	1.3	0.2	0.5
Mannose	-	0.2	-	-
Arabinose	0.4	0.6	0.5	0.5
Ash	1.6 ± 0.1	1.2 ± 0.1	0.3 ± 0.1	2.9 ± 0.3

3.4. Quantification of lignin phenolic hydroxyl groups

3.4.1. Aminolysis method

Several studies have been carried out to determine phenolic hydroxyl group present in various lignins. Among the existing methods, aminolysis is one of the prevalent for researchers because of consistent results and reproducibility (Månsson, 1982; El Mansouri and Salvadó, 2007). This method relies on a two-steps reaction, in which all the hydroxyl groups in lignin are acetylated in the first step

and then, the acetylated lignin undergoes aminolysis using pyrrolidine and regenerates the phenolic hydroxyl group by producing 1-acetylpyrrolidine and the aliphatic acetates remains unchanged. The typical reaction scheme is illustrated in Figure 3.1.

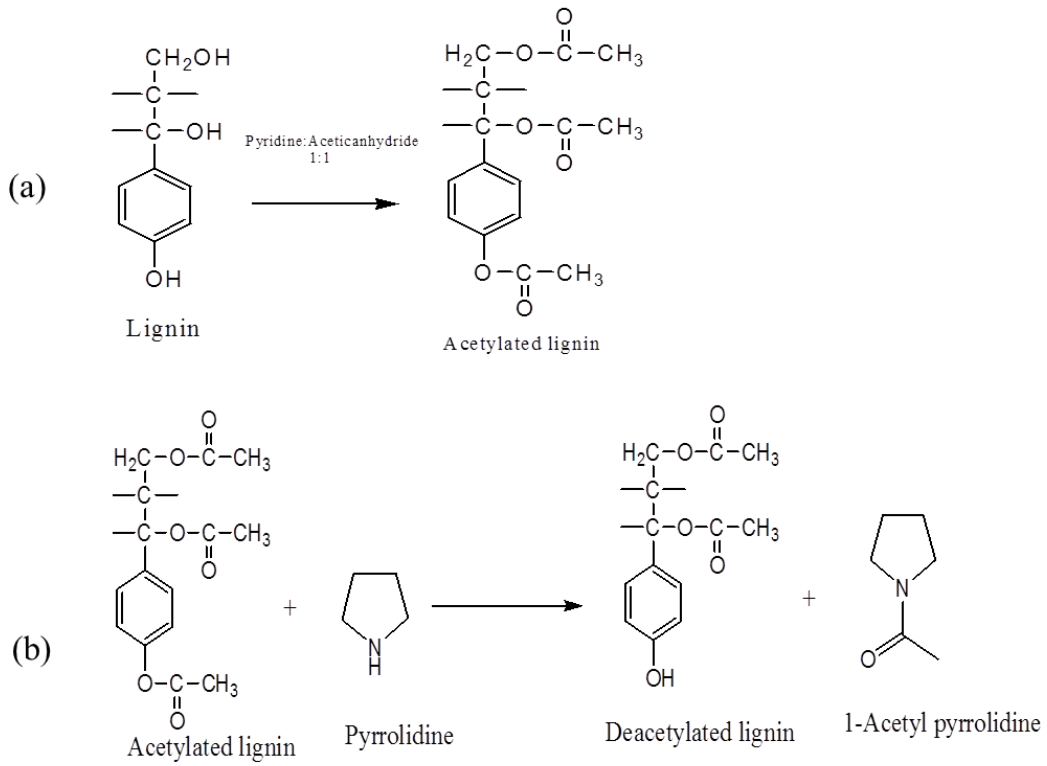

Figure 3.1. (a) Acetylation of lignin – first step (b) Aminolysis of acetylated lignin – second step.

The lignin phenolic hydroxyl groups are thus deduced from the quantification of 1-acetylpyrrolidine using gas chromatography (GC) and a flame-ionization detector (FID).

3.4.2. Aminolysis followed by GC

The GC analyses have been performed for determining the rate of the aminolysis reaction for all investigated lignins. During aminolysis, the rate of deacetylation of phenolic hydroxyl groups is significantly faster than that of aliphatic hydroxyl group in presence of pyrrolidine under mild conditions (Månsson, 1983). Therefore, the formation of acetyl-pyrrolidine corresponds to the amount of aromatic acetyl groups initially present in the lignin. The resulting acetyl-pyrrolidine (the byproduct) formation was analyzed by GC-FID. However, it should be noted that there is a possibility that some aliphatic acetyl groups undergo deacetylation at a prolonged reaction time, leading to overestimated hydroxyl group values.

First, the PB lignin sample was analyzed after different reaction times. The GC chromatograms obtained are gathered in Figure 3.2. It is clearly seen that the acetyl-pyrrolidine formation (area under the signal) increased with the reaction time during the first 20 minutes. After that duration, the quantity of acetyl pyrrolidine stabilizes meaning that deacetylation is completed. Moreover, at 5 min reaction time, the retention time of the product is 10.16 minutes. After, the acetyl pyrrolidine formation increases, and it is eluted at slightly lower retention time: for instance, at 20 min, the elution time found was 10.08 min; similar trend was observed with the higher reaction times.

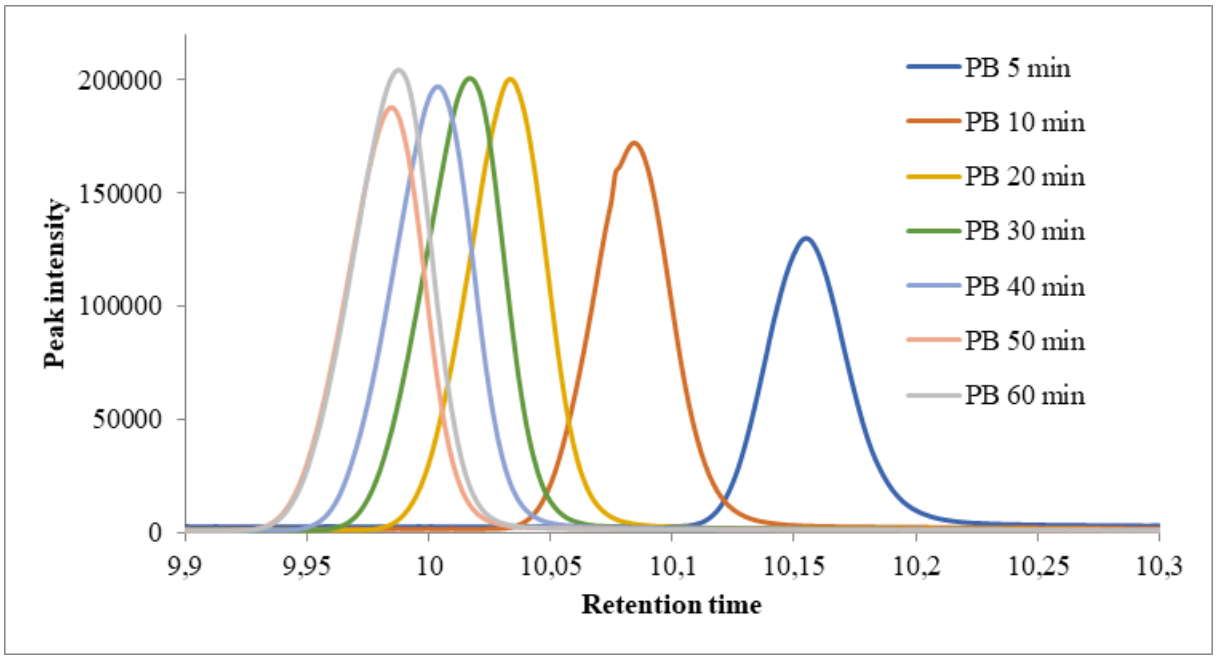

Figure 3.2. GC chromatogram of 1- acetyl pyrrolidine formation during PB1000 lignin de-acetylation

A similar trend was also observed for the ORG lignin sample. The results are given in Figure 3.3. After 5 min of acetyl-pyrrolidine formation, i.e. 5 minutes of reaction, the acetyl-pyrrolidine signal is obtained at 9.98 min of retention time. Again, the quantity of acetyl-pyrrolidine was increasing with reaction time before stabilization after 30 min when deacetylation is completed. However, in this case, the rate of formation of acetyl-pyrrolidine is increased slowly after 5 minutes, whereas in the case of PB lignin (Figure 3.2), the significant difference was obtained between 5 and 10 min. After 12 min of acetyl pyrrolidine production, the variation of retention time is lower. It is also seen from the Figure 3.3 that signal at 50 min has a smaller area compared to 60 min and 43 min and the reason of this variation could be raised from a deficient injection in the GC at this particular reaction time.

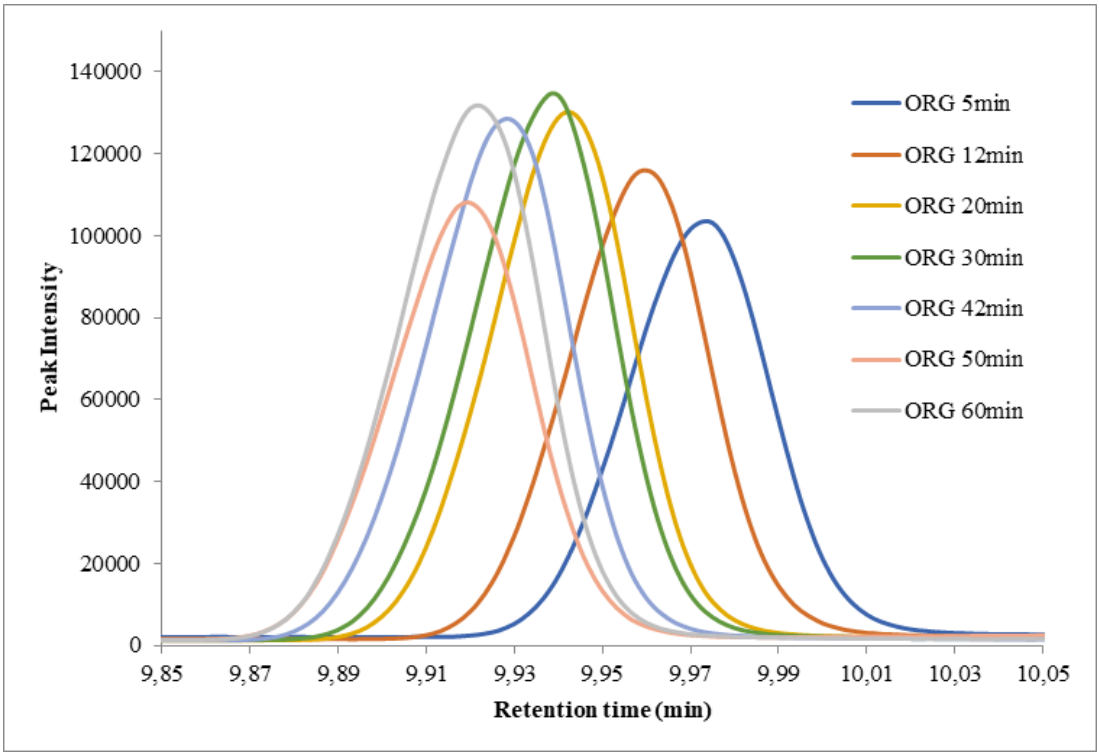

Figure 3.3. GC chromatogram of 1- acetyl pyrrolidine formation during the Organosolv lignin (ORG) de-acetylation

Figure 3.4 presents the GC chromatograms of 1-acetyl pyrrolidine formation during the Kraft lignin de-acetylation. Similar to other lignin samples, Kraft lignin de-acetylation leads to the same behavior. It is interesting to compare the signal area of 1- acetyl pyrrolidine from Figure 3.2, Figure 3.3 and Figure 3.4. Among the tested lignin samples, Kraft lignin leads to the highest signal area. Then PB lignin comes after, followed by ORG lignin. Because the quantity of 1- acetyl pyrrolidine product is proportional to the phenolic hydroxyl content in lignin, it can be concluded that Kraft lignin contains the highest quantity of phenolic hydroxyls. The calculation of phenolic hydroxyl groups is presented in the following section.

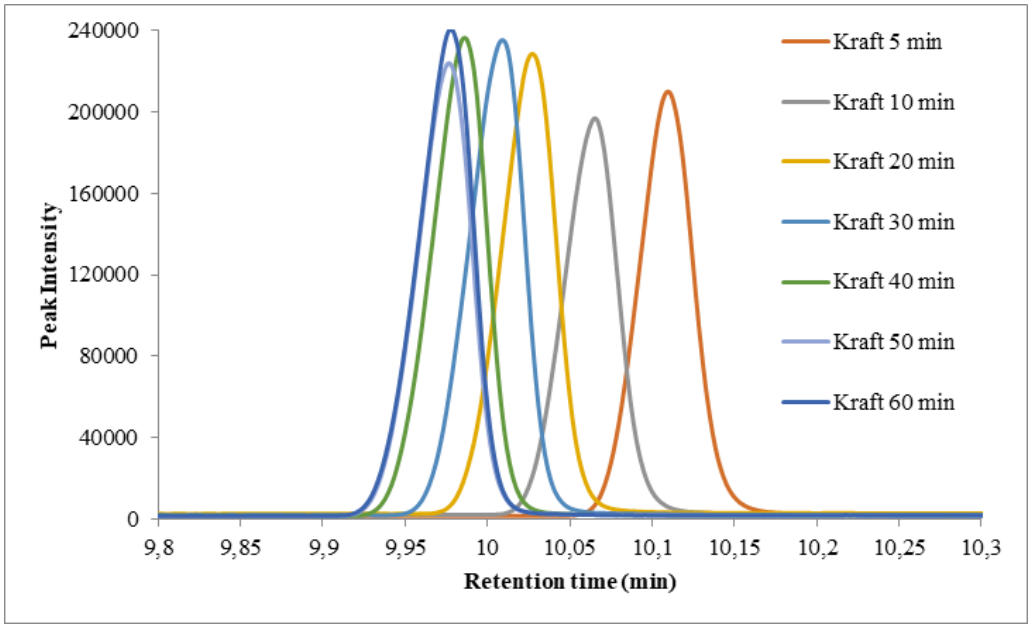

Figure 3.4. GC chromatogram of 1- acetyl pyrrolidine formation during Kraft lignin de-acetylation

The similar GC chromatogram trend is observed for Indulin lignin (chromatogram is not shown here, the aminolysis results are exhibited in Figure 3.5)

Amount (mmol) of acetyl pyrrolidine formation was calculated from the amount of initial lignin and the area obtained from GC chromatogram after aminolysis using the following relation,

$$\text{The formation of acetylpyrrolidine } (mmol/g \text{ lignin}) = \frac{A \times W_s \times 1000}{A_s \times W_L \times k \times 113} \quad \text{Equation 3.1}$$

where A = chromatographic area of the signal corresponding to 1-acetyl pyrrolidine and its retention time obtained at 10 min, As = chromatographic area of the signal corresponding to the internal standard (1-methyl naphthalene) and its retention time found at 13.4 min , L = weight of lignin in mg, W_S = weight of internal standard in mg, 113 = molecular weight of acetyl pyrrolidine (g/mole), k = calibration constant and the detailed procedure for the calculation of k value can be found in the materials and methods chapter (CHAPTER 2)

During aminolysis reaction, the samples were collected at different reaction time and injected into the GC. Figure 3.5 represents the acetyl pyrrolidine formation at different reaction times for all the examined lignin samples. It is clearly seen that within the 5 first minutes of reaction, the acetyl pyrrolidine formation is rapidly increasing. It is continuously rising till 20 min and from 20 to 60 min the acetyl pyrrolidine formation is relatively stable. Moreover, as already seen, Kraft lignin exhibits

higher acetyl pyrrolidine formation than PB, Indulin and ORG lignin samples. Most of the lignins, after 20 min, reach a constant plateau; this clearly demonstrates that the phenolic acetates were de-acetylated during this phase by the aminolysis process. The content of the 1-acetyl pyrrolidine formed was calculated by extrapolating the linear region from 20 to 60 min at zero time (Dence and Lin, 1992). The corresponding value is directly proportional to the phenolic hydroxyl groups present in the lignin samples.

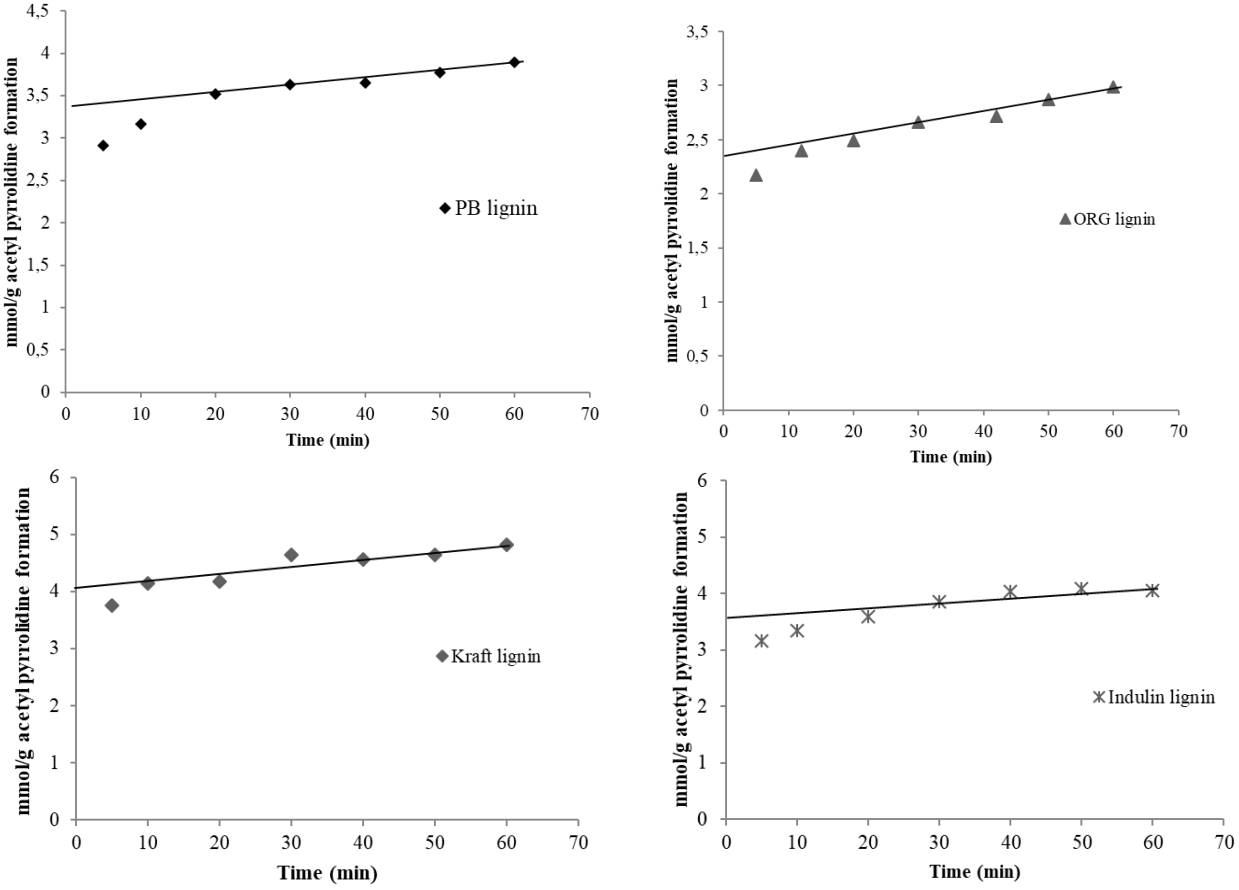

Figure 3.5. Aminolysis of acetylated lignin samples, PB-lignin, ORG lignin, Kraft lignin and Indulin lignin

The amount of phenolic hydroxyl groups in lignin samples is compared in Table 3.2. Each reaction was repeated three times and the standard deviation of the corresponding samples are mentioned in Table 3.2.

Table 3.2. Comparison of phenolic hydroxyl group content in different technical lignins, from lignin aminolysis

Type of the lignin	Phenolic hydroxyl groups mmol/g lignin
PB - Protobind 1000 lignin	3.4 ± 0.18
ORG - Organosolv lignin	2.4 ± 0.12
KF - Kraft lignin	4.0 ± 0.07
IND – Indulin lignin	3.6 ± 0.05

Among the examined lignin samples, Kraft lignin contains the highest amount of phenolic hydroxyl groups, around 4.0 mmol/g, followed by Indulin (3.6 mmol/g) and PB (3.4 mmol/g) lignins. Organosolv lignin exhibits the lowest phenolic hydroxyl group content, i.e. 2.4 mmol/g. It should be stressed that softwood lignins (Kraft and Indulin) are known to contain more phenolic hydroxyl groups than annual plant lignins (PB and ORG). The aminolysis results are thus logical.

It should be noted that PB and Organosolv lignins exhibit high sugar content, 3.1 ± 0.2 and 7.2 ± 0.3 respectively (Table 3.1), which possibly undergo the acetylation and deacetylation leading to an overestimation of the results given by aminolysis. It is evident that the aminolysis method is more sensitive to the sugar impurities than some other methods.

Salvado et al. carried out a similar study on the aminolysis method and lignin phenolic hydroxyl determination. According to their results, Kraft lignin exhibits high phenolic hydroxyl groups quantity, around 4.60 mmol/g with a standard deviation of 0.04. In addition, organosolv lignin displays lower phenolic hydroxyl group content, with around 2.80 ± 0.10 mmol/g. These results are in good agreement with our findings (El Mansouri and Salvadó, 2007).

3.5. Comparison of the aminolysis method with other analytical methods

The results given by the aminolysis method were compared with those obtained by other analytical techniques such as FT-IR, differential UV, NMR and titration method. The following section presents various techniques employed for the analysis and the obtained results.

3.5.1. FT-IR

FT-IR analysis, a non-quantitative analysis, is used to compare crude and acetylated lignins in view of observing structural composition and differences before and after the derivatization. Figure 3.6 gives the FT-IR spectra of the four technical lignin samples used in this study.

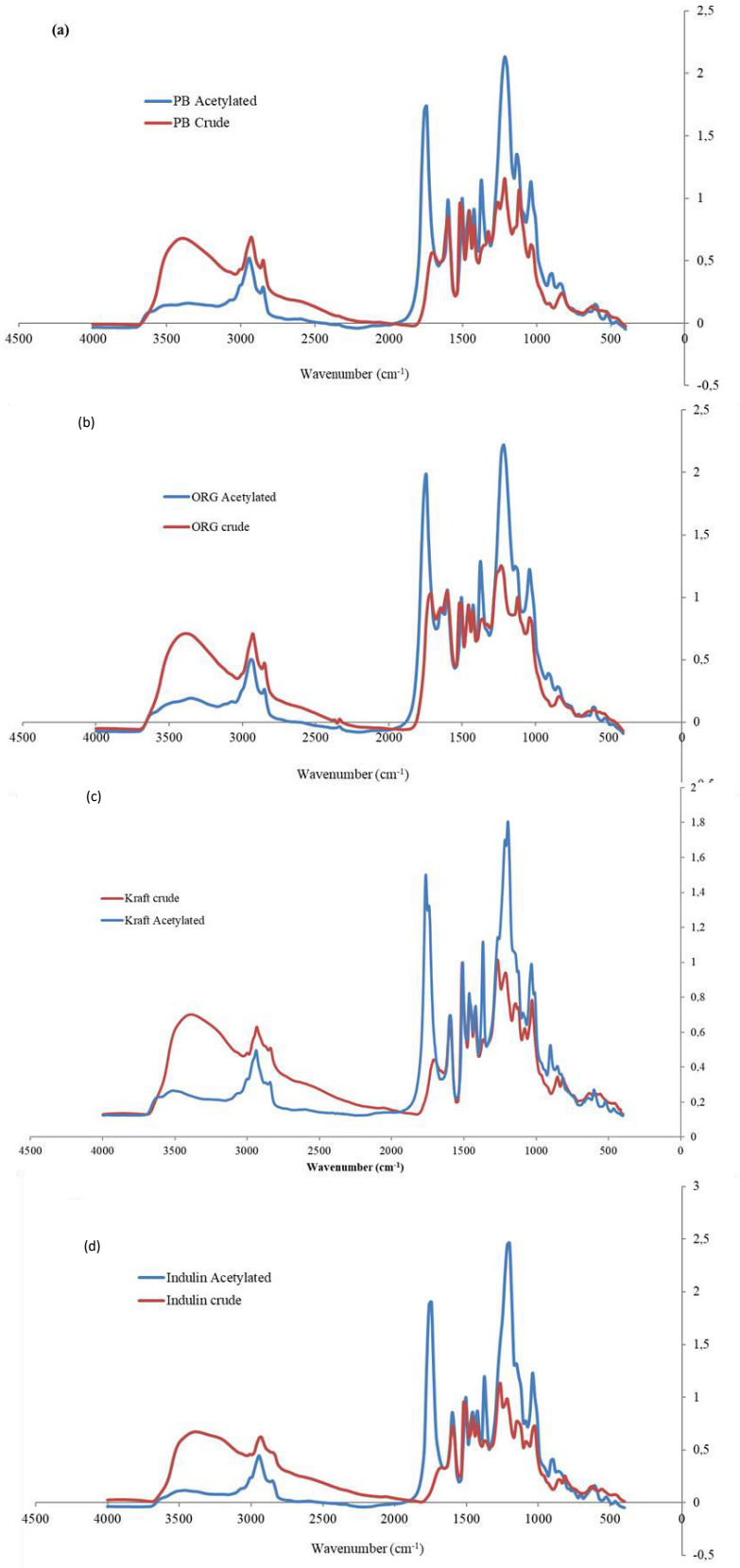

Figure 3.6. FT-IR spectra of crude and acetylated lignins (a) PB - Protobind lignin (b) ORG - Organosolv lignin (c) Kraft lignin (d) IND- Indulin lignin

It is clearly seen from the spectra that, in all cases, similar profiles with slight differences in absorbance bands are obtained. The crude samples showed a typical signal at 3400 cm^{-1} which is attributed to OH groups, and bands around 2950-2830 cm^{-1} corresponding to the vibration of CH bond in methyl and methylene groups. The signals at 1595, 1515 and 1425 cm^{-1} represent typical aromatic vibrations in lignin. The three main lignin structural units (S, G, H) show characteristic signals at 1330 cm^{-1} related to the breathing of the syringyl ring with CO stretching. Two adjacent bands at 1265 and 1210 cm^{-1} are associated to the breathing of the guaiacyl ring with CO stretching. The vibration of CH in guaiacyl and syringyl units appears at 1150 and 1120 cm^{-1}, respectively. Finally, the vibration due to the CH linkage in syringyl and p-hydroxy structures can be observed between 810 cm^{-1} and 850 cm^{-1}.

After acetylation, the typical band of -OH at 3400 cm^{-1} is considerably reduced compared to crude samples, confirming that the corresponding -OH groups were derivatized. It should be noted that a new band is observed at around 1750 cm^{-1}. It is attributed to C=O bond of acetyl groups. Another difference in signal intensity is obtained with derivatized lignins at 1250 cm^{-1}. This is associated to the formation of a new C-O bond in lignins. These results evidenced that there are substantial changes in lignin structure after derivatization. Although, this method is simple and fast, acetylation can cause problems due to incomplete derivatization and therefore the results are only qualitative.

3.5.2. Lignin hydroxyl phenolic group quantification by UV spectrophotometry

UV spectrophotometry is a direct, rapid and easy way for phenolic hydroxyl groups measurement compared to aminolysis. It is applied on crude lignin, without prior lignin derivatization. However, this method (described in chapter 2) only provides the total amount of phenolic hydroxyl groups without any structural specification. Results are presented in **Error! Reference source not found.**.

Table 3.3. Comparison of phenolic hydroxyl group quantification (mmol/g) using aminolysis and UV spectrophotometry

Method	PB-Protobind lignin	ORG-Organosolv lignin	KF-Kraft lignin	IND-Indulin lignin
Aminolysis	**3.4 ± 0.18**	**2.4 ± 0.12**	**4.0 ± 0.07**	**3.6 ± 0.10**
UV-method	2.6 ± 0.02	1.7 ± 0.01	2.8 ± 0.01	3.4 ± 0.01

The UV method estimates lower amount of phenolic hydroxyl groups for all the studied lignins, in particular for the Kraft lignin. The UV method is well known to present limitations; especially for the quantification of some phenolic structures bearing more than one phenolic hydroxyl group (Tiainen et

al., 1999). Another important issue is that the method requires full lignin solubility in the solvents (dioxane mixed with 0,2 M NaOH and dioxane mixed with an aqueous buffer at pH 6) which is not straightforward for some samples. This limitation leads to the underestimation of the lignin phenolic hydroxyl groups.

3.5.3. Lignin hydroxyl group quantification by ^{1}H NMR

Aminolysis, UV and ^{1}H NMR results are presented in Table 3.4. ^{1}H NMR spectra are measured directly on crude lignins. For this analysis, 10 mg of crude lignins are analysed in 5 mm NMR tubes.

Table 3.4. Comparison of phenolic hydroxyl group quantification (mmol/g) using aminolysis and ^{1}H NMR spectroscopy

Method	PB-Protobind lignin	ORG-Organosolv lignin	KF-Kraft lignin	IND-Indulin lignin
Aminolysis	**3.4 ± 0.18**	**2.4 ± 0.12**	**4.0 ± 0.07**	**3.6 ± 0.10**
UV-method	2.6 ± 0.02	1.7 ± 0.01	2.8 ± 0.01	**3.4 ± 0.01**
^{1}H-NMR	1.8 ± 0.13	0.9 ± 0.07	2.7 ± 0.04	**3.1 ± 0.23**

Very low values are obtained with ^{1}H-NMR spectroscopy for all lignins except IND lignin compared to classical aminolysis method. To avoid the acetylation of the sample, the lignin sample should be totally dissolved in deuterated solvents (D_2O) with extreme care, i.e. total dryness in the sample and solvents. These requirements make the method very tedious, time consuming and sometimes lead to undervalued results. The large difference in phenolic hydroxyl group values from ^{1}H NMR clearly indicates that this method fails to associate with other techniques and it evidences the main drawback of this technique. Moreover, the use of a short spectral width range hinders the spectra integration due to overlapping, lack of resolution and large proportion of protons in lignin (Blainski et al., 2013).

3.5.4. Lignin hydroxyl group quantification by ^{13}C NMR

^{13}C NMR technique is an indirect method used for the quantification of phenolic hydroxyl groups in lignin. Lignin samples are acetylated prior to analysis. Fourier transformation is applied to integrate the signals in which the amounts of phenolic hydroxyl group's areas are easily calculated based on the relative integrals with respect to the internal standard. From the ^{13}C NMR, the acetylated groups signal area is quantified that gives the information of number of phenolic hydroxyl groups.

Aminolysis, UV method, ^{1}H and ^{13}C NMR results are presented in Table 3.5. 350 mg of acetylated lignins are analysed in 10 mm NMR tubes used for the analysis.

Table 3.5. Comparison of phenolic hydroxyl group quantification (mmol/g) using aminolysis and ^{13}C NMR spectroscopy

Method	PB-Protobind lignin	ORG-Organosolv lignin	KF-Kraft lignin	IND-Indulin lignin
Aminolysis	**3.4 ± 0.18**	**2.4 ± 0.12**	**4.0 ± 0.07**	**3.6 ± 0.10**
UV-method	2.6 ± 0.02	1.7 ± 0.01	2.8 ± 0.01	3.4 ± 0.01
^{1}H-NMR	1.8 ± 0.13	0.9 ± 0.07	2.7 ± 0.04	3.1 ± 0.23
^{13}C-NMR	2.4 ± 0.04	2.0 ± 0.03	4.2 ± 0.06	3.6 ± 0.05

This method can quantify the total hydroxyl groups, including aromatic and aliphatic hydroxyls. It should be mentioned that in both aminolysis and ^{13}C NMR analyses, acetylated samples have been used. This method shows that Kraft and Indulin lignins possess similar quantities of phenolic hydroxyl groups, in the same range as with aminolysis. PB and organosolv lignin analysed with ^{13}C NMR show lower phenolic hydroxyl content than with the aminolysis method, and the reason can be the interference of high sugar content during aminolysis. Contrary to aminolysis, ^{13}C NMR analysis predicts the phenolic hydroxyl group content regardless of sugar impurities and provides additional structural information. For instance, on the ^{13}C NMR spectra of the Kraft lignin (Figure 3.7), the region between 165 and 175 ppm corresponds to the carboxyl groups issued from aliphatic and aromatic hydroxyl groups acetylation. The spectrum also shows the pyridine residues derived from the acetylation process even after successive evaporation and freeze-drying operations. The limitation of the ^{13}C NMR is incomplete acetylation, signal overlapping and time-consuming process.

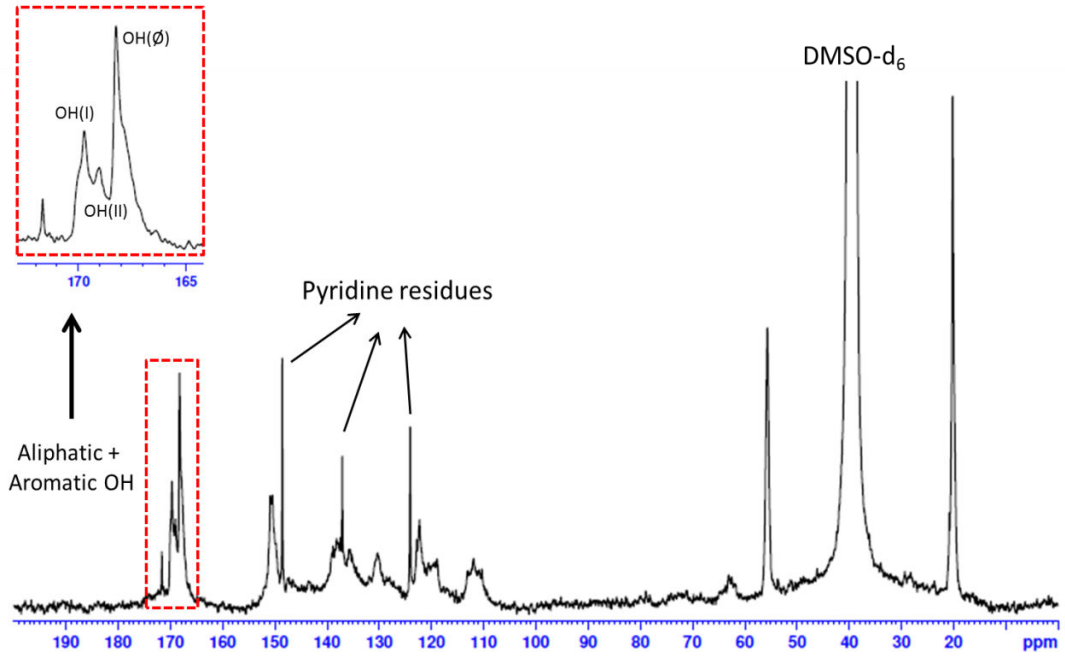

Figure 3.7. KF-Kraft lignin sample ^{13}C-NMR spectrum and detail of the carboxyl zone.

3.5.5. Lignin hydroxyl group quantification by ^{31}P NMR

Nowadays, ^{31}P-NMR is considered as the most referenced method. It provides detailed structural information on lignin. For ^{31}P NMR analysis, in-situ hydroxyl group phosphorylation is necessary, directly in the NMR tube. Comparing with aminolysis, the derivatization reaction is different (acetylation for aminolysis). The use of a phosphorylating agent and of an internal standard (cholesterol) enables the clear differentiation of hydroxyl (aliphatic and aromatic) and carboxyl groups. ^{31}P NMR results are compared with aminolysis, UV and other NMR (^{1}H, ^{13}C) techniques in Table 3.6.

Table 3.6. Comparison of phenolic hydroxyl group quantification (mmol/g) using aminolysis and ^{31}P NMR spectroscopy

Method	PB-Protobind lignin	ORG-Organosolv lignin	KF-Kraft lignin	IND-Indulin lignin
Aminolysis	**3.4 ± 0.18**	**2.4 ± 0.12**	**4.0 ± 0.07**	**3.6 ± 0.10**
UV-method	2.6 ± 0.02	1.7 ± 0.01	2.8 ± 0.01	3.4 ± 0.01
^{1}H-NMR	1.8 ± 0.13	0.9 ± 0.07	2.7 ± 0.04	3.1 ± 0.23
^{13}C-NMR	2.4 ± 0.04	2.0 ± 0.03	4.2 ± 0.06	3.6 ± 0.05
^{31}P-NMR	2.7 ± 0.1	1.3 ± 0.06	3.2 ± 0.16	3.2 ± 0.10

At the same time, ^{31}P-NMR is a non-sensitive method to impurities since sugars are not reactive during phosphorylation (Korntner et al., 2015). This could be the reason why the ^{31}P NMR analysis gives less phenolic hydroxyl groups for all the tested lignins compared to the aminolysis method. As aminolysis, ^{31}P NMR is a tedious and complex determination since it requires a lignin derivatization step and consumes time and expensive chemicals. After phosphorylation, the analysis should be performed rapidly due to derivatized product instability and it requires an access to costly NMR equipment, representing further limitations. The main benefit of the ^{31}P-NMR analysis is that it allows a detailed quantification of syringyl, guaiacyl and p-hydroxyphenyl units (Cateto et al., 2008). Figure 3.8 shows the PB-lignin ^{31}P-NMR spectrum. In the Figure 3.8, the region from 137.5 ppm to 144 ppm is associated to the different phenolic groups in lignin such as p-hydroxy OH (137.5 ppm to 138.5 ppm), guaiacyl OH (139 ppm to 139.8 ppm) and syringyl OH (142.2 ppm to 143 ppm) respectively. The aliphatic OH groups region is found between 145.5 ppm to 149 ppm. Table 3.7 gives the quantification of the different hydroxyl groups.

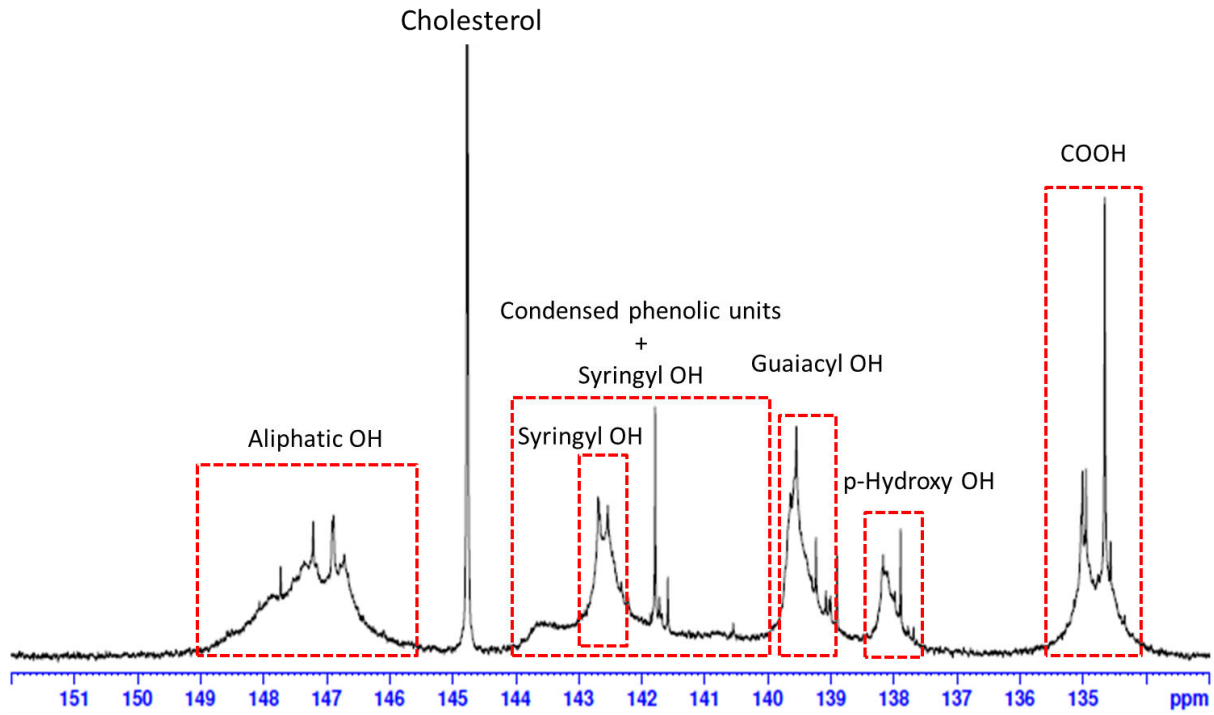

Figure 3.8. ^{31}P-NMR spectrum of the PB-Protobind lignin sample

Table 3.7. Hydroxyl group determination (mmol/g) using ^{31}P NMR spectroscopy

Lignin samples	Aliphatic OH	Syringyl OH	Condensed phenolic OH	Guaiacyl OH	*p*-Hydroxy OH
PB-Protobind lignin	1.50	0.67	0.86	0.82	0.35
ORG-Organosolv lignin	1.23	0.25	0.39	0.45	0.21
KF-Kraft lignin	1.87	0.24	1.30	1.50	0.16
IND-Indulin lignin	2.06	0.20	1.25	1.54	0.21

The detailed hydroxyl group quantification (Table 3.7) reveals the origin of each lignin sample. Softwood lignin samples (Kraft lignin and Indulin lignin) logically present a combination between high amount of guaiacyl units and small amounts of syringyl and p-hydroxyphenyl units. On the other hand, non-wood lignin from agricultural residues (Organosolv lignin and PB lignin) presents comparable structure proportions (Cateto et al., 2008).

3.5.6. Lignin hydroxyl and carboxyl group quantification by conductometric and pH-metric titrations (Fast method)

A fast and easy method for lignin phenolic hydroxyl and carboxyl group determination has been developed at LGP2. The idea is to provide a simple method for lignin producers to easily qualify the technical lignins for various applications. The method is based on the combination of an aqueous acid-base conductometric titration and pH-metric titration. A back titration with HCl is carried out after adding an excess of sodium hydroxide on lignin to convert phenolic and carboxyl acid groups into phenolate and carboxylate ions respectively. The method is presented in detail in CHAPTER 2 .

Figure 3.9 shows the three different end-titration volumes appearing along the conductometric and pH-metric titrations in the tested lignin samples. V_1 is detected by the change in the conductometric curve slope from negative to slightly positive and V_3 is detected by a sharper increase. They correspond to the end-point titration volume of the hydroxyl ions added in excess (V_1) and the start of the hydrochloric acid excess introduced in the medium (V_3). Between V_1 and V_3, phenolic hydroxyl groups first, then carboxyl groups are protonated; but these two functional groups could not be distinguished because they exhibit similar conductivities. However, due to their different pK_a's, a pH-metric titration can discriminate phenolic and carboxyl groups. The titration of free phenols with pKa's in the range of 8-11.5 can be obtained by the volume difference between V_2, corresponding to

pH close to 7, and V_1. The remaining acidic groups, i.e. carboxyl groups, thus correspond to the volume difference between V_3 and V_2.

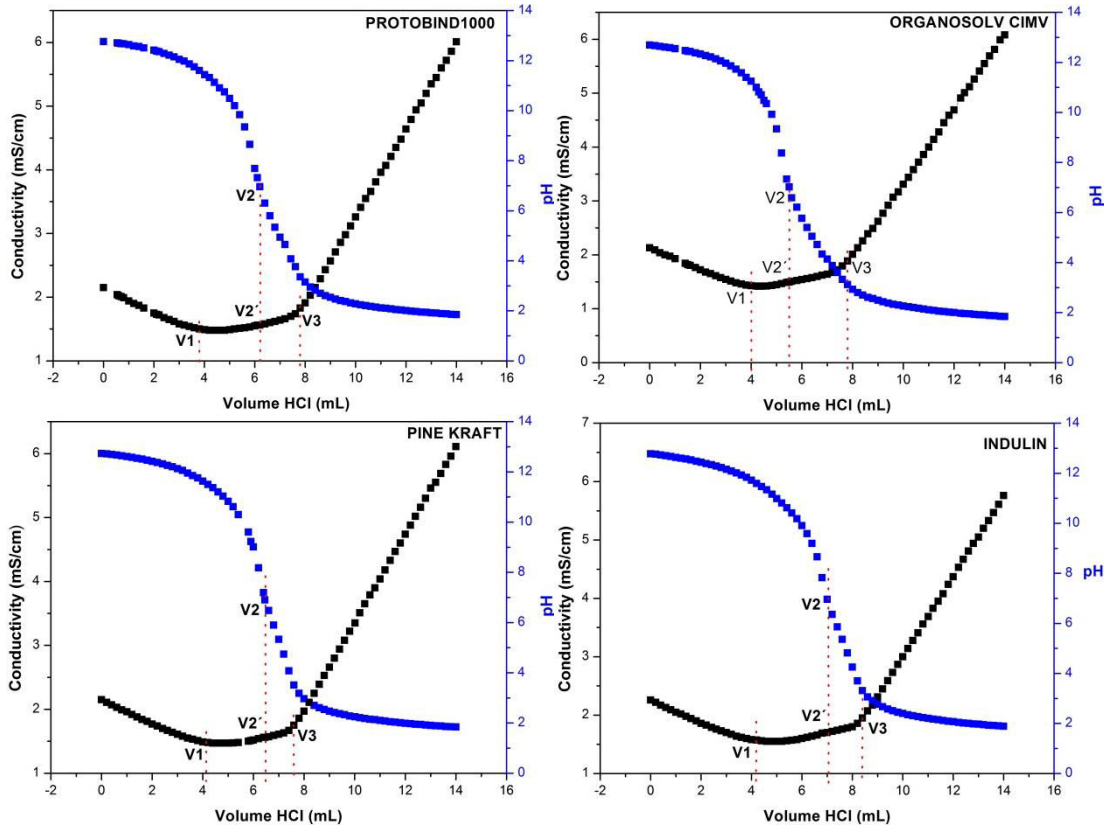

Figure 3.9. Conductometric and acid-base titration curves for lignin samples

As clearly seen in Figure 3.9, all the examined lignin samples undergo a similar profile during the titrations independently of the starting raw material and of the process applied to recover the lignin. However, while the V_3 titration volume is always rather precisely determined (because most carboxylic acids in lignin have a pKa above 4.5, as reported by Zakis (Zakis, 1994)), a significant imprecision may come from the V_1 titration volume determination due to the presence of phenolic components with high pKa values (up to 11.5 in condensed phenolic structures bearing an α-carbon adjacent to the phenolic carbon). This is a limitation of this method.

The quantification of the phenolic hydroxyl groups in the technical lignins by this simple "fast titration method" is given in Table 3.8 and is compared with other methods.

Table 3.8. Phenolic hydroxyl group quantification (mmol/g) using the fast titration method, comparison with aminolysis and other methods

Method	PB-Protobind lignin	ORG-Organosolv lignin	KF-Kraft lignin	IND-Indulin lignin
Aminolysis	**3.4 ± 0.18**	**2.4 ± 0.12**	**4.0 ± 0.07**	**3.6 ± 0.10**
UV-method	2.6 ± 0.02	1.7 ± 0.01	2.8 ± 0.01	3.4 ± 0.01
^{1}H-NMR	1.8 ± 0.13	0.9 ± 0.07	2.7 ± 0.04	3.1 ± 0.23
^{13}C-NMR	2.4 ± 0.04	2.0 ± 0.03	4.2 ± 0.06	3.6 ± 0.05
^{31}P-NMR	2.7 ± 0.1	1.3 ± 0.06	3.2 ± 0.16	3.2 ± 0.10
^{19}F-NMR	2.176	1.673	2.277	2.331
Fast method	2.4 ± 0.03	1.5 ± 0.03	2.4 ± 0.03	2.7 ± 0.05

The fast titration method shows that Indulin, Kraft and PB lignins exhibit the highest phenolic hydroxyl group content. This result is different from those obtained with aminolysis and other NMR techniques, where Kraft lignin contains the highest value. Compared to aminolysis, the fast method underestimates the number of hydroxyl groups in lignin and there is a big difference for the case of Kraft lignin. It is interesting to note that most of the fast titration method results were in close agreement with other conventional methods such as UV, ^{19}F NMR and ^{31}P NMR. The detailed information for the quantification of phenolic hydroxyl groups using ^{19}F NMR can be found in CHAPTER 5.

The fast titration method is also able to provide the quantity of carboxyl groups presents in lignins. Table 3.9 compares the carboxyl groups determination of the analyzed lignin samples obtained by three different methods: the fast method, non-aqueous potentiometric titration by tetra-n-butylammonium hydroxide - TnBAH and ^{31}P NMR (the detailed information on these methods are given in Materials and Methods, CHAPTER 2).

Table 3.9. Comparison of carboxyl group quantification (mmol/g) using the fast method, the TnBAH titration and ^{31}P NMR

Method	PB-Protobind lignin	ORG-Organosolv lignin	KF-Kraft lignin	IND-Indulin lignin
Fast method	1.6 ± 0.02	2.3 ± 0.05	1.2 ± 0.04	1.4 ± 0.02
TnBAH method	1.6 ± 0.04	1.3 ± 0.01	1.2 ± 0.03	1.1 ± 0.01
^{31}P NMR	1.4 ± 0.07	1.1 ± 0.05	0.9 ± 0.04	0.9 ± 0.04

From Table 3.9, the analysis reveals lower carboxyl groups values in the case of ^{31}P NMR and a great similarity between the two titration methods except for the Organosolv lignin sample. Moreover, the carboxyl content of all the analysed lignin samples was lower than the phenolic hydroxyl group amount, except, again, for the Organosolv lignin sample. A higher carboxyl content compared to phenolic hydroxyls is possible since the Organosolv lignin sample extraction process uses oxidative conditions.

Although the fast titration method enables the quantification of both phenolic hydroxyl groups and carboxyl groups, it has some inherent limitations: this method requires a large quantity of sample, around 1g for the analysis, and does not give the structural units (S, G and H) composition present in the lignin. Moreover, an error around 10−15% may be found for phenolic hydroxyl group determination if the lignin samples present phenolic structures with high pKa values. For instance, the calculated phenolic hydroxyl group value is about 2.4 mmol/g from the fast titration method in the case of the PB lignin, whereas it was found around 3.4 mmol/g using aminolysis.

Comparing all analysed samples, the phenolic hydroxyl group values (in mmol/g) range in different methods: 2.4 (ORG) to 4.0 (KF) (aminolysis), 1.7 (ORG) to 3.4 (IND) (UV), 0.9 (ORG) to 3.1 (IND) (^{1}H NMR), 2.0 (ORG) to 4.2 (KF) (^{13}C NMR), 1.3 (ORG) to 3.2 (KF and IND) (^{31}P NMR) and 1.5 (ORG) to 2.7 (IND) (fast titration method). It should be noted that all the methods gave lower phenolic hydroxyl content for Organosolv lignin and higher phenolic hydroxyl content for Indulin or Kraft (softwood lignins). Overall aminolysis method predicted higher phenolic content for all lignins compared to the other analytical techniques and ^{1}H NMR provided lowest phenolic content.

3.6. Conclusion

The aminolysis method was employed for phenolic hydroxyl group quantification in four different technical lignin samples: Protobind 1000 lignin, Organosolv lignin, Kraft lignin and Indulin lignin.

Prior to aminolysis, the lignin samples have been acetylated to convert hydroxyl groups present in lignin into corresponding acetylated derivatives. The derivatization was controlled by FT-IR: the signal corresponding to hydroxyl functional group was significantly reduced after acetylation. The aminolysis GC results revealed that Kraft lignin contains higher phenolic hydroxyl group content than Indulin lignin, followed by Protobind and at least by the Organosolv lignin. The GC results were compared with other analytical techniques such as UV, ^{1}H NMR, ^{13}C NMR, ^{31}P NMR and a fast titration method recently developed at LGP2. The obtained results demonstrated that aminolysis results were comparable to ^{13}C NMR results. This is not surprising since both methods used acetylated derivatives. ^{13}C NMR and ^{31}P NMR are more complete techniques since they provide additional information on the lignin structure. However, it should be stressed that the high complexity of NMR techniques and time consuming associated with high cost of chemicals are the limitations of these analyses. ^{1}H NMR, UV and fast titration methods underestimated the phenolic hydroxyl groups content and are penalized by signal overlapping (^{1}H NMR), more than one phenolic hydroxyl groups in phenyl unit (UV) and large quantity of sample, inability to quantify structural units, and inadequate quantification of high pKa's phenolic structures (fast titration method). However, for the fast titration method, the error has been estimated to be close to 10-15%, which is satisfactory for a first industrial characterization, easy to apply in laboratories without sophisticated analytical equipment. Moreover, classical aminolysis also exhibits some drawbacks such as possible incomplete derivatization and the overestimation of phenolic hydroxyl groups due to sugar impurities present in the samples. Some of these limitations might be avoided by employing new derivatization methods such as fluorobenzylation and fluorobenzoylation. The next chapter will study in detail some fluoro-derivatization reactions on lignin-like model compounds, originally developed by Prof. Barrelle and co-workers about 25 years ago at Grenoble University, but never applied by other groups due to incomplete developments of the methods, to estimate the aromatic and aliphatic hydroxyl groups using ^{19}F NMR, while limiting the interaction with sugars impurities.

CHAPTER 4

4. Study of the reactivity of lignin model compounds toward fluorobenzylation using ^{13}C and ^{19}F NMR: Application to lignin hydroxyl groups quantification by ^{19}F NMR

4.1. Introduction

Two decades ago, Barrelle et al. developed ^{19}F NMR spectroscopic analysis after lignin derivatization by fluorinated compounds to quantify phenolic and aliphatic hydroxyl groups, and carbonyl groups. Fluorobenzylation was used to quantify phenolic hydroxyl groups and primary aliphatic hydroxyl groups, fluorobenzoylation for secondary aliphatic hydroxyl group, whereas trifluoromethylphenylhydrazine derivatization enabled carbonyl groups determination (Barrelle, 1993, 1995; Barrelle et al., 1992; Sevillano et al., 2001). As for ^{13}C NMR analysis, the derivatization was carried out prior to the NMR acquisition. Although not much tested, this method offered several advantages over ^{13}C and ^{31}P NMR techniques: the derivatization reaction is rapid (one day); the derivative is stable so that it can be re-used for other analysis; due the natural abundance of 100% and the high sensitivity of the ^{19}F nucleus, the ^{19}F-NMR acquisition times are quite low (less than 30 min for lignin samples); and the quantitative analysis requires only few amount of lignin derivative (15 mg). However, up to now, the usage of this analytical method has been mostly restricted to carbonyl quantification and not for hydroxyl groups determination, due to the variety of well-tested other methods for –OH evaluation.

Therefore, in this work, we revisited the ^{19}F NMR method to assess the fluorobenzylation reactivity of hydroxyl groups of different natures, using the combination of ^{13}C and ^{19}F NMR analyses performed on lignin model compounds. This work is thus a complement of Barrelle et al. studies, and

intends to prove that the ^{19}F NMR lignin analysis is a robust method for lignin phenolic hydroxyl groups quantification.

Therefore, this chapter is devoted to the study of lignin model compound fluorobenzylation, i.e. to investigate the reactivity of lignin hydroxyl groups in such reaction, with the final objective to quantify phenolic hydroxyl groups of technical lignin.

Five different lignin-like model compounds have been chosen according to the nature of the hydroxyl groups bound to the different sites, such as aromatic and aliphatic hydroxyl groups. Since lignins are often contaminated by sugars, and because sugars also bear hydroxyl groups, a cellulose model compound has been also selected. All the model compounds have been subjected to the fluorobenzylation reaction and the resulting products have been analyzed by ^{13}C and ^{19}F NMR spectroscopy. In the following, ^{19}F NMR analysis was successfully applied on a commercial lignin (Organasolv - ORG) after fluorobenzylation in order to quantify its phenolic group content and also to test its solubility in SEC organic solvent for the molar mass distribution study, presented in the next chapter.

4.2. Materials and methods

The fluorobenzylation reaction is carried out using the 4-fluorobenzyl chloride (FBC) as derivatizing agent. The model compounds and lignin samples are dissolved in tetra N-butylammonium hydroxide in 1M methanol (NBu) solution and stirred for 1h at 50°C, before the addition of the derivatizing agent. Then the reaction is continued at 50°C for overnight. After the reaction time, the model compound derivatives are recovered using EtOAc extraction and successive solvent evaporation. Lignin samples undergo the same reaction conditions whereas the derivatized products are recovered by precipitation in diethyl ether (Barrelle et al., 1992; Barrelle, 1995). The detailed experimental conditions are given in the Materials and Methods Chapter (CHAPTER 2).

The schematic diagram (shown in Figure 4.1) briefly describes the fluorobenzylation of hydroxyl groups of lignin and their conversion into corresponding fluorobenzylated derivatives. Both aliphatic and hydroxyl groups are likely to be derivatized. To investigate the derivatization extend, two NMR techniques, ^{13}C and ^{19}F NMR, have been performed before and after derivatization.

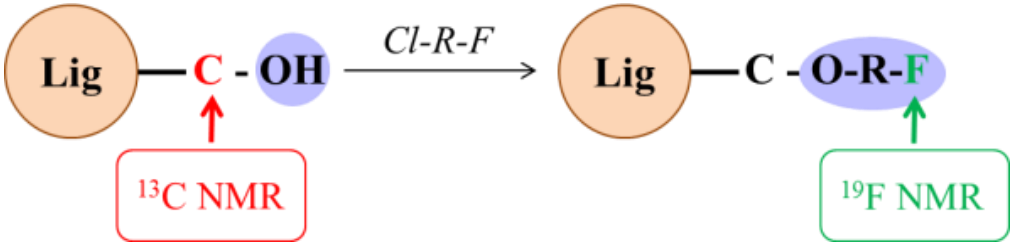

Figure 4.1. Schematic reaction of lignin fluorobenzylation (Cl-R-F: 4-Fluorobenzylchloride, Lig=Lignin).

Five different lignin like model compounds (illustrated in Figure 4.2) have been considered. They were chosen based on the hydroxyl groups location which could be found in lignins. Vanillin (**1**) and Acetovanillone (**2**) attribute a phenolic hydroxyl group with a carbonyl function in α position (aldehyde and ketone respectively). Guaiacol (**3**) is the basic phenolic unit of lignin. Vanillyl alcohol (**4**) consists of both aliphatic and aromatic hydroxyl groups, and Veratryl alcohol (**5**) contains only one aliphatic hydroxyl group. A model of carbohydrate, D(+) Cellobiose (**6**), was also considered because commercial lignins are usually contaminated by sugars containing hydroxyl groups (primary and secondary OH) which may also undergo derivatization.

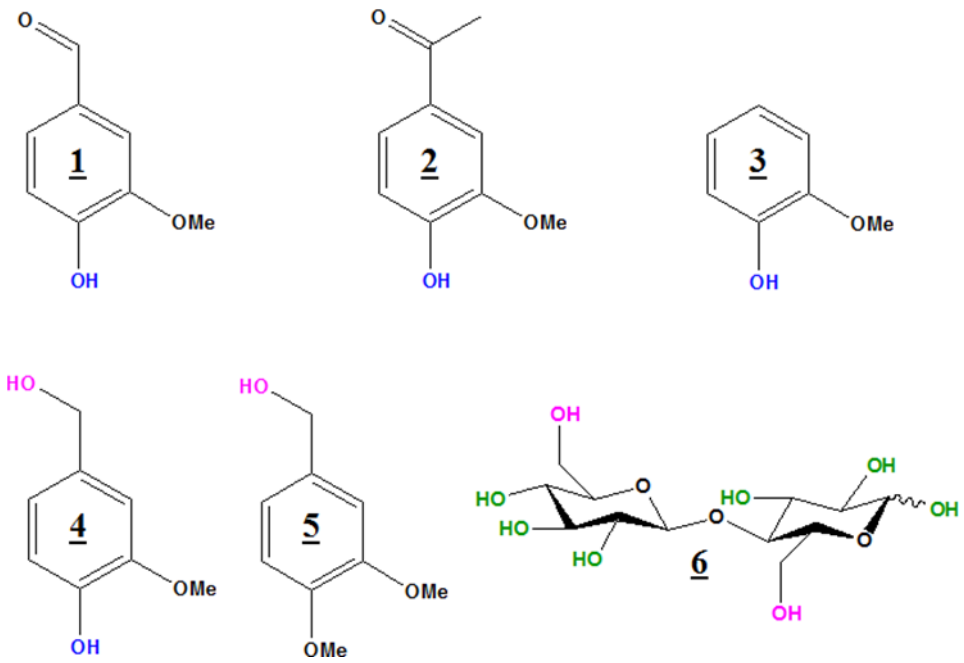

Figure 4.2. Studied model compounds: Vanillin (**1**), Acetovanillone (**2**), Guaiacol (**3**), Vanillyl alcohol (**4**), Veratryl alcohol (**5**) and D(+) Cellobiose (**6**)

In addition to study the lignin fluorobenzylation reaction, the chemical shift assignments given by Barrelle in his former works to quantify phenolic and aliphatic hydroxyl groups and carbonyl groups will be verified (Barrelle et al., 1992; Barrelle, 1993, 1995). Indeed, earlier development of ^{19}F NMR studies was based on spectral folding, leading to possible wrong chemical shifts assignments and sometimes to reverse shaped signals. Considering the current NMR technological development that can now examine the whole spectral window, the present study proposes to re-investigate the ^{19}F NMR analysis in the context of lignin characterization. During our analysis on model compounds, the ^{19}F NMR chemical shift assignments given by Barrelle will be confirmed.

4.3. Lignin model compounds fluorobenzylation followed by HPLC analysis

Qualitative HPLC analyses have been performed to verify the derivatization of the lignin model compounds. The model compounds, before and after derivatization, have been analyzed using the conditions given in the Materials and Methods chapter.

The retention time of Vanillin (**1**) was found at 29.32 min and after derivatization, the signal intensity was significantly reduced. It confirms that most of the vanillin has reacted. Similarly, pure Acetovanillone (**2**), Guaiacol (**3**) and Vanillyl alcohol (**4**) were eluted at 40.62 min, 39.42 min and 12.17 min respectively and after fluorobenzylation, no signal was recorded. These results confirm that these model compounds reacted with FBC, the fluorobenzylated agent and that no more pure compounds were present. As far as Veratryl alcohol (**5**) is concerned, before derivatization the model compound was eluted at 28.38 min. After the fluorobenzylation, the same elution time was observed without any reduction in intensity meaning that the Veratryl alcohol probably exhibits a poor reactivity towards the fluorobenzylation reaction. Unfortunately, the fluoroderivatives did not give any signal, probably because the HPLC analysis conditions (column and eluent) were not suited to these less polar compounds.

As an example, the HPLC chromatogram before and after fluorobenzylation derivatization of acetovanillone is presented in Figure 4.3. Pure acetovanillone provided a signal at a retention time of 40.62 min, whereas fluorobenzylated acetovanillone did not show any signal at this retention time. This confirms the derivatization

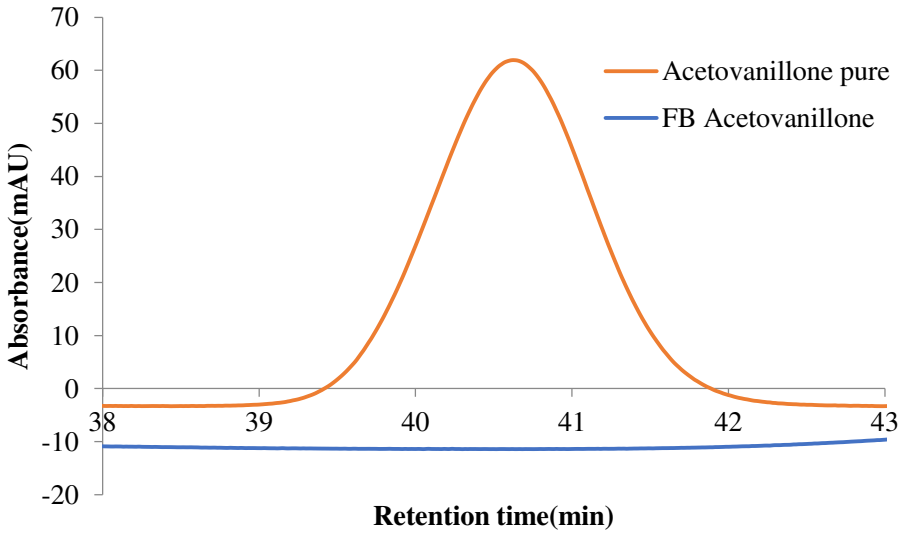

Figure 4.3. HPLC chromatogram of acetovanillone (orange) and fluorobenzylated-acetovanillone (blue)

4.4. NMR analysis of fluorobenzylated model compounds

4.4.1. ^{13}C NMR analysis

First the derivatization reagent FBC and all the fluorobenzylated model compounds and their reaction products after fluorobenzylation have been analyzed by both ^{19}F and ^{13}C NMR in the same way using a quantitative mode. An example of typical fluorobenzylation reaction is shown in Figure 4.4.

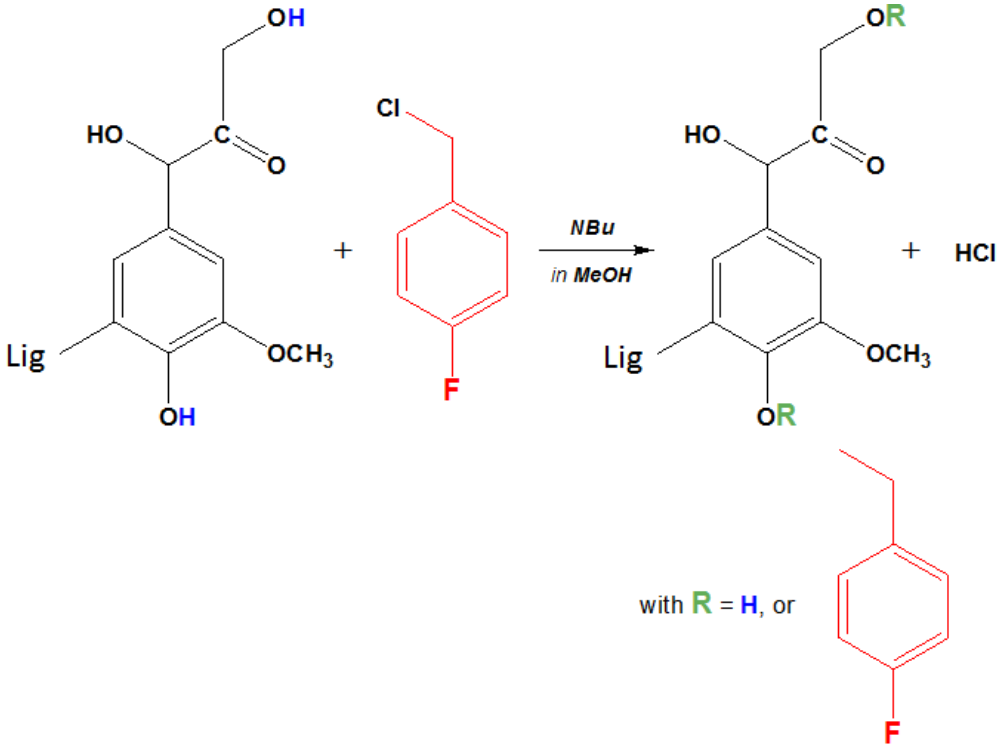

Figure 4.4. Fluorobenzylation reaction of lignin

The following methodology has been adopted to study the fluorobenzylation: after the reaction, distilled water and ethylacetate (EtOAc) were added to quench the reaction. The products of the organic phase were recovered and dried without any purification. After freeze-drying, the products were first analyzed by ^{19}F NMR. After ^{19}F signals detection, ^{13}C NMR analysis was employed to confirm, or not, that the F nucleus belongs to the lignin model derivative. This allows elucidating the structure of the derivatized compounds and detecting all possible non-fluoro substituted products. The chemical shifts and the specific hyperfine structures due to $^{n}J_{CF}$ couplings were used for determining the presence or not of F-$\underline{\Phi}$ (para-fluoro phenyl ring originating from FBC) structure. A complementary DEPT sequence gives access to the unambiguously assignment of the $\underline{C}H_2$' carbons (present in different environments) (Figure 4.5), and the examination of their specific chemical shifts enables to ascertain the occurrence of the fluoro derivatization (or not).

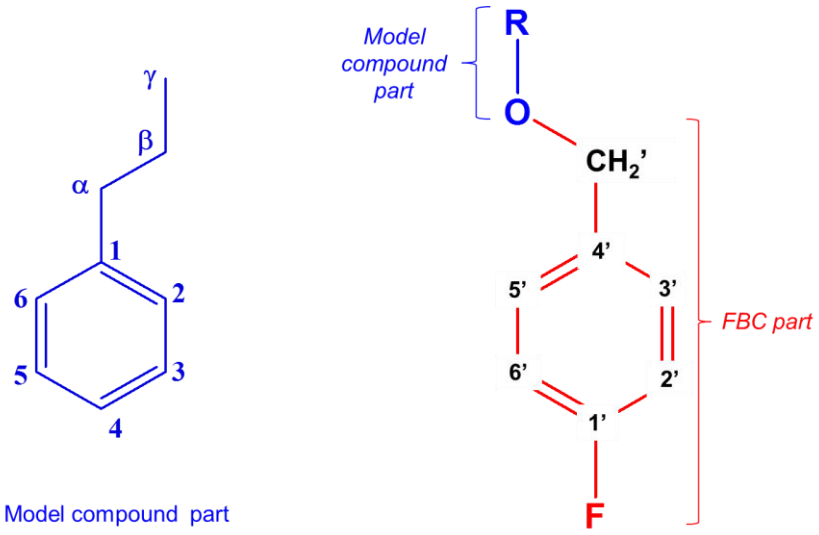

Figure 4.5. Structure and number assignment of fluorobenzylated lignin model compounds

Table 4.1 presents the ^{13}C NMR chemical shift assignments of the methylene group located between FBC and the model (Figure 4.5), of the different products recovered after the lignin model compound derivatization.

Table 4.1. ^{13}C NMR chemical shifts of FBC -CH_2' group (Figure 4.5) of products present in the medium after lignin model compound derivatization

δc (in ppm)	45.3	57.54	62-63	69-71	72.81
Methylene group	-**C**H_2Cl	-**C**H_2N	-**C**H_2OH	-**C**H_2OR	-**C**H_2OMe
Compounds	FBC	NBu	Aliphatic OH FBOH [(a)]	F-derivatized compounds	FBOMe [(b)]

(a) FBOH: resulting product from the reaction of FBC with water.
(b) FBOMe: resulting product from the reaction of FBC with MeOH (solvent of NBu)

The methylene group of FBC, (**C**H_2Cl), and that of N-Bu (**C**H_2N) were detected at 45.3 ppm and 57.54 ppm respectively in relation with the nature of the heteroatom (Cl or N). The FBC reagent could react with water (from moisture) and/or methanol (present in NBu reagent) to form FBOH and/or FBOMe. Their corresponding signals were seen in the range of 62-63 ppm and 72.81 ppm respectively. Finally, the corresponding fluoroderivatized model compounds **C**H_2OR signals were in the range of 69-71 ppm.

To study the reactivity of the fluorobenzylation reaction on lignin model compounds, the reaction products were not purified prior to the ^{13}C NMR analysis. The reaction medium contained a mixture

of products such as the unreacted starting model compounds, fluorobenzylated model compounds (F-derivatized compound), remaining pure reagent (FBC) and by products FBOH (produced by the reaction of FBC with H_2O) and FBOMe (produced by the reaction of FBC with MeOH). To quantify each component at the end of the fluorobenzylation in the reaction medium, the total composition inside the NMR tube was considered as 100%. Then a quantitative ^{13}C NMR analysis was performed on the reaction medium which remained perfectly homogeneous during the analysis time. In this way, the ratio of each present moiety formed during the reaction could be determined (Table 4.2). The fluorobenzylation reagent FBC purity was controlled by taking blank ^{13}C NMR spectrum.

Table 4.2. Mixture ratio of products obtained after the model compound fluorobenzylation, calculated from ^{13}C NMR data (organic part)

Compounds	**Fluorobenzylation** *YIELD, %*	**MIXTURE COMPOSITION**					
		Unreacted starting compound, %	**F-**derivatized Compound, %	**FBC** reagent, %	**FBOH**, %	**FBOMe**, %	**NBu**, %
1	100	-	93.6	6.4	-	-	-
2	100	-	81.3	5.2	-	8.3	5.2
3	100	-	67.6	24.5	-	4.1	3.8
4	100	-	34.0	53.9	Traces	10.1	-
5	9	71.5	7.1	-	Traces	-	21.4
6	-	-	-	-	74.0	-	26
FBC blank		94.1	-	-	5.9	-	-
FBC reacted		-	-	-	7.9	-	92.1

According to ^{13}C results, FBC contains 94.1% of pure FBC and 5.9% of FBOH. Similarly, a "FBC blank reaction" was carried out with all the reagents except the model compound. After reaction, 7.9% of FBOH and 92.1% of NBu reagent have been recovered. No starting FBC signal has been detected (Table 4.2): this clearly shows that the FBC reagent was totally converted into FBOH.

For lignin and carbohydrate model compounds, the fluorobenzylation yield could be calculated by the following relation, *Yield = (F-derivatized compound / (Unreacted pristine compound + F-*

derivatized compound)) × 100. Results are given in Table 4.2. Moreover, the detailed ^{13}C NMR chemical shifts assignment of the fluoroderivatives is given in Table 4.3.

Table 4.3. ^{13}C NMR Chemical shifts (in ppm) of fluorobenzylated model compounds (C numbering according to Figure 4.5)

Compounds		**1**	**2**	**3**	**4**	**5**
Model compounds Part	**C1**	129.8	130.14	120.59	135.75	130.61
	C2	109.9	110.4	112.22	110.76	110.51
	C3	149.4	151.88	149.23	149.05	148.65
	C4	153	148.79	147.66	146.38	148.30
	C5	112.6	112.27	113.88	113.66	111.51
	C6	125.8	122.92	121.25	118.45	120.04
	OCH_3	55.53	55.51	55.44	55.39	55.38 55.46
	C=O	-	196.2	-	-	-
	HC=O	191.34	-	-	-	-
	CH_2 (α)	-	-	-	62.76	71.36
	CH_3	-	26.31	-	-	-
FBC part	**C'H_2**	69.28	69.15	69.15	69.33	70.33
	C'4	132.5	132.74	133.44	133.54	134.71
	$^4J_{CF}$ (Hz)			*2.84*		
	C'3,C'5	130.2	130.14	129.92	129.85	129.57
	$^3J_{CF}$ (Hz)			*9.2*		
	C'2,C'6	115.3	115.29	115.15	115.15	115.40
	$^2J_{CF}$ (Hz)			*21.45*		
	C'1	161.98	161.88	161.7	161.72	161.56
	$^1J_{CF}$ (Hz)			*243*		

As seen in Table 4.2, it is interesting to note that the conversion achieved 100% with the lignin model compounds (**1**), (**2**) and (**3**), containing only phenolic hydroxyl groups.

In the case of Vanillyl alcohol (**4**) bearing both phenolic and aliphatic hydroxyl groups, the absence of starting model compound shows that its conversion was 100% (Table 4.2). Three different compounds were found in the reaction mixture (shown in Figure 4.6): FBC, with its methylenic carbon at 45.3 ppm, was the most abundant product (53.9%); FBOMe, issued from the reaction of methanol with FBC, with its methyl group at 57.40 ppm and its methylenic carbon at 72.81 ppm, represented the minor part (11%); and finally the fluoroderivatized Vanillyl alcohol was present at 35%. From these results, it could be concluded that the fluorobenzylation conversion of lignin phenolic hydroxyl group was quite quantitative, as already seen with previous lignin model compounds (**1**, **2** and **3**). However, the remaining signal at 62.76 ppm corresponding to the methylene carbon covalently bonded to the free aliphatic hydroxyl –**C**H_2OH group and the absence of signal at 71 ppm corresponding to the –**C**H_2OR aliphatic fluoroderivatized group shows that the conversion is due solely to the phenolic hydroxyl (Table 4.3), with no reaction of the aliphatic hydroxyl group. This is also confirmed by the integral measurements: the signal integrals of carbons belonging to the model compound part display the following values: 0.34, 0.31 and 0.29 corresponding to –O**C**H_3 (55.39 ppm), **C**$_1$ (135.75 ppm) and **C**$H_{2\alpha}$ (62.76 ppm), respectively. The integral of the C signal belonging to the FBC part display the following values: 0.32, 0.32 and 0.77 corresponding to **C**H_2' (69.33 ppm), **C**'$_4$ (133.56 ppm) and **C**'$_3$ and **C**'$_5$ (129.87 ppm), respectively. This confirms unambiguously that there is only one FBC moieties per model compound. So, the fluorobenzylation took place on the free phenolic group only, without any reaction on the primary aliphatic hydroxyl function.

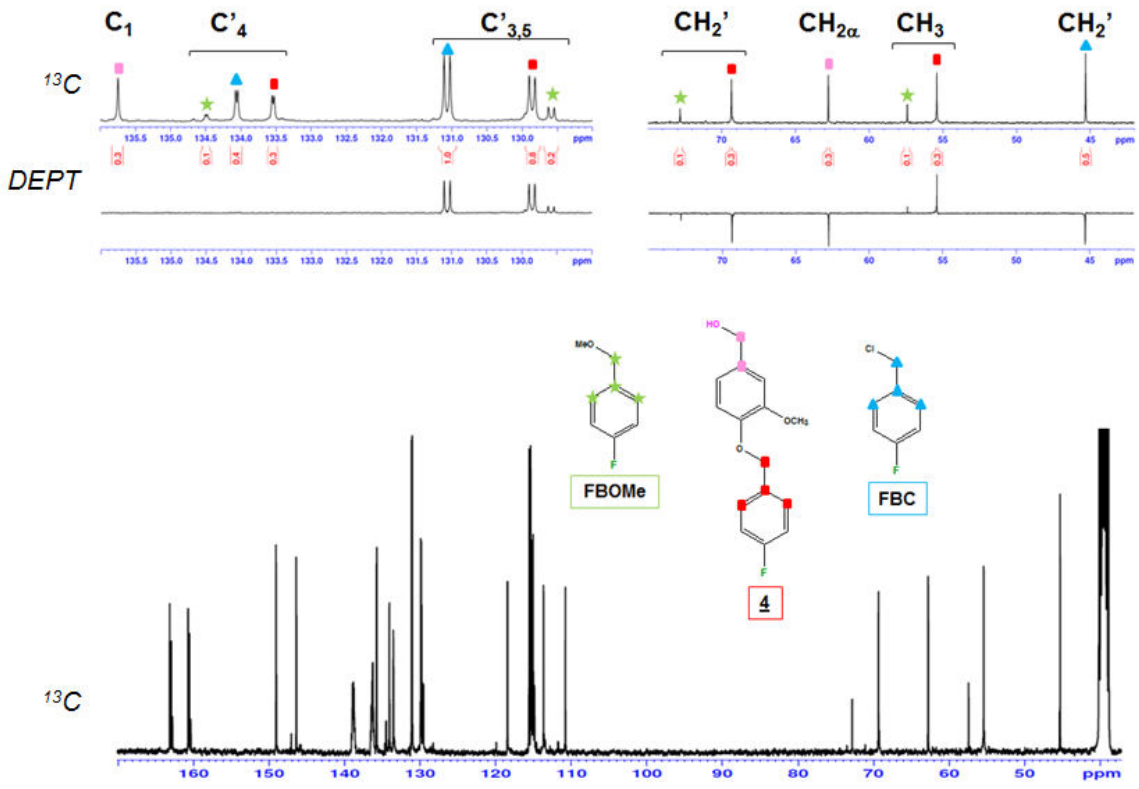

Figure 4.6. ^{13}C-NMR spectra of the mixture issued from the fluorobenzylation of Vanillyl alcohol (**4**) in DMSO-d6.

For the Veratryl alcohol (**5**), bearing only one aliphatic hydroxyl and no phenolic group, three products were found (Table 4.2, Figure 4.7 and Table 4.3): the unreacted starting Veratryl alcohol, with the –**C**H$_2$OH and **C**$_1$ signals respectively at 62.74 ppm and at 135.13 ppm, has been recovered in the largest quantity (71.5%); then 21.4% of butyl ammonium (NBu) was found with its characteristic signals at 13.46, 19.22, 23.09 and 57.54 ppm. This last signal, very close to the chemical shift of the FBOMe methyl group (57.39 ppm), displayed a CH_2 multiplicity (given with the DEPT sequence), instead of CH_3 multiplicity expected in the case of FBOMe, which confirmed undoubtedly the assignment of this signal to the butyl ammonium moiety. Finally, the fluoroderivatized Veratryl alcohol has been recovered as minor compound (7.1%). Its presence was confirmed with the characteristic signal of the FBC part, and the chemical shifts modifications of –**C**H$_2$-OR at 71.36 ppm and of **C**$_1$ at 130.61 ppm. Thus, the fluorobenzylation yield of the Veratryl alcohol (**5**), containing only one aliphatic hydroxyl group, was found very low, about 9%, and most of the starting model compound remained unchanged, which again suggests that aliphatic hydroxyls hardly react with FBC. Moreover, no more FBC remained after the reaction.

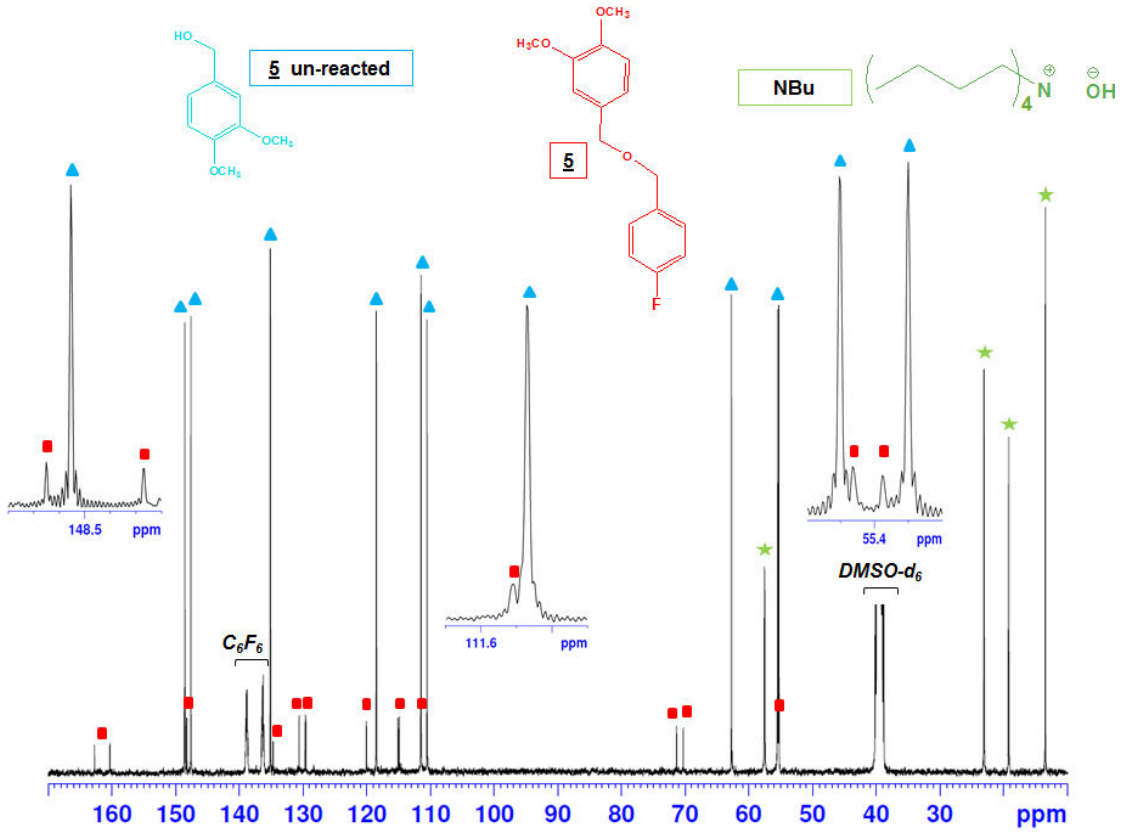

Figure 4.7. ^{13}C-NMR spectra of the mixture issued from the fluorobenzylation of Veratryl alcohol (**5**) in DMSO-d6.

To further study the reactivity of aliphatic hydroxyls towards fluorobenzylation, trials have been conducted with an increasing FBC stoichiometric ratio and with a longer reaction time (3 days instead of 1 day). The final reaction mixture composition is given in Table 4.4.

Table 4.4. Mixture ratio of Veratryl alcohol (**5**) fluorobenzylation carried out with modified conditions, calculated from ^{13}C NMR data

Compounds	Fluorobenzylation *Yield, %*	MIXTURE COMPOSITION					
		Unreacted starting compound, %	**F-derivatized compound, %**	**FBC reagent, %**	**FBOH, %**	**FBOMe, %**	**NBu, %**
5 1 day	9	71.5	7.1	-	Traces	-	21.4
5 3 days	8	27.2	2.7	32.8	traces	30.3	7.0

These new derivatization conditions did not change the fluorobenzylation yield which remained below 10%. In addition, a high quantity of FBC did not react and methanol fluorobenzylation (methanol is the solvent of the added butyl ammonium) has been observed. As a conclusion, it is evident that the fluorobenzylation was more efficient with phenolic hydroxyl than with primary aliphatic hydroxyl groups. Therefore, the derivatization reaction conditions should be improved to get access to all primary aliphatic hydroxyls.

As commercial lignins are usually contaminated by carbohydrates, also containing hydroxyls, the D(+) cellobiose (**6**) was used as a sugar model compound. It was submitted to fluorobenzylation in the same conditions as for the lignin models. The composition of the organic phase recovered after the reaction is given in Table 4.6. The results revealed that no fluorinated product could be identified as well as for the starting carbohydrate model compound. Only N-butyl ammonium (26%) and FBOH (74%) have been detected. Because sugars are water soluble, the aqueous phase was also analyzed. Results show that the aqueous phase reaction mixture contained only the starting cellobiose (10%) and NBu reagent (90%) (Table 4.5). Considering that the total composition inside the NMR tube was 100%, the starting cellobiose (**6**) remained unchanged after the reaction. This clearly indicates that hydroxyls of carbohydrates could not be fluorobenzylated. Therefore, lignin contamination by sugar will not interfere with the ^{19}F NMR analysis of fluorobenzylated lignins.

Table 4.5. Mixture ratio of products obtained after cellobiose (**6**) fluorobenzylation, calculated from ^{13}C NMR data after analysis of the organic and aqueous phases

Compounds	MIXTURE COMPOSITION					
	Unreacted starting compound, %	**F-derivatized Compound**	**FBC reagent, %**	**FBOH, %**	**FBOMe, %**	**NBu, %**
6 Organic phase	-	-	-	74	-	26
6 Aqueous phase	10	-	-	-	-	90

After ^{13}C NMR analysis, ^{19}F NMR analysis has been performed. Results are presented in the following section.

4.4.2. ^{19}F NMR analysis

The reaction medium, obtained after the fluorobenzylation of the model compounds and containing a mixture of different products, has been also analyzed by ^{19}F NMR. According to ^{19}F NMR experiments, only fluorinated compounds can be detected, hence no signal for the starting material, neither NBu, could be detected. So, the reaction mixture composition, expressed in %, exhibits some differences between ^{13}C and ^{19}F NMR data.

^{19}F NMR analysis results are presented in the Table 4.6 and Table 4.7 and the corresponding NMR signals of fluorinated compounds are illustrated in Figure 4.8.

Table 4.6. Conversion rate and mixture ratio of model compound fluorobenzylation, calculated from ^{19}F NMR data

Compounds	F-Compound *Conversion Rate, %*	MIXTURE COMPOSITION			
		F-derivatized compound, %	FBC reagent, %	FBOH, %	FBOMe, %
1	100	94.5	5.5	-	-
2	100	86.3	6.3	-	7.4
3	100	72.3	23.3	-	4.4
4	98	38.8	55.9	1.1	10.2
5	16	89.7	-	10.3	-
6	0	-	-	100	-
FBC	**-**	99.9	-	0.1	-
FBC reacted	**-**	-	-	100	-

Table 4.7. ^{19}F NMR chemical shifts (in ppm) of fluorobenzylated model compounds

Compounds	δ_F (ppm)	Nature
1	-116.36	**Φ**-OH + Aldehyde (α)
2	-116.49	**Φ**-OH + Ketone (α)
3	-116.89	**Φ**-OH
4	-116.99	**Φ**-OH
5	-117.50	**CH_2**OH
6	-	**CH_2**OH
MeOF	-117.49	**CH_3**OH
FBC (blank)	-115.85	**CH_2**Cl
FBOH	-118.7	**CH_2**OH

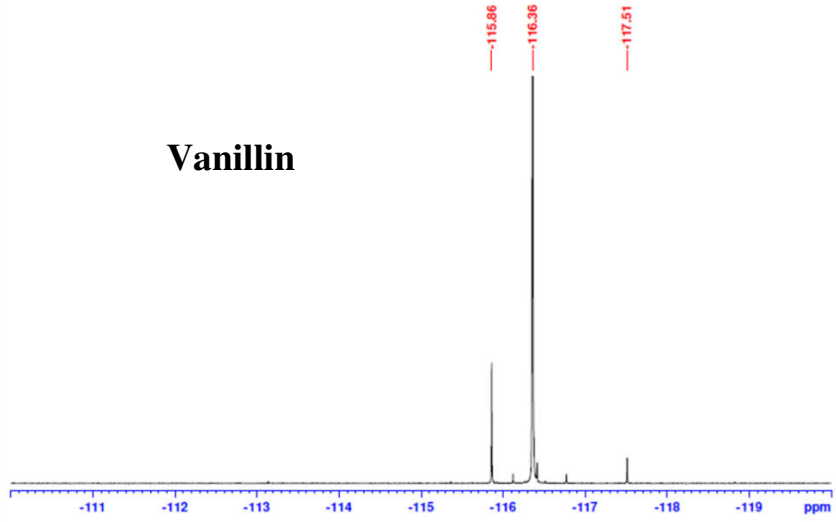

Vanillin

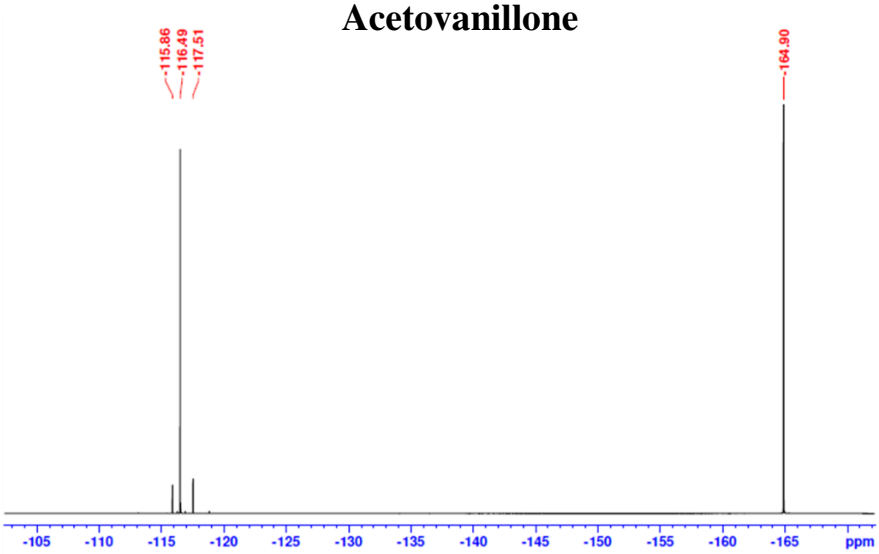

Acetovanillone

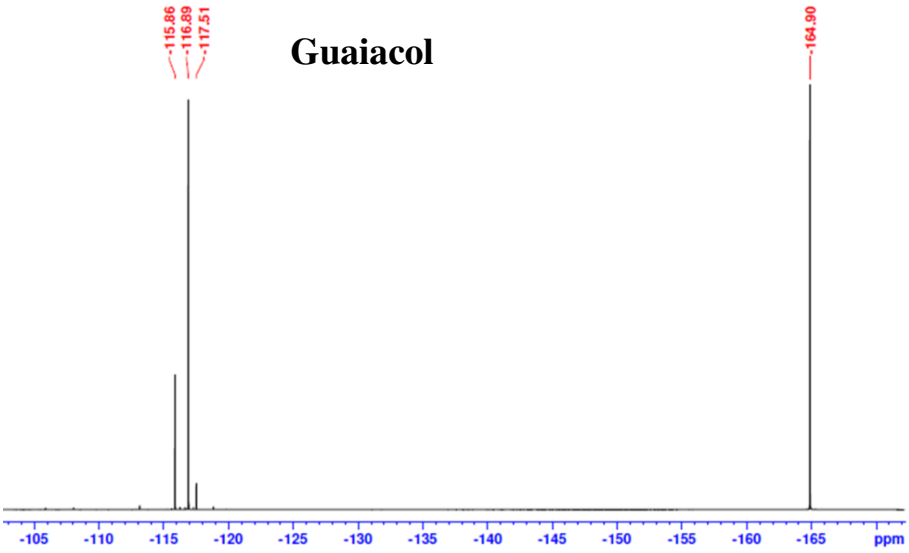

Guaiacol

Vanillylalcohol

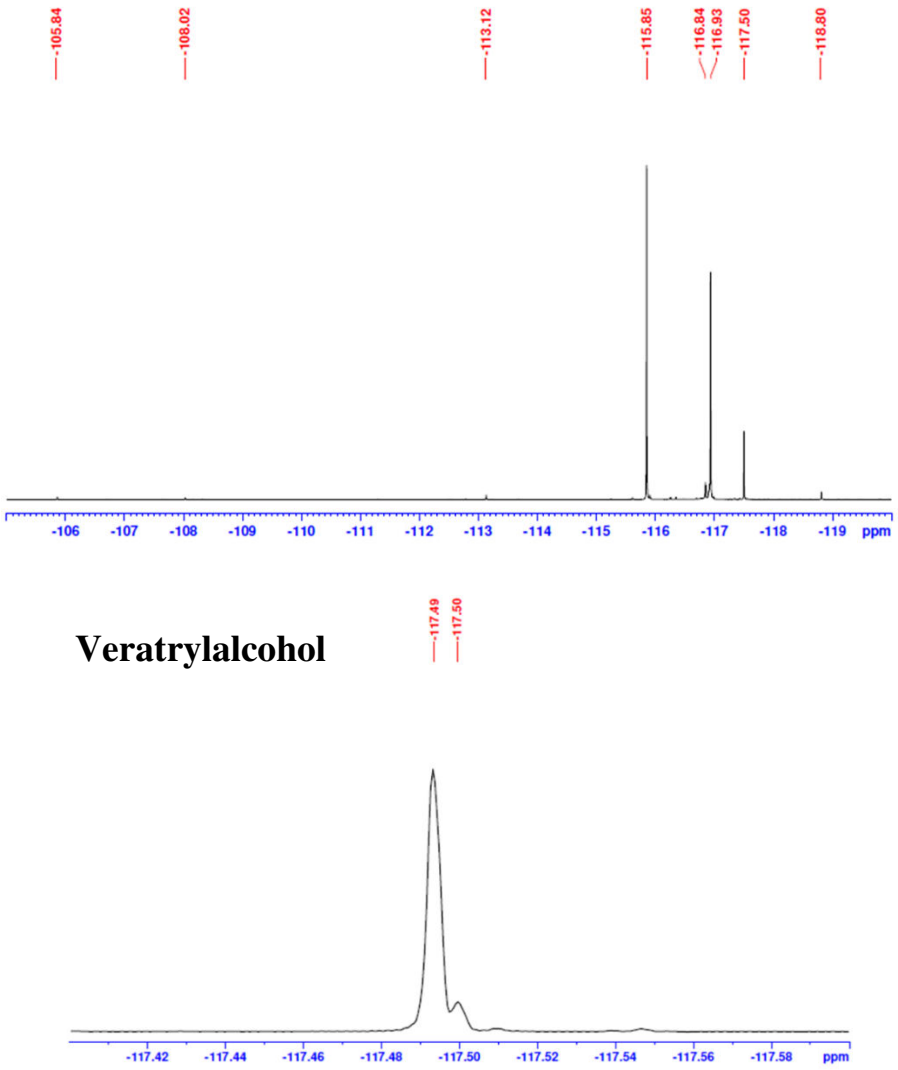

Figure 4.8. ^{19}F-NMR spectra of fluoroderivatized model compounds. From top to bottom: Vanillin, Acetovanillone, Guaiacol, Vanillyl alcohol and Veratryl alcohol.

From ^{19}F NMR results, it could be seen that all the phenolic hydroxyl groups of **1**, **2**, **3** were quantitatively fluorobenzylated giving signals at -116.36 ppm, -116.49 ppm and -116.89 ppm respectively. Concerning the model compound **4**, containing both aliphatic and phenolic OH, ^{19}F NMR confirmed that the conversion took place only in the phenolic region (-116.99 ppm) since no peak has been detected in the aliphatic region. The 98% conversion rate comes from the derivatization of the phenolic hydroxyl group alone. The aqueous phase has also been analyzed but no ^{19}F signal could be detected which confirmed that only phenols could be fluorobenzylated in the studied conditions.

For the model compound **5**, containing only one aliphatic hydroxyl group, after a reaction time of one day, the conversion rate was very low, around 16% (Table 4.6). The signal of the detected fluoroderivatized compound is assigned at -117.50 ppm (Table 4.7). Even after a longer reaction time,

3 days (Table 4.8), F-derivatized compound conversion rate did not increase; and simultaneously the byproduct quantity rose, confirming the ^{13}C NMR results: aliphatic hydroxyls are poorly reactive.

Table 4.8. Conversion rate and mixture ratio of Veratryl alcohol (**5**) fluorobenzylation carried out using modified operating conditions, calculated from ^{19}F NMR data

Compounds	F-Compound *Conversion Rate, %*	MIXTURE COMPOSITION			
		F-derivatized compound	FBC reagent, %	FBOH, %	FBOMe, %
5 1 day	16	89.7	-	10.3	-
5 3 days	12	4.9	46.0	0.6	48.5

In the case of cellobiose (**6**) (Table 4.6 and Table 4.7), no ^{19}F signal could be detected in both aqueous and organic phases. Moreover, it can be seen that the organic phase contained 100% of FBOH originating from the reaction between FBC and water. The result is consistent with ^{13}C NMR data: hydroxyl groups of carbohydrates are not reactive.

Table 4.9. Conversion rate and mixture ratio of cellobiose (**6**) fluorobenzylation, calculated from ^{19}F NMR data after analysis of the organic and aqueous phases

Compounds	F-Compound *Conversion Rate, %*	MIXTURE COMPOSITION			
		F-derivatized compound, %	FBC reagent, %	FBOH, %	FBOMe, %
6 Organic phase	0	-	-	100	-
6 Aqueous phase	0	-	-	-	-

After studying the fluorobenzylation yield of lignin hydroxyl groups, the ^{19}F NMR chemical shift assignments given by Barelle (Barrelle et al., 1992; Barrelle, 1993, 1995) have been controlled since working on folding spectra may have induced wrong assignments. It is pointed out that the whole spectral window has been examined in this study. From the presented ^{19}F NMR chemical shifts for all investigated fluoroderivatized model compounds, it is clearly seen that the general shape of the signal agrees with the work of Barrelle. Chemical shifts from -115 ppm to -117.3 ppm correspond to the phenol group region, whereas poor reactive (16% in the total conversion in the case of veratryl alcohol) primary aliphatic hydroxyl groups give signal between -117.3 ppm to -118.5 ppm. Moreover, in the phenol region, phenol with a C=O in α position could be distinguished since they lead to chemical shifts between -116.2 ppm to -116.6 ppm, which again falls in agreement with the observations of Barrelle.

To conclude, ^{13}C and ^{19}F NMR results are in agreement with HPLC analyses and confirmed that the conversion of phenolic hydroxyl of (**1**), (**2**), (**3**), and (**4**) model compounds was fully achieved whereas the Veratryl alcohol (**5**) conversion was poor. Therefore, the results clearly establish that fluorobenzylation is fully efficient on phenolic hydroxyl groups and less efficient on aliphatic hydroxyls, and that no reaction occurs with saccharides.

4.4.3. Hydroxyl groups quantification of the technical ORG- lignin by ^{19}F NMR

Based on model compounds reactivity towards fluorobenzylation, lignin derivatization and solubility has been controlled. The commercial organosolv lignin sample (ORG) from CIMV Corporation (France) has been analyzed using ^{19}F NMR after fluorobenzylation. The ^{19}F NMR spectrum is given in Figure 4.9. Signal assignment was made with the help of the lignin model compounds ^{19}F NMR spectra. The finest signal at -118.7 ppm was assigned to FBOH originating from the reaction of FBC with water. As seen from the previous sections, signals between -117.3 to -118.5 ppm were associated to aliphatic hydroxyl groups present in the lignin. Aromatic hydroxyl groups region were assigned from -115 to -117.3 ppm in which a part of signal (-116.2 to -116.5 ppm) corresponds to the existence of compounds containing α C=O group and -115.8 ppm was assigned for FBC. The ^{19}F NMR spectrum of analyzed model compounds clearly established the assignment of ORG lignin which therefore can be used for understanding other lignin samples.

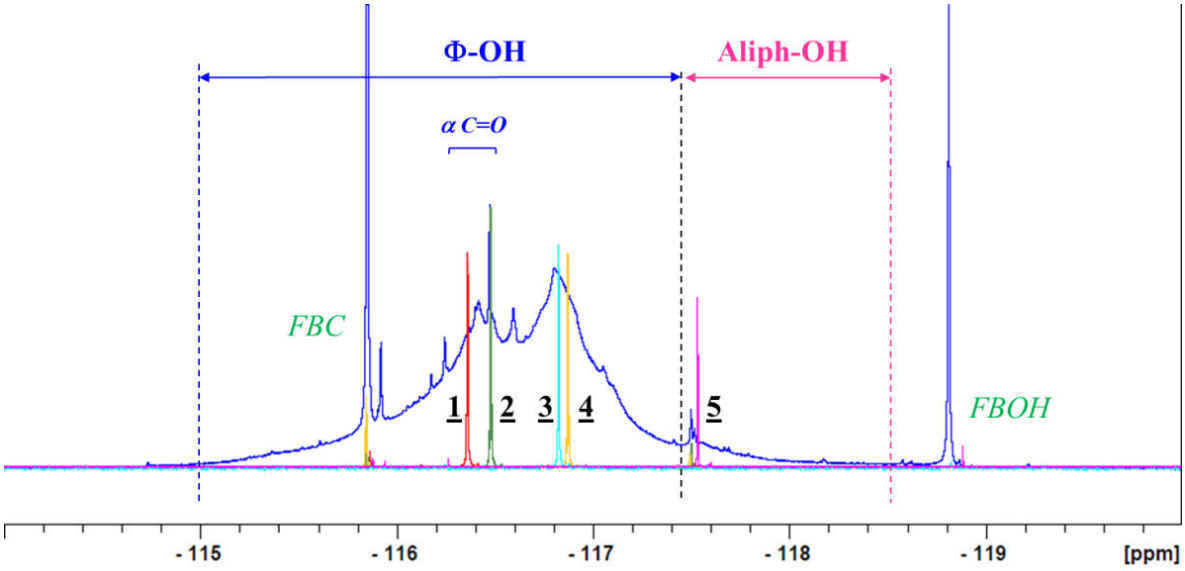

Figure 4.9. Comparison of ^{19}F-NMR spectra of fluorobenzylated ORG lignin (in blue) and derivatized model compounds. (*Note: Only phenol derivatization for* ***4***).

After ^{19}F NMR signal assignment, OH function quantification has been done by integrals comparison with an internal standard, the 2-fluoroacetophenone exhibiting a signal at -112.86 ppm.

According to ^{19}F NMR quantification, the ORG lignin contains 1.71 mmol of phenolic hydroxyl groups per gram of lignin and 0.120 mmol of primary aliphatic hydroxyl groups per gram of lignin. The phenolic hydroxyl group result is in the same order as those obtained using the Fast method (1.5 mmol/g) , UV method (1.7 mmol/g) and ^{13}C NMR after lignin acetylation (2 mmol/g). However aminolysis method overestimated the phenolic hydroxyl group with a quantity of 2.4 mmol/g lignin (Serrano Cantador et al., 2018). This confirmed that ^{19}F NMR is a robust method for phenolic hydroxyl group quantification in lignins.

4.5. Solubility of fluorobenzylated ORG lignin

In this section, the interest of the fluorobenzylation reaction to enhance lignin dissolution prior to size exclusion chromatography (SEC) analysis for lignin molar mass determination is investigated. Indeed free phenolic and aliphatic hydroxyl groups present in the lignin macromolecules increase their polarity and limit their solubility in SEC solvents, either non-polar or partially polar (like THF, DMF or DMAC), due to the formation of aggregates through intermolecular interactions of hydroxyl groups (Sarkanen et al., 1981, 1984; Pellinen and Salkinoja-Salonen, 1985a). To overcome such a difficulty, acetylation is usually performed prior to lignin SEC analysis despite some limitation as an incomplete reaction and aggregates formation. Moreover, acetylation requires long reaction time (Baumberger et al., 2007) to achieve maximum derivatization and even after acetylation, derivatized lignins may not be fully soluble in THF (Asikkala et al., 2012). Incomplete lignin solubility in chromatographic solvents is a major source of error in SEC analysis. Compared to acetylation, the reported fluorobenzylation is easy to handle. In addition, the substitution of hydroxyl functions by fluorobenzyl groups should decrease the polarity of the macromolecule due to the addition of aromatic non-polar fluorobenzyl unit better than acetyl group (acetylation) for polarity reduction and thus increase significantly the solubility in SEC non polar solvent (THF).

The solubility in THF has been examined on the fluorobenzylated ORG lignin using UV spectrophotometry and compared with acetylated and underivatized lignins. Un-derivatized and derivatized lignins were dissolved in THF (5mg/mL). After 1h of dissolution time, the solutions were filtered using a 0.45µm PTFE filter to remove insoluble particles. Then the filtrate was diluted up to 25mL using THF before UV analysis. Underivatized, acetylated and fluoroderivatized ORG lignins were dissolved at the same concentration in THF and analyzed by UV spectrophotometry at a wavelength close to 280 nm, in the region of maximum light absorption by lignin (Figure 4.10).

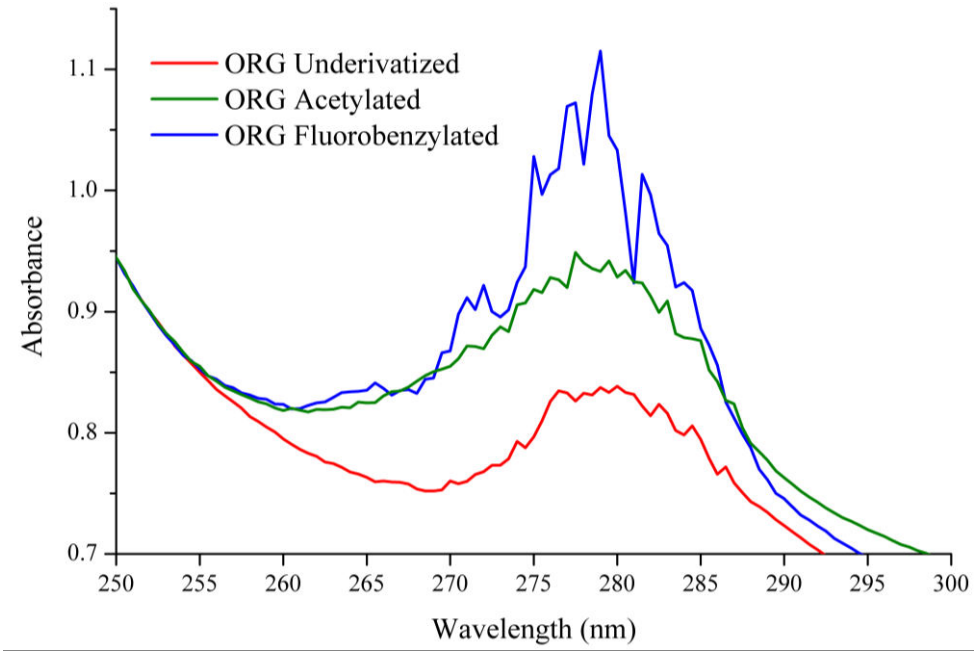

Figure 4.10. Absorbance spectra of dissolved derivatized and underivatized ORG lignins in THF

The comparison of the UV spectra clearly shows that the fluorobenzylated lignin exhibited a higher absorbance. Thus, fluorobenzylation noticeably increased the lignin solubility in THF solvent, more than acetylation, which is suitable for SEC analysis. Thus, the molar mass distribution (MMD) of technical lignins will study after lignin fluorobenzylation. The SEC results and the interest of lignin fluorobenzylation for MMD determination will be discussed in the following Chapter 5.

4.6. Conclusions

This study re-investigated the ^{19}F NMR signal assignment of fluorobenzylated lignin and confirmed the chemical shift values (Sevillano et al., 2001) using lignin based model compounds. Fluorobenzylation reactivity has also been investigated. Complete derivatization is obtained with model compounds containing only phenolic hydroxyl groups whereas for the model compounds containing both aromatic and aliphatic hydroxyls, fluorobenzylation is partial for the aliphatic group. In the case of compounds with only primary aliphatic hydroxyl group, the derivatization is slow and not complete: fluorobenzylation is thus fully efficient on phenolic hydroxyl groups but hardly efficient on aliphatic hydroxyls. Moreover, no fluorobenzylation was observed with a carbohydrate model compound (cellobiose) meaning that lignin sugar contamination should not interfere with the lignin analysis. Fluorobenzylation has also been applied on the commercial organosolv lignin. Based on the obtained results from the model compounds, organosolv lignin signal assignment and chemical shifts were aligned precisely and the hydroxyl groups were quantified using ^{19}F NMR. The obtained phenolic hydroxyl content value is close to those acquired by the Fast, UV and ^{13}C NMR results and aminolysis method overestimated the phenolic hydroxyl content. Fluorobenzylation could also be

successfully applied prior to lignin dissolution for SEC analysis since fluorobenzylation increased the solubility of the macromolecule. The detailed SEC results will be discussed in the following chapter.

CHAPTER 5

5. A new universal calibration method for lignin size exclusion chromatography (SEC) analysis using novel chemical derivatization methods

5.1. Introduction

Molar mass distribution (MMD) is considered the key parameter to understand the reactivity and physiochemical properties of lignin in order to find the alternate way for substituting petrochemical based aromatic compounds (Pellinen and Salkinoja-Salonen, 1985a; Baumberger et al., 2007). For instance, lignin molecule can be used for polymer synthesis applications, but the exact MMD of the lignin sample should be known prior to use (El Mansouri and Salvadó, 2006). Various techniques have been employed to determine the weight-average molar mass of polymers, M_w, and the number-average molar mass of polymers, M_n, such as light scattering, ultra-centrifugation, membrane filtration, mass spectrometry and pulse-field gradient NMR spectroscopy, and some of these methods have been applied to lignin. In principle, crossing some of these methods should help to determine the real molar mass distribution (MMD) of lignin, but still, a large area of uncertainty remains, and some of these techniques are not accessible for routine experiments.

In recent decades, size-exclusion chromatography (SEC) has become the most popular analysis for determining the MMD of various polymers, and it has also been applied for lignin analysis for several decades. The principle of SEC is size separation of macromolecules at different elution time in a column filled with a nanoporous gel, using a suitable, non-interacting solvent as eluent. Complementary to SEC separation, a series of in-line detectors such as UV-visible spectrometer, differential refractometer (DRI), light-scattering (LS) detector, viscometer and fluorescence detector can be placed in-line at the end of the column set, which enables to calculate the MMD independently without relying on the column standard calibration. In general, these detectors also provide complement information to the SEC chromatogram, qualitatively and quantitatively, regarding MMD

and others parameters, such as functional groups content, fluorescent properties, intrinsic viscosity, hydrodynamic radius, gyration radius, which are typical parameters depending of the polymer nature and configuration in the solvent used.

The simplest SEC analysis uses the principle of standard calibration and requires the presence of only in-line concentration detectors, generally UV-visible spectrophotometer or differential refractometer (DRI). Monodisperse polymer standards dissolved in the eluent are used to build a standard calibration curve, which is a linear plot of (log M) as a function of the sample retention time (RT) – or its elution volume (V_r). Unknown polymer sample mass is then calculated from the retention time (RT) in the column. However, in the case of lignin, no standard is commercially available. This is why other polymers standards like polystyrene are often used, which makes quantification inaccurate. Another drawback of methods based on RT only is the phenomenon of flow dispersion through columns, valves and tubing, which is a cause of peak enlargement. Mathematical corrections are theoretically possible to account for this, with more or less accuracy.

To overcome these drawbacks, molar mass detectors have been added in-line, typically light-scattering (LS) detector or viscometric detector. The former measures the static scattered light intensity and by coupling this information with polymer concentration determined by the DRI, the value of M_w is derived, applying Lord Rayleigh's theory. The latter measures the differential pressure between two flow paths in capillaries, one with a higher viscosity containing the polymer in solution, the other containing the pure solvent. Again coupling with the DRI measurement, the polymer intrinsic viscosity is determined as being equal to the specific viscosity calculated at the very low concentration used for these measurements. Both of these coupling techniques, DRI-LS and DRI-viscometry have been slowly developed in-line to SEC for various polymer applications during the last 40 years.

The system used in our laboratory is illustrated in Figure 5.1 below.

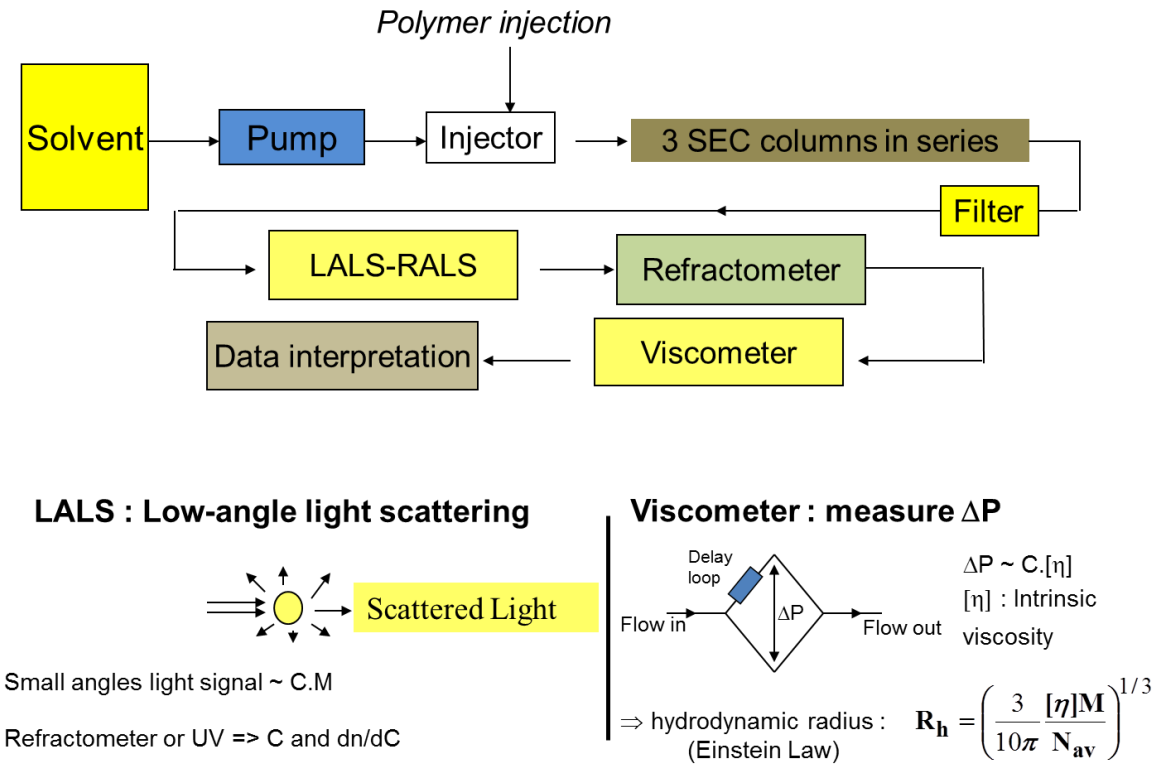

Figure 5.1. A schematic diagram of SEC setup for molar mass distribution, intrinsic viscosity and hydrodynamic radius measurement equipped with several detectors

In principle, LS detector coupled to DRI allows an exact quantification of the molar mass provided the solvent refractive index (n) and the refractive-index increment (dn/dC) of the polymer-solvent system are both accurately known. This is generally not a difficulty, since the dn/dC can be easily determined by injecting a pure polymer sample (mono- or polydisperse) at a known concentration and integrating the DRI signal. A main condition is that the polymer should not be retained in the column.

Unfortunately, in the case of lignin analysis, the DRI-LS coupling method exhibits poor applicability, since several conditions are not satisfied: molecules should be non-light-absorbing, non-asymmetric and non-fluorescent, which is not the case of lignin. Recently, technical progress arose on classical apparatuses: (1) the availability of fluorescent filters; (2) possibilities of light-absorption correction using the signal of one diode in a MALS instrument (Wyatt Co.), and (3), use of polarized light. In theory, corrections of this type should render possible the use of DRI-LS in the case of lignin. But in France, this technique (from Wyatt Co.) is presently available in only one academic laboratory, and there is no current information on the instrument precision in the case of lignin.

As already mentioned, UV-viscometry has also been proposed (Chum et al., 1987; Himmel et al., 1989) as another possible in-line detection technique for lignin analysis. It allows to establish a so-called “universal calibration curve”, following the well-known theory established by Benoit et al.

(1966). In this method, standard polymers of known mass M and intrinsic viscosity [η] (in fact the specific viscosity measured at very low polymer concentration) are eluted through the column. The curve of Ln (M×[η]) versus RT is then constructed, with the noticeable particularity that it should follow a unique straight line for different kind of polymers with rather proximate space configurations, when pure exclusion by apparent volume takes place (ideal behavior). This straight line is called "universal calibration curve". This holds if the hydrodynamic principle of separation applies correctly. Then, simply measuring the RT and [η] value of an unknown polymer, like lignin, allows the calculation of its molar mass, using the universal calibration curve established with other types of polymers for which standards are available.

Numerous SEC studies have been conducted for different lignin samples and model compounds in different media, aqueous or organic, with different polarities (Pellinen and Salkinoja-Salonen, 1985b; Stenlund, 1976). Aqueous SEC is made in alkaline conditions (NaOH), in which lignin dissolves rather well. The advantage is that rather rapid dissolution is obtained, and no pre-derivatization is required. Aqueous media is applied for strong hydrophilic lignin, for example, lignosulfonates. Sarkanan et al. (Sarkanen et al., 1981, 1982) reported the use of mixed Sephadex G gel with 0.1 M NaOH to determine the MMD of lignins. Similarly, various authors used water and dioxane mixture with Sephadex G gel and LH gel to analyse lignin-related materials. However, typically, the acidic groups (phenolic and carboxylic groups) present in the lignin dissociate at high pH and thus form polyelectrolytes. This greatly influenced lignin performance in aqueous SEC. Various factors affected the elution behaviour, such as molecule expansion, ion exchange, ion exclusion, ion inclusion and even adsorption (Barth, 1980). These factors lead to delayed sample elution and obtaining a narrow distribution was difficult. For this reason the use of aqueous GPC has been much discussed (Chen and Li, 2000). Rather recently, Gosselink et al. reported that in aqueous SEC, the use of hydrophilic TSK gel (Toyopearl HW-55(F)) and 0.5 M NaOH as eluent would minimize ionic interactions and adsorption to the column.

In organic SEC systems, two kinds of organic media or eluent have been used: either polar organic solvents, or non-polar solvents (THF, chloroform, toluene). In the former case, dimethysulfoxide (DMSO), dimethyformamide (DMF) and dimethylacetamide (DMAc) are mostly reported, and in the latter case, THF as the most popular non-polar solvent used in SEC. Using polar solvents enables direct lignin dissolution without the requirement of derivatization. However, some association effects remain and this phenomena can be partially reduced by adding lithium salts (LiCl, LiBr) (Chum et al., 1987). Lignosulfonates, Kraft lignin, alkali lignin, steam explosion and Organosolv lignin samples can be analysed with this system (Gosselink et al., 2004; Ringena et al., 2006). Using THF requires derivatization of polar functions (Gellerstedt, 1992). The solubility of lignin in the eluent is also much increased thus inhibiting aggregation or association effects. This particular method is assumed to be

the most efficient and reliable, because of good sample dissolution and stability in the solvent, and narrow distributions can be obtained. Several derivatized lignin samples, such as Milled-Wood-Lignin (MWL), Organosolv lignin, Kraft lignin, Steam-explosion lignin have been accurately analysed using organic THF system (Baumberger et al., 1998; Faix and Beinhoff, 1992; Kubo et al., 1996; Thring et al., 1996). Although, this method has several advantages, the main drawback is the requirement of derivatization that might present conditions for partial degradation or selective recovery of the polymer, depending on size of the recovered fractions. Reaction conditions and lignin recovery by evaporation and/or precipitation should thus be optimized to overcome such issues.

As mentioned before, the effects of polymer association, due to lignin polar interactions, have been studied by several researchers (Lindström, 1979, 1980; Sarkanen et al., 1981, 1982, 1984; Cathala et al., 2003; Connors et al., 1980; Norgren et al., 2002). Such behavior increases LS and viscometric signals, leading to overestimation of the molar mass. The formation of association complexes dominates in the case of underivatized lignins in a variety of solvents, including non-aqueous solvents (DMF, DMSO, THF) and water-NaOH. In non-aqueous solvents without added electrolyte, the formation of such complexes can increase the molar mass by as much as three order of magnitude (Tolbert et al., 2014). Lignin-carbohydrate complexes are also present, and the elution properties of low molar mass carbohydrates in Sephadex G25/dioxane-water (1:1) and Sephadex LH 20/DMF were affected by the existence of aromatic groups in lignin-carbohydrate complexes, which cause retardation due to adsorption effects (Kristersson et al., 1983). Similarly, the adsorption forces between gel and lignin molecule, polarity and poor solubility issues led to elution retardation and apparent underestimation of the molar mass (Chum et al., 1987). Lignin association in DMSO or DMF can be avoided by improving solvation of the sample molecules and by forming H-bonds with electrolytes (Brown, 1967; Connors et al., 1980; Kristersson et al., 1983). The addition of LiCl to DMF decreases lignin association and bimodal elution turned to a single peak (Connors et al., 2009). Similarly, Chum et al. (1987) used HPSEC because of its broad availability and provide a wide range of molar masses (200 to 3.10^6 Da) of acetylated alkali lignin, organosolv lignin and ball-milled lignin in styrene-divinyl benzene (SDVB) copolymer gels with DMF alone or DMF/LiBr as eluents. The result of DMF alone exhibited multimodal elution behaviour due to aggregation phenomena, whereas the addition of 0.1M LiBr reduced lignin aggregates. Gosselink et al. studied molar mass determination of Alcell^{TM} Organosolv lignin using HPSEC with different organic solvents: DMF/LiCl 0.2 M, and THF. The weight-average molar mass (Mw) was considerably lower in THF. It was concluded that HPSEC of lignin in organic solvents provides poorly comparable inter-laboratory results (Gosselink et al., 2004). Previously, the same conclusion had been drawn by Milne et al. on different lignins analysed under identical standard conditions (Milne et al., 1992).

The early studies from Brown et al., and Faix et al., had evidenced that to decrease aggregates for SEC analysis due to polar hydroxyl groups, derivatization by various methods, typically acetylation, silylation and methylation was crucial (Brown, 1967; Faix et al., 1981). Plant source, isolation method, functionality and molar mass distribution are determining factors for the solubility of lignin in chromatographic solvents. Moreover no universal SEC method is available for all types of lignins and in most of studies in the past, columns containing non-polar polystyrene gels, eluted with THF, have been used to calculate the more reliable MMD for different variety of lignins (Faix, 1992).

In most studies, the SEC columns are calibrated by polystyrene standards which are commercially available. Lignin model compounds have also been used as standards, with molar mass determined by ultracentrifugation. The molecular weight is calculated by Svedberg equation taking into account sedimental and diffusion coefficients (Umoren and Solomon, 2016). Siochi et al. performed hydroxypropylation of Organosolv red oak lignin and determined the absolute molecular weight using SEC/LALLS (low-angle light scattering detector) and SEC/viscometry (differential viscosity detector). Using SEC/LALLS, M_w of Organosolv red oak lignin was found to be 11500 Da, whereas SEC/viscometry provided a M_w value of 3852 Da. Thus the obtained values with SEC/LALLS were three times higher than with GPC/DV. The authors suggested that the obtained results from SEC/LALLS were complicated because of the influence of sample absorbance and fluorescence, and the need for light-polarization correction. Nevertheless, the author proposed SEC/viscometry as convenient and quite acceptable to study the absolute lignin MMD (Siochi et al., 1990).

Glasser et al. (1993.a) studied the absolute MMD of hardwood, softwood and annual plant lignins produced by Kraft and Organosolv pulping processes, also using SEC/viscometry. A universal calibration curve was established with polystyrene standards. The results illustrated that the investigated lignins (Indulin AT, Indulin, Eucalin, Organosolv lignin, Alcell lignin, HSPA-bagasse) have M_w values between 3000 and 20000 Da, polydispersity values between 2 and 12, Mark-Houwink-Sakurada exponential factors (α) value in the range of 0.17 to 0.35, and intrinsic viscosities between 3.7 and 8 mL/g.

Cathala et al. (2003) stated that DMF is known for lignin aggregation effect in SEC. To investigate this effect the author has chosen spruce milled-wood-lignin (MWL) and guaiacyl lignin polymers model (DHP) for MMD study in SEC – DMF solvent using light scattering detector. The results showed that bimodal elution profile occurred due to association effects between the molecules. To account for these effects, the authors fractionated the lignin samples in THF and stated that THF-soluble fractions were responsible for low molar mass part and THF-insoluble fractions were responsible for higher molar mass corresponding to DMF elution profile. The different molar mass

fractions were acetylated to break the association effect and characterized by SEC in THF and THF-LiBr, combined with online viscometric detection and universal calibration. The authors observed that Mark-Houwink-Sakurada plots exhibited low MH-α exponents, which clearly indicates that the polymers matrixes are collapsed in THF and THF-LiBr. These results apparently revealed that THF and THF-LiBr would be rather poor solvents even for acetylated samples. Moreover, the authors concluded that MWL and DHP molar mass in DMF was higher than 50000 – 60000 Da, due to aggregation (Cathala et al., 2003).

Collaborative study of SEC analysis on technical lignins has been performed by the Eurolignin network in an effort to standardize the SEC method. The authors performed acetylation using 1:2 v/v of pyridine/acetic acid anhydride, stirring at room temperature for 6 days prior to the SEC analysis in THF and styrene-divinylbenzene columns. The authors studied acetylated bagasse soda lignin without and with removal of insoluble fractions in the acetylation mixture. They reported that removal of insoluble fraction led to a lower proportion of higher molar mass fractions (Baumberger et al., 2007).

Nowadays, HPSEC are commonly operated using acetylated lignins and styrene-divinylbenzene columns and the results are referred to polystyrene calibration, although unprecise for lignin derivatives, because of still-existing unclear association effects of non-polar lignin even after derivatization (Pellinen and Salkinoja-Salonen, 1985a).

Incomplete lignin solubility in chromatographic solvents is also an important source of error to investigate lignin molar mass. As already discussed, derivatization partially overcomes this difficulty and acetylation is most often used (Baumberger et al., 2007; Hatfield et al., 1999). The latter studies have shown that using long reaction time, over 6 days, more than 90% dissolution in THF is attained. But with same duration, Asikkala et al. reached only about 60% solubility in THF of Norway spruce MWL (Asikkala et al., 2012). These authors developed a “universal derivatization” using acetylbromide in glacial acetic acid to obtain complete dissolution in 30 min in THF. In these conditions, derivatized sample degradation appears after one month of aging at room temperature.

As already mentioned, polystyrene is the most often used standard although its linear structure differs much of that of lignin, partially cross-linked. Lignin-like model compounds have been used for calibration and the obtained M_w values were 2 to 3 times higher than with polystyrene calibration (Faix and Beinhoff, 1992). DRI, LALLS and RALS (right-angle LS detector) coupled detectors were used to measure the molar mass of acetylated lignin samples in THF, although with some difficulties linked to imperfect solubilisation. In another study, lignin fractions were separated by preparative SEC, reaching dispersity value near to one, and such fractions were compared to polystyrene standards. Lignin fractions and polystyrene standards exhibited similar behaviour over a wide range of molecular weight (Botaro and Curvelo, 2009).

Viscometry and other techniques, like MALDI-TOF-MS (matrix-assisted laser desorption ionization time-of-flight mass spectrometry) have been reported in several studies to measure absolute mass values. MMD by universal calibration was carried out on acetylated and hydroxypropylated lignins in THF (Himmel et al., 1989; Siochi et al., 1990; Cathala et al., 2003; Gosselink et al., 2004; Glasser et al., 1993). SEC with off-line MALDI-TOF-MS was originally proposed by Jacobs and Dahlman (Jacobs, 2000; Jacobs and Dahlman, 2001; Rönnols et al., 2016) and later also studied by Gosselink (Gosselink, 2011). However, MALTI-TOF has a limitation that the matrix plays a major role in desorption/ionization process. This is illustrated for instance in the study of Wetzel et al., that dealt with the analysis of polyethylene glycol, which showed two different fragmentation pattern in 2,5-dihydroxybenzoicacid and dithranol matrixes (Wetzel et al., 2003).

As a summary, despite the number of studies and techniques investigated until now, there is still a significant uncertainty about the real lignin molar mass values, and about the choice of a reliable method to use. There is still room for improvement, as illustrated by the recent work of C. Crestini's group (Lange et al., 2016). This author studied the accurate MMD of different derivatized lignins (acetobromination, acetylation and benzoylation) with three column setup connections and standard calibration. The results stated that three column setup and two detectors set up (poly diode array- PDA and RI) significantly influenced the quality of SEC results.

Therefore, this chapter focuses on SEC analysis (SEC) of 5 different commercial lignins, using different types of derivatization and different solvents systems: Protobind 1000 (PB), Organosolv (ORG), Indulin (IND), softwood kraft (KR) and Eucalyptus kraft (EU-KR) in organic solvents (DMAc/LiCl and THF). Washing as a pretreatment has been carried out with different solvents (ethanol, ethylacetate and hexane) prior to SEC analysis. MMD of the different derivatives (acetylation, fluorobenzylation and fluorobenzoylation) where compared to that of underivatized lignins. MMD obtained using direct dissolution in DMAc/LiCl, PolarGel M (Agilent Co.) column setup, and direct dissolution and standard calibration, were compared to using derivatization, PLgel column setup, dissolution of derivatives in THF solvent, and universal calibration using an in-line coupling DRI-viscometry.

5.2. Materials and Methods

5.2.1. Technical lignins

5.2.1.1. *Commercial lignin samples*

Four industrial lignin samples were used in this study: (i) Soda lignin from wheat straw (Protobind 1000) (PB) was purchased from Green Value Enterprises LLC, (ii) Kraft lignin from pine (KL) was provided by the Centre Technique du Papier (CTP) (Grenoble, France), (iii) Organosolv lignin (ORG)

(namely BioLignin® CIMV process using formic acid/acetic acid/water at 185-210ºC) from wheat straw was purchased from CIMV Company, and (iv) Kraft Indulin AT lignin (IND) was purchased from DKSH Switzerland Ltd (Serrano et al., 2018).

5.2.1.2. *Eucalyptus Kraft lignin preparation at lab scale*

Eucalyptus chips were cooked using the Kraft pulping process. 3 batches of 1200 g of wood chips were cooked using technical grade Na_2S and NaOH solutions. Effective and active alkalis were respectively 25 and 30% of NaOH on wood. Sulphidity was adjusted to 30% and the liquor on wood ratio was 8. Dry matter content of wood chips was measured as 87.4%. Cooking conditions used were heat up time of 40 min from 20˚C to 165˚C followed by plateau time of 80 min at 165˚C. After completion of cooking, 9.5 L of black liquor was extracted and transferred to CTP (Centre Technique du Papier) Grenoble, France, where the lignin was recovered using CO_2 precipitation method followed by washing with diluted sulfuric acid. Around 100 g of Eucalyptus cooked Kraft lignin were obtained from 4 L of black liquor. Kappa number of the pulp was found to be 12.4% and the measured pulp yield was 50.02%.

Chemical compositions including acid soluble and insoluble lignin, total sugar and ash content of the investigated lignin samples can be found in Chapter 3 (Table 3.1).

5.2.2.Derivatizations

5.2.2.1. Acetylation

100 mg of lignin samples (dry matter content basis) were acetylated with 5 ml of pyridine and acetic anhydride mixture (1/1: V/V) at room temperature for 15 h in a round bottom flask with continuous stirring. After the reaction time, the mixture was quenched with 40 ml of 50% aqueous methanol and dried under vacuum. After methanol evaporation, the product was washed with toluene three times (3 x 40ml) to remove residual pyridine and once with 40 ml of 99.5% methanol. Finally, the samples were freeze-dried to ensure total solvent removal.

5.2.2.2. Fluorobenzylation

100 mg of lignin samples were dissolved in 1 mL of NBu (tetra N-butylammonium hydroxide in 1M methanol) and stirred for 1 h at 50°C. Then 10 mL of acetonitrile were added followed by 300 mg of 4-fluorobenzyl chloride (FBC), the derivatizing agent. The reaction mixture was stirred at 50°C for overnight. After the reaction time, the derivatized lignin recovery was performed by precipitation in diethyl ether. Lignin produced a viscous precipitate in diethylether, precipitated again in ice-cold distilled water. This precipitate was filtered through a 0.45 µm PTFE filter, washed with distilled water several times and oven-dried at 50˚C (Barrelle et al., 1992; Barrelle, 1995).

5.2.2.3. Fluorobenzoylation

Fluorobenzylated lignins (100 mg) were dissolved in 2.5 mL of pyridine. After, 4-dimethyl-aminopyridine (DMAP, 2.5 mg) and 4-fluorobenzoic acid anhydride (150 mg) were progressively added into the reaction medium. The mixture was stirred for 48 h at 60˚C. Then derivatized lignins were poured into ice-cold water. The obtained precipitate was washed with distilled water several times and filtered through 0.45µm PTFE filters and dried in the oven at 40˚C followed by FT-IR, SEC and ^{19}F NMR analyses.

5.2.3. Lignin molar mass distribution analyses by SEC

5.2.3.1. SEC conditions

Table 5.1 demonstrates the conditions used for SEC analyses using different columns and different organic solvents DMAc/LiCl and THF.

Table 5.1. SEC conditions used for analysis of lignin samples using DMAc/LiCl and THF systems

	System A: DMAc/LiCl	**System B: THF**
System	Malvern GPCmax + column oven + separate detectors (DiALS + DRI) & Omnisec 4.6	Malvern TDA 302 & Omnisec 4.5
Column	Two polargel M (30 cm x 7 mm) + one pre-column (Agilent Co.)	Three (300 cm x 7.5 mm) PLGel mixed B (10 µm mixed B LS) + one pre-column (Agilent Co.)
Eluent	0.5% of DMAc/LiCl (5g of LiCl dissolved in 1L of DMAc)	Pure THF (HPLC grade)
Flow rate	1 mL/min	1 mL/min
Column temperature	70°C	35°C
Detector	DRI (Differential Refractive Index) (the DiALS detector is not used for data treatment)	DRI, RALS-LALS and in-line viscometer detectors

Standard	Polystyrene (PS) 1660, 10050, 65500, 426600	PS: 1670, 4970, 10030, 28400, 64200 Polymethylmethacrylate (PMMA): 1520, 6840, 13200, 31380, 73850, 135300, 342700, 525K, 1026K, 2095K Cellulose acetate (CA) – polydispersed polymer sample (Aldrich) used as standard
Sample injection volume	100 µL of lignin samples and standards	100 µL of lignin samples and standards
Lignin sample concentration	2 mg/mL	10 mg/mL
Derivatization	Acetylation, Fluorobenzylation, Fluorobenzoylation	Acetylation, Fluorobenzylation, Fluorobenzoylation

5.2.3.2. Calibration curves

5.2.3.2.1. SEC-DMAc/LiCl system – Conventional calibration

Firstly, the calibration curve has been made using system A, with homologous series of PS standards, using the Polargel M column setup in DMAc/LiCl and DRI detection. The logarithm of each molar mass was plotted against the retention volume (V_r) and the plot is illustrated in Figure 5.2.

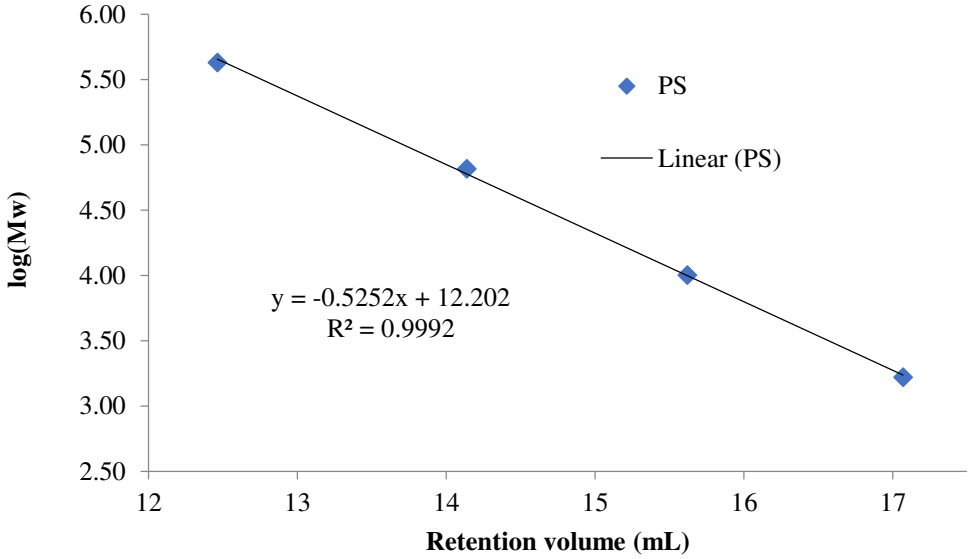

Figure 5.2. Calibration curve of PS in DMAc/LiCl (system A, Polargel column setup)

Recalculated molar mass of PS standards is presented in Table 5.2. It is clearly seen that the deviation between recalculated molar mass and true molar mass for the low molar mass standards is less than 4 % (1660 Da and 10050 Da). However, for higher molar mass standards, the error is significantly higher. Therefore, this method may lead to estimation errors for high-molar mass lignin fractions, above 50 kDa.

Table 5.2. Molar mass (Da) of known PS standards with deviations between recalculated and true M values

M_{true} (Da)	Retention volume (Vr) (ml)	log M_{true}	Recalculated mass (M_{calc})*	Deviation**
1660	17.07	3.22	1726	-4.0%
10050	15.62	4.00	9970	0.8%
65500	14.14	4.82	59700	8.9%
426600	12.463	5.63	453656	-6.3%

* Recalculated mass from the calibration curve obtained by linear regression of log M_{true} vs. Vr

** Deviation = $(M_{true}-M_{cal})/M_{true}$

5.2.3.2.2. SEC-THF – Conventional calibration

For SEC-THF analysis, three different polymer standards were selected (two monodisperse and one polydisperse), with a common point, their linear molecular structure: PS (polystyrene), PMMA (poly methylmethacrylate) and cellulose acetate (polydisperse). The molar mass of each sample is known, either from manufacturer data (case of monodisperse standards), or from the analysis by SEC-LALS/RALS-DRI coupling (using system B in THF, case of cellulose acetate). The plot of log (M) against V_r using system A with DRI detection is shown in Figure 5.3. It is obvious that this conventional method does not produce a unique curve for these different samples, all the data cannot be aligned in a straight line. To estimate the magnitude of the differences in the molar mass estimations using these different calibration curves, different retention times were chosen to calculate the corresponding log (M). Table 5.3 shows that large differences in the estimated molar mass arise from these different calibration curves. The same trend as in Figure 5.3 can be observed, *i.e.,* at the highest mass (lower retention volume), differences in the estimated molar mass M, calculated from the different calibration curves, increases. This is a logical consequence of the fact that the three calibration curves do not align, and moreover, they have different slopes. The general interpretation is that polymers of different chemical nature have not the same density when they are dissolved in the SEC solvent. Since chromatographic separation in SEC columns is based on apparent volume or polymer pellet size rather than by apparent mass, the principle of universal calibration should lead to much improved accuracy for the estimation of the true mass of the polymer.

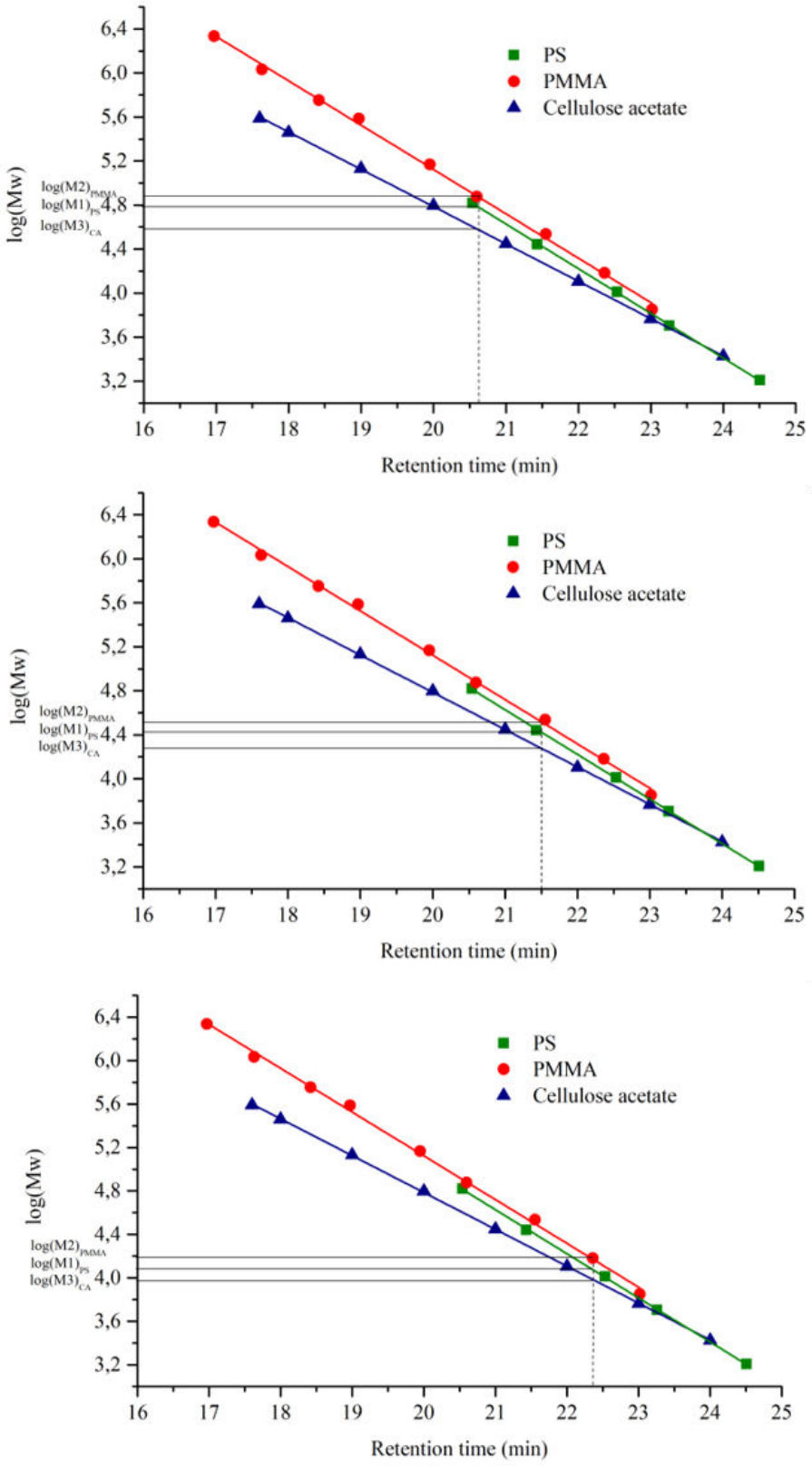

Figure 5.3. Conventional calibration curves of PS, PMMA and Cellulose acetate (CA). Different retention times are chosen to calculate and compare the corresponding log (M).

Table 5.3. Calculation of MW (g mol^{-1}) of different polymer standards obtained from conventional calibration curve at different retention volumes (min)

Retention volume (ml)	Chosen calibration curve						Standard Deviation for M
	PS (standard 1)		PMMA (standard 2)		CA (standard 3)		
	log (M)*	M**	log (M)*	M**	log (M)*	M**	
20.6	4.8	63100	4.9	79430	4.59	38905	20390
21.5	4.42	26300	4.52	33110	4.28	19054	7031
22.4	4.1	12590	4.2	15850	3.97	9333	3258

* read on the corresponding calibration curve at given retention volume

** recalculated from log M

Advantages and disadvantages of conventional calibration method

Advantages: (1) Conventional calibration is the simplest method to find MMD from SEC experiments. Because of its simplicity, this method is still popular and widely used in industries although the accuracy could be questioned. (2) The samples can be thoroughly analyzed in one hour or less. (3) One single detector, providing a stable and accurate response at given polymer concentration, is required for obtaining a chromatogram in order to calculate the MMD of the polymer.

Drawbacks: Accuracy of MMD is guaranteed only when mono-disperse standards for a given polymer are available. For an unknown polymer, the latter should possess the same apparent density in solution as the known standards available, whatever the molar mass in the explored area. Mostly, polystyrene is used as standard for lignin determination. Considering polystyrene, its linear structural arrangement is far from three dimensional cross-linked network of lignin and therefore this method should lead to erroneous estimation of the MMD in the case of lignin.

5.2.3.2.3. SEC-THF – Universal calibration

Universal calibration principle:

This concept relies on the Mark-Houwink-Sakurada (MHS) relationship and was first tested on polystyrene polymers by Benoit et al. (Benoit et al., 1966) who stated that samples were eluted in a SEC column on the basis of their hydrodynamic volume V_h, which determines the elution volume.

The MHS relationship is expressed as: $[\eta] = K'M^a$

where [η] is the intrinsic viscosity of the polymer, expressed in dL/g or in mL/g; *K'* and *a* are Mark-Houwink constants, depending on the polymer-solvent system; M is the molar mass of the polymer in g/mol.

Based on the above equation, different polymer samples with same [η] and M should possess the same hydrodynamic volume (proportional to the product [η].M), if they follow the same MHS relation (same K and a). Thus, they will be eluted at same retention times in a given SEC column. The plot of log ([η].M) vs. retention time should be unique, which is called the "universal calibration curve".

In our study, we have used narrowly distributed standards to calibrate the SEC columns setup of system B. The universal calibration curve was constructed using the in-line SEC-viscometry detector available on system B. Monodispersed (PS, PMMA) and polydispersed (cellulose acetate) polymer standards have been used. The curve of log ([η].M) vs. retention time is presented on Figure 5.4. It should be mentioned that only 8 points were considered for the cellulose acetate calibration curve. It is shown that all samples align on a single linear curve. Himmel et al., (Himmel et al., 1989) stated that according to MHS relationship, "*a"* values of linear and flexible polymers were limited between 0.50 to 0.80. Indeed we found that for all of our investigated polymer standards, *a* and *–K* values lie in this range: for PS, *a* values lie between 0.5 to 0.8, and *–K* between 3.1 and 5.1, respectively; for PMMA, we found 0.6 to 0.8 for a, and 3.5 to 4.9 for K; and finally for cellulose acetate, we found 0.815 for a and 3.94 for -K.

In this method the molar mass of an unknown polymer sample is calculated based on the viscometric response (intrinsic viscosity) and retention volume, and then, substituting these values to the universal calibration curve provides the absolute molar mass of the sample.

In our study, we have made the universal calibration curve using global curve fit and individual curve fit. Global curve fit means that all the three polymer data points were used together, and linearly correlated to build a unique straight-line calibration curve. Individual fit means that one straight-line calibration curve is based on the data of one given polymer. Results of both types of calibration curves were compared.

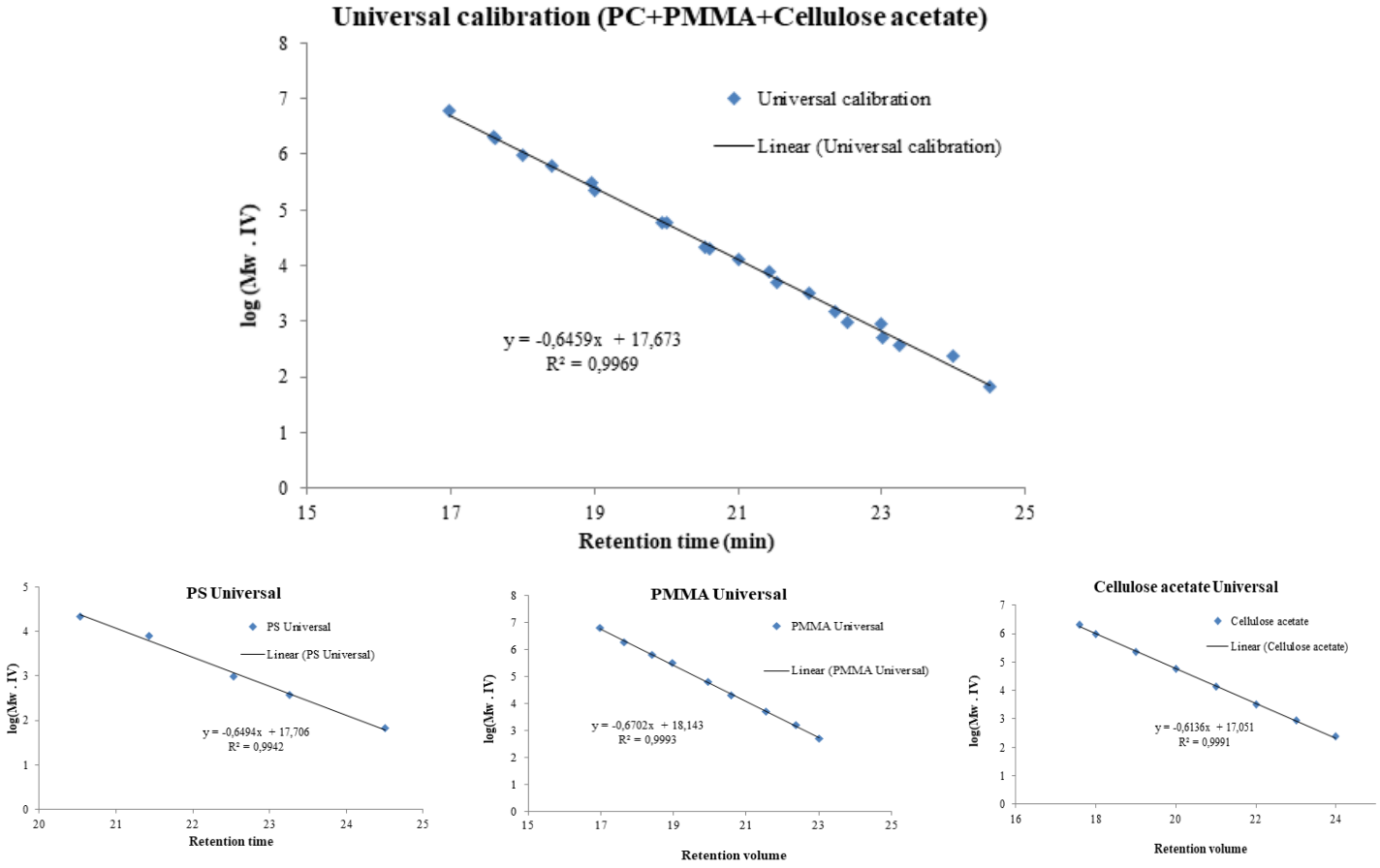

Figure 5.4. *Top:* Global universal calibration curve including all points of PS, PMMA and Cellulose acetate; and *bottom:* Individual universal calibration curves including data of each type of polymer

5.2.3.2.4. Calibration Strategy for the integration of SEC chromatogram

In this study, two different columns (Polargel M and PLgel columns, based on polystyrene divinylbenzene gel) and solvent systems (DMAc/LiCl and THF) were used and five different technical lignins were analyzed.

In the case of system A (DMAc/LiCl and two Polargel M columns), bimodal and trimodal elution curves were found for some typical examples of technical lignins: Indulin and Eucalyptus Kraft lignins chromatogram, as shown in Figure 5.5.

Similarly, in system B using THF and PLgel columns, bimodal elution and long tail in the high molar mass region was found for Organosolv lignin (ORG). In this particular cases, integration of all SEC peaks including the main peak and all the smallest peaks at high elution time, leads to very extended MMD and an unacceptable range of molar mass, considering ORG lignin. In this regard, the

main peak of the chromatogram was only considered for MMD calculation, excluding front-tail and small peaks that arise after the main peak.

In our study, single-peak chromatograms were observed in most of the analysis. In the cases when additional peaks were observed (ex. EU-KR and Indulin), Figure 5.5 shows the procedure for MMD calculation by selecting the particular area of the peak. From the obtained SEC chromatogram, baseline should be adjusted because it is one important parameter in the calculation of the MMD. In our case, the baseline is drawn for the selected peaks, from V_0 (starting of the considered peak region) to V_t (end point of the peak) which is then further integrated. The presented Indulin lignin SEC profile (Figure 5.5) shows a uniform distribution and V_t point is selected when the distribution is close to baseline. However, in the case of EU-KR lignin, the V_t point is chosen from the end of distribution in order to eliminate the second peak on the integration calculation. In the present study, we use this methodology to calculate MMD of lignin samples under study.

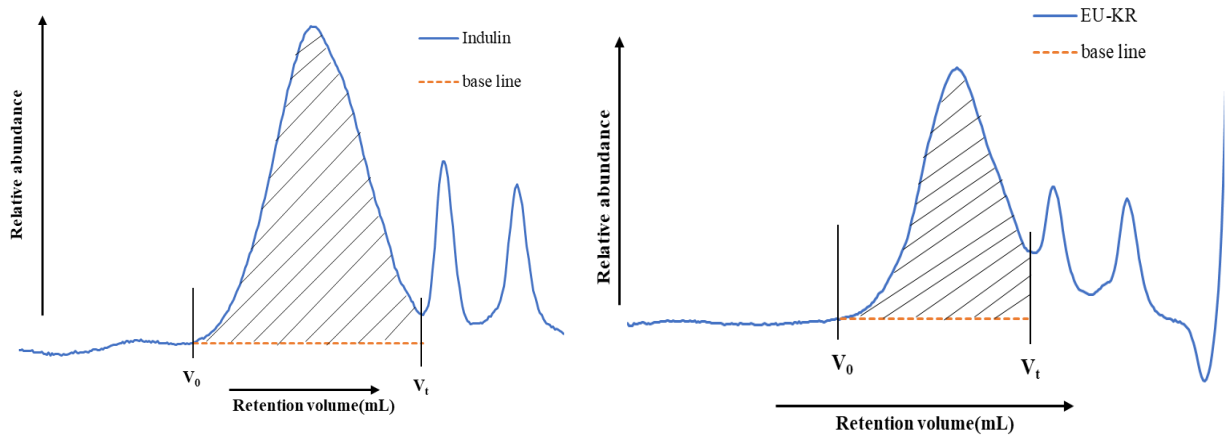

Figure 5.5. SEC chromatograms of underivatized technical lignins, Indulin (*left*) and EU-KR (Eucalyptus-Kraft) lignin, using system A in DMAc/LiCl (*right*). V_0 and V_t represent the start and end volumes used for peak area integration and calculation of the average molar masses.

5.3. Results and Discussion

5.3.1. Molar mass distribution study of crude lignin samples in DMAc/LiCl

Molar mass study of different commercial lignin samples was first performed using system A (SEC- DMAc/LiCl system with Polargel M columns, direct dissolution without derivatization). The obtained SEC and MMD curves are plotted in Figure 5.6. The calculated average molar masses and DP values are reported in Table 5.4.

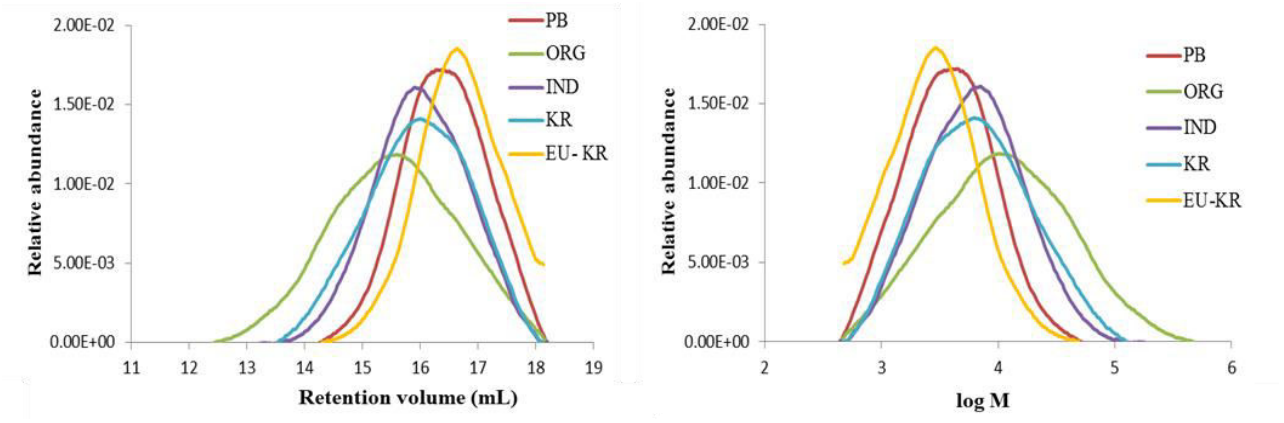

Figure 5.6. SEC chromatograms of underivatized technical lignins in DMAc/LiCl. *Left:* Relative abundance Vs Retention volume (mL). *Right:* Relative abundance Vs log M.

Figure 5.6 shows that the SEC chromatograms exhibit regular profiles except for the ORG lignin with possibly a phenomenon of aggregation, considering the very early elution and more irregular profile. Among the investigated lignin samples, Organosolv lignin contains higher amount of sugar impurities because of lighter extraction process conducted. These molecularly dispersed species interact with different structural elements, resulting in the association of molecular clusters of different densities and resulting in broader distribution curve. The corresponding M_w (25270 Da) value is considerably higher than for other lignins. Eucalyptus-Kraft (Hardwood lignin) and PB (Grass lignin) exhibit the lowest Mw (in Table 5.4) (4080 and 5470). This could be due to more severe cooking conditions: EU-KR was produced by Kraft cooking and PB was recovered from wheat straw cooking using Soda process. Mw of softwood Kraft lignin (Pine Kraft lignin sample and Indulin) were between 9000 – 11500 Da. EU-KR and PB lignins led to low Mn (2000 Da for EU-KR, and 2600 Da for PB). Indulin and Pine Kraft are medium (3400 – 4000 Da). The highest M_n was observed for Organosolv lignin (around 5000 Da). The ratio of Mw/Mn (dispersity) is below 3 for most lignins, except for ORG (equal to 5), revealing more disperse population (likely due to aggregates). Indulin and EU-Kraft exhibited some additional peaks possibly due to sugar or small oligomeric impurities. In the case of EU-KR, only the main peak observed until 18.5 min was considered for the comparison (full chromatogram shown in calculation strategy).

Table 5.4. Average molar mass data (M_n, M_w) / g mol^{-1}, polydispersity (Mw/Mn) and average degree of polymerization (*DPn, DPw*) of underivatized technical lignins in SEC-DMAc/LiCl systems

Sample Name	M_n	M_w	M_w/M_n	DP_n	DP_w
PB1000 (grass lignin)	2,650	5,470	2.1	13	27
Organosolv (CIMV)	4,970	25,270	5.1	25	126
Indulin (softwood)	3,430	9,620	2.8	17	48
Kraft (softwood - Pine)	4,090	11,500	2.8	20	57
Eucalyptus – Kraft (hardwood)	2,030	4,080	2.0	10	20

Note: calculated DP values are based on a mean monomer mass of 200 g/mol for underivatized lignin

Advantages and drawbacks of direct lignin analysis using DMAc/LiCl

Advantages: (1) The analysis can be performed with crude samples, therefore no washing is needed, and it reduces the risk of losing small lignin fractions, and (2) no derivatization is required for lignin samples and hence it avoids the potential risk of sample degradation or small fractions loss during derivatization.

Drawbacks: (1) a very long dissolution time is required for technical lignins, about 4 to 5 weeks, (2) higher probability of forming aggregates in the column could be responsible for obtaining high M_W in some cases, which affects the M_W value in a significant manner, (3) the presence of impurities like residual extractives and sugars may interfere in the apparent MMD determination.

5.3.2.Solvent wash study

Extraction of lignin from lignocellulosic biomass involves tedious chemical processes and the extracted lignin contains certain amount of impurities such as sugars, organic extractives, fatty acids and minerals. The washing of lignin can be performed to remove those impurities to avoid interference with analysis and also increase the purity of the lignin. Numerous studies have been attempted to extract/fractionate as well as enhance the purity of the lignin using various solvents such as water/ethanol mixture, sulfuric acid, deionized water, acetone, dioxane, dichloromethane, ethyl acetate, etc. (Alvarez-Vasco et al., 2016; Barta et al., 2013; Bauer et al., 2012; El Hage et al., 2009; Mansouri and Salvadó, 2006; Schorr et al., 2014).

In this regards, three different solvents are chosen for this thesis work based on their polarity, for instance, highly polar (ethanol), moderately polar (ethyl acetate) and non-polar (hexane) to select a suitable solvent for the rest of the study. Table 5.5 summarizes the solvent properties of the considered solvents and some physical properties (data from website[2]). The relative polarity and dielectric constant of the ethanol are significantly higher than ethyl acetate and hexane. In addition, the hexane has the relative polarity value of 0.009 which is almost negligible compared to the other two solvents.

Table 5.5. Solvent parameters for ethanol, ethylacetate and hexane

Solvent	Formula	Relative polarity*	Dielectric constant (ε)	Boiling point (°C)	Melting point (°C)	Density (g/ml)
Ethanol	C_2H_6O	0.654	24.5	78.5	-114.4	0.789
Ethyl acetate	$C_4H_8O_2$	0.228	6.02	77	-83.6	0.894
Hexane	C_6H_{14}	0.009	1.89	69	-95	0.655

* Relative polarity is normalized with respect to water polarity value of 1.

In the case of solvent wash study, we have considered only PB lignin for benchmark purposes. 1g PB lignin was washed using approximately 60 mL of respective solvent (approximately 16.5 g/L). The obtained results are illustrated in Table 5.6.

Table 5.6. Before and after washing of PB lignin in different solvents and final yield in %

	Solvent	Starting quantity (in g)	After washing (in g)
PB1000 lignin	Ethanol	1	0.291
	Ethyl acetate	1	0.598
	Hexane	1	0.903

It is clearly seen from the Table 5.6 that ethanol-washed PB lignin exhibits lower yield than other solvent-washed lignin samples. The reason of small yield can be directly related to the polarity of ethanol which is relatively high compared to ethyl acetate and cellulose acetate solvents. The obtained yield from our study can be compared with references (Alvarez-Vasco et al., 2016; Bauer et al., 2012) where it is reported that in the case of water/ethanol mixture, the increasing ethanol composition

[2] https://sites.google.com/site/miller00828/in/solvent-polarity-table

produces lower yield of lignin. The obtained results lead to conclude that high polar nature of the ethanol removes not only impurities but also lignin polymer chains of various size, because of the very low yield. In contrary ethyl acetate wash produces a moderate effect which probably removes only small lignin molecules. However, due to non-polarity, hexane solvent is not efficient for lignin washing, it removes only non-polar impurities but is probably insufficient to remove polar ones.

5.3.3. SEC analysis of solvent washed PB lignin – Crude and Derivatized

In this section, SEC analysis was performed in DMAc/LiCl system with polystyrene standard for washed PB lignin in different solvents to see the effect on the molar mass distribution, and compare the results between crude and derivatized (acetylated and fluorobenzylated) lignins.

The obtained chromatograms can be compared in Figure 5.7 and the corresponding average molar mass and degree of polymerization are presented in Table 5.7. It should be noted that the chromatographic curves and the obtained M_n and M_w values showed that no significant differences were observed for underivatized crude and hexane-washed PB. The results confirm that hexane as non-polar solvent was not efficient for removing the smaller molar mass lignin fractions. In the case of ethanol-washed PB, higher M_w (13310 Da) and M_n (6890 Da) values and sharp molecular weight distribution curve in higher molar mass region explain that ethanol removes both impurities and small molar mass lignin molecules present in the crude. In contrary, ethyl acetate washed PB exhibited a uniform distribution curve and the MMD starts at lower molar mass region and the corresponding M_w and M_n values are 10230 Da and 4380 Da, respectively. The obtained results revealed that ethyl acetate is capable of washing lignin polymer without removing small lignin molecules and works as a better solvent than other ones.

Figure 5.7 shows that the acetylated crude PB sample exhibits a broad distribution of retention time and log M compared to derivatized washed lignins. DP_n and DP_w values were calculated by assuming a mean molar mass value of 240 g/mol for the acetylated lignin monomer, and the results are presented in Table 5.7. A clear difference is observed between crude-acetylated and washed-acetylated lignin samples, except for hexane-washed lignin. M_n and M_w values of crude-acetylated lignin were comparatively lower than other solvent-washed lignin samples, but only a small variation occurred in the case of hexane-washed lignin. Ethanol-washed lignin exhibits higher M_n and M_w values compared to the ethyl acetate-wash due to lack of small lignin molecules.

Like acetylation, fluorobenzylated PB lignin also shows similar trends (Figure 5.7) and the calculated M_n, M_w and dispersity values are presented in Table 5.7, where it is shown that M_n and M_w values of crude were smaller than ethyl acetate and hexane washed samples. Fluorobenzylated ethanol washed sample showed higher M_n and M_w values that can be due to large tail in the high molar mass

region. DP_n and DP_w values were calculated on the basis of assuming a molar mass value of 251 g/mol for the fluorobenzylated lignin monomer. This value was obtained from preliminary result of ^{19}F NMR (a detailed calculation is given in the following section).

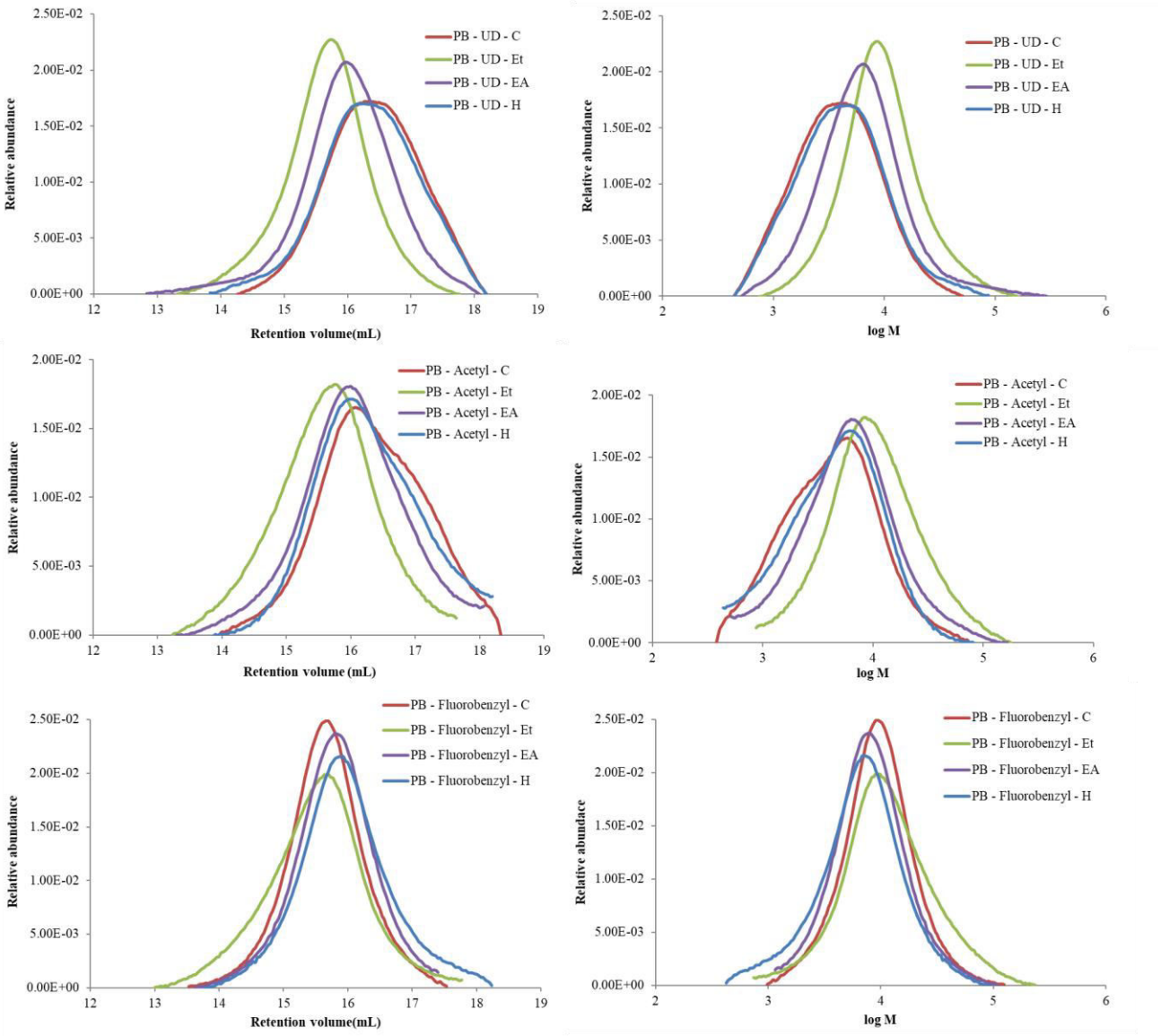

Figure 5.7. SEC chromatogram profiles of PB washed underivatized lignins, acetylated and fluorobenzylated lignin samples in different solvents. Plot: Relative abundance vs Retention volume (*left*) and Relative abundance vs log (M) (*right*).

Abbreviations: UD – Underivatized, C – Crude, Et – ethanol, EA – ethyl acetate, H – Hexane.

Table 5.7. Average molar mass data (M_n, M_w in Da), polydispersity (M_w/M_n) and average degree of polymerization (DP_n, DP_w) of crude PB lignin, washed PB lignin and derivatized (acetylated and fluorobenzylated) PB lignin samples in SEC system A (direct dissolution, Polargel M column setup, DMAc/LiCl as solvent, DRI detection, std. calibration with monodisperse polystyrene calibrants)

PB lignin / SEC-DMAc/LiCl	**M_n**	**M_w**	**M_w/M_n**	**DP_n**	**DP_w**
Underivatized					
PB crude	2650	5470	2.1	13	27
PB Ethanol	6890	13310	1.9	34	67
PB Ethyl acetate	4380	10230	2.0	22	51
PB Hexane	2802	6397	2.3	14	32
PB – Acetylated					
Crude	2390	6030	2.5	12	30
Ethanol	5900	14300	2.4	30	72
Ethyl acetate	3400	8900	2.6	17	44
Hexane	2540	6240	2.5	13	31
PB -Fluorobenzylated					
Crude	5780	9860	1.7	29	49
Ethanol	5940	14150	2.4	30	71
Ethyl acetate	4910	8550	1.7	25	43
Hexane	3410	7380	2.2	17	37

By comparing the SEC profiles of the crude PB, with and without derivatization, it is shown that the underivatized sample exhibits a broader distribution than the acetylated sample. In addition, there is no significant difference in M_n and M_w values, with and without acetylation. In the case of the fluorobenzylated crude lignin, SEC profiles exhibit a more uniform distribution compared to underivatized and acetylated samples.

Therefore, it is clearly demonstrated that lignin fluorobenzylation yields to sufficient derivatization to produce a uniform molar mass distribution. Furthermore, fluorobenzylation enhances lignin solubility in other organic solvents like THF for SEC analysis.

Among the investigated washing solvents, ethyl acetate significantly removes the impurities present in the lignin crude sample and the lignin polymer molecules are preserved.

5.3.4. Chemical derivatization of technical lignins

In this section, various technical lignins such as PB, ORG, IND, KR and EU-KR were subjected to different chemical derivatizations such as acetylation, fluorobenzylation and fluorobenzoylation and chemical analyses are described in the following sections.

5.3.4.1. FT-IR analysis

FT-IR analysis was performed for underivatized and derivatized (acetylated, fluorobenzylated and fluorobenzoylated) lignins and spectra are shown in to confirm the derivatization. In particular, we considered three different frequencies to understand the derivatization of lignin, such as –OH, -CH and aromatic ring vibrations. From the Figure 5.8, in the case of underivatized lignin, –OH stretching frequency is broad and easily seen in the range of 3600-3100 cm^{-1}. –CH, $–CH_2$ and $–CH_3$ stretching frequencies lies between 2800-3000 cm^{-1}. Aromatic ring vibration is observed around 1600-1500 cm^{-1} and aromatic C-H out of plane absorption band visible at 856 cm^{-1}. Guaiacyl, Syringyl and p-hydroxyl phenolic C-H out of plane absorption can be seen at 754 cm^{-1}.

According to FTIR spectra shown in Figure 5.8, –OH groups intensity in derivatized lignin was decreased noticeably, compared to underivatized lignin. In particular, fluorobenzylated lignin –OH groups intensity was slightly higher than in acetylated lignins, because of fluorobenzylation selectivity toward phenolic and primary –OH groups, without significant reaction on secondary –OH groups. For acetylated lignin, derivatization occurs on all types of –OH groups. This is clearly seen from –OH peak intensity, which is significantly lower than in the case of fluorobenzylation. However the remained –OH peak shows that acetylation on all –OH groups is incomplete. In the case of fluorobenzoylation, the absence of –OH band indicates that all –OH groups were derivatized successfully. Other IR region, 3000-2800 cm^{-1} belongs to the formation of new –CH, $–CH_2$ and $–CH_3$ groups and the corresponding IR intensity increased compared to underivatized lignin.

The frequency, 1750-1720 cm^{-1} is assigned to non-conjugated C=O of ester, ketones, aldehydes and acids. Acetylated lignin increased band intensity ranges 1900-1700 cm^{-1}, illustrates large extent of esterification. Similarly, in the case of fluorobenzoylation, the formation of new ester groups increases the band intensity in this region. 1700-1550 cm^{-1} is classified for conjugated C=O and C=C stretching and the region of 1180-1080 cm^{-1} refers for new ether bond formation. Therefore, FTIR analysis revealed that all investigated lignin samples were derivatized and can be used for further analysis.

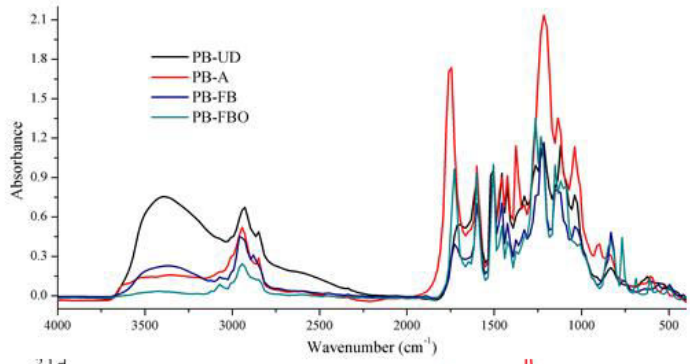
PB-UD
PB-A
PB-FB
PB-FBO
Absorbance
Wavenumber (cm-1)

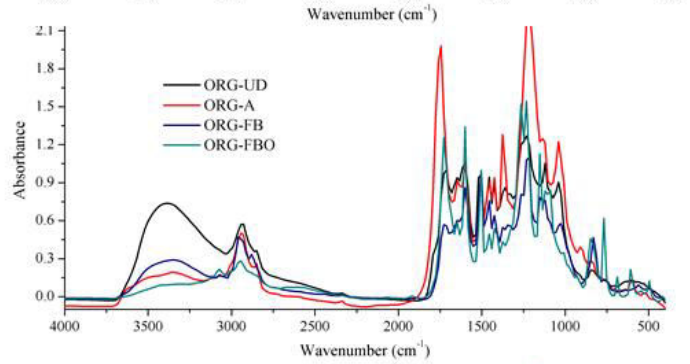
ORG-UD
ORG-A
ORG-FB
ORG-FBO
Absorbance
Wavenumber (cm-1)

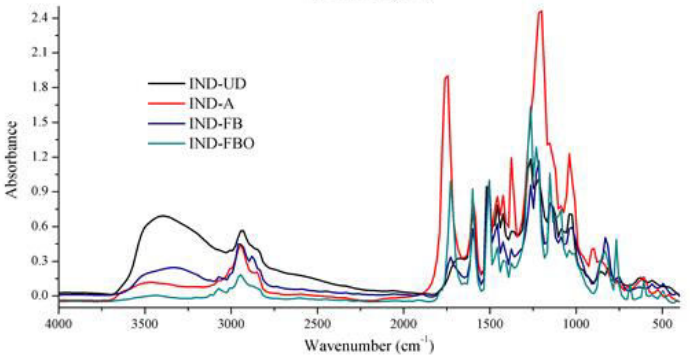
IND-UD
IND-A
IND-FB
IND-FBO
Absorbance
Wavenumber (cm-1)

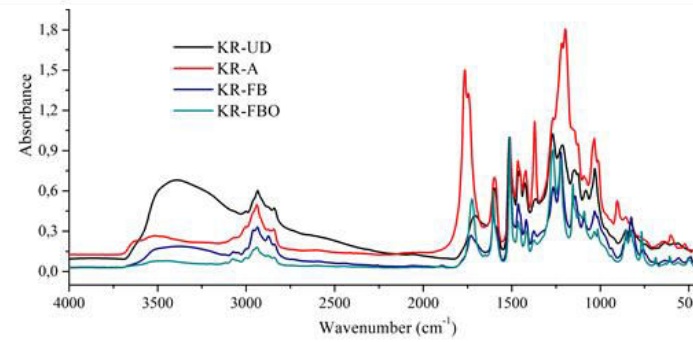
KR-UD
KR-A
KR-FB
KR-FBO
Absorbance
Wavenumber (cm-1)

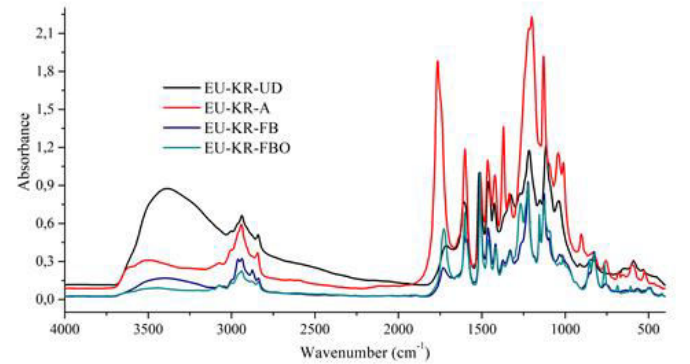
EU-KR-UD
EU-KR-A
EU-KR-FB
EU-KR-FBO
Absorbance
Wavenumber (cm-1)

Figure 5.8. FTIR spectra of ethyl acetate washed PB, ORG, Indulin, KR (Kraft) and EU-KR (Eucalyptus kraft) lignins, A – Acetylated, FB- Fluorobenzylated, FBO- Fluorobenzoylated

5.3.4.2. ^{19}F NMR spectra

Fluoro-derivatized lignins were analysed by ^{19}F NMR to determine the extent of hydroxyl groups derivatization, based on the fluoro-derivatization work described in the previous chapters (Barrelle, 1995; Barrelle et al., 1992). As a summary, phenolic and primary aliphatic hydroxyl groups were derivatized using 4-fluorobenzyl chloride and converted into their corresponding ether derivatives. The fluorobenzylated lignin derivatives were forwarded to fluorobenzoylation using 4-fluorobenzoic acid anhydride. Particularly, the secondary hydroxyl groups and remained phenolic groups from fluorobenzylation were converted into their ester derivatives. All derivatized lignins were analyzed by ^{19}F NMR. Figure 5.9 depicts ^{19}F NMR spectra of all investigated fluorobenzylated and fluorobenzoylated lignins. In the case of fluorobenzylation spectra, the broad spectral region corresponds to fluorobenzylated lignin and phenolic hydroxyl groups, ranging from -115 to -117.48 ppm (relative to C_6F_6) and primary aliphatic hydroxyl groups signals are assigned from -117.48 to -118.5 ppm. In fluorobenzylated + fluorobenzoylated samples spectra, the right side broad spectral region belongs to fluorobenzylated lignin, and the left side to fluorobenzoylated lignin. In fluorobenzoylation region, phenolic hydroxyl groups were assigned from -104.6 to -107.24 ppm and secondary hydroxyl groups from -107.24 to -108.64 ppm. Number of phenolic and aliphatic hydroxyl groups was proportional to the area of the peak which is normally quantified based on the internal standard, and the area of the internal standard (2-fluoroacetophenone) was fixed to 1. This method provides the information about the number of total hydroxyl groups per gram of derivatized lignin (mmol/g), which can be expressed as:

$$n_{OH} = A_L * m_{IS} * 1000/(m_{LF} * 138.14) \quad \textit{in mmol/g lignin derivatized} \qquad \text{Equation 5.1}$$

where: nOH= mmol/g lignin derivatized
A_L = Area of lignin
m_{IS} = mass of internal standard
M_{IS} = molar mass of internal standard (138.14 g)
m_{LF} = mass of lignin derivatized
Internal standard IS = 2-fluoroacetophenone

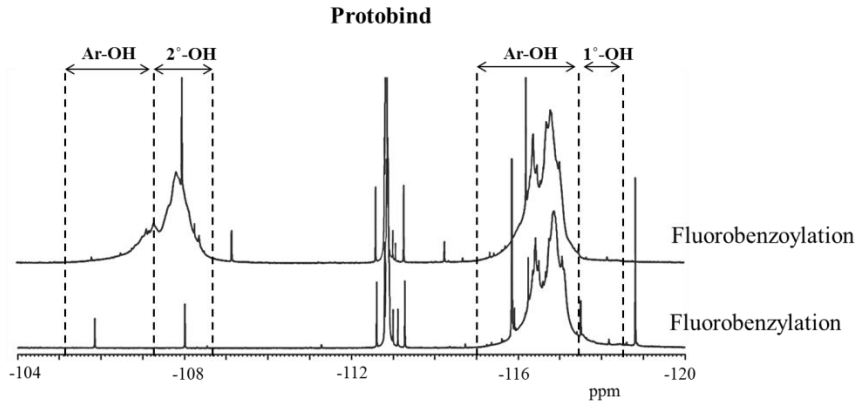
Protobind
Ar-OH
2°-OH
Ar-OH
1°-OH
Fluorobenzoylation
Fluorobenzylation
-104
-108
-112
-116
-120
ppm

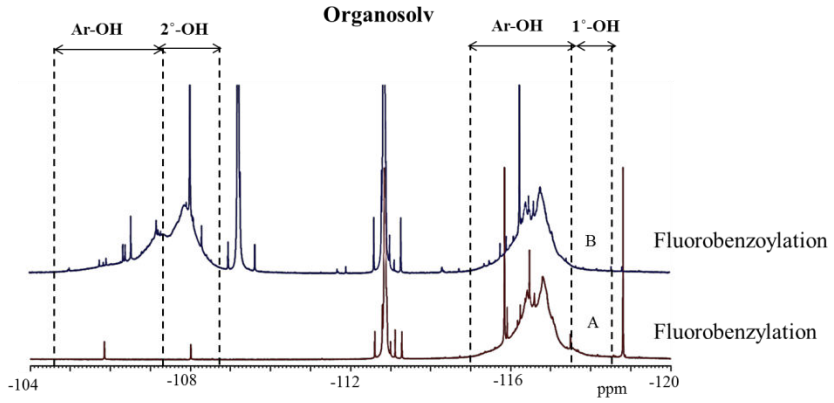
Organosolv
Ar-OH
2°-OH
Ar-OH
1°-OH
B
A
Fluorobenzoylation
Fluorobenzylation
-104
-108
-112
-116
-120
ppm

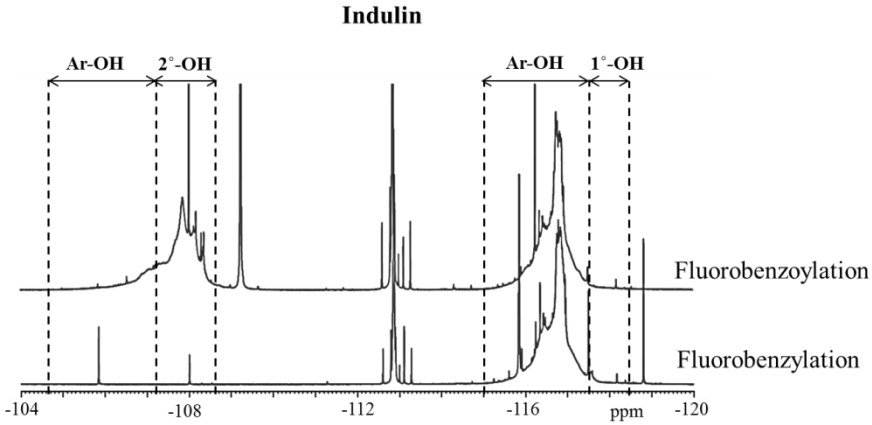
Indulin
Ar-OH
2°-OH
Ar-OH
1°-OH
Fluorobenzoylation
Fluorobenzylation
-104
-108
-112
-116
-120
ppm

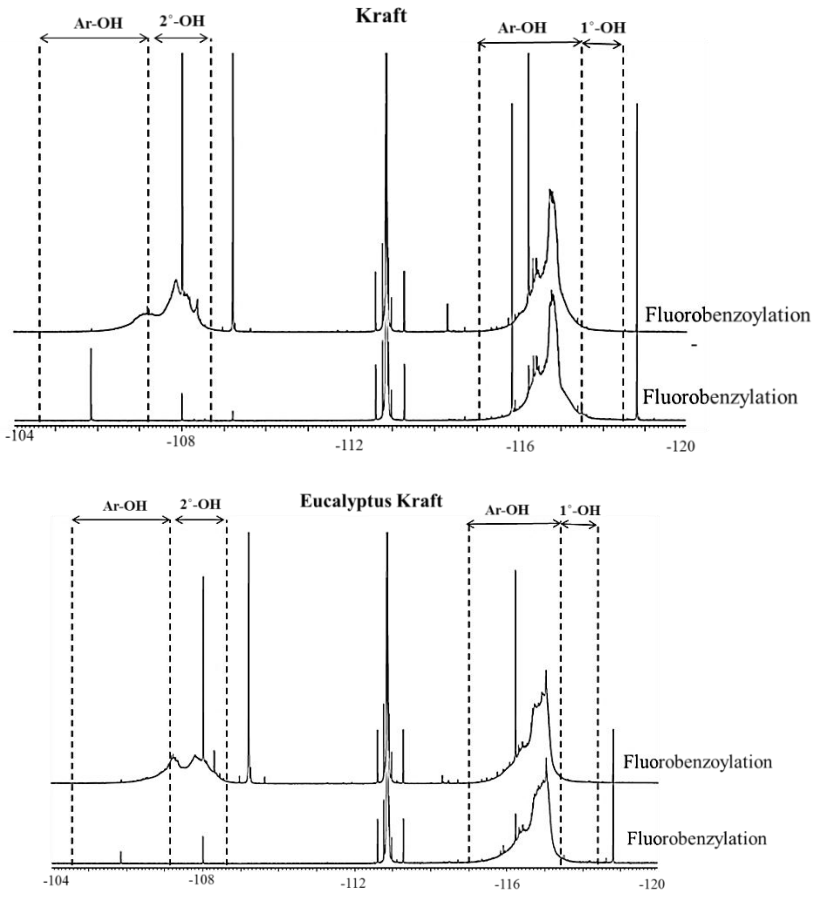

Figure 5.9. ^{19}F NMR spectra of fluorobenzylated and fluorobenzoylated Protobind, Organosolv, Indulin, Kraft and Eucalyptus-Kraft lignins. Chemical shifts relative to $CFCl_3$. Internal standard: 2-fluoroacetophenone

It should be clarified that the fluorobenzylation reaction was employed for derivatization and subsequent analysis of ^{19}F NMR analysis. From this reaction, the phenolic and primary hydroxyl groups were calculated in different lignins, as reported in Table 5.8. From this Table, the indulin Kraft lignin shows higher amount of phenolic hydroxyl group than other types of Kraft lignins. Among the investigated lignins, the annual plant ORG lignin contains the lowest amount of hydroxyl groups.

Table 5.8. Total number of OH groups (in mmol/g) in fluorobenzylated lignin samples, determined by ^{19}F NMR spectroscopy

Lignin	Fluorobenzylated		Total $OH_{Calculated}$ mmol/g lignin derivatized
	Ph-OH	*1°-OH*	
PB	1.785	0.106	1.891
ORG	1.708	0.120	1.828
IND	2.451	0.078	2.529
KR	2.252	0.089	2.341
EU-KR	2.322	0.059	2.381

From the ^{19}F NMR fluorobenzylation spectra, the areas of aromatic and aliphatic hydroxyl groups were taken into account to calculate the number of moles of lignin derivatives, using the following Equation 5.2, and values are presented in Table 5.9. In order to calculate the number of moles of hydroxyl groups, the following parameters are required: M_L = molar mass of lignin, M_{IS} = molar mass of internal standard, $A_{LAr\text{-}OH}$ = Area of lignin aromatic hydroxyl group, $A_{LAli\text{-}OH}$ = Area of lignin aliphatic hydroxyl group, m_L= Mass of lignin, m_{IS} = mass of internal standard, M_F = molar mass of fluorobenzylated lignin, M_{HCl} = molar mass of HCl. The step-by-step explanation of this equation can be found in the Appendix B.

$$n_{OH} = \frac{M_L}{M_{IS}} * A_{LAr-OH} * m_{IS}/m_L \\ * 1 / \left(1 - (M_F - M_{HCl}) * \left(\frac{m_{IS}}{m_L}\right) * A_{LAr-OH} * \left(1 + \left(\frac{A_{LAli-OH}}{A_{LAr-OH}}\right)\right)\right)$$

Equation 5.2

Among the investigated lignins, fluorobenzylation reaction predicted that IND lignin contains the highest total number of phenolic hydroxyls and little part of primary hydroxyls, totally about 0.697 mol/mol aromatic unit. It is followed by EU-KR lignin (0.642 mol/mol) and by KR lignin (0.628 mol/mol). The least hydroxyl content was obtained for the case of ORG lignin (0.456 mol/mol). It can be pointed out that wheat straw or annual grass plants present lower hydroxyl groups content than hardwood and softwood lignins.

Table 5.9. Total OH groups (in mol/mol aromatic unit) in fluorobenzylated lignin samples, determined by ^{19}F NMR spectra

Lignin (mg)	IS (mg)		FB carbonylated-ArOH	FB Ar-OH	Total Ar-OH	primary-OH	Total OH
					x	y	
PB (15.5)	4.3	A	0.328	0.561	0.889	0.053	
		N			0.449	0.027	0.476
ORG (15.5)	3.3	A	0.505	0.603	1.108	0.078	
		N			0.426	0.030	0.456
IND (15.5)	3.2	A	0.494	1.146	1.640	0.052	
		N			0.675	0.021	0.697
KR (15)	5.1	A	0.282	0.633	0.915	0.036	
		N			0.604	0.024	0.628
EU-KR (15.4)	5.2	A	0.251	0.699	0.95	0.024	
		N			0.626	0.016	0.642

A – Area of the peak, N – number of moles, x and y represents number of moles of aromatic and aliphatic hydroxyl groups (mol/mol), IS – internal standard.

From the fluorobenzylation spectra, the number of moles of aromatic (x) and aliphatic hydroxyl groups (y) were calculated, and these values were used for the calculation of the monomer molar mass based on the equation below (Equation 5.3), with M_L = 200 g/mol, M_F = 144.5 g/mol (FBC) and M_{HCl} = 36.5 g/mol. The calculated "M" value represents the monomer molar mass of fluorobenzylated lignin which therefore will be used for determining the degree of polymerization of all lignin samples, reported in Table 5.10..

$$M = M_L + (x + y)M_F - (x + y)M_{HCl} \qquad \text{Equation 5.3}$$

The fluorobenzylated lignin samples were forwarded to fluorobenzoylation in which the remained hydroxyl groups are fluorobenzoylated. After the derivatization, the total number of hydroxyl groups, including total phenolic and aliphatic hydroxyls in all lignins were calculated; values are reported in Table 5.10. Comparing the two-wheat straw lignins (PB and ORG), the total phenolic hydroxyl group content differs. Such a difference can be attributed to the totally different cooking processes employed for their extraction. The PB lignin produced by soda cooking has higher phenolic and aliphatic hydroxyl groups than the ORG lignin (from the CIMV organosolv cooking process which uses acetic and formic acid at temperatures above 100°C). Considering various Kraft process lignins, IND lignin showed highest total hydroxyl content, followed by the KR lignin (from pine) and the least quantity was found for the EU-KR lignin. For instance, IND has 3.42 mmol/g and KR contains 3.145 mmol/g

of total hydroxyl groups, of which 2.33 and 2.277 mmol/g corresponds to phenolic hydroxyl for IND and KR, 1.09 and 0.868 mmol/g aliphatic hydroxyl groups for IND and KR, respectively.

Chapter 3 has been dedicated to the quantification of phenolic hydroxyl groups using classical aminolysis with NMR and fast wet chemistry methods. Comparing all analysed samples, the calculated phenolic hydroxyl group content (in mmol/g) range from different methods:

(1) Aminolysis: PB-3.4, ORG-2.4, IND-3.6, KR-4.0
(2) UV-differential spectrometry: PB-2.6, ORG-1.7, 3.4-IND, KR-2.8
(3) ^{1}H NMR: PB-1.8, ORG-0.9, IND-3.1, KR-2.7
(4) ^{13}C NMR: PB-2.4, ORG-2.0, IND-3.6, KR-4.2
(5) ^{31}P NMR: PB-2.7, ORG-1.3, IND-3.2. KR-3.2
(6) Fast wet chemical method: PB-2.4, ORG-1.5, IND-2.7, KR-2.7

It should be noted that all the above analysis exhibited lower phenolic hydroxyl content for Organosolv lignin and higher phenolic hydroxyl group content for Indulin or Kraft (softwood lignins). It is interesting to note that total phenolic content after fluorobenzoylation using ^{19}F NMR results were consistent with the result obtained by other methods. Detailed information can be found in Chapter 3.

From the analysis of fluorobenzoylated lignins ^{19}F NMR spectra and the determination of each peak area, the following Equation 5.4 was used to calculate the –OH content in derivatized lignins.

Table 5.10. Total number of OH groups (in mmol/g) in fluorobenzoylated lignin samples, determined by ^{19}F NMR spectra

Lignin	**Fluorobenzylated**		**Fluorobenzoylated**		**Total OH_{Phenol}**	**Total OH_{aliph}**	**Total $OH_{Calculated}$ mmol/g derivatized lignin**
	Ar-OH	*1°-OH*	Ar-OH	*2°-OH*			
PB	1.802	0.051	0.374	0.851	2.176	0.902	3.078
ORG	1.110	0.057	0.563	0.643	1.673	0.700	2.373
IND	1.901	0.051	0.430	1.036	2.331	1.087	3.418
KR	1.938	0.060	0.339	0.808	2.277	0.868	3.145
EU-KR	1.840	0.058	0.397	0.490	2.237	0.548	2.785

The following parameters are used for the calculations and detailed derivation of this equation can be found in Appendix C. M_{FBC} = 144.5 g/mol, FBC = 4-fluorobenzyl chloride, M_{HCl} = 36.47 g/mol, HCl = hydrochloric acid, M_{FBAA} = 262.2 g/mol, FBAA = 4-fluorobenzoic acid anhydride,

M_{FBA} = 140.1 g/mol, FBA = Fluorobenzoic acid, M_{IS} = 138.14 g/mol IS = Internal standard (2-fluoroacetophenone), m_{IS} = mass of internal standard, m_{Li} = mass of lignin, A_{Liu} = Area corresponding to fluorobenzylated aromatic hydroxyl, A_{LiV} = Area corresponding to fluorobenzoylated aromatic hydroxyl, A_{Liy} = Area of primary hydroxyls, A_{LiZ} =Area of secondary hydroxyls.

$$n_{OHx} = \frac{M_L}{M_{IS}} * A_{Lix} * (m_{IS}/m_{Li}) * 1 / \left[(1 - (A_{Liu} * m_{IS})/(M_{IS} * m_{Li}) * (M_{F1} - M_{HCl}) * \left(1 + \left(\frac{A_{LiY}}{A_{Liu}}\right) + (M_{F2} - M_{FBA}) * \frac{(A_{LiV} + A_{LiZ})}{A_{Liu}}\right)\right]$$

Equation 5.4

The calculated total number of hydroxyl groups present in the lignin are reported in Table 5.11. From fluorobenzoylation, it is estimated that IND lignin possesses the highest total number of hydroxyl groups, followed by KR lignin. This trend differs from the results obtained by fluorobenzylation, where EU-KR lignin exhibited more hydroxyl group than KR lignin. PB hydroxyl group content is lower than for KR lignin, but higher than for EU-KR; ORG has the lowest content, typically about one-half of the IND lignin. Considering the extraction process employed for the investigated lignins, ORG lignin was extracted by the "lighter process", in comparison to the aqueous alkaline cooking processes that take place at much higher temperatures. This could play a significant role on the total hydroxyl group quantity.

In order to calculate the monomer molar mass of fluorobenzoylated lignin samples, u, v, y and z values were extracted from the fluorobenzoylated lignin ^{19}F NMR spectra (in Table 5.11) and these values were further substituted in the Equation 5.5 to find out monomer molar mass of fluorobenzoylated lignin. The following components are considered for the monomer molar mass estimation: M_{F2} = molar mass of fluorobenzoic acid anhydride (FBAA), M_{FBA} = molar mass of fluorobenzoic acid produced as by-product during fluorobenzoylation, F_1= FBC molar mass of 4-fluorobenzyl chloride = 144.5 g/mol, M_L = 200 g/mol (molar mass of lignin monomer unit, assumed to 200 g/mol in all the calculations)

$$M = M_L + (u + y)(M_{F1} - M_{HCl}) + (v + z)(M_{F2} - M_{FBA})$$

Equation 5.5

Table 5.11. Total OH groups in fluorobenzoylated lignin in mmol/mol, determined by ^{19}F NMR spectroscopic analysis

Lignin (mg)	IS (mg)		FBO Ar-OH	FB Ar-OH	Total Ar-OH	2°-OH	1°-OH	TOTAL OH_{aliph}	Total OH
			v	u		z	y		
PB	4.4	A	0.196	0.945		0.446	0.027		
(16.7)		n	0.115	0.554	0.669	0.262	0.016	0.277	0.931
ORG	4.2	A	0.287	0.566		0.328	0.029		
(15.5)		n	0.155	0.305	0.460	0.177	0.016	0.193	0.637
IND	4.8	A	0.187	0.826		0.450	0.022		
(15.1)		n	0.141	0.623	0.764	0.339	0.017	0.356	1.119
KR	4.8	A	0.159	0.909		0.379	0.028		
(16.3)		n	0.105	0.601	0.706	0.251	0.019	0.269	0.957
EU-KR (16.2)	5.2	A	0.171	0.792		0.211	0.025		
		n	0.116	0.536	0.652	0.143	0.017	0.160	0.794

A – Area of the peak, n – number of moles, u and v describes the number of moles of aromatic hydroxyl groups fluorobenzylated (mol/mol) and fluorobenzoylated (mol/mol), y and z represents the number of moles of primary aliphatic hydroxyl groups fluorobenzylated (mol/mol) and fluorobenzoylated (mol/mol) respectively.

Based on the ^{19}F NMR results, the monomer molar mass of all lignins samples were calculated using Equation 5.4 and Equation 5.5). As already mentioned, the average molar mass of the lignin monomer was assumed to be 200 g/mol, and 240 g/mol for the acetylated lignin monomer. Values for fluorobenzylated and flurobenzoylated lignin monomers are reported in Table 5.12. In the case of fluorobenzylated monomers, the highest molar masses were found for the Kraft lignins, such as IND, KR and EU-KR, followed by PB and ORG lignins. However, in the case of fluorobenzoylated monomers, the trend is IND > KR > PB > EU-KR > ORG.

These results can be compared to hydroxyl groups contents in each lignin samples (given in Table 5.8 and Table 5.10). Softwood KR and IND lignins exhibited higher total hydroxyl group number than hardwood Kraft and annual plant lignins, in which most of the phenolic hydroxyl groups were derivatized during fluorobenzylation. IND lignin contains significant amount of aliphatic hydroxyl groups which are derivatized during fluorobenzoylation. It is interesting to note that the wheat straw PB lignin showed higher hydroxyl content than hardwood (Eucalyptus) Kraft lignin. ORG lignin (also from wheat straw) exhibited least total hydroxyl content, however its aliphatic hydroxyl content was

higher than EU-Kraft lignin. Overall, these results revealed that Indulin lignin contains higher amount of total hydroxyl groups than all other lignins.

Table 5.12. Calculated monomer molar mass in $g.mol^{-1}$ of fluorobenzylated and fluorobenzoylated lignin samples from ^{19}F NMR

Lignin Samples	Molar mass of monomer	
	FB	FBO
PB	251	308
ORG	249	275
IND	275	328
KR	268	310
EU-KR	269	291

5.3.5. Derivatized lignin analysis in SEC-DMAc/LiCl system

All the investigated lignin samples were derivatized (acetylated, fluorobenzylated and fluorobenzoylated) and the corresponding SEC-DMAc/LiCl chromatogram are shown in Figure 5.10 and the obtained molar mass data can be compared in Table 5.13. Comparing all lignin samples, a narrow distribution of both underivatized and derivatized lignin is predominant in the case of PB, Indulin and Eucalyptus Kraft lignin. Values in Table 5.13 shows no significant change in polydispersity values.

The intriguing phenomenon has been obtained for the case of ORG lignin samples. Both underivatized and fluorobenzoylated lignin show more uniform molar mass distribution than acetylated and fluorobenzylated samples. It is clearly seen from the profile (in Figure 5.10) that acetylated and fluorobenzylated ORG lignin showed higher proportion of higher-molar-mass fragments in the low molar mass region, which clearly impacts the calculation of M_w (Table 5.13): acetylated and fluorobenzylated samples have higher M_w than underivatized and flurobenzoylated samples. This might be due to aggregation inside the column, and then, DMAc/LiCl system may not be always appropriate for acetylated and fluorobenzylated samples.

In the case of acetylated KR lignin, a broad distribution was obtained and the SEC peak starts earlier, i.e. in the higher molar mass region. The apparent M_w value (in Table 5.13) is twice higher than for underivatized lignin. Lower polydispersity was found for fluorobenzylated lignin than underivatized lignin.

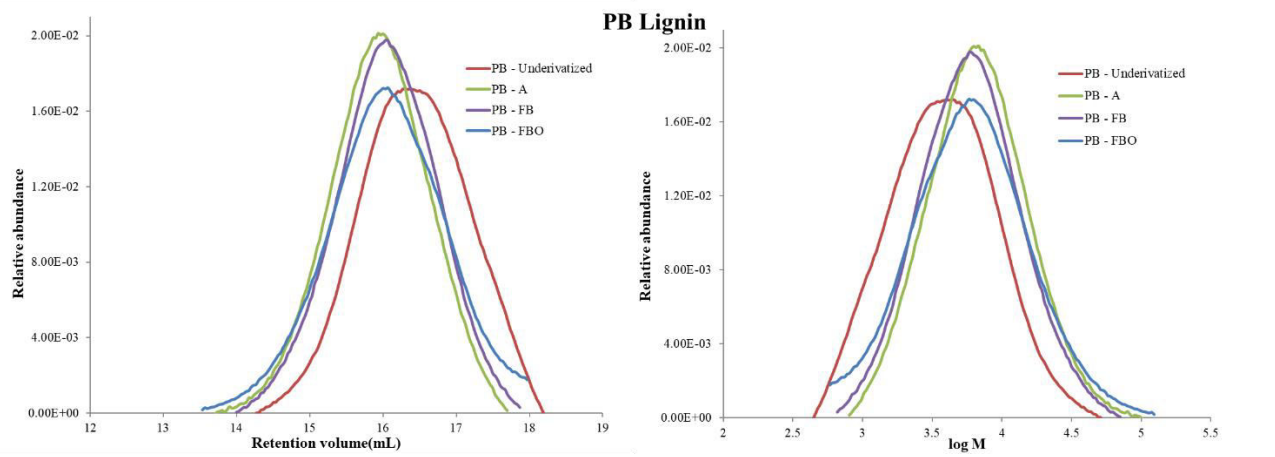
PB Lignin
Relative abundance
Retention volume(mL)
log M
PB - Underivatized
PB - A
PB - FB
PB - FBO

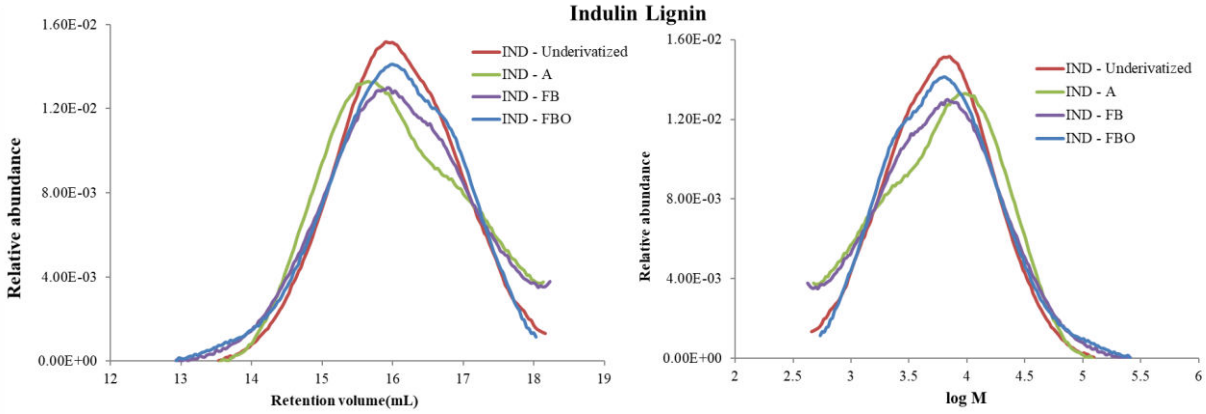
Indulin Lignin
Relative abundance
Retention volume(mL)
log M
IND - Underivatized
IND - A
IND - FB
IND - FBO

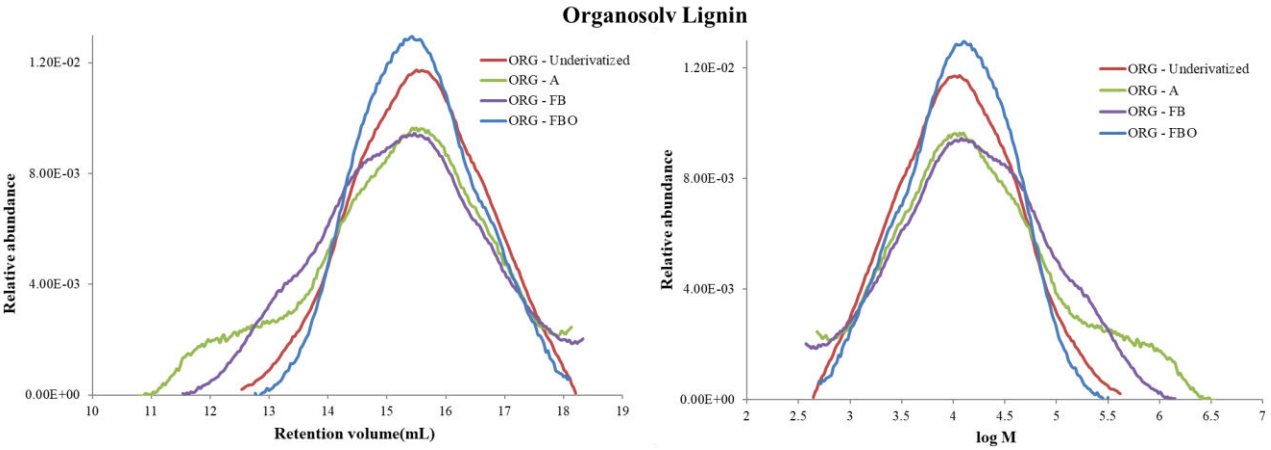
Organosolv Lignin
Relative abundance
Retention volume(mL)
log M
ORG - Underivatized
ORG - A
ORG - FB
ORG - FBO

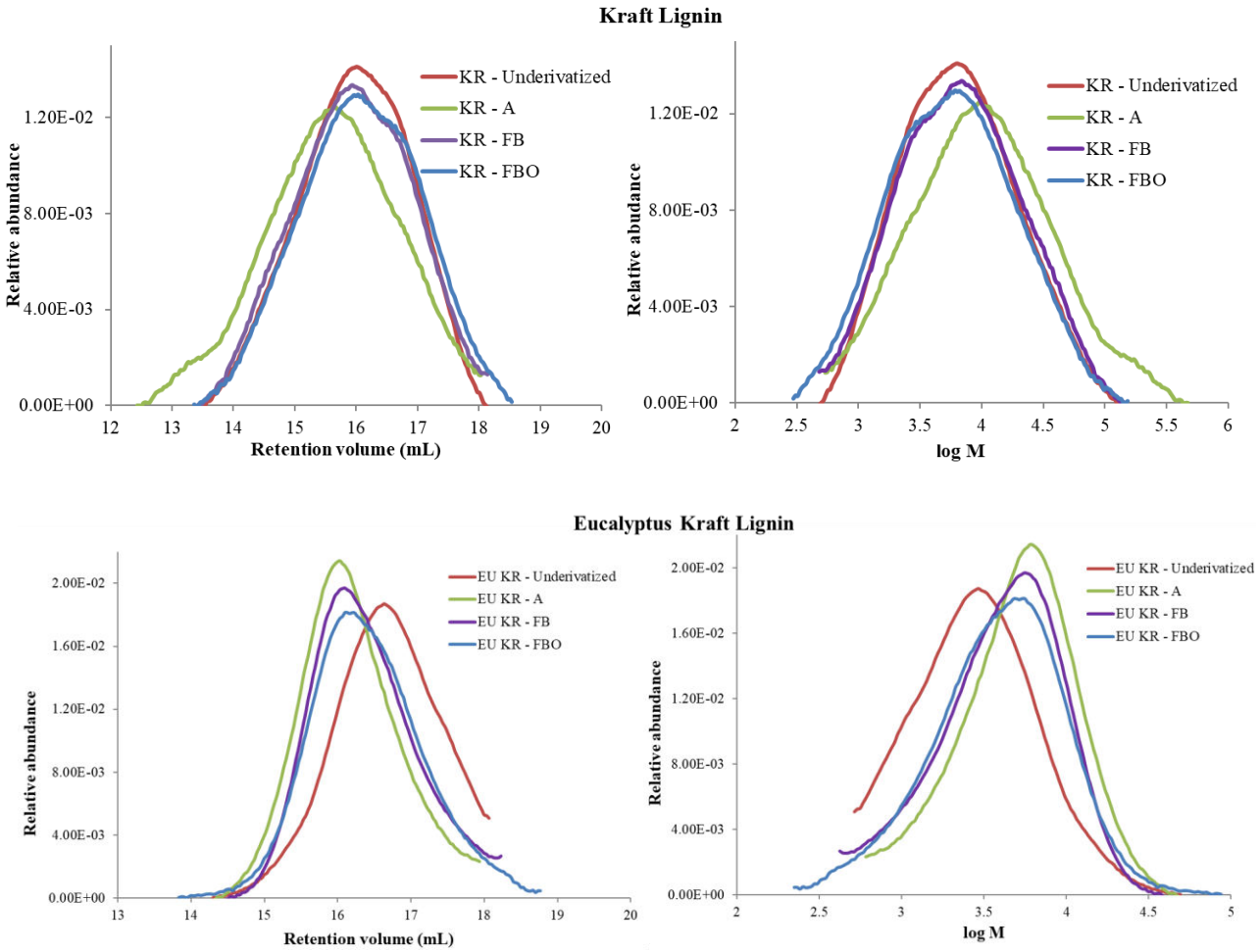

Figure 5.10. SEC chromatogram profiles of underivatized and derivatized (acetylated, fluorobenzylated and fluorobenzoylated) of all studied lignin samples. Relative abundance vs Retention volume (*left*) and Relative abundance vs log (M) (*right*)

Table 5.13. Average molar mass data (M_n, M_w in g.mol^{-1}), polydispersity (M_w/M_n) and average degree of polymerization (DP_n, DP_w) of underivatized and derivatized lignin samples in SEC-DMAc/LiCl system (system A)

	M_n	M_w	M_w/M_n	DP_n	DP_w
PB					
underivatized	2650	5470	1.9	13	27
Acetylated	4140	7820	1.9	21	39
Fluorobenzylated	3400	6580	1.9	17	33
Fluorobenzoylated	2490	6200	2.5	12	31
IND					
underivatized	3430	9610	2.8	17	48
Acetylated	2540	8970	3.5	13	45
Fluorobenzylated	2070	8210	4.0	10	41
Fluorobenzoylated	2190	7300	3.3	11	36
ORG					
underivatized	4970	25270	5.1	25	126
Acetylated	4170	79600	19.1	21	398
Fluorobenzylated	3670	43200	11.8	18	216
Fluorobenzoylated	4040	15560	3.9	20	78
KR					
underivatized	3890	11340	2.9	19	57
Acetylated	4020	19690	4.9	20	98
Fluorobenzylated	2750	9150	3.3	14	46
Fluorobenzoylated	1970	7050	3.6	10	35
EU-KR					
underivatized	2030	4080	2.01	10	20
Acetylated	3000	5690	1.9	15	28
Fluorobenzylated	1990	4060	2.0	10	20
Fluorobenzoylated	1680	3910	2.3	8	20

Comparing underivatized lignin samples, the highest molar mass was found for ORG lignin, followed by Kraft, Indulin, and least value for PB and EU-KR. The broad distribution of ORG lignin is due to the abundance of high molar mass components. However, in the case of EU-KR underivatized sample, the peak does not start from the baseline and the lower mass region was excluded for the calculation. Our obtained M_w values of Kraft underivatized lignin were in rather

good accordance with the data of Ringena al. (Ringena et al., 2006). However, the difference in M_n introduced a small discrepancy in M_w/M_n (the author reported 5.5). The source of lignin and the presence of low-molar mass components, and impurities, has a strong effect on the calculation of the apparent M_n.

From overall SEC-DMAc/LiCl experiments, the results have evidenced that the different derivatization methods significantly enhance the SEC profiles. Overall, the obtained results seem to reflect the apparent M_w of the samples. Indeed, looking at the good regularity and good Gaussian shape of the chromatographic profiles, aggregation behavior should be rather minimized; except maybe for the case of acetylated lignin which for all samples exhibited much higher M_w and dispersity. Another point which probably should play a favorable role is the polarity of both the SEC columns (Polargel M type) and of the solvent used, DMAc/LiCl. Indeed, Li-salts (LiCl) are known to counteract aggregation by ionic strength effects (Connors et al., 1980).

The DS (degree of substitution) of the acetylated lignin samples can be done by considering the following expressions:

The lignin monomer mass is assumed to be: $M_{Lignin\ monomer} = 200$ g/mol Equation 5.6

The acetylated lignin monomer mass is: $M_{Ac\text{-}Lignin\ monomer} = 200 + 42 \times DS$ g/mol Equation 5.7

Assuming same DP for lignin and acetylated lignin:

$DP = M_{Lignin}/ M_{Lignin\ monomer} = M_{Ac\text{-}Lignin}/ M_{Ac\text{-}Lignin\ monomer}$ Equation 5.8

From Equation 5.6Equation 5.7Equation 5.8, one obtains:

$M_{Lignin}/ 200 = M_{Ac\text{-}Lignin}/ (200 + 42 \times DS)$ Equation 5.9

Then, after rearrangement: $DS = [(M_{Ac\text{-}lignin}/M_{Lignin}) - 1] \times 200/42$ Equation 5.10

Based on the apparent M_w and M_n data in Table 5.13 and on a molar mass of 220 g/mol for the acetylated lignin monomer, DS values are reported in Table 5.14. Based on M_w, calculation leads to rather high estimation for the DS of PB, Kraft and Eucalyptus Kraft lignin samples (since expected values would be in a range of 1 - 2.5), negative DS for IND lignin (which has no meaning), and very high substitution for ORG. This calculation is therefore not correct, probably because a unique molar mass value was taken for the acetylated lignin monomer, without accounting for the DS itself.

As an overall conclusion of this paragraph, one can say that, despite good apparent solubility of lignin samples in DMAc/LiCl, SEC behaviour remained at least partially imperfect with some samples.

Table 5.14. Calculated degree of substitution (DS) based on M_n and M_w values for all lignin samples

	DS using M_n value	DS using M_w value
PB	2.7	2.0
ORG	-0.8	10.2
IND	1.2	-0.3
KR	0.2	3.5
EU-KR	2.3	1.9

5.3.6. Derivatized lignin analysis in THF system (system B)

In this section, the chosen lignin derivatives were analysed in SEC-THF, using PLGel columns. Prior to the analysis, lignin samples were washed with ethyl acetate and derivatized (acetylated, fluorobenzylated and fluorobenzoylated). We used chromatographic system B, working in THF and 3 PLgel columns (non-polar PSDVB gel), and 3 different polymers as standards (PS, PMMA, cellulose acetate) to established standard and universal calibration curves:

(1) Universal calibration by plotting log ([η].M) vs. retention volume as linear calibration curve, either using individual polymer fit, or global fit (gathered data of all standard polymers)
(2) Conventional calibration by plotting log (M) vs. retention volume as linear calibration curve using individual polymers as standard calibrants.

5.3.6.1. Derivatized Protobind (PB) lignin SEC-THF analysis using universal and conventional calibration methods (system B)

Solubility tests of derivatized PB were performed in THF. The results showed that derivatization enhanced the solubility in THF, and SEC single peak elution profile was found for all lignin samples. In particular, PB derivatives exhibited better solubility in THF than the other lignin samples. PB derivatives chromatograms are illustrated in Figure 5.11. Rather uniform Gaussian-type distributions can be observed, except for the acetylated lignins which appears less regular and exhibits long tail in the low-molar-mass region. Acetylation would retain lower molar fractions than the other derivatization treatments. In the case of fluoro-derivatization, both the effect of the added mass, which increases the hydrodynamic volume, and the decrease of polymer polarity, reduces the macromolecular interaction in solution and with the column gel, and reduces the retention volume.

Applying universal or conventional calibration can be compared in Figure 5.12. From SEC-THF chromatograms, the main peak has been chosen to determine the MMD. Using universal calibration

shifts the MMD towards higher molar mass. Such an effect can be observed for the three kinds of derivatives (acetylation, fluorobenzylation and fluorobenzoylation).

In Table 5.15, M_n, M_w and polydispersity values of acetylated, fluorobenzylated and fluorobenzoylated PB derivatives obtained by universal calibration can be compared with values obtained by conventional calibration. In all cases of universal calibration, average molar mass values using PS and PMMA as standards were rather close, whereas values using cellulose acetate as standard were more distant. Again, the difference between universal and conventional calibration is significant: M-average and M_w/M_n values obtained by conventional calibration appear 3 to 5 times lower than those obtained by universal calibration.

As main conclusion of this paragraph focused on the study of PB lignin, it appears that the choice of the calibration method plays a main role on the determination of the molar mass of the lignin.

An important difference was found between universal calibration and conventional calibration. Universal calibration should be in principle a much better method than conventional calibration. Universal calibration yielded significantly higher molar mass than conventional calibration, which provided molar mass values of the same order of magnitude as values mainly reported in the literature.

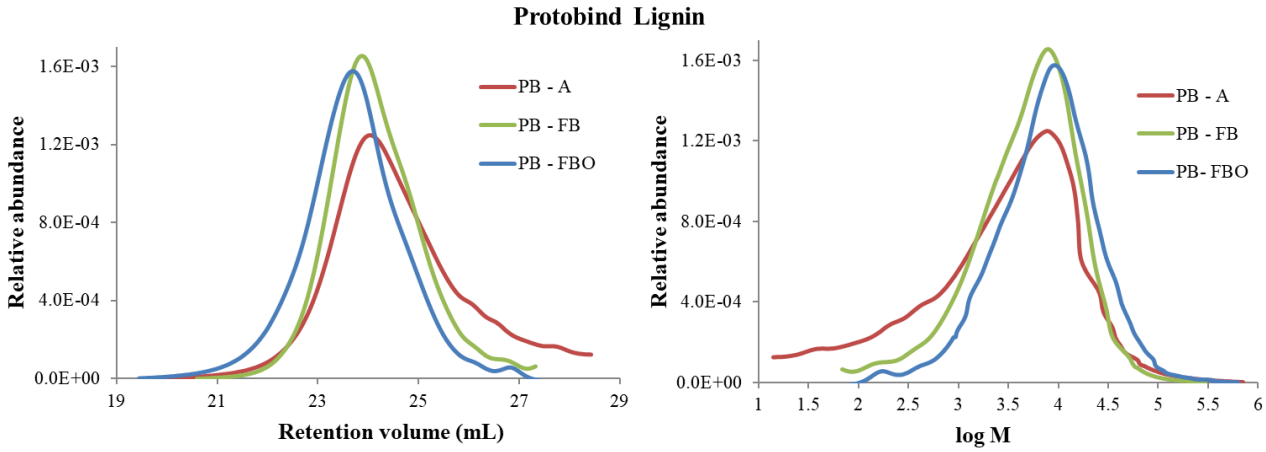

Figure 5.11. SEC – MMD universal calibration curve of PB lignin: relative abundance Vs retention volume (*left*) and relative abundance Vs log (Mw) (*right*) (A - acetylated, FB - fluorobenzylated and FBO - fluorobenzoylated)

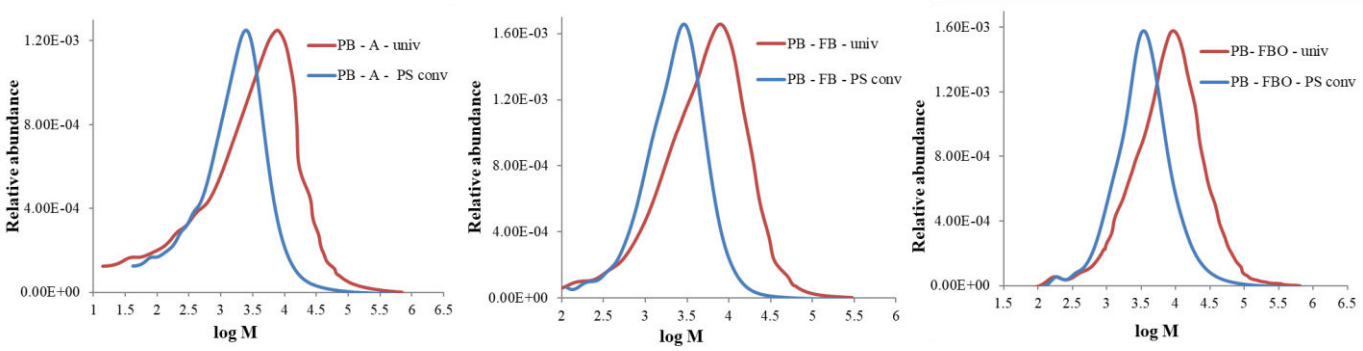

Figure 5.12. Comparison of universal and conventional SEC – MMD curves of relative abundance Vs log(Mw) for A - acetylated, FB - fluorobenzylated and FBO - fluorobenzoylated PB lignin samples

Table 5.15. MMD of derivatized PB lignin from universal calibration with global curve fit and individual curve fit and comparison with conventional calibration. M_n and M_w values in Da.

	Universal (viscometric detector)				**Conventional (RI detector)**			
PB-Acetylated	M_n	M_w	M_w/M_n	M_p	M_n	M_w	M_w/M_n	M_p
Fit with Global curve[a]	380	10060	26.5	7780	-	-	-	-
PS	330	9030	27.4	6910	560	2890	5.2	2500
PMMA	240	8260	34.4	5981	725	3640	5.0	3150
Cellulose acetate	700	13260	18.9	11090	856	2720	3.2	2620
PB-Fluorobenzylated								
Fit with Global curve[a]	2000	9560	4.8	7980	-	-	-	-
PS	1760	8570	4.9	7110	1450	3180	2.2	2930
PMMA	1400	7700	5.5	6200	1840	4000	2.2	3690
Cellulose acetate	3220	12890	4.0	11230	1770	3060	1.7	2990
PB-Fluorobenzoylated								
Fit with Global curve[a]	3690	16140	4.4	9240	-	-	-	-
PS	3230	14550	4.5	8250	2140	5390	2.5	3430
PMMA	2640	13510	5.1	7250	2710	6740	2.5	4320
Cellulose acetate	5640	20680	3.7	12850	2450	4660	1.9	3420

a = fit with global curve (PS, PMMA, Cellulose acetate)

5.3.6.2. Derivatized Indulin (IND) lignin SEC-THF analysis using universal and conventional calibration methods (system B)

Indulin AT lignin is purchased from DKSH Switzerland Ltd., prepared using Kraft cooking process on softwood tree. Fluoroderivatized Indulin AT lignin exhibited single peak elution profile in THF. Acetylated and fluoroderivatized IND lignin SEC chromatogram profiles are shown in Figure 5.13. During the dissolution, acetylated IND lignin solubility in THF was poor compared to fluoro-derivatives. From the Figure 5.13, more or less uniform MMD profiles for fluoro-derivatives can be observed (less uniform than for PB lignin, see previous paragraph), while a broad and irregular distribution was obtained for the acetylated derivative. It is due to the fact of incomplete solubility of the acetylated IND sample. Elimination of the insoluble portion from acetylated IND led to extended distribution towards lower molar mass regions.

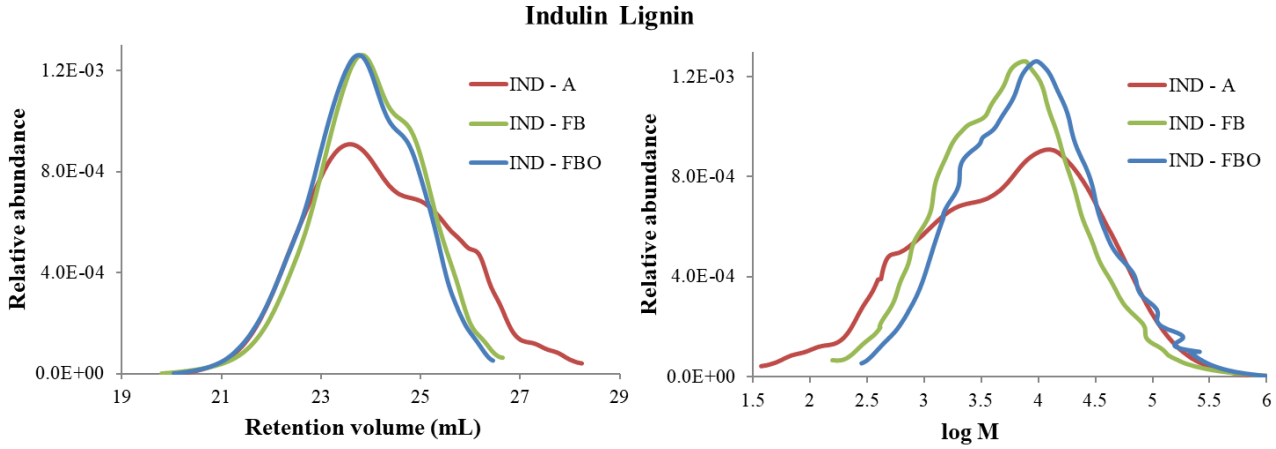

Figure 5.13. SEC – MMD universal calibration curve of Indulin (IND) lignin: relative abundance vs retention volume (*left*) and relative abundance vs log (M) (*right*) (A - acetylated, FB - fluorobenzylated and FBO - fluorobenzoylated)

Comparing the MMD curves of the different derivatives (Figure 5.14) shows the same effect as already observed with the PB lignin: a shift towards higher molar mass for the universal calibration curves. Another visible shift is due to the added mass introduced by fluoro-derivatization, as compared to the acetylation that introduces a smaller added mass on lignin monomers. Overall, as in the case of PB lignin, the better global shape of the fluoro-derivatives curves indicates that fluoro-derivatization promotes a better SEC behavior in non-polar columns.

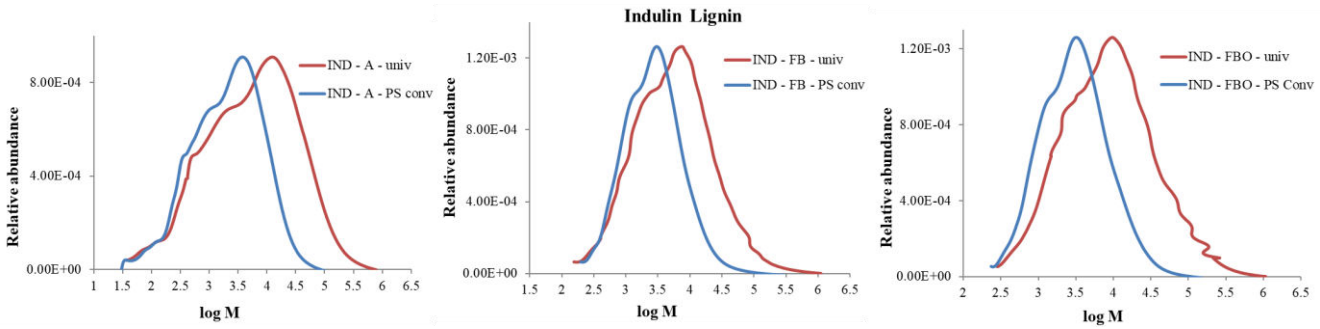

Figure 5.14. Comparison of universal and conventional SEC – MMD curves of relative abundance Vs log(Mw) for A - acetylated, FB - fluorobenzylated and FBO - fluorobenzoylated Indulin lignin samples

Table 5.16 reports average mass and dispersity values for the IND derivatives. Acetylated IND showed M_w values closer to fluorobenzoylated IND than to fluorobenzylated IND. This is due to the width of the acetylated lignin MMD which extends in the high mass region, increasing the apparent M_w. Also because the large width of the distribution, M_n value appears considerably lower than for fluoroderivatives, which clearly explains the large variations in dispersity index. It is likely that compared to the other derivatives, acetylated lignin contains larger number of small molecules which contributes to the decrease of the M_n value. Probably because of the size selection process during the precipitation procedure, fluoro-derivatives contain bigger molecular fractions, thus contributing to an increase of M_n and decrease of dispersity index.

Table 5.16. MMD of derivatized IND lignin from universal calibration with global curve fit and individual curve fit and comparison with conventional calibration. M_n and M_w values in Da.

	Universal (viscometric detector)				Conventional (RI detector)			
IND-Acetylated	M_n	M_w	M_w/M_n	M_p	M_n	M_w	M_w/M_n	M_p
Fit with Global curve[a]	1090	19920	18.3	12300	-	-	-	-
PS	950	17980	18.9	10990	820	4530	5.5	3770
PMMA	720	16860	23.4	9690	1040	5680	5.5	4750
Cellulose acetate	1880	25150	13.4	16970	1160	3940	3.4	3700
IND-Fluorobenzylated								
Fit with Global curve[a]	2440	15390	6.3	7600	-	-	-	-
PS	2150	13890	6.5	6780	1660	4490	2.7	3040
PMMA	1750	13020	7.4	5920	2110	5630	2.7	3830
Cellulose acetate	3790	19480	5.1	10670	1970	3980	2.0	3090
IND-Fluorobenzoylated								
Fit with Global curve[a]	3760	22270	5.9	9700	-	-	-	-
PS	3320	20100	6.1	8650	1910	5040	2.6	3210
PMMA	2730	18870	6.9	7570	2420	6310	2.6	4050
Cellulose acetate	5780	28080	4.9	13550	2210	4400	2.0	3230

a = fit with global curve (PS, PMMA, Cellulose acetate)

5.3.6.3. Derivatized Organosolv (ORG) lignin SEC-THF analysis using universal and conventional calibration methods (system B)

Organosolv lignin is obtained from the CIMV process i.e. cooking with a mixture of (formic acid/acetic acid/water) at 105-110ºC for about 2-3 hours. As already mentioned, the ORG lignin showed a bimodal elution behaviour in THF, and only the main peak was considered in our study for comparison with the other lignin samples. The additional much smaller peak, observed in the very high molar mass region, could be due to poor solubility and association effects.

From the Figure 5.15, it is observed that a broad distribution was obtained for ORG acetylated lignin. It is clearly seen that a significant part of ORG acetylated lignin eluted outside the calibration range or in the low-molar-mass region. Acetylated lignin solubility was very poor and only smaller molar mass fractions were likely to dissolve. However, fluorobenzylated lignin solubility was much better, although a small part of the lignin was still insoluble. It is therefore evident that a major part of the distribution curve lies in the low molar mass region for acetylated samples. In the case of

fluorobenzoylated lignin, the uniform distribution obtained shows the good column behaviour toward this sample. Consequently, the increased hydrodynamic volume drives the system at lower retention time. Fluorobenzylated MMD exhibited an irregular curve due to poor viscometric response, which affected the calculated log (M) value by universal calibration.

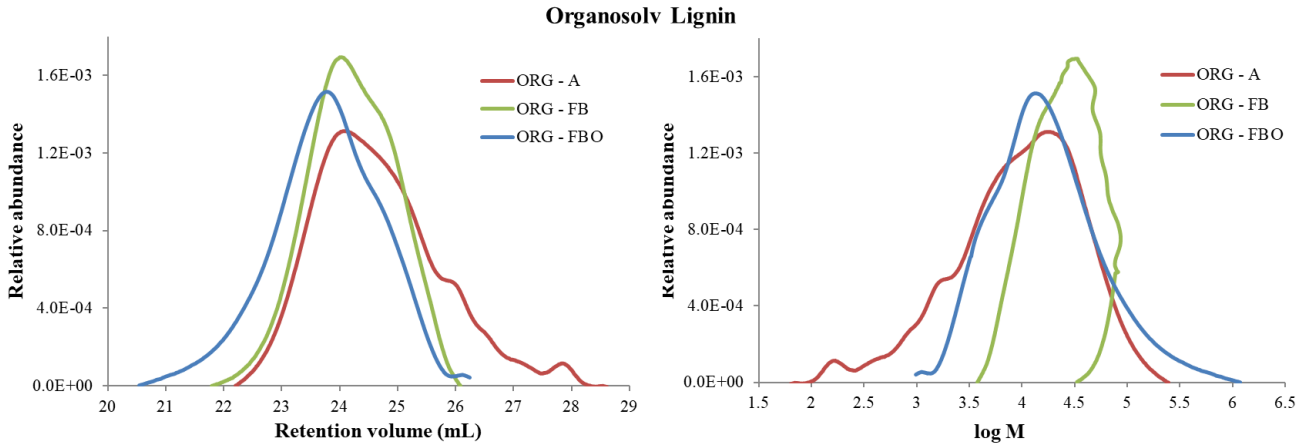

Figure 5.15. SEC – MMD universal calibration curve of Organosolv (ORG) lignin: relative abundance vs retention volume (*left*) and relative abundance vs log (M) (*right*) (A - acetylated, FB - fluorobenzylated and FBO - fluorobenzoylated)

The obtained MMD curves from universal and conventional methods can be compared in Figure 5.16. A large shift is observed between the methods. It should be noted that the conventional method used polystyrene as standard and the molar mass of ORG lignin could probably not fit in the range of the standard. This may explain the huge difference with the values obtained from universal calibration.

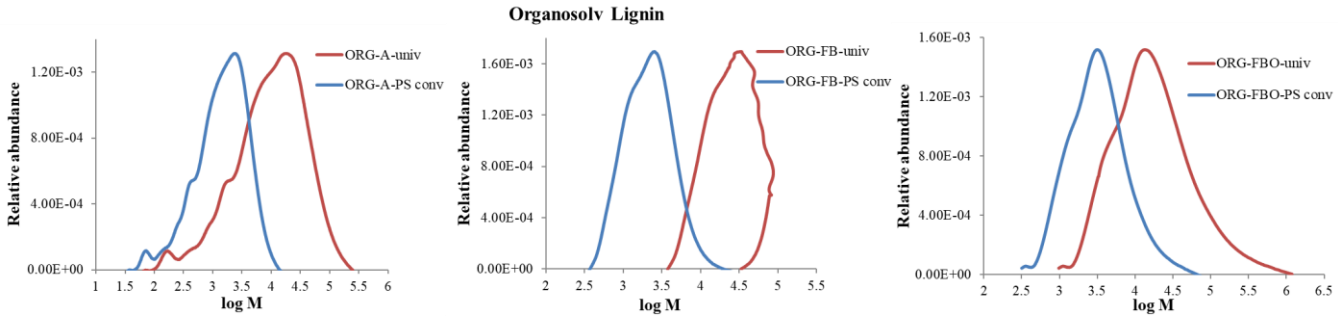

Figure 5.16. Comparison of universal and conventional SEC – MMD curves of relative abundance vs log (M) for A - acetylated, FB - fluorobenzylated and FBO - fluorobenzoylated ORG lignin samples

From Table 5.17, although extreme variations in apparent M_n and M_w values, the acetylated ORG lignin dispersity index (M_w/M_n) is higher than for fluoro-derivatives. Dispersity index values around 1.5 to 2 for fluorobenzylated ORG lignin reveals that the partially soluble lignin contains uniform

molar mass fractions. In the case of fluorobenzoylated lignin, the solubility is even better than for the two other derivatives and major part of the higher-molar-mass lignin increases the apparent M_w values.

Table 5.17. MMD of derivatized ORG lignin, from universal calibration with global curve fit and individual curve fit, and comparison with conventional calibration. M_n and M_w values in Da.

	Universal (viscometric detector)				Conventional (RI detector)			
ORG-Acetylated	M_n	M_w	M_w/M_n	M_p	M_n	M_w	M_w/M_n	M_p
Fit with Global curve[a]	2900	18950	6.5	17810	-	-	-	-
PS	2530	16930	6.7	15850	770	2100	2.7	2380
PMMA	1940	14920	7.7	13660	980	2650	2.7	3010
Cellulose acetate	4950	26270	5.3	25500	1070	2160	2.0	2520
ORG-Fluorobenzylated								
Fit with Global curve[a]	19750	32700	1.7	32630	-	-	-	-
PS	17480	29170	1.7	29050	1680	2690	1.6	2500
PMMA	14610	25550	1.7	25100	2130	3390	1.6	3150
Cellulose acetate	29610	45760	1.5	46540	1930	2700	1.4	2620
ORG-Fluorobenzoylated								
Fit with Global curve[a]	8600	34410	4.0	13540	-	-	-	-
PS	7620	31030	4.1	12080	2240	4800	2.1	3180
PMMA	6400	28970	4.5	10570	2850	6020	2.1	4015
Cellulose acetate	12800	43720	3.4	18940	2500	4270	1.7	3210

a = fit with global curve (PS, PMMA, Cellulose acetate)

5.3.6.4. Derivatized Kraft (KR) lignin SEC-THF analysis using universal and conventional calibration methods (system B)

Kraft lignin is obtained from pine softwood. Figure 5.17 exhibits almost similar SEC curves for fluoroderivatives, and like for the other lignins, acetylated lignin displays a broad profile. MMD curves for different derivatized KR lignin samples using conventional and universal method and compared in Figure 5.18. The curve of acetylated lignin is shifted at higher log (M) and this clearly shows the presence of higher molar fragments in the acetylated samples. From Table 5.18, the acetylated lignin using universal calibration showed highest MMD compared to fluoro derivatives.

However, the M_n value is very low and greatly influences the dispersity value, compared to other derivatization methods. Fluorobenzoylated lignin dispersity value is lower than for other derivatives and the higher molar mass addition significantly increased the average M_w and M_n in this case.

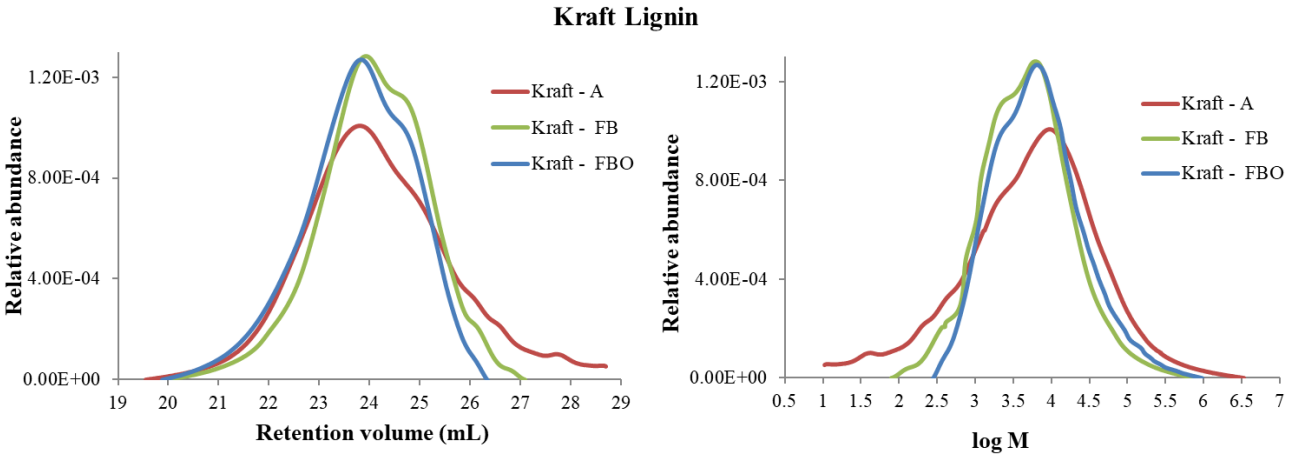

Figure 5.17. SEC – MMD universal calibration curve of Kraft (KR) lignin: relative abundance vs retention volume (*left*) and relative abundance vs log (Mw) (*right*) (A - acetylated, FB - fluorobenzylated and FBO - fluorobenzoylated)

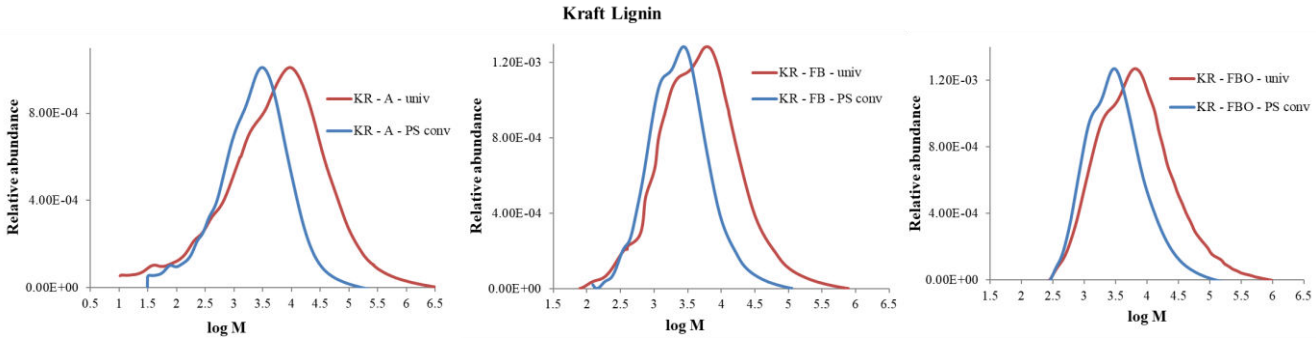

Figure 5.18. Comparison of universal and conventional SEC – MMD curves of relative abundance vs log (M) for A - acetylated, FB - fluorobenzylated and FBO - fluorobenzoylated Kraft lignin samples

Table 5.18. MMD of derivatized Kraft pine lignin, from universal calibration with global curve fit and individual curve fit, and comparison with conventional calibration. M_n and M_w values in Da.

	Universal (viscometric detector)				Conventional (RI detector)			
KR-Acetylated	M_n	M_w	M_w/M_n	M_p	M_n	M_w	M_w/M_n	M_p
Fit with Global curve[a]	540	31060	57.5	9520	-	-	-	-
PS	470	28190	60.0	8490	750	5110	6.8	3100
PMMA	350	27270	77.9	7420	960	6380	6.6	3910
Cellulose acetate	990	37450	37.8	13340	1110	4290	3.9	3130
KR-Fluorobenzylated								
Fit with Global curve[a]	2190	13670	6.2	6250	-	-	-	-
PS	1930	12340	6.4	5570	1510	4170	2.8	2770
PMMA	1560	11550	7.4	4840	1920	5230	2.7	3490
Cellulose acetate	3430	17340	5.1	8840	1820	3710	2.0	2850
EU-KR-Fluorobenzoylated								
Fit with Global curve[a]	3210	18190	5.7	6530	-	-	-	-
PS	2840	16450	5.8	5830	2020	5580	2.8	3040
PMMA	2350	15630	6.7	5090	2570	6980	2.7	3830
Cellulose acetate	4860	22540	4.6	9170	2310	4730	2.0	3090

a = fit with global curve (PS, PMMA, Cellulose acetate)

5.3.6.5. Derivatized Eucalyptus-Kraft (EUCA-KR) lignin SEC-THF using universal and conventional calibration methods (system B)

Hardwood Eucalyptus Kraft lignin was prepared using Kraft cooking at laboratory scale. The SEC and MMD curves in Figure 5.19 exhibit more uniform distribution for all derivatized lignins. A long tail can be seen for acetylated samples. Comparing universal and conventional calibrations from

Figure **5.20**, a rather small shift (compared to other lignins) towards higher molar mass region can be observed. Average molar mass values in Table 5.19 indicate that conventional calibration yields to about 2 – 2.5 times lower average mass than universal calibration. With universal calibration, acetylated and fluorobenzylated lignins showed similar M_w values, but as already seen for other lignins, the acetylated lignin M_n value is lower than for the fluorobenzylated sample, which leads to higher dispersity index for the acetylated EUCA-KR lignin.

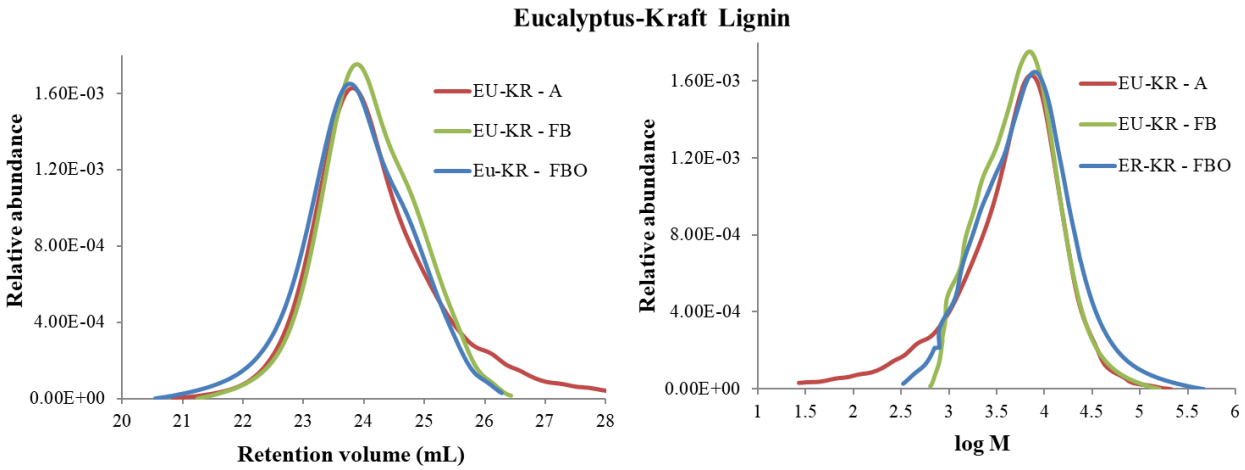

Figure 5.19. SEC – MMD universal calibration curve of EUCA-KR lignin: relative abundance vs retention volume (*left*) and relative abundance vs log (M) (*right*) (A - acetylated, FB - fluorobenzylated and FBO - fluorobenzoylated)

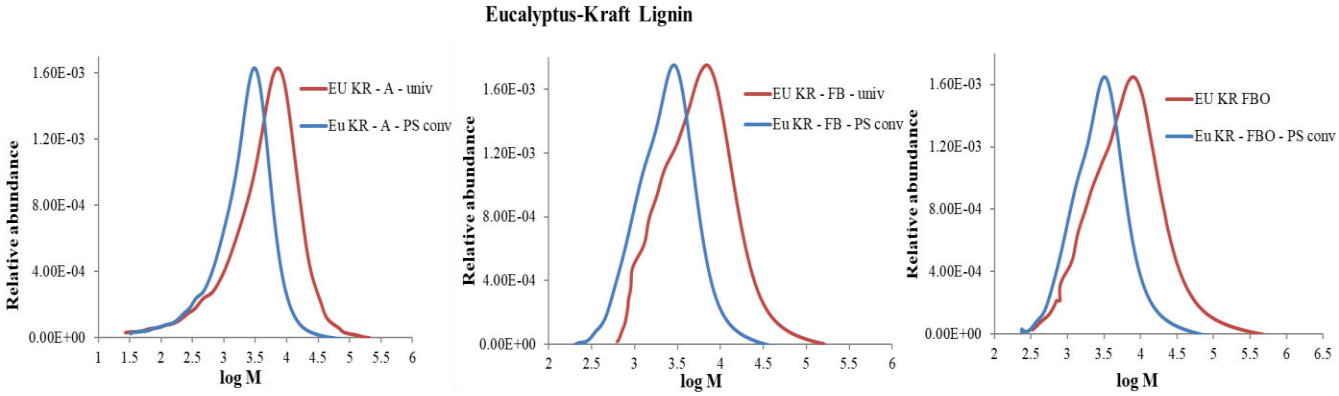

Figure 5.20. Comparison of universal and conventional SEC – MMD curves for EUCA-KR lignin; A - acetylated, FB - fluorobenzylated and FBO - fluorobenzoylated .

Table 5.19. MMD of derivatized EUCA-KR lignin from universal calibration with global curve fit and individual curve fit, and comparison with conventional calibration. M_n and M_w values in Da.

	Universal (viscometric detector)				Conventional (RI detector)			
EU-KR-Acetylated	M_n	M_w	M_w/M_n	M_p	M_n	M_w	M_w/M_n	M_p
Fit with Global curve[a]	1260	8460	6.7	7270	-	-	-	-
PS	1100	7580	6.9	6480	1010	3210	3.2	3070
PMMA	840	6820	8.1	5660	1300	4040	3.1	3870
Cellulose acetate	2150	11370	5.3	10200	1390	3080	2.2	3110
EU-KR-Fluorobenzylated								
Fit with Global curve[a]	3390	8580	2.5	7000	-	-	-	-
PS	3000	7680	2.6	6240	1780	3130	1.8	2870
PMMA	2500	6880	2.8	5430	2260	3940	1.7	3630
Cellulose acetate	5120	11610	2.3	9870	2040	3050	1.5	2940
EU-KR-Fluorobenzoylated								
Fit with Global curve[a]	3630	13210	3.6	7990	-	-	-	-
PS	3210	11890	3.7	7130	2040	4060	2.0	3200
PMMA	2670	10930	4.1	6240	2580	5100	2.0	4040
Cellulose acetate	5470	17200	3.1	11170	2300	3740	1.6	3230

a = fit with global curve (PS, PMMA, Cellulose acetate)

5.3.7. General Discussion

Our results are consistent with previously reported results using conventional SEC (Faix and Beinhoff, 1980; Himmel et al., 1989). Faix et al. calculated MMD of various acetylated lignin samples (Spruce, Bamboo, Beech, Aspen and Milled wood) using conventional calibration and polystyrene standard. They found higher M_w and M_n for the acetylated lignin than for underivatized lignin, and the dispersity values lie in the range of 1.8 to 3.6. Himmel et al. carried out SEC analysis of different aspen lignin samples after acetylation using conventional calibration with UV and RI detection, and universal method with viscometric detection. The author found dispersity values for conventional calibration ranging from 3.4 to 4.2. Universal calibration yielded to higher M_w values, about 1.5 to 2.5 times higher than conventional calibration. Moreover, M_w values determined by universal calibration were in the same range than those determined by the sedimentation equilibrium method.

Similarly, Nascimento et al. (Nascimento et al., 1992) calculated the apparent M_w values of four lignins of *eucalyptus grandis* wood (milled wood lignin, Organosolv, Kraft-mild conditions, Kraft-vigorous conditions) after acetylation with conventional calibration and polystyrene standards. The author obtained broad MMD's in all the cases, with two maxima found in the case of milled wood and Organosolv process lignin samples, and thus excluded some macromolecular fractions for the calculation of apparent M_w value. Like these researchers, we faced the same difficulty with the CIMV Organosolv lignin. After peak selection Organosolv lignins exhibited higher M_w values than Kraft lignin samples. On the other hand, Ringena et al. (Ringena et al., 2006) carried out SEC analysis of various technical lignins without derivatization in DMSO/H_2O/LiBr and DMAC/LiCl, and molar mass values were calculated from conventional and universal calibration methods. Again, the calculated apparent M_w values determined by conventional calibration were found lower than by universal calibration. In conventional calibration, the result is much affected by the standards used as well as by the linearity and slope of the calibration curve. Moreover, systematic deviation increases as far as lignin fractions are of higher mass.

Among the three derivatization methods employed, acetylated samples exhibited the poorest solubility in THF whereas fluorobenzylated and fluorobenzoylated lignin exhibited higher solubility. Such a difference in solubility eventually affects the elution behaviour in the SEC column and results in broad MMD.

It can also be noticed that acetylated derivatives were recovered by solvent evaporation instead of liquid precipitation, and contain many smaller molecules, readily soluble in the chromatographic solvents during dissolution. However, higher molar mass fractions still have solubility issues. Precipitation methods used in the case of fluoroderivatization lead to a selection of higher molar mass derivatives. Moreover fluoro-derivatives have a much-decreased polarity which enhances their solubility while decreasing interactions with the column gel and association phenomena, especially in THF as a non-polar solvent. All these effects contribute to an improvement of SEC profiles.

From the above discussion and observations, it can be concluded that all fluoro-derivatized lignin samples showed uniform SEC and MMD profiles except Indulin and Organosolv lignin. Profiles were generally better than for acetylated lignin samples. A more logical evolution for the molar mass data can also be noticed, also characterized by higher M_w and dispersity's (the data of acetylated lignin may not be considered, due to the imperfection of the SEC profile). Higher dispersity might be explained either by better solubility and SEC behaviour of the fluoro-derivatives in THF, or by the better resolution obtained with the three PLGel columns in THF, compared to the two PolarGel columns in DMAC-LiCl. Fluoroderivatization and universal calibration is a better choice to find

lignin absolute molar mass, to analyse the structural and chemical characteristics of lignin for biorefinery application.

5.3.8. Calculation of the degree of polymerization (DP)

The degree of polymerization was calculated from the values of monomer molar mass. The monomer molar mass of all derivatized lignins were calculated from the results of ^{19}F NMR spectroscopy. The average DP is simply equal to the average molar mass divided by the monomer molar mass.

In table 5.20, the reported DP_n and DP_w values correspond to the use of chromatographic system B (SEC in THF) and universal calibration with global curve fit. As already mentioned, it should be noted that the molar mass for acetylated lignin was fixed at 240 g/mol. Similarly, DP_n, DP_w were calculated using conventional calibration and values are reported in Table 5.21.

Table 5.20. Calculated average DP's from universal calibration – Global curve fit.

		Molar mass of monomer (g/mol)	**DP_n**	**DP_w**	**$Q=DP_w/DP_n$**
PB	Acetylated	240	2	42	26.2
	FB	251*	8	38	4.8
	FBO	308*	12	52	4.4
IND	Acetylated	240	5	83	18.3
	FB	275*	9	56	6.3
	FBO	328*	11	68	5.9
ORG	Acetylated	240	12	79	6.5
	FB	249*	79	131	1.7
	FBO	275*	31	125	4
KR	Acetylated	240	2	129	57.5
	FB	268*	8	51	6.2
	FBO	310*	10	59	5.7
EU-KR	Acetylated	240	5	35	6.7
	FB	269*	13	32	2.5
	FBO	291*	12	45	3.6

*Monomer molar mass of FBZ and FBO lignins calculated from ^{19}F NMR; $Q = DP_w/DP_n$ = dispersity.

Table 5.21. Calculated average DP's from conventional calibration (using polystyrene standards)

			Conventional Calibration								
			PS			PMMA			Cellulose acetate		
		Molar mass of monomer	DP_n	DP_w	Q	DPn	DPw	Q	DPn	DPw	Q
PB	Acetylated	240	2	12	5	3	15	5	4	11	3
	FB	251*	6	13	2	7	16	2	7	12	2
	FBO	308*	7	18	3	9	22	2	8	15	2
IND	Acetylated	240	3	19	6	4	24	5	5	16	3
	FB	275*	6	16	3	8	20	3	7	14	2
	FBO	328*	6	15	3	7	19	3	7	13	2
ORG	Acetylated	240	3	9	2.7	4	11	2.7	4	9	2.0
	FB	249*	7	11	1.6	9	14	1.6	8	11	1.4
	FBO	275*	8	17	2.1	10	22	2.1	9	16	1.7
KR	Acetylated	240	3	21	6.81	4	27	6.65	5	18	3.86
	FB	268*	6	16	2.76	7	20	2.72	7	14	2.04
	FBO	310*	7	18	2.76	8	22	2.72	7	15	2.05
EU-KR	Acetylated	240	4	13	3.18	5	17	3.11	6	13	2.22
	FB	269*	7	12	1.76	8	15	1.74	8	11	1.50
	FBO	291*	7	14	1.99	9	18	1.98	8	13	1.63

*Monomer molar mass of FBZ and FBO lignins calculated from ^{19}F NMR; Q = DP_w/DP_n = dispersity.

According to Table 5.20, universal calibration method predicted that polydispersity (Q) values for acetylated lignins are considerably higher than for all other derivatives. This clearly demonstrates acetylated lignin samples have the broadest distribution. Dispersity values in the case of conventional calibration (Table 5.21) are much lower than with universal calibration.

5.4. Conclusion

Size exclusion chromatography analysis (SEC) was performed on five different commercial lignin samples (Protobind 1000 (PB), Organosolv CIMV (ORG), Indulin (IND), pine Kraft (KR) and Eucalyptus Kraft (EU-KR)) in two organic solvents (DMAc/LiCl and THF).

Solvent washing study on lignins showed that ethyl acetate, which exhibits an intermediate polarity, works better than ethanol and hexane for lignin sample washing. MMD's of underivatized and derivatized lignins were studied in DMAc/LiCl solvent using conventional calibration as a first classical method. The obtained results for all ethyl acetate-washed lignin samples demonstrated that long dissolution time is needed for full dissolution of underivatized lignin, but washing improves solubility. Different derivatizations (acetylation, fluorobenzylation and fluorobenzoylation) were performed to overcome the long dissolution time. The results of FTIR, ^{19}F NMR spectra confirmed the derivatization and quantify the hydroxyl groups. Despite apparently good solvent solubility, SEC behavior of underivatized and derivatized lignins in DMAc/LiCl remained imperfect. Moreover, conventional calibration depends on the nature of the calibrant used and molar mass results are significantly affected.

Universal calibration using DRI and viscometric detection (system B, in THF) was investigated to develop a method that allows the determination of absolute lignin molar mass values. The obtained MMD were compared to results from conventional calibration using different polymer standards. It was well observed on the SEC curves that fluoro-derivatization enhanced the lignin solubility and uniform MMD curves in THF could be obtained, a better result than for acetylated lignin samples. However, it was found that universal calibration predicts 3 to 5 times higher molar mass compared to conventional calibration. Compared to fluoro-derivatives, acetylated lignins exhibited lower M_n, due to poor solubility of higher molar mass fractions, and higher dispersity index (M_w/M_n).

Comparing the results of DMAc/LiCl and THF system, differences between the two set of results are significant. Each one is referred to different column systems and calibration methods, universal calibration versus conventional calibration. In the DMAc system, results are based on calibration by an inappropriate mono-disperse polymer, polystyrene, which differs from the cross-linked structure of lignin and leads to an erratic estimation of the MMD (Jacobs, 2000). The non-uniform distribution as well as aggregation behaviour in the conventional SEC method, using DMAc/LiCl, lead to a significant deviation on the calculation of apparent M_w values. Introducing viscometry and universal calibration lead to significantly different results.

However, despite promising results, we think that the FB and FBO derivatization methods followed by SEC in THF, established at the moment, are still perfectible. Indeed, the quality of SEC

curves obtained were not good enough on some lignin samples, not as good as in DMAc-LiCl without derivatization (as seen in the 1st part of the chapter). Only for the EU-KR and PB lignin, the curves were rather good and fully regular, thus giving reliable M_w and M_n values. In the other cases, the values were extremely affected by the high mass tailing and possibly also affected by retention in the SEC columns used (PLgel in THF, maybe not the best column-solvent system to use with lignin fluoro-derivatives). Both derivatization conditions and chromatographic conditions should still be improved, paying attention to preserving the polymer from degradation during the derivatization reactions.

As a summary, it was found that the new fluoro-derivatives exhibited an improved solubility and a rather good behaviour in the SEC system used, at least for some of the lignin samples tested. Work is still needed for optimisation of the SEC conditions, by testing other columns and solvents, like for instance the Polargel M column system using DMAc-LiCl as solvent associated with a SEC system allowing universal calibration. Moreover, derivatization conditions should be improved to increase the recovery yield of the derivatized lignin, without excluding lowest molar mass fractions. Also, the reason why such molar mass differences are observed between standard calibration and universal calibration should be elucidated by further tests using other derivatives and columns.

Conclusions and Perspectives

The thesis objective was to investigate lignin derivation methods for lignin analysis, to quantity functional groups and to determine lignin molar mass by size exclusion chromatography, the main issue being to establish the structure and reactivity of technical lignins for value-added applications.

Lignin is a branched, three-dimensional aromatic polymer with a large variety of functional groups, including hydroxyl, methoxyl, carbonyl and carboxyl groups. Lignin analysis is of primary importance because of its possible usage as precursor for different applications such as for instance in phenolic resins, polyurethanes, epoxides and acrylics, and other usages. However, lignin structure and functional groups composition remain difficult to characterize, which limits the extent of possible new applications. Another important parameter which influences the lignin usage is its molar mass which can vary significantly, depending on the process type and conditions used for its extraction.

In general, molar mass distribution (MMD) can be determined by size exclusion chromatography (SEC) analysis with column packed with either aqueous or organic polar or non-polar nanoporous gels. Numerous studies have shown that lignins do not need to be derivatized. Direct lignin SEC analysis, in alkaline-aqueous or in organic medium (DMF, DMAc, DMSO), are the simplest methods employed in research laboratories. Some lignins, especially samples with highly polar character, may form strong aggregates inside the SEC system which therefore significantly impacts the calculated MMD. To overcome this issue, lignin functional group derivatization may be employed, especially on hydroxyl groups since they are highly reactive and mainly responsible for lignin polarity. Among possible derivatization methods, acetylation is the reference. Acetylated lignin derivatives exhibit lower sample-column interaction, compared to underivatized lignin. SEC columns are usually calibrated using standard calibration with polystyrene polymers of different known molar masses, and the MMD is calculated from the (log M vs. Retention time) calibration plot. However, polystyrene is a polymer with a linear structure, far from the lignin branched structure; thus, the obtained lignin MMD value is not reliable and must be questioned.

In the present work, another derivatization method has been explored and compared with the well-known acetylation, the lignin fluorobenzylation and fluorobenzoylation to further decrease lignin polarity. All this work was done using five different technical lignin samples: Protobind 1000 lignin (commercial lignin originated from soda cooking of wheat straw), Organosolv lignin (from the CIMV process applied on wheat straw), Kraft lignin from pine and from Eucalyptus (prepared at lab. scale), and Indulin lignin (commercial Kraft lignin).

First, lignin acetylation was applied on the technical lignins to study their reactivity through the quantification of phenolic hydroxyl groups by aminolysis. Indeed, prior to aminolysis, the lignin samples were acetylated to convert hydroxyl groups into their corresponding acetylated derivatives. FT-IR spectroscopy confirmed that lignin hydroxyl groups were acetylated since the intensity of the hydroxyl groups region significantly decreased. De-acetylation carried out during the aminolysis reaction and followed by GC analysis, revealed that the Kraft lignin contains a higher phenolic hydroxyl group content (4.0 mmol/g) than the Indulin lignin (3.6 mmol/g), followed by the Protobind lignin (3.4 mmol/g) and by the Organosolv lignin (2.4 mmol/g). All these results are logical; softwood lignins (Kraft and Indulin) are known to contain more phenolic hydroxyl groups than annual plant lignins (PB and ORG). The aminolysis was compared with other analytical techniques such as UV, ^{1}H NMR, ^{13}C NMR, ^{31}P NMR and a "fast method" developed recently at LGP2 (by simultaneous conductometric and potentiometric titration). It was demonstrated that aminolysis gave comparable results as ^{13}C NMR spectroscopy. This is not surprising since both methods used acetylated derivatives. ^{1}H NMR, UV and "fast method" underestimate the phenolic hydroxyl group content for different reasons: in the case of ^{1}H NMR, signal overlapping occurs; in the UV method, some phenolic hydroxyl groups are not accounted; and the conductometric and potentiometric methods do not quantify all the phenolic structural units (with the highest pKa's). However, in the case of the titration methods, the error has been estimated to be close to 10-15%, which is satisfactory for a first industrial characterization. Moreover, classical aminolysis also exhibits some drawbacks such as an incomplete derivatization and the overestimation of phenolic hydroxyl groups due to sugar impurities present in the samples. For example, Protobind and Organosolv lignins display high sugars content, 3.1 ± 0.2 and 7.2 ± 0.3 mmol/g respectively. Polysaccharides possibly undergo the acetylation and deacetylation reactions leading to an overestimation of the hydroxyl content results.

All these limitations, incomplete derivatization and the influence of impurities, can be avoided by employing new derivatization methods such as fluorobenzylation and fluorobenzoylation. Our herein reported studies on this topic have completed the original work from Barrelle and co-workers during the 1990's. The reactivity of hydroxyl groups typically encountered in lignin was first studied using lignin model compounds submitted to fluorobenzylation. Lignin like model compounds were chosen according to the nature of the hydroxyl groups bound to the different sites, such as aromatic and aliphatic hydroxyl groups in order to better assess and precise fluorobenzylation reactivity towards a variety of hydroxyl groups, as well as ^{19}F NMR signal assignment. The selected model compounds were the vanillin, the acetovanillone and the guaiacol, all containing an aromatic hydroxyl group, the vanillyl alcohol with both aliphatic and aromatic hydroxyl groups, the veratryl alcohol bearing only an aliphatic hydroxyl group, and finally a model of carbohydrate, the cellobiose, to study the possible effect of polysaccharides impurities in lignins. Complete derivatization was obtained with purely

phenolic model compounds, whereas for the model compound containing both aromatic and aliphatic hydroxyls, or only aliphatic, fluorobenzylation was partial. Fluorobenzylation is thus fully efficient on phenolic hydroxyl groups but aliphatic hydroxyls are poorly reactive. Moreover, no fluorobenzylation was observed with cellobiose, therefore, sugar contamination in lignin sample should not interfere with the phenolic hydroxyl analysis. After the study of lignin model reactivity, the fluorobenzylation reaction was applied on the Organosolv lignin and ^{19}F NMR spectroscopy analysis was carried out for hydroxyl group quantification. The obtained ^{19}F NMR chemical shift assignments on the lignin polymer were aligned precisely with chemical shifts obtained with lignin model compounds. According to ^{19}F NMR quantification, Organosolv lignin contains 1.71 mmol of phenolic hydroxyl groups per gram of lignin, and only 0.120 mmol of primary aliphatic hydroxyl groups per gram of lignin, which is a low and probably underestimated value, because of the lack of reactivity of fluorobenzylation on aliphatic hydroxyls, as observed on model compounds. The phenolic hydroxyl group content is in the same order as those obtained using the Fast method (1.5 mmol/g), UV method (1.7 mmol/g), ^{31}P NMR method (1.3 mmol/g) and ^{13}C NMR after lignin acetylation (2 mmol/g). However, the aminolysis method apparently overestimated phenolic hydroxyls, with a quantification of 2.4 mmol/g lignin. These results confirmed that ^{19}F NMR is a robust method for phenolic hydroxyl group quantification in lignins. It is also stressed that fluorobenzylation significantly increases the solubility of the lignin macromolecule meaning that this derivatization method could also be used to enhance lignin behaviour in SEC systems.

Prior to MMD analysis, lignins have been washed to remove impurities. For that purpose, several solvents have been tested on the Protobind 1000 lignin. Results revealed that ethyl acetate worked as a better solvent for lignin washing than the two other selected solvents, ethanol and hexane, because of the moderate polar nature of ethyl acetate. It was observed that during washing, the higher polarity of ethanol leads to an important removal of all molar mass fractions of the lignin polymer, including the higher mass, along with impurities, and an important decrease of washing yield.

Size exclusion chromatography (SEC) analysis was performed on five different commercial lignins, i.e. Protobind, Organosolv, Indulin, Kraft and Eucalyptus Kraft lignins in organic solvents (DMAc/LiCl and THF). As a first step, molar mass distributions of underivatized and derivatized lignins were studied in a SEC system working in DMAc/LiCl as solvent (chromatographic system A equipped with two Polargel M columns and a DRI detector) and using conventional standard calibration. Three standard polymers used for calibration were compared (polystyrene, PMMA and cellulose acetate). They exhibited fully linear calibration curves which significantly differed from each other in terms of slope and Y-ordinate. The obtained results for all ethyl acetate washed underivatized lignin samples showed that long dissolution time, about 4 to 5 weeks, was required to fully solubilize all the lignins. In addition, the different derivatives (acetylated and fluorobenzylated

and fluorobenzoylated derivatives) were also tested in the same solvent system. FTIR and ^{19}F NMR analyses confirmed the derivatization and enabled hydroxyl groups quantification. The added mass on each lignin samples during fluoro derivatization was calculated from ^{19}F NMR spectra. Then the MMD was analysed and the apparent M_n, M_w values determined through the conventional calibration method with polystyrene standards. Although, fluoro-derivatization enhanced lignin solubility and SEC behaviour in DMAc/LiCl, the molar mass results remain imprecise because of standard calibration with polymers that do not fit correctly the structure of the lignin macromolecule. To circumvent this, the universal calibration method was used to determine absolute molar mass values of lignins, using viscometry as a complementary in-line detector, coupled to DRI detector (chromatographic system B working in THF, equipped with three PLGel columns). It was first verified that all standard polymers (polystyrene, PMMA and cellulose acetate) followed a unique universal calibration straight line with the chromatographic system used. Lignin derivatives were then tested, all of them being soluble in THF, and the obtained MMD results were compared to conventional calibration. SEC results showed that fluoro-derivatives had a better solubility and exhibited nicer MMD profiles in THF solvent, compared to acetylated lignins. It was found that universal calibration calculation predicts 3 to 5 times higher molar mass values, compared to conventional calibration. Acetylated lignin derivatives presented significantly lower M_n and higher dispersity values than the fluoro-derivatives, for which the lowest molar mass fractions are not retained during the recovery step by precipitation in ethyl-ether, in the derivatization protocol used.

Therefore, comparing the results of the two chromatographic systems used, one in DMAc/LiCl and the other in THF, and the different calibration methods used, it can be conclude that important differences were found. It seems that the fluorobenzylation and fluorobenzoylation protocols, followed by SEC in THF, are not good enough at the moment. A molar mass selection occurs during the final precipitation step that enables the recovery of the derivatives. Moreover, in the non-polar solvent used (THF), the quality of SEC profiles of the fluoro-derivatives, although better than with acetylation, was not good enough for some of the samples tested, not as good as in DMAc-LiCl without derivatization with long dissolution time. Only for the Eucalyptus-Kraft and Protobind lignin, the SEC profiles were fully regular, thus giving reliable M_w and M_n values. For the other samples, the apparent M_w and M_n values for Indulin, Organosolv and Kraft lignins were extremely affected by tailing in the high mass region, possibly due to some retention effect in columns (PLGel in THF is suited for fully non-polar polymers, maybe not the best column-solvent system to be used if lignin derivatives remain slightly polar). Therefore, fluoro-derivatization protocols and the column-solvent system to use still need some improvement. As long as size-exclusion chromatograms will present some insufficiencies, the uncertainty on the real lignin molar mass will remain, whatever the method used for quantification (universal or conventional calibration). Therefore, to pursue the research on

fluoro-derivatives, which keep the advantage of low polarity and rapid dissolution, other solvents and SEC systems should be employed, and as a first test to set-up, using DMAc-LiCl, Polargel M columns and a SEC system that enables universal calibration should be attempted.

As final conclusion, the obtained results from this work on the different lignin samples investigated can be used for the development of various value-added applications for lignin utilization. Indeed, the number and types of hydroxyl groups were quantified by different methods, and the molecular size and dissolution properties of the different lignins were comparatively investigated. Moreover, fluoro-derivatization methods may also give a new insight for decreasing lignin polarity, and further developments of well-established protocols will open a new route for changing the polarity of lignins originated from different sources.

References

Achyuthan, K.E., Achyuthan, A.M., Adams, P.D., Dirk, S.M., Harper, J.C., Simmons, B.A., Singh, A.K., Achyuthan, K.E., Achyuthan, A.M., Adams, P.D., et al. (2010). Supramolecular Self-Assembled Chaos: Polyphenolic Lignin's Barrier to Cost-Effective Lignocellulosic Biofuels. Molecules *15*, 8641–8688.

Adler, E. (1957). Structural elements of lignin. Ind. Eng. Chem. *49*, 1377–1383.

Adler, E. (1977). Lignin chemistry—past, present and future. Wood Sci. Technol. *11*, 169–218.

Adler, E., Hernestam, S., Boss, E., and Caglieris, A. (1955). Estimation of Phenolic Hydroxyl Groups in Lignin. I. Periodate Oxidation of Guaiacol Compounds. Acta Chem. Scand. *9*, 319–334.

Adler, E., Magnusson, R., Hansen, S.E., Sömme, R., Stenhagen, E., and Palmstierna, H. (1959). Periodate Oxidation of Phenols. I. Monoethers of Pyrocatechol and Hydroquinone. Acta Chem. Scand. *13*, 505–519.

Ahvazi, B.C., and Argyropoulos, D.S. (1996a). 19F Nuclear Magnetic Resonance Spectroscopy for the Elucidation of Carbonyl Groups in Lignins. 1. Model Compounds. J. Agric. Food Chem. *44*, 2167–2175.

Ahvazi, B.C., and Argyropoulos, D.S. (1996b). Quantitative trifluoromethylation of carbonyl-containing lignin model compounds. J. Fluor. Chem. *78*, 195–198.

Ahvazi, B., Wojciechowicz, O., Ton-That, T.-M., and Hawari, J. (2011). Preparation of Lignopolyols from Wheat Straw Soda Lignin. J. Agric. Food Chem. *59*, 10505–10516.

Ahvazi, B.C., Crestini, C., and Argyropoulos, D.S. (1999). 19F Nuclear Magnetic Resonance Spectroscopy for the Quantitative Detection and Classification of Carbonyl Groups in Lignins. J. Agric. Food Chem. *47*, 190–201.

Albertsson, A.-C., Edlund, U., and Varma, I.K. (2011). Synthesis, Chemistry and Properties of Hemicelluloses. In Biopolymers – New Materials for Sustainable Films and Coatings, (John Wiley & Sons, Ltd), pp. 133–150.

Allan, G.G. (1969). Hydroxyesters of bark phenolic acids.

Alvarez-Vasco, C., Ma, R., Quintero, M., Guo, M., Geleynse, S., Ramasamy, K.K., Wolcott, M., and Zhang, X. (2016). Unique low-molecular-weight lignin with high purity extracted from wood by deep eutectic solvents (DES): a source of lignin for valorization. Green Chem. *18*, 5133–5141.

Aniceto, J.P.S., Portugal, I., and Silva, C.M. (2012). Biomass-Based Polyols through Oxypropylation Reaction. ChemSusChem *5*, 1358–1368.

Anjos, O., Santos, A., and Simões, R. (2004). Influence of hemicelluloses content on the paper quality produced with Eucalyptus globulus fibres. In Progress in Paper Physics Seminar 2004, pp. 50–52.

Argyropoulos, D.S. (1994). Quantitative Phosphorus-31 NMR Analysis of Six Soluble Lignins. J. Wood Chem. Technol. *14*, 65–82.

Argyropoulos, D.S. (2013). High value lignin derivatives, polymers, and copolymers and use thereof in thermoplastic, thermoset, composite, and carbon fiber applications.

Argyropoulos, D.S., and Zhang, L. (1998). Semiquantitative Determination of Quinonoid Structures in Isolated Lignins by 31P Nuclear Magnetic Resonance. J. Agric. Food Chem. *46*, 4628–4634.

Argyropoulos, D.S., Heitner, C., and Morin, F.G. (1992). P NMR Spectroscopy in Wood Chemistry - Part III. Solid State 31P NMR of Trimethyl Phosphite Derivatives of Chromophores in Mechanical Pulp. Holzforsch. - Int. J. Biol. Chem. Phys. Technol. Wood *46*, 211–218.

Argyropoulos, D.S., Bolker, H.I., Heitner, C., and Archipov, Y. (1993). 31P NMR Spectroscopy in Wood Chemistry. Part IV. Lignin Models: Spin Lattice Relaxation Times and Solvent Effects in 31P NMR. Holzforsch. - Int. J. Biol. Chem. Phys. Technol. Wood *47*, 50–56.

Aro, T., and Fatehi, P. (2017). Production and Application of Lignosulfonates and Sulfonated Lignin. ChemSusChem *10*, 1861–1877.

Asikkala, J., Tamminen, T., and Argyropoulos, D.S. (2012). Accurate and reproducible determination of lignin molar mass by acetobromination. J. Agric. Food Chem. *60*, 8968–8973.

Atalla, R.H., and Agarwal, U.P. (1985). Raman Microprobe Evidence for Lignin Orientation in the Cell Walls of Native Woody Tissue. Science *227*, 636–638.

Bajpai, P. (2018). Chapter 2 - Wood and Fiber Fundamentals. In Biermann's Handbook of Pulp and Paper (Third Edition), P. Bajpai, ed. (Elsevier), pp. 19–74.

Balogh, D.T., Curvelo, A.A.S., and De Groote, R. (1992). Solvent effects on organosolv lignin from Pinus caribaea hondurensis. Holzforsch.-Int. J. Biol. Chem. Phys. Technol. Wood *46*, 343–348.

Barrelle, M. (1993). A New Method for the Quantitative 19F NMR Spectroscopic Analysis of Hydroxyl Groups in Lignins. Holzforsch. - Int. J. Biol. Chem. Phys. Technol. Wood *47*, 261–267.

Barrelle, M. (1995). Improvements in the Structural Investigation of Lignins by 19F NMR Spectroscopy. J. Wood Chem. Technol. *15*, 179–188.

Barrelle, M., Fernandes, J.C., Froment, P., and Lachenal, D. (1992). An Approach to the Determination of Functional Groups in Oxidized Lignins by 19F Nmr. J. Wood Chem. Technol. *12*, 413–424.

Barta, K., D. Matson, T., L. Fettig, M., L. Scott, S., V. Iretskii, A., and C. Ford, P. (2010). Catalytic disassembly of an organosolv lignin via hydrogen transfer from supercritical methanol. Green Chem. *12*, 1640–1647.

Barta, K., Warner, G.R., Beach, E.S., and Anastas, P.T. (2013). Depolymerization of organosolv lignin to aromatic compounds over Cu-doped porous metal oxides. Green Chem. *16*, 191–196.

Barth, H.G. (1980). A Practical Approach to Steric Exclusion Chromatography of Water-Soluble Polymers. J. Chromatogr. Sci. *18*, 409–429.

Bauer, S., Sorek, H., Mitchell, V.D., Ibáñez, A.B., and Wemmer, D.E. (2012). Characterization of Miscanthus giganteus Lignin Isolated by Ethanol Organosolv Process under Reflux Condition. J. Agric. Food Chem. *60*, 8203–8212.

Baumberger, S., Lapierre, C., and Monties, B. (1998). Utilization of Pine Kraft Lignin in Starch Composites: Impact of Structural Heterogeneity. J. Agric. Food Chem. *46*, 2234–2240.

Baumberger, S., Abaecherli, A., Fasching, M., Gellerstedt, G., Gosselink, R., Hortling, B., Li, J., Saake, B., and de Jong, E. (2007). Molar mass determination of lignins by size-exclusion chromatography: towards standardisation of the method. Holzforschung *61*, 459–468.

Belgacem, M.N., Blayo, A., and Gandini, A. (2003). Organosolv lignin as a filler in inks, varnishes and paints. Ind. Crops Prod. *18*, 145–153.

Benoit, H., Grubisic, Z., Rempp, P., Decker, D., and Zilliox, J.-G. (1966). Étude par chromatographie en phase liquide de polystyrènes linéaires et ramifiés de structures connues. J. Chim. Phys. *63*, 1507–1514.

Berlin, A., and Balakshin, M. (2014). Chapter 18 - Industrial Lignins: Analysis, Properties, and Applications. In Bioenergy Research: Advances and Applications, (Amsterdam: Elsevier), pp. 315–336.

Biermann, C. (1996). Handbook of Pulping and Papermaking - 2nd Edition. In Handbook of Pulping and Papermaking, p.

Binh, N.T.T., Luong, N.D., Kim, D.O., Lee, S.H., Kim, B.J., Lee, Y.S., and Nam, J.-D. (2009). Synthesis of Lignin-Based Thermoplastic Copolyester Using Kraft Lignin as a Macromonomer. Compos. Interfaces *16*, 923–935.

Blainski, A., Lopes, G.C., and De Mello, J.C.P. (2013). Application and Analysis of the Folin Ciocalteu Method for the Determination of the Total Phenolic Content from Limonium Brasiliense L. Molecules *18*, 6852–6865.

Botaro, V.R., and Curvelo, A.A. da S. (2009). Monodisperse lignin fractions as standards in size-exclusion analysis. J. Chromatogr. A *1216*, 3802–3806.

Brandt, A., Gräsvik, J., Hallett, J.P., and Welton, T. (2013). Deconstruction of lignocellulosic biomass with ionic liquids. Green Chem. *15*, 550–583.

Brogdon, D.B.N., Mancosky, D.G., and Lucia, L.A. (2005). New Insights into Lignin Modification During Chlorine Dioxide Bleaching Sequences (I): Chlorine Dioxide Delignification. J. Wood Chem. Technol. *24*, 201–219.

Brown, W. (1967). Solution properties of lignin. Thermodynamic properties and molecular weight determinations. J. Appl. Polym. Sci. *11*, 2381–2396.

Buhner, J., and Agblevor, F.A. (2004). Effect of detoxification of dilute-acid corn fiber hydrolysate on xylitol production. Appl. Biochem. Biotechnol. *119*, 13–30.

Buono, P., Duval, A., Verge, P., Averous, L., and Habibi, Y. (2016). New Insights on the Chemical Modification of Lignin: Acetylation versus Silylation. ACS Sustain. Chem. Eng. *4*, 5212–5222.

Calvo-Flores, F.G., Dobado, J.A., Isac-García, J., and Martín-Martínez, F.J. (2015). Lignin and Lignans as Renewable Raw Materials: Chemistry, Technology and Applications (John Wiley & Sons).

Capanema, E.A., Balakshin, M.Yu., and Kadla, J.F. (2005). Quantitative Characterization of a Hardwood Milled Wood Lignin by Nuclear Magnetic Resonance Spectroscopy. J. Agric. Food Chem. *53*, 9639–9649.

Carlos Serrano-Ruiz, J., Luque, R., and Sepúlveda-Escribano, A. (2011). Transformations of biomass-derived platform molecules: from high added-value chemicals to fuels via aqueous-phase processing. Chem. Soc. Rev. *40*, 5266–5281.

Casey, J.P. (1960). Pulp and Paper: Chemistry and Chemical Technology, Volume 2, 3rd Edition.

Cateto, C.A., Barreiro, M.F., Rodrigues, A.E., Brochier-Salon, M.C., Thielemans, W., and Belgacem, M.N. (2008). Lignins as macromonomers for polyurethane synthesis: A comparative study on hydroxyl group determination. J. Appl. Polym. Sci. *109*, 3008–3017.

Cathala, B., Saake, B., Faix, O., and Monties, B. (2003). Association behaviour of lignins and lignin model compounds studied by multidetector size-exclusion chromatography. J. Chromatogr. A *1020*, 229–239.

Cen, Y.-P., Turpin, D.H., and Layzell, D.B. (2001). Whole-Plant Gas Exchange and Reductive Biosynthesis in White Lupin. Plant Physiol. *126*, 1555–1565.

Chakar, F.S., and Ragauskas, A.J. (2004). Review of current and future softwood kraft lignin process chemistry. Ind. Crops Prod. *20*, 131–141.

Chen, F., and Li, J. (2000). Aqueous Gel Permeation Chromatographic Methods for Technical Lignins. J. Wood Chem. Technol. *20*, 265–276.

Chen, P., Zhang, L., Peng, S., and Liao, B. (2006). Effects of nanoscale hydroxypropyl lignin on properties of soy protein plastics. J. Appl. Polym. Sci. *101*, 334–341.

Cherubini, F. (2010). The biorefinery concept: using biomass instead of oil for producing energy and chemicals. Energy Convers. Manag. *51*, 1412–1421.

Christian, D.T., Nobell, A., Armstrong, T.S., and Look, M. (1972). Process for producing polyoxyalkylene ether-polyols from lignin and tannin and products so made.

Chum, H.L., Johnson, D.K., Tucker, M.P., and Himmel, M.E. (1987). Some Aspects of Lignin Characterization by High Performance Size Exclusion Chromatography Using Styrene Divinylbenzene Copolymer Gels. Holzforschung *41*, 97–108.

Connors, W.J., Sarkanen, S., and McCarthy, J.L. (1980). Gel Chromatography and Association Complexes of Lignin. Holzforschung *34*, 80–85.

Connors, W.J., Sarkanen, S., and McCarthy, J.L. (2009). Gel Chromatography and Association Complexes of Lignin. Holzforsch. - Int. J. Biol. Chem. Phys. Technol. Wood *34*, 80–85.

Constant, S., Lancefield, C.S., Weckhuysen, B.M., and Bruijnincx, P.C.A. (2017). Quantification and Classification of Carbonyls in Industrial Humins and Lignins by 19F NMR. ACS Sustain. Chem. Eng. *5*, 965–972.

Credou, J., and Berthelot, T. (2014). Cellulose: from biocompatible to bioactive material. J. Mater. Chem. B *2*, 4767–4788.

Cross, C.F., and Bevan, E.J. (1882). XVI.—The chemistry of bast fibres. J. Chem. Soc. Trans. *41*, 90–110.

Cyr, A., Chiltz, F., Jeanson, P., Martel, A., Brossard, L., Lessard, J., and Ménard, H. (2000). Electrocatalytic hydrogenation of lignin models at Raney nickel and palladium-based electrodes. Can. J. Chem. *78*, 307–315.

Davin, L.B., and Lewis, N.G. (2005). Lignin primary structures and dirigent sites. Curr. Opin. Biotechnol. *16*, 407–415.

Deguchi, S., Tsujii, K., and Horikoshi, K. (2006). Cooking cellulose in hot and compressed water. Chem. Commun. *0*, 3293–3295.

Demirbaş, A. (2001). Relationships between lignin contents and heating values of biomass. Energy Convers. Manag. *42*, 183–188.

Dence, C.W., and Lin, S.Y. (1992). Introduction. In Methods in Lignin Chemistry, (Springer, Berlin, Heidelberg), pp. 3–19.

Deng, D., Deng, P., Wang, X., and Hou, X. (2009). Direct Determination of Sodium Fluoride and Sodium Monofluorophosphate in Toothpaste by Quantitative 19F-NMR: A Green Analytical Method. Spectrosc. Lett. *42*, 334–340.

Dilling, P., and Samaranayake, G.S. (1999). Mixtures of amine modified lignin with sulfonated lignin for disperse dye.

Dorrestijn, E., Kranenburg, M., Poinsot, D., and Mulder, P. (1999). Lignin depolymerization in hydrogen-donor solvents. Holzforschung *53*, 611–616.

Dorrestijn, E., Laarhoven, L.J., Arends, I.W., and Mulder, P. (2000). The occurrence and reactivity of phenoxyl linkages in lignin and low rank coal. J. Anal. Appl. Pyrolysis *54*, 153–192.

Ebringerová, A., Hromádková, Z., and Heinze, T. (2005). Hemicellulose. In Polysaccharides I: Structure, Characterization and Use, T. Heinze, ed. (Berlin, Heidelberg: Springer Berlin Heidelberg), pp. 1–67.

El Hage, R., Brosse, N., Chrusciel, L., Sanchez, C., Sannigrahi, P., and Ragauskas, A. (2009). Characterization of milled wood lignin and ethanol organosolv lignin from miscanthus. Polym. Degrad. Stab. *94*, 1632–1638.

El Mansouri, N.-E., and Salvadó, J. (2006). Structural characterization of technical lignins for the production of adhesives: Application to lignosulfonate, kraft, soda-anthraquinone, organosolv and ethanol process lignins. Ind. Crops Prod. *24*, 8–16.

El Mansouri, N.-E., and Salvadó, J. (2007). Analytical methods for determining functional groups in various technical lignins. Ind. Crops Prod. *26*, 116–124.

Evtuguin, D.V., Pascoal Neto, C., Rocha, J., and Pedrosa de Jesus, J.D. (1998). Oxidative delignification in the presence of molybdovanadophosphate heteropolyanions: mechanism and kinetic studies. Appl. Catal. Gen. *167*, 123–139.

Faix, O. (1991). Classification of Lignins from Different Botanical Origins by FT-IR Spectroscopy. Holzforsch. - Int. J. Biol. Chem. Phys. Technol. Wood *45*, 21–28.

Faix, O. (1992). In Methods in Lignin Chemistry; Lin, SY; Dence, CW, Eds. Berl. Heidelb. Springer Berl. Heidelb. Doi *10*, 978–3.

Faix, O., and Beinhoff, O. (1980). Short Note. Holzforsch. - Int. J. Biol. Chem. Phys. Technol. Wood *34*, 174–176.

Faix, O., and Beinhoff, O. (1992). Improved calibration of highperformance sizeexclusion chromatography of lignins using lignin-like model compounds. Holzforschung *46*, 355–360.

Faix, O., Lange, W., and Salud, E.C. (1981). The Use of HPLC for the Determination of Average Molecular Weights and Molecular Weight Distributions of Milled Wood Lignins from Shorea polysperma (Blco.). Holzforsch. - Int. J. Biol. Chem. Phys. Technol. Wood *35*, 3–9.

Faix, O., Meier, D., and Fortmann, I. (1990). Thermal degradation products of wood. Holz Als Roh-Werkst. *48*, 281–285.

Faix, O., Grünwald, C., and Beinhoff, O. (1992). Determination of Phenolic Hydroxyl Group Content of Milled Wood Lignins (MWL's) from Different Botanical Origins Using Selective Aminolysis, FTIR, 1H-NMR, and UV Spectroscopy. Holzforsch. - Int. J. Biol. Chem. Phys. Technol. Wood *46*, 425–432.

Faix, O., Argyropoulos, D.S., Robert, D., and Neirinck, V. (1994). Determination of Hydroxyl Groups in Lignins Evaluation of 1H-, 13C-, 31P-NMR, FTIR and Wet Chemical Methods. Holzforsch. - Int. J. Biol. Chem. Phys. Technol. Wood *48*, 387–394.

Faix, O., Andersons, B., and Zakis, G. (1998). Determination of Carbonyl Groups of Six Round Robin Lignins by Modified Oximation and FTIR Spectroscopy. Holzforsch. - Int. J. Biol. Chem. Phys. Technol. Wood *52*, 268–274.

Fernandes, J. (1992). Modifications structurales apportées à la lignine lors de la cuisson kraft et des stades de blanchiment des pâtes papetières. PhD Diss. INPG Grenoble Fr.

Fox, S.C., and McDonald, A.G. (2010). Chemical and Thermal Characterization of Three Industrial Lignins and Their Corresponding Lignin Esters. BioResources *5*, 990–1009.

Fromm, J., Rockel, B., Lautner, S., Windeisen, E., and Wanner, G. (2003). Lignin distribution in wood cell walls determined by TEM and backscattered SEM techniques. J. Struct. Biol. *143*, 77–84.

Froschauer, C., Hummel, M., Iakovlev, M., Roselli, A., Schottenberger, H., and Sixta, H. (2013). Separation of Hemicellulose and Cellulose from Wood Pulp by Means of Ionic Liquid/Cosolvent Systems. Biomacromolecules *14*, 1741–1750.

Gang, D.R., Costa, M.A., Fujita, M., Dinkova-Kostova, A.T., Wang, H.-B., Burlat, V., Martin, W., Sarkanen, S., Davin, L.B., and Lewis, N.G. (1999). Regiochemical control of monolignol radical coupling: A new paradigm for lignin and lignan biosynthesis. Chem. Biol. *6*, 143–151.

Gellerstedt, G. (1992). Gel Permeation Chromatography. In Methods in Lignin Chemistry, (Springer, Berlin, Heidelberg), pp. 487–497.

Gellerstedt, G. (2009). Chemistry of chemical pulping. Pulping Chem. Technol. *2*, 91–120.

Gellerstedt, G., and Lindfors, E.-L. (1984). Structural Changes in Lignin During Kraft Pulping. Holzforschung *38*, 151–158.

Ghatak, H.R. (2008). Spectroscopic comparison of lignin separated by electrolysis and acid precipitation of wheat straw soda black liquor. Ind. Crops Prod. *28*, 206–212.

Gierer, J. (1980). Chemical aspects of kraft pulping. Wood Sci. Technol. *14*, 241–266.

Gierer, J., and Soderberg, S. (1959). Über die Carbonylgruppen des Lignine. Acta Chern Scand *13*, 127–137.

Gierer, J., Lindeberg, O., and Noren, I. (1979). Alkaline delignification in the presence of anthraquinone/anthrahydroquinone. Holzforschung *33*, 213–214.

Gírio, F.M., Fonseca, C., Carvalheiro, F., Duarte, L.C., Marques, S., and Bogel-Łukasik, R. (2010). Hemicelluloses for fuel ethanol: A review. Bioresour. Technol. *101*, 4775–4800.

Glasser, W.G., Drew, S.W., and Hall, P.L. (1980). Annual Report to NSF. 150.

Glasser, W.G., Davé, V., and Frazier, C.E. (1993). Molecular weight distribution of (semi-) commercial lignin derivatives. J. Wood Chem. Technol. *13*, 545–559.

Glasser, W.G., Atalla, R.H., Blackwell, J., Malcolm Brown, R., Burchard, W., French, A.D., Klemm, D.O., and Nishiyama, Y. (2012). About the structure of cellulose: debating the Lindman hypothesis. Cellulose *19*, 589–598.

Gosselink, R.J.A. (2011). Lignin as a renewable aromatic resource for the chemical industry.

Gosselink, R.J., van Dam, J.E., de Jong, E., Gellerstedt, G., Scott, E.L., and Sanders, J.P. (2011). Effect of periodate on lignin for wood adhesive application. Holzforschung *65*, 155–162.

Gosselink, R.J.A., Abächerli, A., Semke, H., Malherbe, R., Käuper, P., Nadif, A., and van Dam, J.E.G. (2004). Analytical protocols for characterisation of sulphur-free lignin. Ind. Crops Prod. *19*, 271–281.

Granata, A., and Argyropoulos, D.S. (1995). 2-Chloro-4,4,5,5-tetramethyl-1,3,2-dioxaphospholane, a Reagent for the Accurate Determination of the Uncondensed and Condensed Phenolic Moieties in Lignins. J. Agric. Food Chem. *43*, 1538–1544.

Gu, J., Catchmark, J.M., Kaiser, E.Q., and Archibald, D.D. (2013). Quantification of cellulose nanowhiskers sulfate esterification levels. Carbohydr. Polym. *92*, 1809–1816.

Gupta, K.C., Kumar Sutar, A., and Lin, C.-C. (2009). Polymer-supported Schiff base complexes in oxidation reactions. Coord. Chem. Rev. *253*, 1926–1946.

Habibi, Y., Lucia, L.A., and Rojas, O.J. (2010). Cellulose Nanocrystals: Chemistry, Self-Assembly, and Applications. Chem. Rev. *110*, 3479–3500.

Hao, N., Ben, H., Yoo, C.G., Adhikari, S., and Ragauskas, A.J. (2016). Review of NMR Characterization of Pyrolysis Oils. Energy Fuels *30*, 6863–6880.

Harman-Ware, A.E., Crocker, M., Kaur, A.P., Meier, M.S., Kato, D., and Lynn, B. (2013). Pyrolysis–GC/MS of sinapyl and coniferyl alcohol. J. Anal. Appl. Pyrolysis *99*, 161–169.

Harris, E.E., D'Ianni, J., and Adkins, H. (1938). Reaction of Hardwood Lignin with Hydrogen. J. Am. Chem. Soc. *60*, 1467–1470.

Hatakeyama, H., and Hatakeyama, T. (2010). Lignin Structure, Properties, and Applications. In Biopolymers: Lignin, Proteins, Bioactive Nanocomposites, A. Abe, K. Dusek, and S. Kobayashi, eds. (Berlin, Heidelberg: Springer Berlin Heidelberg), pp. 1–63.

Hatakeyama, T., Hirose, S., and Hatakeyama, H. (1983). Differential scanning calorimetric studies on bound water in 1,4-dioxane acidolysis lignin. Makromol. Chem. *184*, 1265–1274.

Hatfield, R.D., Grabber, J., Ralph, J., and Brei, K. (1999). Using the acetyl bromide assay to determine lignin concentrations in herbaceous plants: some cautionary notes. J. Agric. Food Chem. *47*, 628–632.

HAUSALO, T. (1985). Analysis of wood and pulp carbohydrates by anion exchange chromatography with pulsed amperometric detection. Proc. 8th Int. Sympoium Wood Pulp Chem. Hels. 1985.

He, W., Du, F., Wu, Y., Wang, Y., Liu, X., Liu, H., and Zhao, X. (2006). Quantitative 19F NMR method validation and application to the quantitative analysis of a fluoro-polyphosphates mixture. J. Fluor. Chem. *127*, 809–815.

Hedges, J.I., and Mann, D.C. (1979). The characterization of plant tissues by their lignin oxidation products. Geochim. Cosmochim. Acta *43*, 1803–1807.

Heitner, C., Dimmel, D., and Schmidt, J. (2016). Lignin and lignans: advances in chemistry (CRC press).

Heuser, E. (1953). Analytik der Carbonylgruppe. Anal. Methoden George Thieme Stuttg. Fed. Repub. Ger. 434–472.

Heuser, E., and Sieber, R. (1913). Über die Einwirkung von Chlor auf Fichtenholz. Angew. Chem. *26*, 801–806.

Himmel, M.E., Tatsumoto, K., Oh, K.K., Grohmann, K., Johnson, D.K., and Chum, H.L. (1989). Molecular Weight Distribution of Aspen Lignins Estimated by Universal Calibration. In Lignin, (American Chemical Society), pp. 82–99.

Hoareau, W., Trindade, W.G., Siegmund, B., Castellan, A., and Frollini, E. (2004). Sugar cane bagasse and curaua lignins oxidized by chlorine dioxide and reacted with furfuryl alcohol: characterization and stability. Polym. Degrad. Stab. *86*, 567–576.

Hoftiezer, H.W., Watts, D.J., and Takahashi, A. (1984). Cationic reaction product of kraft lignin with aldehyde and polyamine.

Holzgrabe, U., Deubner, R., Schollmayer, C., and Waibel, B. (2005). Quantitative NMR spectroscopy—Applications in drug analysis. J. Pharm. Biomed. Anal. *38*, 806–812.

Hon, D.N.-S. (1996). Cellulose and its derivatives: structures, reactions, and medical uses. Polysacch. Med. Appl. N. Y. USA Marcel Dekker 87–105.

Horst H. Nimz, Uwe Schmitt, Eckart Schwab, Otto Wittmann, Franz Wolf. (2005). "Wood" in Ullmann's Encyclopedia of Industrial Chemistry, Wiley-VCH, Weinheim.

Hortling, B., Tamminen, T., and Kenttä, E. (1997). Determination of Carboxyl and Non-Conjugated Carbonyl Groups in Dissolved and Residual Lignins by IR Spectroscopy. Holzforsch. - Int. J. Biol. Chem. Phys. Technol. Wood *51*, 405–410.

Huang, F., Pan, S., Pu, Y., Ben, H., and J. Ragauskas, A. (2014). 19 F NMR spectroscopy for the quantitative analysis of carbonyl groups in bio-oils. RSC Adv. *4*, 17743–17747.

Ince, P.J. (1979). How to estimate recoverable heat energy in wood or bark fuels. Gen Tech Rep FPL–GTR–29 Madison WI US Dep. Agric. For. Serv. For. Prod. Lab. 7 P 27 Cm *029*.

Jacobs (2000). Absolute molar mass of lignins by size exclusion chromatography and MALDI-TOF mass spectroscopy. Nord. Pulp Pap. Res. J. *15*, 120–127.

Jacobs, A., and Dahlman, O. (2001). Characterization of the Molar Masses of Hemicelluloses from Wood and Pulps Employing Size Exclusion Chromatography and Matrix-Assisted Laser Desorption Ionization Time-of-Flight Mass Spectrometry. Biomacromolecules *2*, 894–905.

Jacobson, M.Z., and Delucchi, M.A. (2009). A path to sustainable energy by 2030. Sci. Am. *301*, 58–65.

Januszkiewicz, K.R., and Alper, H. (1983). Exceedingly mild, selective and stereospecific phase-transfer-catalyzed hydrogenation of arenes. Organometallics *2*, 1055–1057.

Javaid, R., Sabir, A., Sheikh, N., and Ferhan, M. (2019). Recent Advances in Applications of Acidophilic Fungi to Produce Chemicals. Molecules *24*, 786.

Jia, Q., Zhang, W., Li, D., Liu, Y., Che, Y., Ma, Q., and Meng, F. (2017). Hydrazinolyzed cellulose-g-polymethyl acrylate as adsorbent for efficient removal of Cd(II) and Pb(II) ions from aqueous solution. Water Sci. Technol. *75*, 1051–1058.

Jiang, X., Liu, J., Du, X., Hu, Z., Chang, H., and Jameel, H. (2018). Phenolation to Improve Lignin Reactivity toward Thermosets Application. ACS Sustain. Chem. Eng. *6*, 5504–5512.

Jones, D., Ormondroyd, G.O., Curling, S.F., Popescu, C.-M., and Popescu, M.-C. (2017). 2 - Chemical compositions of natural fibres. In Advanced High Strength Natural Fibre Composites in Construction, M. Fan, and F. Fu, eds. (Woodhead Publishing), pp. 23–58.

Kadla, J.F., and Kubo, S. (2004). Lignin-based polymer blends: analysis of intermolecular interactions in lignin–synthetic polymer blends. Compos. Part Appl. Sci. Manuf. *35*, 395–400.

Kai, D., Tan, M.J., Chee, P.L., Chua, Y.K., Yap, Y.L., and Loh, X.J. (2016). Towards lignin-based functional materials in a sustainable world. Green Chem. *18*, 1175–1200.

Kamm, B., and Kamm, M. (2004). Principles of biorefineries. Appl. Microbiol. Biotechnol. *64*, 137–145.

Kamm, B., Kamm, M., Schmidt, M., Hirth, T., and Schulze, M. (2008). Lignocellulose-based Chemical Products and Product Family Trees. In Biorefineries-Industrial Processes and Products, (Wiley-Blackwell), pp. 97–149.

Kaplan, D.L. (1998). Introduction to Biopolymers from Renewable Resources. In Biopolymers from Renewable Resources, D.L. Kaplan, ed. (Berlin, Heidelberg: Springer Berlin Heidelberg), pp. 292–322.

Kim, D., Park, K.Y., and Yoshikawa, K. (2017). Conversion of Municipal Solid Wastes into Biochar through Hydrothermal Carbonization. Eng. Appl. Biochar 31.

Klason, P. (1920). Constitution of the lignin of pine wood. Ber Dtsch Chem Ges B *53*, 1864–1873.

Korntner, P., Sumerskii, I., Bacher, M., Rosenau, T., and Potthast, A. (2015). Characterization of technical lignins by NMR spectroscopy: optimization of functional group analysis by 31P NMR spectroscopy. Holzforschung *69*.

Krässig, H.A. (1993). Cellulose – Structure, Accessibility and Reactivity (M. B. Huglin, Gordon & Breach Science Pub., Yverdon).

Kristersson, P., Lundquist, K., Simonson, R., and Tingsvik, K. (1983). Gel permeation chromatography of lignin carbohydrate compounds. Holzforsch.-Int. J. Biol. Chem. Phys. Technol. Wood *37*, 51–53.

Krolikowski, P. (2004). The Use of 19F NMR to Monitor Organic Reactions on Solid Supports.

Kubo, S., Uraki, Y., and Sano, Y. (1996). Thermomechanical Analysis of Isolated Lignins. Holzforschung *50*, 144–150.

Kühnel, I., Podschun, J., Saake, B., and Lehnen, R. (2015). Synthesis of lignin polyols via oxyalkylation with propylene carbonate. Holzforschung *69*, 531–538.

Kuwahara, M., Glenn, J.K., Morgan, M.A., and Gold, M.H. (1984). Separation and characterization of two extracelluar H2O2-dependent oxidases from ligninolytic cultures of Phanerochaete chrysosporium. FEBS Lett. *169*, 247–250.

Lachenal, D., Benattar, N., Allix, M., Marlin, N., and Chirat, C. (2005). Bleachability of Alkaline Pulps: Effect of Quinones Present in Residual Lignin. In 59th Appita Annual Conference and Exhibition: Incorporating the 13th ISWFPC (International Symposium on Wood, Fibre and Pulping Chemistry), Auckland, New Zealand, 16-19 May 2005: Proceedings, (Appita Inc.), p. 23.

Lai, Y.-Z., Guo, X.-P., and Situ, W. (1990). Estimation of Phenolic Hydroxyl Groups in Wood by a Periodate Oxidation Method. J. Wood Chem. Technol. *10*, 365–377.

Lammers, G., Stamhuis, E.J., and Beenackers, A.A.C.M. (1993). Kinetics of the hydroxypropylation of potato starch in aqueous solution. Ind. Eng. Chem. Res. *32*, 835–842.

Lange, H., Rulli, F., and Crestini, C. (2016). Gel Permeation Chromatography in Determining Molecular Weights of Lignins: Critical Aspects Revisited for Improved Utility in the Development of Novel Materials. ACS Sustain. Chem. Eng. *4*, 5167–5180.

Lapierre, C., Pollet, B., and Monties, B. (1991). Heterogeneous distribution of diarylpropane structures in spruce lignins. Phytochemistry *30*, 659–662.

Laurichesse, S., and Avérous, L. (2014). Chemical modification of lignins: Towards biobased polymers. Prog. Polym. Sci. *39*, 1266–1290.

Le Floch, A., Jourdes, M., and Teissedre, P.-L. (2015). Polysaccharides and lignin from oak wood used in cooperage: Composition, interest, assays: A review. Carbohydr. Res. *417*, 94–102.

Lewis, H.F., Shaffer, S., Trieschmann, W., and Cogan, H. (1930). Methylation of Phenol by Dimethyl Sulfate1. Ind. Eng. Chem. *22*, 34–36.

Li (1994). A new method for the analysis of phenolic groups in lignins by ¹H NMR spectrometry. Nord. Pulp Pap. Res. J. *09*, 191–195.

Lin, S.Y. (1985). Reaction product of lignosulfonate and unsaturated fatty amine.

Lin, S.Y. (1992). Ultraviolet Spectrophotometry. In Methods in Lignin Chemistry, S.Y. Lin, and C.W. Dence, eds. (Berlin, Heidelberg: Springer Berlin Heidelberg), pp. 217–232.

Lin, S.Y., and Dence, C.W. (1992). Methods in lignin chemistry (Springer Science & Business Media).

Lindner, A., and Wegener, G. (1988). Characterization of Lignins from Organosolv Pulping According to the Organocell Process Part 1. Elemental Analysis, Nonlignin Portions and Functional Groups. J. Wood Chem. Technol. *8*, 323–340.

Lindsey, J.B., and Tollens, B. (1892). Ueber Holz-Sulfitflüssigkeit und Lignin. Justus Liebigs Ann. Chem. *267*, 341–366.

Lindström, T. (1979). The colloidal behaviour of kraft lignin. Colloid Polym. Sci. *257*, 277–285.

Lindström, T. (1980). The colloidal behaviour of kraft lignin. Colloid Polym. Sci. *258*, 168–173.

Llevot, A., Monney, B., Sehlinger, A., Behrens, S., and R. Meier, M.A. (2017). Highly efficient Tsuji–Trost allylation in water catalyzed by Pd-nanoparticles. Chem. Commun. *53*, 5175–5178.

Lora, J.H., and Glasser, W.G. (2002). Recent industrial applications of lignin: a sustainable alternative to nonrenewable materials. J. Polym. Environ. *10*, 39–48.

Ludwig, C.H., Nist, B.J., and McCarthy, J.L. (1964a). Lignin. XII.1 The High Resolution Nuclear Magnetic Resonance Spectroscopy of Protons in Compounds Related to Lignin. J. Am. Chem. Soc. *86*, 1186–1196.

Ludwig, C.H., Nist, B.J., and McCarthy, J.L. (1964b). Lignin. XIII.1 The High Resolution Nuclear Magnetic Resonance Spectroscopy of Protons in Acetylated Lignins. J. Am. Chem. Soc. *86*, 1196–1202.

Lundquist, K. (1992). Proton (1H) NMR spectroscopy. In Methods in Lignin Chemistry, (Springer), pp. 242–249.

Lundquist, K., Sjöholm, R., Teien, G., Pakkanen, T., Servin, R., Sternerup, H., Wistrand, L.-G., Nørskov, L., and Schroll, G. (1979a). NMR Studies of Lignins. 2. Interpretation of the 1H NMR Spectrum of Acetylated Birch Lignin. Acta Chem. Scand. *33b*, 27–30.

Lundquist, K., Mannervik, B., Nordfors, K., Nishida, T., Enzell, C.R., Reid, W.W., Yanaihara, N., and Yanaihara, C. (1979b). NMR Studies of Lignins. 3. 1H NMR Spectroscopic Data for Lignin Model Compounds. Acta Chem. Scand. *33b*, 418–420.

Lundquist, K., Aasen, A.J., Daasvatn, K., Forsgren, B., Gustafsson, J.-Å., Högberg, B., and Becher, J. (1980). NMR Studies of Lignins. 4. Investigation of Spruce Lignin by 1H NMR Spectroscopy. Acta Chem. Scand. *34b*, 21–26.

Lvova, L., Kirsanov, D., Natale, C.D., Legin, A., Kirsanov, D., Natale, C.D., and Legin, A. (2014). Multisensor Systems for Chemical Analysis : Materials and Sensors (Pan Stanford).

Lynd, L.R., Weimer, P.J., van Zyl, W.H., and Pretorius, I.S. (2002). Microbial cellulose utilization: fundamentals and biotechnology. Microbiol. Mol. Biol. Rev. *66*, 506–577.

Magina, S., Marques, A.P., and Evtuguin, D.V. (2014). Study on the residual lignin in Eucalyptus globulus sulphite pulp. Holzforschung *69*, 513–522.

Mansouri, N.-E.E., and Salvadó, J. (2006). Structural characterization of technical lignins for the production of adhesives: Application to lignosulfonate, kraft, soda-anthraquinone, organosolv and ethanol process lignins. Ind. Crops Prod. *24*, 8–16.

Månsson, P. (1982). Selective deacetylation of aromatic acetates by aminolysis. Tetrahedron Lett. *23*, 1845–1846.

Månsson, P. (1983). Quantitative determination of phenolic and total hydroxyl groups in lignins. Holzforsch.-Int. J. Biol. Chem. Phys. Technol. Wood *37*, 143–146.

Marques, A.P., Evtuguin, D.V., Magina, S., Amado, F.M.L., and Prates, A. (2009). Structure of Lignosulphonates from Acidic Magnesium-Based Sulphite Pulping of Eucalyptus globulus. J. Wood Chem. Technol. *29*, 337–357.

Martino, R., Gilard, V., Desmoulin, F., and Malet-Martino, M. (2005). Fluorine-19 or phosphorus-31 NMR spectroscopy: A suitable analytical technique for quantitative in vitro metabolic studies of fluorinated or phosphorylated drugs. J. Pharm. Biomed. Anal. *38*, 871–891.

Marton, J., and Adler, E. (1961). Carbonyl groups in lignin III. Mild catalytic hydrogenation of Bjorkman lignin. Acta Chern Scand 370–383.

Marton, J., Adler, E., and Persson, K.-I. (1961). Carbonyl groups in lignin IV. Infrared absorption studies and examination of the volumetric borohydride method. Act Chern Scand *15*, 384–392.

Masingale, M.P., Alves, E.F., Bose, S.K., and Francis, R.C. (2009). An Oxidant to Replace Nitrobenzene in Lignin Analysis. BioResources *4*, 1139–1146.

Matera, R., Gabbanini, S., Valvassori, A., Triquigneaux, M., and Valgimigli, L. (2012). Reactivity of (E)-4-Hydroxy-2-nonenal with Fluorinated Phenylhydrazines: Towards the Efficient Derivatization of an Elusive Key Biomarker of Lipid Peroxidation. Eur. J. Org. Chem. *2012*, 3841–3851.

McDonough, T.J. (1993). The chemistry of organosolv delignification. Tappi J. USA.

Meister, J. (2000). Polymer modification: principles, techniques, and applications (CRC Press).

Meister, J.J. (2002). Modification of lignin. J. Macromol. Sci. Part C Polym. Rev. *42*, 235–289.

Milne, T.A., Chum, H.L., Agblevor, F., and Johnson, D.K. (1992). Standardized analytical methods. Biomass Bioenergy *2*, 341–366.

Milton, F. (1995). The preservation of wood. Self-Study Man. Wood Treat. Coll. Nat. Resour. Univ. Minn. 102.

M.N. Mohamad, I., I. Nur, A., M.Y. Nor, N., and I. Mohd, S. (2006). Lignin Graft Copolymer as a Drilling Mud Thinner for High Temperature Well. J. Appl. Sci. *6*, 1808–1813.

Mosier, N., Wyman, C., Dale, B., Elander, R., Lee, Y.Y., Holtzapple, M., and Ladisch, M. (2005). Features of promising technologies for pretreatment of lignocellulosic biomass. Bioresour. Technol. *96*, 673–686.

Muurinen, E. (2000). Organosolv pulping – A review and distillation study related to peroxyacid pulping.

Nadif, A., Hunkeler, D., and Käuper, P. (2002). Sulfur-free lignins from alkaline pulping tested in mortar for use as mortar additives. Bioresour. Technol. *84*, 49–55.

Nasar, K., Fache, F., Lemaire, M., Béziat, J.-C., Besson, M., and Gallezot, P. (1994). Stereoselective reduction of disubstituted aromatics on colloidal rhodium. J. Mol. Catal. *87*, 107–115.

Nascimento, E.A., Morais, S.A., Machado, A.E., and Veloso, D.P. (1992). Studies of Eucalyptus grandis Lignin. Part II: High-Performance Size-Exclusion Chromatography of Milled Wood Lignin, Kraft and Organosolv Lignins. J Braz Chem Soc *3*, 61–64.

Naven, T.J.P., and Harvey, D.J. (1996). Cationic Derivatization of Oligosaccharides with Girard's T Reagent for Improved Performance in Matrix-assisted Laser Desorption/Ionization and Electrospray Mass Spectrometry. Rapid Commun. Mass Spectrom. *10*, 829–834.

Norgren, M., Edlund, H., and Wagberg, L. (2002). Aggregation of lignin derivatives under alkaline conditions. Kinetics and aggregate structure. Langmuir *18*, 2859–2865.

O'Sullivan, A.C. (1997). Cellulose: the structure slowly unravels. Cellulose *4*, 173–207.

Parpot, P., Bettencourt, A.P., Carvalho, A.M., and Belgsir, E.M. (2000). Biomass conversion: attempted electrooxidation of lignin for vanillin production. J. Appl. Electrochem. *30*, 727–731.

Patil, P.T., Armbruster, U., Richter, M., and Martin, A. (2011). Heterogeneously Catalyzed Hydroprocessing of Organosolv Lignin in Sub- and Supercritical Solvents. Energy Fuels *25*, 4713–4722.

Paulsson, M., and Simonson, R. (2002). Acetylation of Lignin and Photostabilization of Lignin-Rich Mechanical Wood Pulp and Paper. In Chemical Modification, Properties, and Usage of Lignin, T.Q. Hu, ed. (Boston, MA: Springer US), pp. 221–245.

Pellinen, J., and Salkinoja-Salonen, M. (1985a). High-performance size-exclusion chromatography of lignin and its derivatives. J. Chromatogr. A *328*, 299–308.

Pellinen, J., and Salkinoja-Salonen, M. (1985b). Aqueous size exclusion chomatography of industrial lignins. J. Chromatogr. A *322*, 129–138.

Pepper, J.M., and Supathna, P. (1978). Lignin and related compounds. VI. A study of variables affecting the hydrogenolysis of spruce wood lignin using a rhodium-on-charcoal catalyst. Can. J. Chem. *56*, 899–902.

Pepper, J.M., Steck, W.F., Swoboda, R., and Karapally, J.C. (1966). Hydrogenation of Lignin Using Nickel and Palladium Catalysts. In Lignin Structure and Reactions, (AMERICAN CHEMICAL SOCIETY), pp. 238–248.

Pizzi, A., and Walton, T. (1992). Non-Emulsifiable, Water-Based, Mixed Diisocyanate Adhesive Systems for Exterior Plywood - Part I. Novel Reaction Mechanisms and Their Chemical Evidence. Holzforsch. - Int. J. Biol. Chem. Phys. Technol. Wood *46*, 541–547.

Podschun, J., Stücker, A., Saake, B., and Lehnen, R. (2015). Structure–Function Relationships in the Phenolation of Lignins from Different Sources. ACS Sustain. Chem. Eng. *3*, 2526–2532.

Polčín, J. (1954). Study of alkali sulfite-lignin. I. Chlorination with hypochlorites. Chem. Pap. *4*, 227–234.

Pouteau, C., Dole, P., Cathala, B., Averous, L., and Boquillon, N. (2003). Antioxidant properties of lignin in polypropylene. Polym. Degrad. Stab. *81*, 9–18.

Prakobna, K., Kisonen, V., Xu, C. and Berglund, L, A. (2015). Strong reinforcing effects from galactoglucomannan hemicellulose on mechanical behavior of wet cellulose nanofiber gels. J Mater Sci 50, 7413–7423.

Puls, J., Janzon, R., and Saake, B. (2006). Comparative Removal of Hemiceluloses from Paper Pulps Using Nitren, Cuen, NaOH and KOH. Lenzing. Berichte *86*, 63–70.

Ragauskas, A.J., Williams, C.K., Davison, B.H., Britovsek, G., Cairney, J., Eckert, C.A., Frederick, W.J., Hallett, J.P., Leak, D.J., Liotta, C.L., et al. (2006a). The Path Forward for Biofuels and Biomaterials. Science *311*, 484–489.

Ragauskas, A.J., Nagy, M., Kim, D.H., Eckert, C.A., Hallett, J.P., and Liotta, C.L. (2006b). From wood to fuels: Integrating biofuels and pulp production. Ind. Biotechnol. *2*, 55–65.

Ralph, J., Lundquist, K., Brunow, G., Lu, F., Kim, H., Schatz, P.F., Marita, J.M., Hatfield, R.D., Ralph, S.A., Christensen, J.H., et al. (2004). Lignins: Natural polymers from oxidative coupling of 4-hydroxyphenyl- propanoids. Phytochem. Rev. *3*, 29–60.

Ramos, L.P. (2003). The chemistry involved in the steam treatment of lignocellulosic materials. Quím. Nova *26*, 863–871.

Ringena, O., Lebioda, S., Lehnen, R., and Saake, B. (2006). Size-exclusion chromatography of technical lignins in dimethyl sulfoxide/water and dimethylacetamide. J. Chromatogr. A *1102*, 154–163.

Robert, D.R., and Brunow, G. (1984). Quantitative estimation of hydroxyl groups in milled wood lignin from spruce and in a dehydrogenation polymer from coniferyl alcohol using 13C NMR spectroscopy. Holzforsch.-Int. J. Biol. Chem. Phys. Technol. Wood *38*, 85–90.

Rönnols, J., Larsson, K., Jacobs, A., and Aldaeus, F. (2016). Absolute determination of softwood kraft lignin molar mass using MALDI-TOF mass spectrometry and pulsed field gradient NMR. In DIVA, pp. 143–146.

S. Aziz, and G.C. Goyal (1993). Kinetics of Delignification from Mechanistic and Process Control Point of View in Solvent Pulping Processes. In Proceedings of the TAPPI Pulping Conference, TAPPI, Atlanta, Georgia.

Saake, B., and Lehnen, R. (1990). Lignin in Ullmanns Encyclopedia of industrial chemistry. (American Cancer Society), pp. 303–315.

Sadeghifar, H., Cui, C., and Argyropoulos, D.S. (2012). Toward Thermoplastic Lignin Polymers. Part 1. Selective Masking of Phenolic Hydroxyl Groups in Kraft Lignins via Methylation and Oxypropylation Chemistries. Ind. Eng. Chem. Res. *51*, 16713–16720.

Saito, T., H. Brown, R., A. Hunt, M., L. Pickel, D., M. Pickel, J., M. Messman, J., S. Baker, F., Keller, M., and K. Naskar, A. (2012). Turning renewable resources into value-added polymer : development of lignin -based thermoplastic. Green Chem. *14*, 3295–3303.

Sannigrahi, P., and Ragauskas, A.J. (2013). Fundamentals of Biomass Pretreatment by Fractionation. In Aqueous Pretreatment of Plant Biomass for Biological and Chemical Conversion to Fuels and Chemicals, (Wiley-Blackwell), pp. 201–222.

Sarkanen, K.V., and Ludwig, C.H. (1971). Liguins. Occurrence, formation, structure, and reactions (New York.; Wiley-Interscience).

Sarkanen, S., Teller, D.C., Hall, J., and McCarthy, J.L. (1981). Lignin. 18. Associative Effects among Organosolv Lignin Componentst. *14*, 9.

Sarkanen, S., Sarkanen, S., Teller, D.C., Abramowski, E., and McCarthy, J.L. (1982). Lignin. 19. Kraft Lignin Component Conformation and Associated Complex Configuration in Aqueous Alkaline Solution. Macromolecules *15*, 1098–1104.

Sarkanen, S., Teller, D.C., Stevens, C.R., and Mccarthy, J.L. (1984). Lignin. 20. Associative Interactions Between Kraft Lignin Components. Macromolecules *17*, 2588–2597.

Sasaki, M., Adschiri, T., and Arai, K. (2003). Production of Cellulose II from Native Cellulose by Near- and Supercritical Water Solubilization. J. Agric. Food Chem. *51*, 5376–5381.

Schorr, D., Diouf, P.N., and Stevanovic, T. (2014). Evaluation of industrial lignins for biocomposites production. Ind. Crops Prod. *52*, 65–73.

Sen, S., Patil, S., and Argyropoulos, D.S. (2015). Thermal properties of lignin in copolymers, blends, and composites: a review. Green Chem. *17*, 4862–4887.

Serrano, L., Esakkimuthu, E.S., Marlin, N., Brochier-Salon, M.-C., Mortha, G., and Bertaud, F. (2018). Fast, Easy, and Economical Quantification of Lignin Phenolic Hydroxyl Groups: Comparison with Classical Techniques. Energy Fuels *32*, 5969–5977.

Serrano Cantador, L., Esakkimuthu, E.S., Marlin, N., Brochier-Salon, M.-C., Mortha, G., and Bertaud, F. (2018). Fast, easy and economical quantification of lignin phenolic hydroxyl groups. Comparison with classical techniques. Energy Fuels *32*, 5969–5977.

Sévillano, R.M. (1999). Structures des lignines résiduelles des pâtes chimiques: influence des méthodes d'extraction, des procédés de délignification et des essences de bois. Thesis.

Sevillano, R.M., Mortha, G., Barrelle, M., and Lachenal, D. (2001). 19F NMR Spectroscopy for the Quantitative Analysis of Carbonyl Groups in Lignins. Holzforschung *55*, 286–295.

Shrotri, A., Kobayashi, H., and Fukuoka, A. (2018). Cellulose Depolymerization over Heterogeneous Catalysts. Acc. Chem. Res. *51*, 761–768.

Siochi, E.J., Ward, T.C., Haney, M.A., and Mahn, B. (1990). The absolute molecular weight distribution of hydroxypropylated lignins. Macromolecules *23*, 1420–1429.

Siró, I., and Plackett, D. (2010). Microfibrillated cellulose and new nanocomposite materials: a review. Cellulose *17*, 459–494.

Sixta, H. (2006). Handbook of pulp. In Handbook of Pulp, (Wiley-VCH ; John Wiley, distributor]), p.

Sixta, H. (2008). Introduction. In Handbook of Pulp, (Wiley-Blackwell), pp. 2–19.

Sjöholm, E., Gustafsson, K., Norman, E., and Colmsjö, A. (1997). The effect of degradation on the strength of hardwood kraft pulp fibres. In Proc. 9th Int. Symp. Wood Pulping Chem, p. 106.

Sjostrom, E. (1993). Wood Chemistry: Fundamentals and Applications (Elsevier).

Spellman, F. (2011). Forest-Based Biomass Energy : Concepts and Applications (CRC Press).

Sridach, W. (2010). The environmentally benign pulping process of non-wood fibers. *17*, 20.

Stankovikj, F., McDonald, A.G., Helms, G.L., and Garcia-Perez, M. (2016). Quantification of Bio-Oil Functional Groups and Evidences of the Presence of Pyrolytic Humins. Energy Fuels *30*, 6505–6524.

Stein, T. vom, Grande, P., Sibilla, F., Commandeur, U., Fischer, R., Leitner, W., and María, P.D. de (2010). Salt-assisted organic-acid-catalyzed depolymerization of cellulose. Green Chem. *12*, 1844–1849.

Stenius, P. (2000). Forest Products Chemistry - Part 3 (TAPPI).

Stenlund, B. (1976). Polyelectrolyte effects in gel chromatography. Adv. Chromatogr. *14*, 38–74.

Strassberger, Z., Tanase, S., and Rothenberg, G. (2014). The pros and cons of lignin valorisation in an integrated biorefinery. RSC Adv. *4*, 25310–25318.

Suib, S. (2013). New and future developments in catalysis: catalytic biomass conversion (Newnes).

Sun, Y., and Cheng, J. (2002). Hydrolysis of lignocellulosic materials for ethanol production: a review. Bioresour. Technol. *83*, 1–11.

Syrjänen, K., and Brunow, G. (2000). Regioselectivity in lignin biosynthesis. The influence of dimerization and cross-coupling. J. Chem. Soc. Perkin 1 *0*, 183–187.

Tamminen, T., and Hortling, B. (1999). Isolation and characterization of residual lignin. In Progress in Lignocellulosics Characterization, (TAPPI Press), p.

Thielemans, W., and Wool, R.P. (2005). Lignin Esters for Use in Unsaturated Thermosets: Lignin Modification and Solubility Modeling. Biomacromolecules *6*, 1895–1905.

Thring, R.W., Vanderlaan, M.N., and Griffin, S.L. (1996). Fractionation Of Alcell® Lignin By Sequential Solvent Extraction. J. Wood Chem. Technol. *16*, 139–154.

Tiainen, E., Drakenberg, T., Tamminen, T., Kataja, K., and Hase, A. (1999). Determination of Phenolic Hydroxyl Groups in Lignin by Combined Use of 1H NMR and UV Spectroscopy. Holzforschung *53*, 529–533.

Tien, M., and Kirk, T.K. (1983). Lignin-Degrading Enzyme from the Hymenomycete Phanerochaete chrysosporium Burds. Science *221*, 661–663.

Tolbert, A., Akinosho, H., Khunsupat, R., Naskar, A.K., and Ragauskas, A.J. (2014). Characterization and analysis of the molecular weight of lignin for biorefining studies. Biofuels Bioprod. Biorefining *8*, 836–856.

Tupciauskas, R., Gravitis, J., Abolins, J., Veveris, A., Andzs, M., Liitia, T., and Tamminen, T. (2017). Utilization of lignin powder for manufacturing self-binding HDF. Holzforschung *71*, 555–561.

Umoren, S.A., and Solomon, M.M. (2016). Polymer Characterization : Polymer Molecular Weight Determination. p.

Vanholme, R., Demedts, B., Morreel, K., Ralph, J., and Boerjan, W. (2010). Lignin Biosynthesis and Structure. Plant Physiol. *153*, 895–905.

Walther, T., Hensirisak, P., and Agblevor, F.A. (2001). The influence of aeration and hemicellulosic sugars on xylitol production by Candida tropicalis. Bioresour. Technol. *76*, 213–220.

Wang, M., Sjöholm, E., and Li, J. (2016). Fast and reliable quantification of lignin reactivity via reaction with dimethylamine and formaldehyde (Mannich reaction). Holzforschung *71*, 27–34.

Wegener, G., Przyklenk, M., and Fengel, D. (2009). Hexafluoropropanol as Valuable Solvent for Lignin in UV and IR Spectroscopy. Holzforsch. - Int. J. Biol. Chem. Phys. Technol. Wood *37*, 303–307.

Wetzel, S., Guttman, C.M., and Flynn, K.M. (2003). The Influence of the Laser Energy and Matrix of MALDI on the Molecular Mass Distribution of Poly(ethylene glycol) | NIST. ACS PMSE Prepr. *88*.

Windeisen, E., and Wegener, G. (2012). Lignin as Building Unit for Polymers-10.15.

Wu, L.C.-F., and Glasser, W.G. (1979). Utility of oxidative lignin determination methods for biodegraded lignocellulosic substrates. Biotechnol. Bioeng. *21*, 1679–1683.

Wu, L.C.-F., and Glasser, W.G. (1984). Engineering plastics from lignin. I. Synthesis of hydroxypropyl lignin. J. Appl. Polym. Sci. *29*, 1111–1123.

Wyman, C.E. (1994). Alternative fuels from biomass and their impact on carbon dioxide accumulation. Appl. Biochem. Biotechnol. *45*, 897–915.

Xu, F., Sun, J.-X., Sun, R., Fowler, P., and Baird, M.S. (2006). Comparative study of organosolv lignins from wheat straw. Ind. Crops Prod. *23*, 180–193.

Yue, X., Chen, F., and Zhou, X. (2011). Improved interfacial bonding of PVC/wood-flour composites by lignin amine modification. BioResources *6*, 2022–2044.

Zakis, G.F. (1994). Functional analysis of lignins and their derivatives (TAPPI Press).

Zakzeski, J., Bruijnincx, P.C.A., Jongerius, A.L., and Weckhuysen, B.M. (2010). The Catalytic Valorization of Lignin for the Production of Renewable Chemicals. Chem. Rev. *110*, 3552–3599.

Zawadzki, M. Quantitative Determination of Quinone Chromophore Changes during ECF Bleaching of Kraft Pulp; Institute of Paper Science and Technology: Atlanta, August 1999. PhD Thesis. Ph. D. Dissertation.

Zawadzki, M., and Ragauskas, A. (2001). N-Hydroxy Compounds as New Internal Standards for the 31P-NMR Determination of Lignin Hydroxy Functional Groups. Holzforschung *55*, 283–285.

Zawadzki, M.A., and Ragauskas, A.J. (1999). Pulp properties influencing oxygen delignification bleachability.

Zhang, Y.-H.P. (2008). Reviving the carbohydrate economy via multi-product lignocellulose biorefineries. J. Ind. Microbiol. Biotechnol. *35*, 367–375.

Zhang, J., Deng, H., Lin, L., Zhang, J., Deng, H., and Lin, L. (2009). Wet Aerobic Oxidation of Lignin into Aromatic Aldehydes Catalysed by a Perovskite-type Oxide: LaFe1-xCuxO3 (x=0, 0.1, 0.2). Molecules *14*, 2747–2757.

Zhang, K., Bhuiya, M.-W., Pazo, J.R., Miao, Y., Kim, H., Ralph, J., and Liu, C.-J. (2012). An Engineered Monolignol 4-O-Methyltransferase Depresses Lignin Biosynthesis and Confers Novel Metabolic Capability in Arabidopsis. Plant Cell *24*, 3135–3152.

Zhou, X., Li, W., Mabon, R., and Broadbelt, L.J. (2018). A mechanistic model of fast pyrolysis of hemicellulose. Energy Environ. Sci. *11*, 1240–1260.

Zoia, L., Salanti, A., Frigerio, P., and Orlandi, M. (2014). Exploring Allylation and Claisen Rearrangement as a Novel Chemical Modification of Lignin. BioResources *9*, 6540–6561.

Appendix A: Derivatization and Classification of model compounds containing aldehyde and ketone functional groups using ^{1}H, ^{13}C and ^{19}F NMR: Application to lignin carbonyl groups quantification by ^{19}F NMR

a) Introduction

^{13}C NMR and ^{19}F NMR techniques have been widely employed for the quantification of functional groups present in lignin. For example, ^{13}C NMR can be used for direct hydroxyl functional groups measurement but some phenolic functionals were overlapped and therefore this technique couldn't be precisely assigned the spectrum. Labelling the position with either a most sensitive isotope nucleus (^{19}F, ^{31}P), giving a new function, is another way around this problem. These techniques were commonly used for OH functions measurements via acetylation, fluorosilylation or phosphitylation(Zakis, 1994). Also, the absolute sensitivity and very good S/N (Signal/Noise) ratio of ^{19}F NMR allow quantitative acquisitions rather rapid. In fact, it has been shown in chapter 4 that ^{19}F NMR technique has been used to understand the difference in chemical assignments of both aliphatic and aromatic hydroxyls present in the model compounds. In addition, this method provides the significant information regarding the reactivity of investigated model compounds towards fluorobenzylation. The model compounds results were successfully incorporated into a lignin compound (ORG lignin) to illustrate the chemical assignment as well as quantification of hydroxyl groups. Therefore, it is evident that ^{19}F NMR potentially offers a detailed picture for analyzing fluoro-derivatized compounds.

In 2001, Sevillano et al., (Sévillano, 1999; Sevillano et al., 2001) performed ^{19}F NMR analysis for the quantification of carbonyl groups present in the lignin after different derivatizations such as trifluoromethylphenylhydrazine, fluorobenzoylation of alcohol groups formed after $NaBH_4$ reduction of lignin. These derivatizations were compared with oximation method. The authors also investigated five different model compounds containing aldehydes, ketones and quinones to assign the ^{19}NMR chemical shifts after trifluoromethylphenylhydrazine derivatization. The reaction between carbonyl functional group of lignin with the trifluoromethyl phenylhydrazine is shown in Figure 1, followed by ^{19}F NMR measurements to detect the resulting new hydrazone function and thus to quantify carbonyl groups.

Figure 1. Carbonyl labelling with fluorinated hydrazine

The authors were able to well-distinguish the carbonyl groups present in the aliphatic chain (aldehydes and ketones) and aromatic ring (quinone) from the results and the peak assignments were successfully applied to lignin sample. The results revealed that trifluoromethylphenylhydrazine is fast and efficient method that provides a clear view of different carbonyls present in the system, i.e., aldehydes, ketones and quinone groups. This new method was applied and reported by several authors as a specific technic for carbonyl measurements for lignin and lignocellulosic materials ((Brogdon et al., 2005; Deng et al., 2009; El Mansouri and Salvadó, 2007; He et al., 2006; Holzgrabe et al., 2005; Krolikowski, 2004; Lachenal et al., 2005; Martino et al., 2005; Matera et al., 2012; Zawadzki; Zawadzki and Ragauskas, 1999). More recently, the Sévillano's method had been used to quantify the carbonyl functional groups in different bio-oils materials (Hao et al., 2016; Huang et al., 2014; Stankovikj et al., 2016)

This section presents a more systematic study of the fluorination reaction with the fluorinated hydrazine in order to validate this method as a technique for analyzing aldehyde and ketone groups in lignins. The operating conditions of the fluorination reaction have been investigated in order to carry out quantitative ^{19}F NMR analysis. For that purpose, around twenty aldehyde and ketone model compounds with the carbonyl function at α, β, and γ position with respect to the aromatic ring have been selected. All the fluorination reactions have been carried out under *in-situ* condition (direct reaction between the model and the derivatizing agent in the NMR tube) and the reaction kinetics have been monitored by NMR to find the optimal operating conditions for obtaining a total chemical reaction.

At the same time of this PhD work, Constant & al., (Constant et al., 2017) had undertaken a similar study in the lignin field but more in the direction of industrial humin derivatives. The author has studied different model compounds (which are byproduct in the lignin process and not the part of the lignin structure) and modified some experimental conditions (for instance temperature, time). The reactions were performed inside the NMR tube to minimize the potential loss during the handling, and for non-symmetrical ketones the E and Z isomers were reported. However, there is no information about the kinetics of the reaction and the authors considered that after 24 h the reaction was finished as there is no significant evolution on the spectra.

In the present work, it is proposed to focus on the reaction kinetics using model compounds and after to extend the study to the quantification of carbonyl groups in the technical Protobind 1000 (PB) lignin using different conditions: conventional method (fluorination followed by the derivatized lignin

recovery using precipitation method) and comparison with the *in-situ* reaction kinetics with Sévillano's and Constant's conditions.

b) Materials and methods

i) ^{19}F NMR analysis conditions

Internal standard: First, the choice of the fluorinated compound as internal standard for both chemical shifts analysis and quantification has been made. Sévillano made the choice of the guaiacyl 4-fluorobenzoate (GFB), a monofluorinated synthesized product. In our study, the trifluoromethylbenzophenone (F_3BP: mp = 114-116° C) (Figure 2) was chosen because it is a trifluoromethyl compound more similar to fluorine-containing hydrazine : in our case, the internal standard and the labelled compound to quantify exhibit same functional groups, which was not the case with the GFB. Moreover, the fluorine atom directly borne by the aromatic carbon of GFB is coupled with the aromatic protons which should be decoupled to avoid obtaining a "multiplet signal" due to hetero coupling constant $^3J_{HF}$ (to avoid the nOe).

In addition, a C**F$_3$** group has a higher intensity than a single C**F**. The three fluorine atoms of the trifluoromethyl group in **F$_3$**BP are equivalent and give a single signal because the closest protons are 4 bonds distant ($^4J_{HF}$). It is then possible to work without any proton decoupling and therefore without any integral perturbations due to the heteronuclear nOe

On the other hand, the chemical shifts of the C**F$_3$**s atoms are close, making it possible to work with a small acquisition spectral width, while C**F** and C**F$_3$** signals are separated from more than 50 ppm leading to resolution decrease because most points of the acquisition are used to describe background noise instead of the signal.

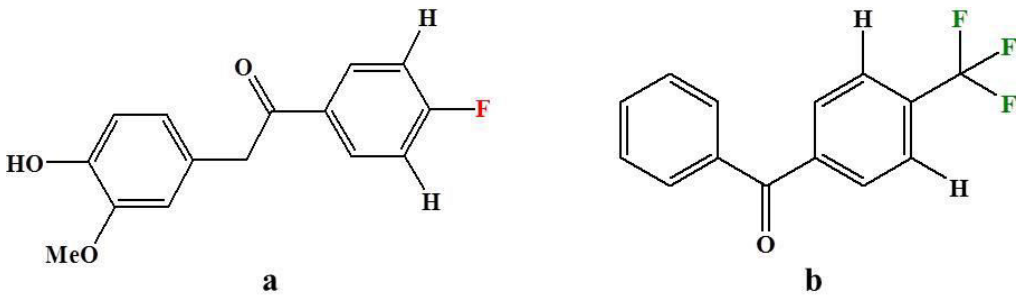

Figure 2. Internal standards: a) GFB: Guaiacyl 4-fluorobenzoate, b) F_3BP: Trifluoromethylbenzophenone

Relaxation delay: For quantitative measurements, it is very important to ensure that the chosen relaxation delay d1 allows a full turn back to equilibrium for each compound (starting carbonyl compound, hydrazine and resulting hydrazone). So, T_1 relaxation time measurements have been investigated for the internal standard, the fluorinated hydrazine, the resulting hydrazones, as well as for the derivatized lignins using the inversion - recovery method. The measured times being less than 2 s for all compounds, a relaxation delay of 10 s has been chosen. In these conditions, all the species present in solution have time to return to equilibrium and the measurements are carried out in a quantitative mode.

Chemical shifts: The chemical shift of the internal standard F_3BP in solution in DMSO-d_6 is compared to that of the hexafluorobenzene (C_6F_6) 101.025 ppm (-63.875 ppm / $CFCl_3$).

Quantification.

As seen from the above section that F_3BP compound contains a keto group which could easily react with phenyl hydrazine. This compound was used as internal standard (IS) initially for conventional measurement, however, no remaining hydrazine in the NMR tube, so no possibility of reaction. For the kinetics study, at the beginning, F_3BP was used with an internal coaxial tube (no contact between IS and hydrazine). However, F_3BP compound was placed with 4-Methylbenzotrifluoride (MBTF), contains no keto group and therefore used for the kinetic measurements. Moreover, no insert coaxial tube needed and hence easy for handling and calculation.

For the kinetics studies and conventional measurements, the internal standard (MBTF for kinetics, F3BP for conventional) was weighed exactly and then added to the reaction medium. The amount of lignin was also weighed precisely.

ii) Choice of model compounds

In their studies Sévillano & al., considered a limited number of model compounds with α – carbonyls: 3 aldehydes and 1 ketone. Our work has been extended for a more systematic study, considering around thirty commercial compounds, containing aldehyde or ketone functional groups in the α-position (Table 1), β-position (Table 2) and γ-position (Table 3) of the aromatic ring. In addition, compounds with hydroxyl or methoxy groups in 3 and 4 positions and 3, 4-ethylenedioxy group have been selected. Compounds with a more complex structure have been also investigated: for example, compounds **16**, **21** and **24** containing aldehyde or ketone functions in a saturated aliphatic chain and compounds **25**, **26** and **27** carrying an additional aromatic unsaturation. These model compounds could be encountered in lignocellulosic materials.

Table 1. Model compounds owing α-position carbonyl

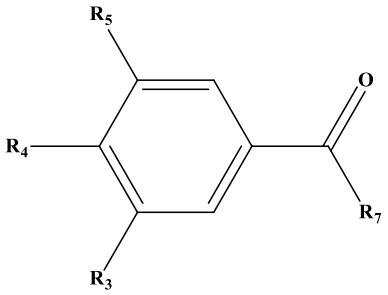

Compound n°	R_3	R_4	R_5	R_7	Name
1	OMe	OH	H	H-	4-Hydroxy-3-methoxy benzaldehyde
2	OMe	OH	OMe	H-	4-Hydroxy-3,5-dimethoxybenzaldehyde
3	OMe	OMe	OMe	H-	3,4,5-Trimethoxybenzaldehyde
4	H	OH	H	Me-	4-Hydroxyacetophenone
5	OMe	OH	OMe	Me-	4-Hydroxy-3,5-dimethoxyacetophenone
6	H	H	H	Me(C=O)Et-	1-Phenyl-1,4-pentanedione
7	H	H	H	PhEt-	1,3-Diphenyl-1-propaneone
8	H	OH	H	PhCH=CH-	Benzylidene-(4-hydroxyacetophenone)
9	H	OMe	H	PhCH=CH-	Benzylidene-(4-Methoxyacetophenone)
10	OMe	OMe	H	2-(OMe)PhOCH(CH_2OH)-	1-(3,4-dimethoxy-phenyl)-3-hydroxyl-2-(2-methoxy-phenoxy)-propan-1-one
11	OMe	OH	H	2-(OMe)PhOC(Me)(CH_2OH)-	3-hydroxy-1-(4-hydroxy-3-methoxyphenyl)-2-(2-methoxyphenoxy)propan-1-one

Table 2. Model compounds owing β-position carbonyl

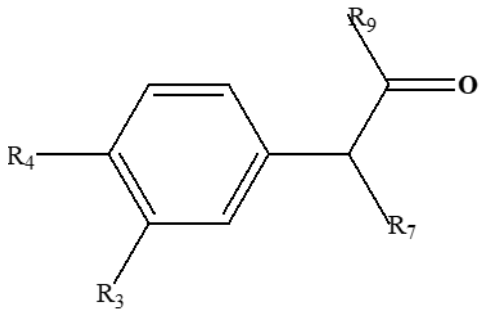

Compounds n°	R_3	R_4	R_7	R_9	Name
12	H	H	H	H-	Phenylacetaldehyde
13	H	OMe	H	Me-	4-Methoxyphenylacetone
14	H	H	Me	H-	2-Phenylpropionaldehyde
15	H	H	H	iPropyl-	3-Methyl-1-phenyl-2-butanone
16	OCH_2O	OCH_2O	H	Et-	1-(3,4-Methylenedioxy)-phenyl-2-butanone

Table 3. Model compounds owing γ-position carbonyl

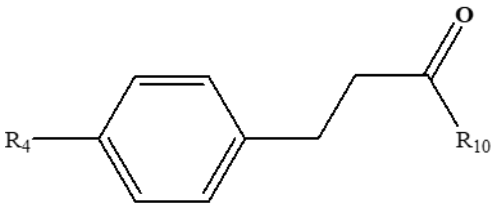

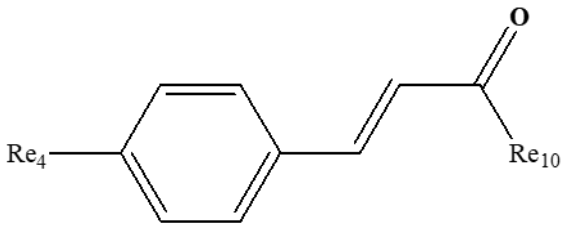

Compounds n°	R_4	R_{e4}	R_{10}	R_{e10}	Name
17	OMe		Me-		4-(4-Methoxyphenyl)-2-butanone
18	OH		Me-		Hydroxy-phenyl-2-butanone
19	H		H		3-Phenylpropionaldehyde
20	OH		2,4,6-$(OH)_3$Ph-		2',4',6'-Trihydroxy-3-(4-hydroxyphenyl)propiophenone
21	OCH_2O		Me		3,4-Methylenedioxybenzylacetone
22		OH		Me	4-Hydroxybenzylideneacetone
23		OMe		H	4-Methoxycinnamaldehyde
24		OCH_2O		Me	3,4-(Methylenedioxy)benzylideneacetone
25		OMe		Ph-	4-Methoxybenzylideneacetophenone
26		OH		Ph-	4-Hydroxybenzylideneacetophenone
27		OMe		4-(OMe)Ph-	4,4'-Dimethoxybenzylideneacetophenone
28		OMe		Ph_2-	3-(4-Methoxyphenyl)-1-(2-Naphtyl)-prop-2-en-1-one

Other typical derivatives (Table 4), without any carbonyl group, but containing reactive functions such as ethylenic bond, phenolic hydroxyl and carboxylic acid groups, have been tested. Normally, none of these compounds should lead to the formation of hydrazine. Because lignin is a natural macromolecule with numerous functional groups, it is important to control the selectivity of the reaction and the absence of any secondary reaction which may lead to the detection of fluorinated parasitic signals in the observation zone.

Table 4. Other typical model compounds, without carbonyl functions

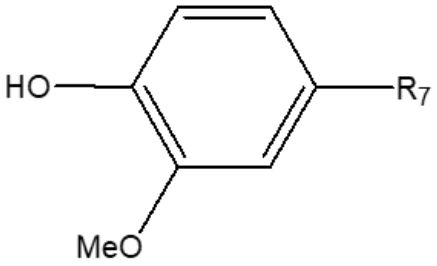

Compound n°	R_7	Name
29	CO_2H-CH_2-	4-Hydroxy-3-methoxybenzoicacid
30	CH_2OH-	4-Hydroxy-3-methoxybenzylicalcohol
31	CH_2=CH-CH_2-	4-Allyl-2-methoxyphenol
32	CH_3-CH=CH-	2-Methoxy-4-propenylphenol

c) Model Compound fluorination - in-situ kinetics

i) Identification of the initial and reaction products

Before the derivatization, 1M solutions of carbonyl containing model compound (**1** to **28**) have been prepared separately in DMSO-d_6. Each model compound was analysed, and all its proton and carbon chemical shifts were assigned using ^{13}C and ^{1}H NMR (Table 5 and Table 6)

Table 5. Model compounds ^{13}C chemical shifts δ(ppm) in DMSO-d6 at 25°C, in bold δ of C=O groups

N°	C_1	C_2	C_3	C_4	C_5	C_6	R_3	R_4	R_5	R_7	R_8	R_9	R_{10}
1	129.66	114.42	131.73	164.20	131.73	114.42	55.56			**191.13**			
2	127.24	107.10	148.17	142.17	148.17	107.10	56.06		56.06	**191.09**			
3	131.34	106.68	153.31	142.87	153.31	106.68	55.95	60.12	55.95	**191.68**			
4	128.65	115.67	130.69	162.65	130.69	115.17				**195.98**	26.17		
5	127.49	106.25	147.54	141.00	147.54	106.25	56.09		56.09	**196.20**	26.22		
6	136.45	128.63	127.77	133.46	127.77	128.63				**198.52**	36.34 ;32.14 ; **207.03** ; 29.62		
7	141.20	128.60	127.85	133.0	127.85	128.60				**198.97**	28.44 ; 136.57 ; 128.20 ; 128.32 ; 125.79		
8	142.67	131.32	115.52	162.61	115.52	131.32				**187.16**	130.26 ; 129.01 ; 134.94 ; 128.7 ; 122.2		
9	143.04	130.84	113.93	163.18	113.93	130.84		55.44		**187.35**	130.44 ; 130.29 ; 134.78 ; 128.7 ; 128.8 ; 121.99		
10	128.06	112.77	148.71	153.61	114.72	123.43	55.54	55.54		**195.37**	81.52 ; 62.68 ; 147.07 ; 149.32 ; 121.75 ; 110.9 ; 120.65 ; 55.81		
11	126.7	111.8	146.7	152.43	116.6	122.0	55.53			**196.27**	92.2 ; 18.1 ; 75.12 ; 147.8 ; 149.3 ; 55.53 ; 114.7 ; 121.1 ; 121.4 ; 115.2		
12	129.66	127.90	128.56	126.84	128.56	127.90				49.56	**200.25**		
13	128.75	130.48	113.75	158.0	113.75	130.48		54.90		48.76	**206.21**	29.07	
14	138.13	128.23	128.79	127.11	128.79	128.23				51.71 ;	**201.62**		

									14.40			
15	134.99	129.51	128.10	126.29	128.10	129.51			46.53	**211.18**	39.53 ; 17.94	
16	128.63	122.49	147.17	145.86	109.88	108.01	100.76		48.02	**208.48**	34.50 ; 7.54	
17	131.95	129.06	113.64	157.47	113.64	129.06		54.86	28.24	44.42	**207.57**	29.58
18	131.17	129.0	115.1	155.47	115.1	129.0			28.39	44.57	**207.81**	29.68
19	125.88	128.17	128.28	128.28	128.28	128.17			27.47	44.33	**202.52**	
20	131.64	129.16	115.06	164.6	115.06	129.16			29.44	45.46	**204.23**	155.39 ; 164.6
21	134.93	120.86	147.14	145.26	108.63	107.93	100.56		29.57	44.39	**207.53**	29.81
22	125.29	130.88	115.82	159.85	115.82	130.88			143.42	123.99	**197.63**	27.0
23	126.65	130.57	114.50	161.71	114.50	130.57		55.27	152.97	126.26	**193.88**	
24	128.78	124.95	148.04	149.34	106.54	108.44	101.57		143.01	125.38	**197.75**	27.12
25	137.86	130.64	114.31	161.32	114.31	130.64		55.17	143.93	119.48	**188.99**	132.71 ; 128.6 ; 128.3 ; 127.24
26	125.73	130.98	115.87	160.2	115.87	130.98			144.54	118.53	**189.05**	138.02 ; 128.66 ; 128.3 ; 132.72
27	127.42	130.55	114.27	161.15	114.27	130.55		55.17	143.02	119.43	**187.23**	130.48 ; 113.81 ; 162.98 ; 55.34
28	127.34	130.65	114.29	161.29	114.29	130.65		55.16	143.79	119.54	**188.72**	132.29 ; 124.13 ; 134.89 ; 126.7 ; 128.23 ; 127.6 ; 135.2 ; 129.5

Table 6. Model compounds ^{1}H NMR chemical shifts δ(ppm) in DMSO-d_6 à 25°C

N°	H_2	H_3	H_4	H_5	H_6	R_3	R_4	R_5	R_7	R_8	R_9	R_{10}
1	7.08	7.84		7.84	7.08		3.84			9.85		
2	7.18				7.18	3.83		3.83		9.75		
3	7.21				7.21	3.84	3.76	3.84		9.85		
4	6.84	7.81		7.81	6.84		10.29			2.45		
5	7.45				7.45	4.05	9.48	4.05		2.73		
6	7.96	7.51	7.63	7.51	7.96					2.80 ; 3.21 ; 2.15		
7	7.97	7.49	7.60	7.49	7.97					3.36 ; 2.95 ; 7.27 ; 7.16		
8	8.1	6.93		6.93	8.1					7.7 ; 7.89 ; 7.83 ; 7.41 ; 7.42		
9	8.16	7.06		7.06	8.16		3.83			7.91 ; 7.72 ; 7.84 ; 7.43 ; 7.42		
10	7.29			6.74	7.34	3.73	3.73			5.28 ; 4.10 ; 6.66 ; 6.71 ; 3.75		
11	6.75			7.65	6.80	3.8	10.15			1.56 ; 3.8 ; 5.76 ; 7.65 ; 6.80 ; 6.85 ; 3.80		
12	7.24	7.30	7.35	7.30	7.24				3.22		9.69	
13	6.87	7.10		7.10	6.87		3.72		3.65		2.08	
14	7.29	7.24	7.36	7.24	7.29				3.75 ; 1.32		9.62	
15	7.18	7.29	7.21	7.29	7.18				3.80		2.72 ; 1.02	
16	6.73			6.80	6.62	5.95			3.61		2.44 ; 0.89	
17	6.39	6.12		6.12	6.39		3.0		2.0	2.0		1.36
18	6.96	6.66		6.66	6.96		9.10		2.65	2.65		2.05
19	7.18	7.26	7.21	7.26	7.18				2.74	2.85		9.71

20	7.0	6.65		6.65	7.0			2.75	3.21	5.79
21	6.76			6.76	6.63	5.93		2.68	2.68	2.06
22	7.51	6.82		6.86	7.51		10.04	6.58	7.50	2.26
23	7.56	6.98		6.98	7.56		3.78	6.69	7.60	9.59
24	7.30			6.92	7.15	6.06		6.65	7.50	2.27
25	8.13	6.98		6.98	8.13		3.77	7.75	7.75	7.80 ; 7.53 ; 7.62
26	8.11	6.87		6.87	8.11		10.2	7.61	7.51	7.73 ; 7.70 ; 7.53
27	8.13	6.98		6.98	8.13		3.78	7.69	7.72	7.80 ; 7.04 ; 3.82
28	8.00	6.99		6.99	8.0		3.77	7.78	7.97	7.84 ; 8.15 ; 8.20 ; 7.60 ; 7.60 ; 7.95 ; 8.89

The exact quantities were calculated based on the number of C=O groups present in the model compounds. For instance, if the model compound contains one C=O groups the one mole of CF_3PH is added in 1M/1M ratio. Similarly, if there are two C=O in the model compounds, the CF_3PH quantity was twice in comparison to only one C=O.

The quantities were calculated in mg to obtain final solutions one molar for carbonyl group. The starting compound was dissolved with solvent in the NMR tube, and at time 0(t0), CF_3PH solution was added (for better handling CF_3PH was previously dissolved with the same solvent, and the quantity was previously calculated to lead a complete reaction 1:1 for each carbonyl group of the compound). The total volume was 0.7mL for 5mm tubes, and 4mL for 10mm tubes.

Records of ^{1}H, ^{13}C and ^{19}F NMR signals were performed at regular intervals after t0. The derivatization reaction was followed directly in the NMR tube, following the evolution of the fluorine signals. As the starting ratio of carbonyl / trifluoromethyl phenylhydrazine was 1 M / 1 M, the decrease of the pristine hydrazine signal corresponds with the concomitantly occurrence and growth of the new signal attributing to the hydrazone formation.

The control of the reacting products as well as the progress of the reaction was made by combining the results obtained with the three nuclei: fluorine, carbon and proton. With ^{19}F, the decrease of the pristine hydrazine signal and the appearance of that of the resulting hydrazone, is followed. ^{13}C NMR analysis makes it possible to control the disappearance of **C**=O carbonyl, the appearance of the signal corresponding to the formation of the **C**=N bond (region 145 ppm and 138 ppm) and the modification

of the aromatic carbon (**C$_1$**) in para-position of CF_3 (shift from 155 ppm towards 149 ppm). Moreover ^{1}H NMR enables to follow the disappearance of the N**H**$_2$ and that of the aldehyde proton. All other C and H nuclei chemical shifts are slightly modified after reaction.

Table 7 summarizes the main changes, evidencing the hydrazone formation. In this table, compound **0** corresponds to the starting reagent, the trifluoromethyl phenylhydrazine CF_3PH. ^{19}F NMR also provides the additional information of E/Z isomers that exist in double bonds. In this case, E isomer represents the higher priority groups or substituents present in the opposite side and vice-versa. It is clearly seen form the Table 7 that the obtained values show no characteristic difference between investigated aldehydes and ketone. These results are in well-agreement with recently reported work from Constant et al(Constant et al., 2017).

Table 7. Main chemical shifts as hydrazone formation evidence δ (ppm) ^{1}H, ^{13}C and ^{19}F in DMSO-d6 at 25°C

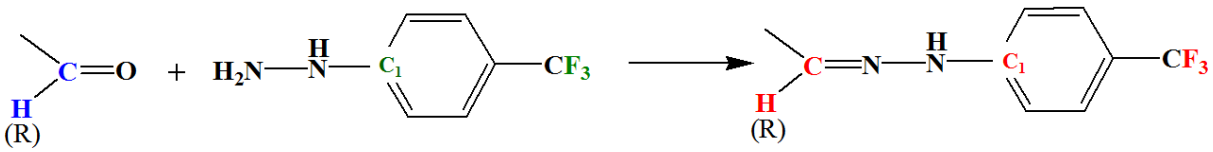

No.	*C=O*	C=N	C_1	H_{ald}	H_{hydr}	F	
0			*155.22*			*-61.14*	
						E	Z
1	*191.13*	139.13	148.56	*9.85*	7.92	-61.54	-61.69
2	*191.09*	139.94	148.58	*9.75*	7.87	-61.53	-61.71
3	*191.68*	139.08	148.36	*9.85*	7.89	-61.61	-61.73
4	*195.98*	143.76	149.42			-61.51	-61.71
5	*196.20*	143.88	149.35			-61.56	-61.70
6	*198.52*	147.70	149.78			-61.52	-61.66
	207.50	149.91	150.42			-61.49	-61.56
7	*198.97*	147.72	149.80			-61.67	-61.62
8	*187.16*	137.69	149.32			-61.85	-61.95
9	*187.35*	137.75	149.33			-61.91	-62.01
10	*195.37*	144.68	148.66			-62.05	-62.06
11	*196.27*	135.51	149.41			-61.67	-61.73
12	*200.25*	148.07	148.95	*9.69*	7.32	-61.54	
13	*206.21*	148.05	149.55			-61.51	-61.52
14	*201.62*	145.52	148.92	*9.62*	7.27	-61.54	-61.69
15	*211.18*	149.66	153.64			-61.49	-61.50
16	*208.48*	149.54	151.74			-61.50	-61.51
17	*207.57*	149.95	150.34			-61.47	
18	*207.81*	149.95	150.34			-61.47	
19	*202.52*	142.26	148.86	*9.71*	7.28	-61.52	-61.67
20	*204.23*	149.12	149.81			-61.22	-61.45
21	*207.53*	150.07	150.46			-61.48	
22	*197.63*	146.19	149.14			-61.51	-61.60
23	*193.88*	143.23	148.15	*9.59*	7.24	-61.62	-61.66
24	*197.75*	146.20	149.18			-61.71	-61.78
25	*188.99*	146.20	149.15			-61.94	-62.00
26	*189.05*	146.74	149.41			-61.99	-62.01
27	*187.23*	148.00	148.85			-61.41	-61.50
28	*188.72*	148.02	148.96			-61.90	-61.94

d) Fluorination kinetic study of model compounds

In this section, the kinetics of all considered model compounds against fluorination were evaluated. It should be mentioned that there are two different conditions employed for this study: (1) neutral medium – no additional reagent was added in NMR tube (2) acidic medium – in this case, a small amount of orthophosphoric acid (2 drops) was added in the NMR tube. Only less reactive model compounds were followed in acidic medium. The obtained kinetic results are discussed below.

i) Model compound fluorination kinetics in neutral medium

The fluorination kinetics of model compounds bearing α-position carbonyl (**2** to **11**) is presented in Figure 3 and in Table 8. The obtained results illustrated that the compounds **2**, **3** and **6** are rapidly derivatized and derivatization is total in less than 24 hours. For compounds **4** and **5**, the reaction is slower but again derivatization is efficient since after 72 hours the conversion is around 80%. On the other hand, model compounds **7**, **8** and **11** lead to around 25 to 30% hydrazone conversion after 72 hours reaction, which is very low compared to the above-mentioned compounds. Moreover, the derivatization rate is also low. As for as model compounds **9** and **10** are concerned, the carbonyl conversion is very low or almost null in neutral condition.

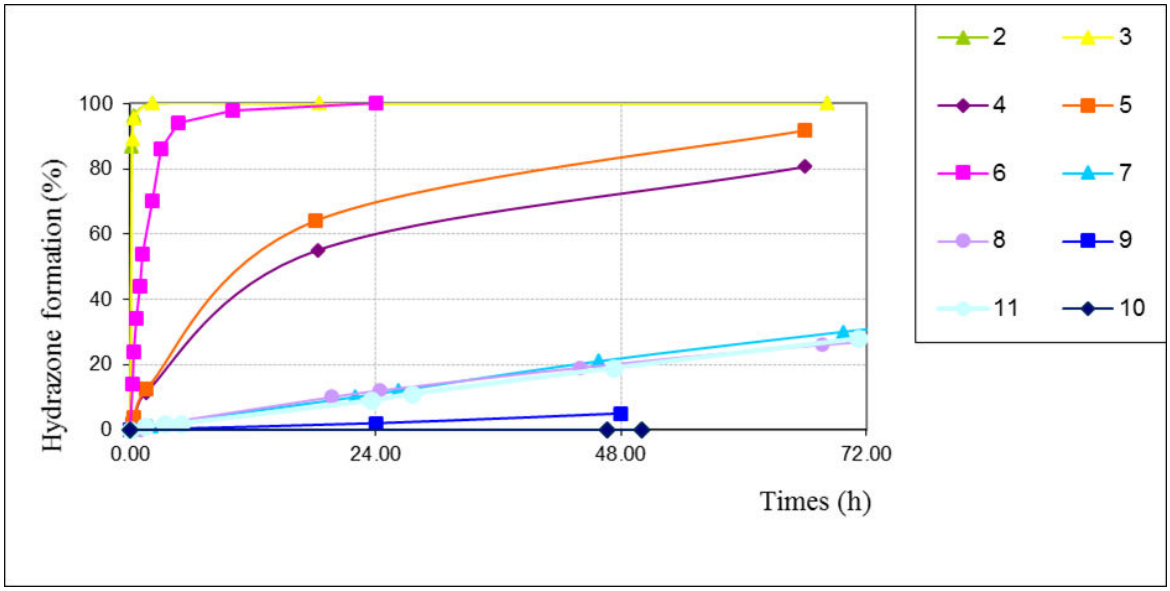

Figure 3. Fluorination kinetics of model compounds bearing α-position carbonyl group in neutral condition

Table 8. Kinetic results (conversion in % and time in hours) and E/Z isomer in % of all model compounds were compared in neutral and acetic medium.

Compound n°	Species	Neutral medium		*Acidic medium*		Isomer E	Isomer Z
		conversion	time	*conversion*	*time*		
		%	(h)	*Rate, %*	*(h)*	%	%
1	Ald α	**100**	**3**	-	-	98	2
2	Ald α	**100**	**3**	-	-	99	1
3	Ald α	**100**	**3**	-	-	97	3
4	Ket α	**72**	**48**	-	-	99	1
5	Ket α	**83**	**48**	-	-	98	2
6	Ket α +	**0**	**24**	***100***	***1.5***	*20*	*80*
	(Ket δ)	**100**	**24**	***100***	***0.5***	20	80
7	Ket α(γ)	**22**	**48**	-	-	25	75
8	Ket α(γ) + Alkene	**20**	**48**	***100***	***20***	*69*	*31*
9	Ket α(γ) + Alkene	**6**	**48**	***100***	***18***	*67*	*33*
10	Ket α	**0**	**48**	***100***	***16***	*55*	*45*
11	Ket α	**19**	**48**	-	-	45	55
12	Ald β	**91**	**48**	-	-	100	0
13	Ket β	**93**	**48**	-	-	25	75
14	Ald β	**100**	**4**	-	-	95	5
15	Ket β	**85**	**48**	-	-	54	46
16	Ket β	**90**	**48**	-	-	60	40
17	Ket γ	**100**	**8**	-	-	100	0
18	Ket γ	**99**	**48**	-	-	100	0
19	Ald γ	**78**	**48**	-	-	83	17
20	Ket γ(α)	**2**	**48**	***100***	***20***	*85*	*15*
21	Ket γ	**97**	**48**	-	-	100	0
22	Ket γ + Alken	**65**	**48**	-	-	38	62
23	Ald γ + Alken	**100**	**23**	-	-	75	25
24	Ket γ + Alken	**61**	**48**	***100***	***0.25***	*32*	*68*
25	Ket γ(α) + Alken	**6**	**48**	***100***	***14***	*61*	*39*
26	Ket γ(α) + Alken	**26**	**48**	***100***	***15***	*58*	*42*
27	Ket γ(α) + Alken	**0**	**48**	***100***	***18***	*65*	*35*
28	Ket γ(α) + Alken	**0**	**48**	***100***	***16***	*61*	*39*
29	Acid	**0**	**48**	***0***	***24***	x	x
30	Alcool + Phenol	**0**	**48**	***0***	***24***	x	x
31	Alken + Phenol	**0**	**48**	***0***	***24***	x	x
32	Alken + Phenol	**0**	**48**	***0%***	***24***	x	x

Ald - aldehyde, Ket – Ketone, E and Z isomer ratios (italic numbers and red color correspond to the reaction in acidic medium)

Results for β-position carbonyl model compounds are shown in the Figure 4. The derivatization of β-position carbonyl model compounds was achieved faster compared to α carbonyls. In particular, the model compound **14** reached 100% conversion quite immediately and compounds **12**, **13** and **16** reached 80 to 90% conversion within 24 hours. It is also noted that compound **15** reaches around 75% conversion after around 24 hours and it attains the maximum conversion, around 90%, after 72 hours reaction.

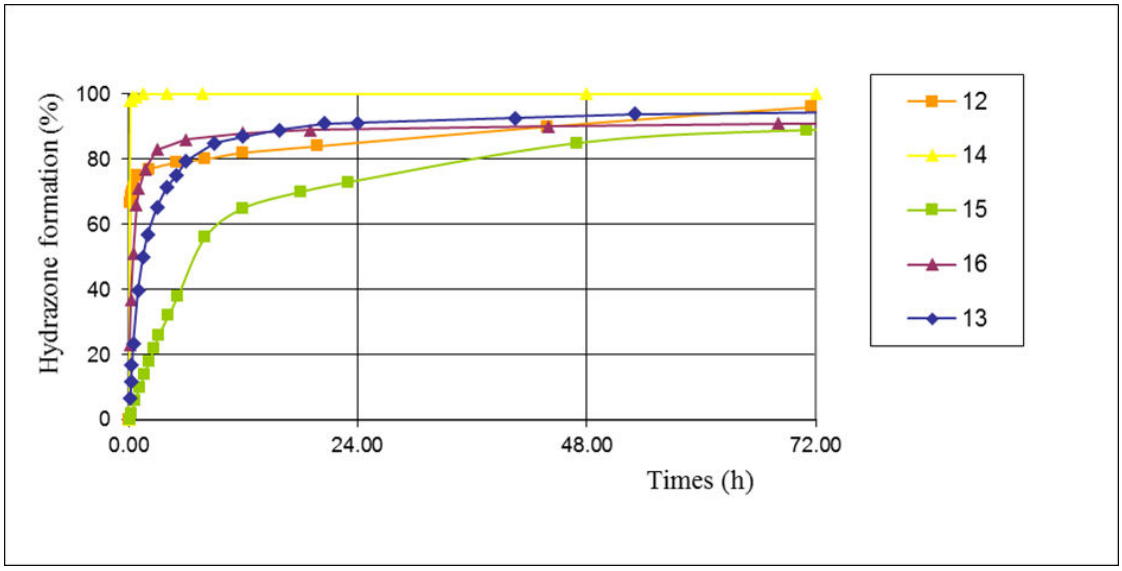

Figure 4. Fluorination kinetics of model compounds bearing β-position carbonyl group in neutral condition

Fluorination kinetics of model compounds bearing γ-position carbonyl group in neutral condition is shown in Figure 5. Compounds **20**, **25**, **26**, **27** and **28**, all bearing phenyl group at γ – position, show poor reactivity with the CF_3PH reagent in neutral condition and their corresponding conversion rate is significantly low, around 30% or almost zero conversion. This low conversion could be explained by the steric hindrance caused by phenyl ring. However, in the case of compounds **17**, **18**, **21** and **23**, the aliphatic substitution present at γ – position, enhances the conversion rate which reached 100% after 72 hours reaction. However, even after 48 hours reaction, the conversion rate was about 60 – 80 % for compounds **19**, **22**, and **24**.

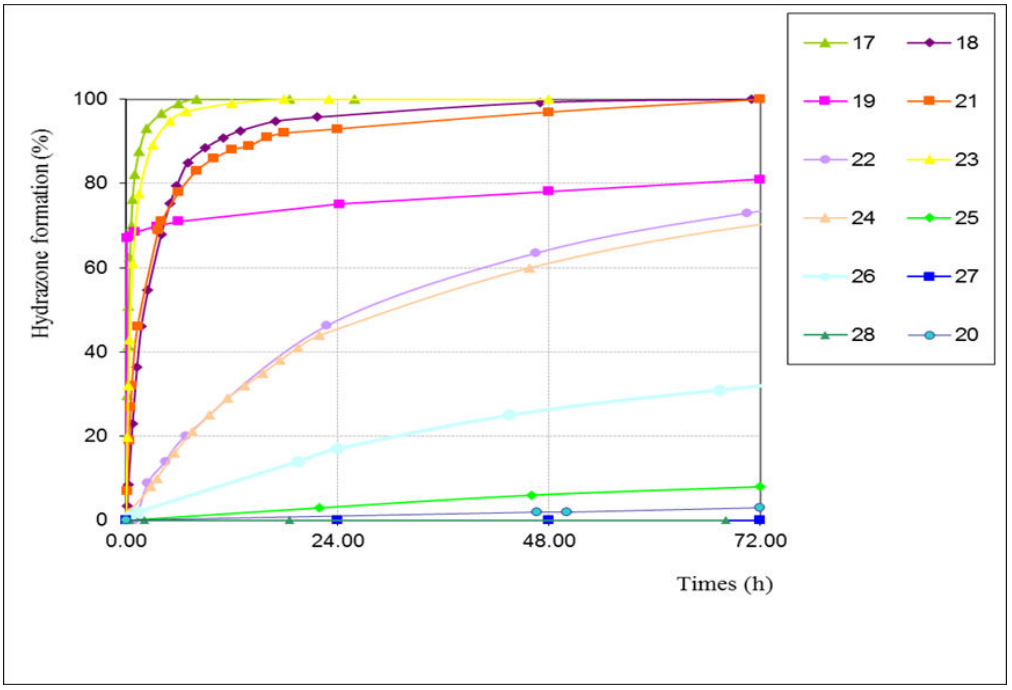

Figure 5. Fluorination kinetics of model compounds bearing γ -position carbonyl group in neutral condition

Comparing the conversion rate of model compounds with substituents at α, γ positions, the compounds α: **9**, **10** γ: **20**, **25**, **27**, **28** revealed low conversion than other compounds. The low conversion rate is directly associated to the polarization of C=O bonds. The carbonyl bond of aldehydes and ketones has a high dipole moment (2.8 Debye on average) and this permanent double bond polarization varies according to the substituents present in α and γ positions. The polarization of C=O order is shown in Figure 6. The C=O groups with no or lower substituents at neighbouring positions show a higher polarization than with higher number substitutions. Since, nitrogen from hydrazine molecule is a nucleophilic atom with paired electrons, it is expected that nitrogenous compounds could be linked to the carbonyl group.

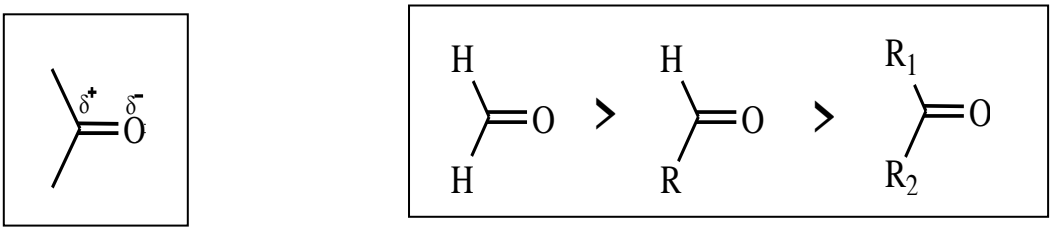

Figure 6. Polarisation of the carbonyl bond and polarization order according to substituents

It can be seen from the Table 8 and Figure 3, Figure 4 and Figure 5 that aldehydes are found much more reactive than the corresponding ketones due to rather high polarization of aldehydes than ketones. Among the investigated aldehydes, aldehydes at α position are the most reactive since the conversion reached 100% in 3 hours. The more the carbonyl position is far from the aromatic ring, the compound is less reactive by the cause of decreasing polarization of carbonyl bond. In fact, the aldehyde at γ-position as in **19** compound (in Table 8) does not lead to a total reaction even after 48 hours (78% conversion), even if the reaction seems to be fast during the first minutes of reaction (Figure 5). On the other hand, if a double bond is conjugated to the γ aldehyde, **23** for example, the reactivity of the latter is much activated since there is total reaction after 24 hours.

As explained in the previous paragraph, ketones exhibit lowest reactivity. No complete reaction, even after 48 hours, is observed, except for the compound **6** which is somewhat particular because it is composed of two ketone groups, one in α position and the other in δ position, the latter one being included in the aliphatic chain. In fact, in the case of compound **6**, only the δ ketone is converted into hydrazone after 24 hours whereas ketone α exhibits a poor reactivity since the C=O groups is still clearly visible in ^{13}C NMR (Figure 7). The corresponding chemical shift is lower than that of the δ C=O group because of the conjugation with the aromatic ring. Finally, half of the CF_3PH reagent remained in the mixture as seen in ^{19}F NMR spectra (Figure 8), which confirms that the derivatization is not total.

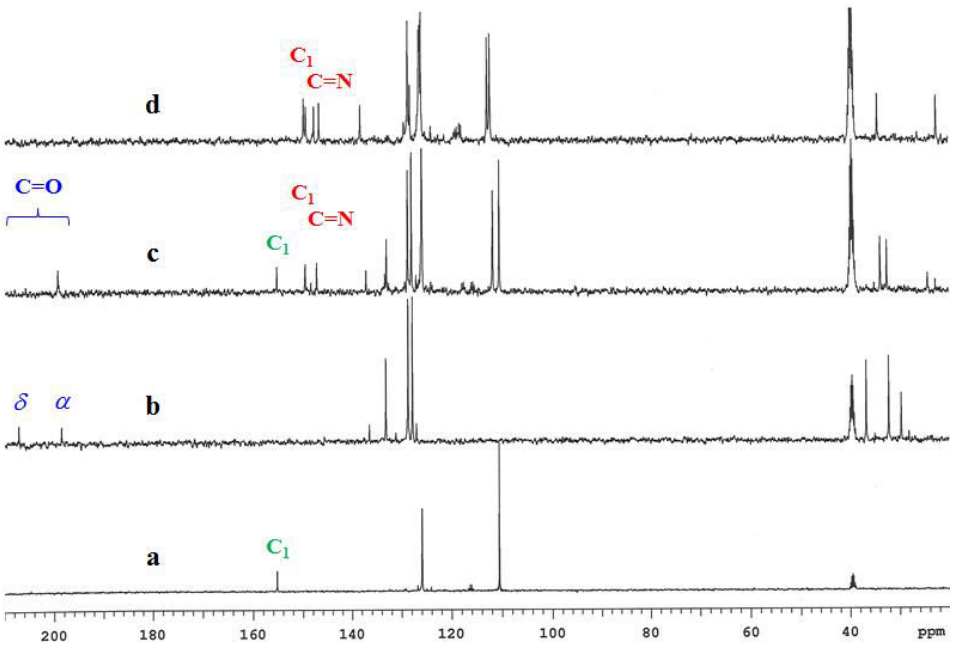

Figure 7. ^{13}C NMR spectra in DMSO-d6 of: (**a**) CF_3PH, (**b**) model compound **6** before derivatization, (**c**) model compound **6** kinetic in neutral medium after 1 day, (**d**) model compound **6** kinetic in acidic medium after 1h

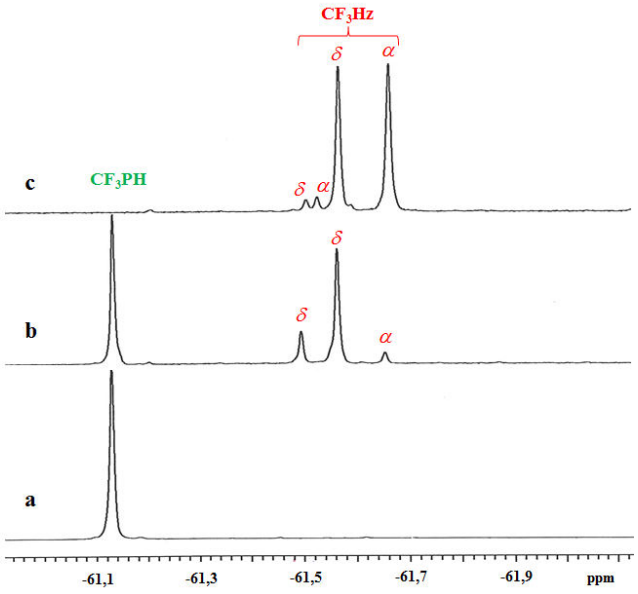

Figure 8. ^{19}F NMR spectra in DMSO-d6 of: (a) CF3PH, (b) model compound 6 kinetic in neutral medium after 1 day, (c) model compound 6 kinetic in acidic medium after 1h

Pursuing the analysis of ketone model compounds, it can be seen that carbonyl functions in γ-position, as in compounds **17**, **18** and **21** are more reactive than those in β-position, as in compounds **13**, **15** and **16**, with conversion rates respectively close to 100 and 90% after 48 hours reaction (Table 8). On the other hand, the ketones α (**4**, **5**) are less reactive and their conversion is 72 % and 83 % after 48 hours of reaction and compounds **10** and **11** are much less reactive or almost no reaction after 48 hours reaction time. The presence of conjugated ethylenic unsaturation greatly reduces reactivity; the latter is even more affected by the presence of a second substituted or unsubstituted aromatic ring. For compounds **8**, **9**, **20**, **26**, **25**, **27** and **28,** the choice of labelling the carbonyl in α or γ "priority" position was chosen in comparison with lignin "fragment". The position of the carbonyl groups mainly referred for the lignin monomer unit (aromatic ring with OH and OMe group at position 3 and 4). In any case, for all these compounds, the conversion yield into hydrazone drops drastically or even remains zero. The presence of an additional aromatic ring or ethylenic unsaturation completely deactivates the reactivity by decreasing the polarization of the carbonyl bond.

ii) Model compound fluorination kinetics in acidic medium - results

The carbonyl group reacted with hydrazine in acidic medium and the possible reaction mechanism is presented in Figure 9. The similar derivatization trials have been performed in the same operating conditions, the only difference being the addition of orthophosphoric acid (2 drops) in the NMR tube. The derivatization kinetics was followed only for the less reactive model compounds and the results are illustrated in the Table 8.

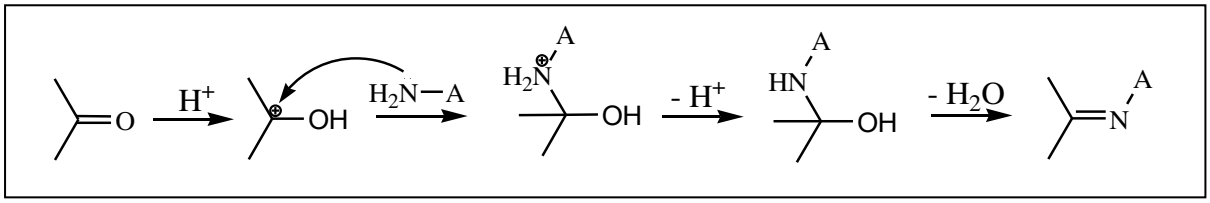

Figure 9. Reaction mechanism of the formation of hydrazine into acidic medium

The fluorination reaction was studied in acidic medium because it is known that acidic conditions increase the polarity of the starting carbonyl bond thus leading to the catalysis of the reaction. Model compound fluorination kinetics are presented in Figure 10 and Figure 11. Only compounds exhibiting low reactivity are investigated.

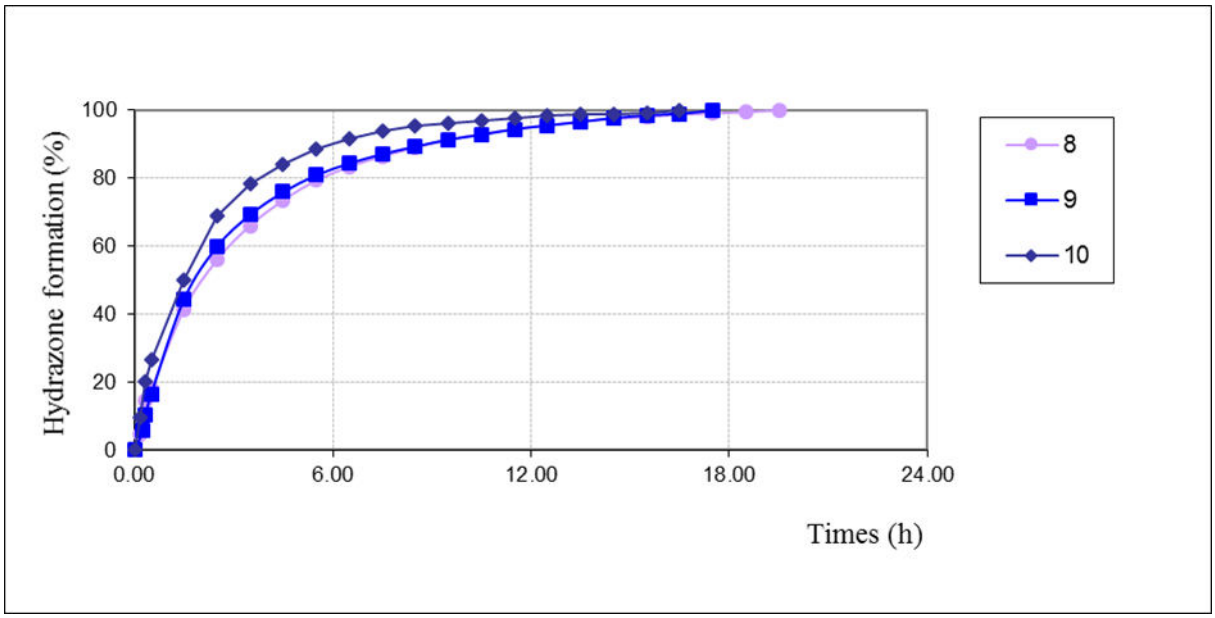

Figure 10. Fluorination kinetics of model compounds bearing α -position carbonyl group in acidic condition

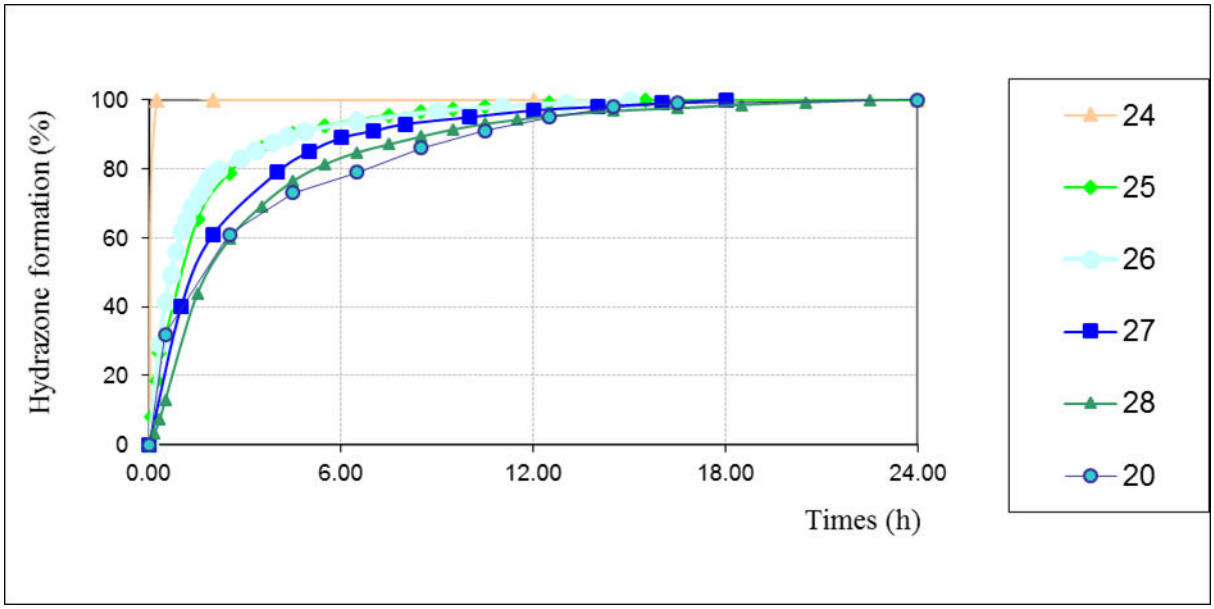

Figure 11. Fluorination kinetics of model compounds bearing γ -position carbonyl group in neutral condition

Figure 10 and Figure 11 show that α – position carbonyl (**8**, **9**, **10**) and γ-position carbonyl (**20**, **24**, **25**, **26**, **27** and **28**) unreactive model compounds in neutral condition, are much more reactive in acidic medium and that the reaction is completed within a day. In all cases, 100% conversion rates are achieved in less than 24 hours. It has been also observed that a reaction conversion rate for **24** was only 61% after 48 hours of reaction in neutral medium and however, it becomes almost immediate in acidic conditions.

As it could be seen on the ^{13}C and ^{19}F NMR spectra for model compound **6** (Figure 7 and Figure 8) with ketone α– and δ- carbonyl positions. The compound **6** was chosen for acidic conditions, since α– one does not react in neutral conditions 0% after 24 hours. Only the δ- position carbonyl react faster in neutral medium, nevertheless the conversion of carbonyl at α– position becomes predominant in acidic conditions. It should be mentioned that the compounds with β-position carbonyl exhibited a rather good conversion rate in neutral conditions, thus testing acidic conditions were unnecessary.

After full derivatization, in all cases, only one product has been identified by ^{1}H and ^{13}C NMR. However, using ^{19}F NMR analysis, two isomers E and Z (isomerism around the C = N double bond) are found. E and Z isomers are present in variable proportions depending on the steric hindrance around the carbonyl function. These isomers were detected more easily with ^{19}F NMR than with ^{1}H or ^{13}C due to the higher sensitivity of fluorine nucleus in term of spectral width.

Moreover, in lignin macromolecule, carbonyl groups are "overlooked" among a multitude of other functional groups. To be sure that the reaction with fluorinated hydrazine did not lead to the production of spurious signals disturbing the NMR observations, lignin model compounds without any carbonyl group have been investigated: phenol, methoxy, alcohol, ethylenic and carboxylic acid groups containing model compounds, such as compounds **29** to **32**. The fluorination reaction has been performed first in neutral condition and then in acidic medium. ^{1}H and ^{13}C NMR spectra confirmed that the starting compounds remain unchanged, even after longer (48 h) reaction time: all the starting signals were detected without any modification. On ^{19}F NMR spectra, the CF_3PH signal and the internal standard are detected only, with their initial ratios and without any change. Therefore, it is clearly demonstrated that CF_3-hydrazine derivatization is highly selective for carbonyl groups only.

All the results on model compounds are consistent with Constant's work(Constant et al., 2017): non-symmetrical ketone compounds lead to fluorinated derivatives with two forms, E and Z isomers. Besides confirming the production of isomers, the ratio of each of them was calculated (Table 8). From our analysis, it should be stressed that in order to derivatize all types of carbonyl group (α, β, γ), the reaction should be performed in the acidic condition. In neutral medium, the conversion rate is very low and takes a long reaction time. Finally, it is important to stress that other functional groups such as hydroxyl, phenolic, carboxyl, etc., which are present in lignin macromolecule were not sensitive to the derivatizing agent CF_3PH.

e) Lignin Carbonyl group quantification after fluorination

i) Lignin derivatization with CF_3PH, followed by ^{19}F NMR analysis

The above method has been extended for lignin carbonyl group quantification, using only acidic conditions to ensure that all possible aldehyde and / or ketone functional groups fully reacted regardless of their chemical environment. Thus, several lignin samples (100mg) have been derivatized with the trifluoromethyl phenylhydrazine (120mg) agent in acidic medium(4 drops of orthophosphoric acid) and 4 mL of DMSO during 48 hours. After the reaction time, the derivatized product were precipitated in large volume of distilled water(around 500 mL), then washed with cold water several times to remove the residual reactants and the washed precipitate were dried in oven at 40°C. ^{19}F NMR analysis was carried out in a quantitative mode to determine the carbonyl group content. A 50 mg of derivatized lignin was solubilized into 0.7 mL of DMSO-d_6. Then the internal standard 4 trifluoromethylbenzophenone (F_3BP) (used for conventionally derivatized lignin samples) and 4-Methylbenzotrifluoride-MBTF (used in in-situ reaction kinetics) was added to the solution. The exact amounts of derivatized lignin and internal standard dissolved in DMSO-d_6 were noted. The quantitative ^{19}F spectrum is recorded in less than 30 minutes. After ^{19}F NMR quantitative data

acquisition and integral measurements, the number of aldehyde and ketone functions were calculated according to the *Equation* , *Equation* 2 and *Equation* 3.

in **mmol.g^{-1}** derivatized lignin

$$n_{C=O\ F3L} = \frac{A_L \times m_{IS} \times 1000}{(A_{IS} \times m_{F3L} \times M_{IS})} \qquad \text{Equation 1}$$

in **mmol.g^{-1}** non-derivatized lignin

$$n_{C=O\ L} = \frac{n_{C=O\ F3L}}{\left[1 - \left(n_{C=O\ F3L} \times 0.001 \times (M_{F3PH} - M_{H2O})\right)\right]} \qquad \text{Equation 2}$$

in **mmol.mol^{-1}** non-derivatized lignin

$$n_{C=O\ L} = \frac{A_L \times m_{IS} \times 1000}{\left[(A_{IS} \times m_{F3L} \times M_{IS}) - \left(A_L \times m_{IS} \times (M_{F3PH} - M_{H2O})\right)\right]} \qquad \text{Equation 3}$$

Where,

$n_{C=O\ F3L}$ = number of carbonyl groups in lignin derivatized

$n_{C=O\ L}$ = number of carbonyl groups in lignin non-derivatized

IS = Internal standard

A_{IS} = Integral of the IS signal recorded in the ^{19}F NMR signal, Generally = 1

m_{IS} (mg) = mass of internal standard amount inside the tube

M_{IS} (g) = molar mass of internal standard

M_{F3PH} (g) = molar mass of 4-(trifluoromethyl)phenylhydrazine

m_{F3L} (mg) = mass of derivatized lignin amount inside the tube

A_L = Area of the lignin signal in the ^{19}F NMR spectrum

Several lignin's (after ethyl acetate washing) have been tested. Results are summarized in Table 9. They are expressed in mmoles of carbonyl per mole or gram of non-derivatized lignin and in g of carbonyl per g of derivatized lignin.

Table 9. Lignin carbonyl group quantification by ^{19}F NMR analysis after lignin derivatization using the trifluoromethyl phenylhydrazine agent

Ethylacetate washed lignin	mmol of C=O (ketones, aldehydes)		
	per mol non-derivatized L	per g non-derivatized L	per g F_3-derivatized L
Indulin	0.157	0.784	0.698
Organosolv	0.246	1.232	1.031
Protobind	0.136	0.669	0.605
Kraft	0.210	1.044	0.932

Table 9 shows the results of mmol of C=O per gram of non derivatized and fluoroderivatized lignin samples and mmol of C=O group per mol of non-derivatized lignin from the equation 1.1 to 1.3 based on the ^{19}F NMR results. Four different technical lignins C=O groups were quantified using ^{19}F NMR, according to the results Organosolv lignin contains highest number of carbonyl groups than the other lignins, next higher carbonyl group quantity observed with pine kraft lignins which is a softwood lignin, indulin and Protobind lignins showed the lowest number of carbonyl groups. Indulin and pine kraft lignin both were produced using kraft cooking process however the origin of the wood is different. Pine is a softwood lignin and indulin is hardwood lignin. Softwood pine kraft lignin showed higher carbonyl groups than hardwood indulin lignin sample, and Protobind lignin produced from annual plant showed the least number of carbonyl groups.

To assess these results, complementary analyses have been done on the CTP Pine Kraft lignin. The objective is to estimate the carbonyl group content via ^{13}C NMR. For that purpose, a ^{13}C NMR quantitative analysis has been done on the lignin sample before and after the derivation with the trifluoromethyl phenylhydrazine. Then the integrals of aromatic carbons from 160 to 100 ppm and of the methoxy groups one at 56 ppm have been measured. Results are given in Table 10.

Table 10. ^{13}C NMR integral value of lignin (aromatic and methoxy groups) before and after F_3PH derivatization.

	^{19}F NMR	^{13}C NMR	
	Number of C=O / C9 unit	$I_{Aromatic}$ 160 ppm to 100 ppm	$I_{Methoxy}$ 56 ppm
Pristine Lignin	-	6	0.87
Derivatized Lignin	0.209	6	0.68
Derivatized Lignin after ^{13}C integrals normalization	-	7.6764	0.87

In ^{13}C NMR lignin quantitative analysis, the quantification per C9 skeletal unit (per mole) is usually done by aromatic carbon integral normalization to 6 (6 aromatic carbons per skeletal C9 units). However, considering the lignin before and after derivatization, the only functional group remaining unchanged is the methoxy one. The similar procedure has been tested with the systematic study on model compounds. For an accurate ^{13}C spectra normalization, the methoxy integral should be kept constant, by multiplying all the integrals with the **0.87 / 0.68 ratio** = 1.2794 (Table 10). Then, the new value of the aromatic carbon integral becomes 7.6764, which represents 1.6764 increase in comparison with that of the pristine lignin. This integral increase is only due to the following structure modification:

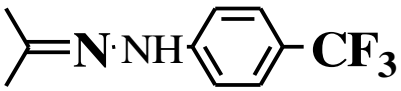

i.e. after the reaction with trifluoromethylphenylhydrazine, every carbonyl carbon (210 to 180 ppm) disappears, at the same time, 8 supplementary carbon atoms appear, in the aromatic region between160 to 100 ppm (CF_3 125 ppm, C=N 160 ppm to 135ppm).

Finally, it could be assumed that the 1.6764 increase for the aromatic carbon integral corresponds to 8 times carbon number per C9 unit. This gives 0.209 C=O. This value is similar to the ^{19}F NMR results (0.21) confirming that both methods consistent to the quantification of aldehyde and keto groups quantification, especially for lignin materials.

i) **Lignin derivatization kinetics studied in-situ in the ^{19}F NMR tube**

Constant et al. (Constant et al., 2017) studied the carbonyl quantification of humin materials, by CF_3PH derivatization at 40°C for 24 h, before NMR acquisition. In the present study, three methods (our method, Constant and Sevillano) have been compared.

This work has been carried out on the Protobind1000 (PB) lignin after ethyl acetate washing. The reaction was done using trifluoromethylphenylhydrazine (CF_3PH) as derivatizing agent, in the following conditions (Table 11):

Condition1: at room temperature in acidic medium - our present work

Condition2: at room temperature in neutral medium (Sevillano et al.,)

Condition3: at 40°C in neutral medium for 24 h (Constant et al)

Comparing all conditions, the present work followed the derivatization kinetics with ^{19}F NMR for 72 h (3 days) at minimum in acidic medium.

Table 11. Different kinetic conditions investigated for carbonyl group study of PB Lignin

CONDITIONS		1 This work	2 Sevillano (2001)	3 Constant (2017)
REAGENTS	**Lignin**	100 mg	100 mg	100 mg
	Reagent			
	4-Trifluoromethylphenyl hydrazine (CF_3PH)	120 mg	150 mg	93 mg
	Internal sta60ndard			
	4-methylbenzotrifluoride	10 mg	10 mg	10 mg
	Ortho phosphoric acid (H_3PO_4)	2 drops	-	-
REACTION TEMPERATURE (°C)		25	25	40
REACTION DURATION (hours)		48	24	24

The 4-methylbenzotrifluoride has been chosen as internal standard in in-situ reaction kinetics since it does not react with 4-(trifluoromethyl) phenylhydrazine (CF_3PH). After ^{19}F NMR quantitative data acquisition and integral measurements, the aldehyde and ketone function quantity is deduced from the Equation 4.

in **mmol.g^{-1}**$_{\text{non-derivatized lignin}}$

$$n_{C=O\ L} = \frac{A_L \times m_{IS} \times 1000}{(A_{IS} \times m_L \times M_{IS})} \qquad \text{Equation 4}$$

Where,

A_{IS} = Integral of IS, usually = 1

m_{IS} (mg) = mass of internal standard amount inside the tube

M_{IS} (g) = molar mass of internal standard

m_L (mg) = mass of non-derivatized lignin amount inside the tube

A_L = Area of the lignin integral

The results are given in mmol of C=O per gram of pristine lignin (starting before derivatization) (Table 12 and Figure 12). In general, the reactions are carried in the lab scale (without using in situ) which is referred as conventional method. The conventional method results were compared with other conditions performed by in-situ method.

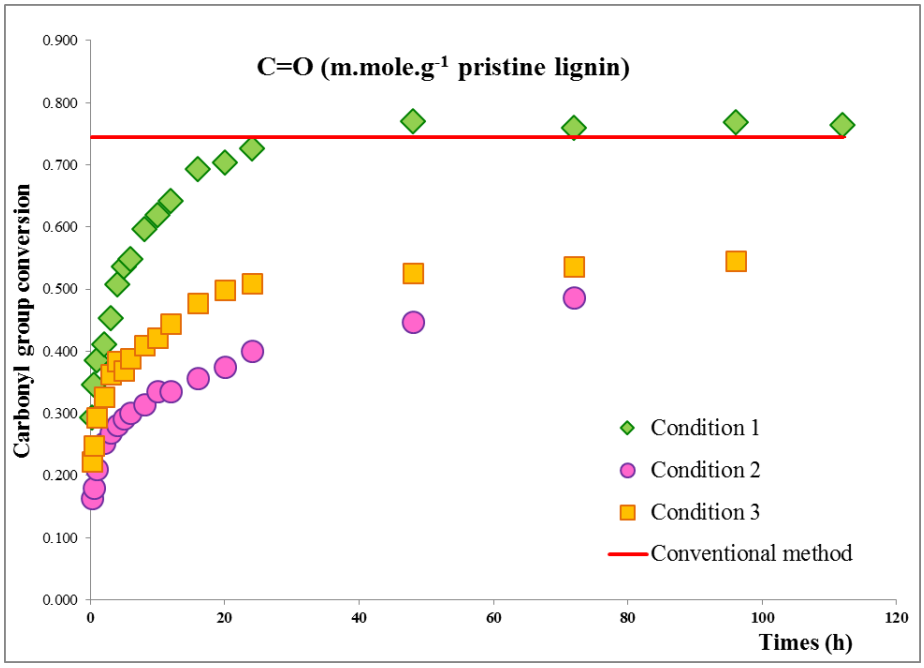

Figure 12. Carbonyl group conversion ratio with different experimental conditions

From Figure 12, after 24 h reaction, the maximum conversion of 0.72 was achieved with **condition 1** (reaction in acidic medium). The final reached value was 0.76 mmol of C=O per gram of pristine lignin. With **condition 3**, the conversion reached a plateau after 24 h reaction and no further spectral changes on the ^{19}F spectra after 24 h reaction. The obtained value for the carbonyl group conversion 0.545 was one-third smaller compared to that of our work.

With Sévillano conditions, **condition 2**, the result of model compounds showed that even after 3 days (72 h) no full carbonyl conversion was not achieved as confirmed with the low conversion rate (0.486). The reaction was followed for 4 days reaction, there is no significant changes on the conversion value.

Table 12. Reaction kinetics (mmol of C=O per gram) comparisons of in-situ method (Conditions 1 to 3) with conventional method

Time (h)	$n_{C=O}$ *Condition 1*	$n_{C=O}$ *Condition 2*	$n_{C=O}$ *Condition3*	$n_{C=O}$ *Conventional method*
0.25	0.293	0.164	0.222	0.744
0.5	0.346	0.180	0.248	0.744
1	0.385	0.210	0.293	0.744
2	0.411	0.253	0.327	0.744
3	0.454	0.269	0.363	0.744
4	0.508	0.282	0.384	0.744
5	0.536	0.292	0.369	0.744
6	0.549	0.301	0.389	0.744
8	0.596	0.314	0.409	0.744
10	0.620	0.336	0.422	0.744
12	0.642	0.336	0.444	0.744
16	0.693	0.357	0.478	0.744
20	0.704	0.375	0.499	0.744
24	0.726	0.401	0.509	0.744
48	0.770	0.448	0.525	0.744
72	0.760	0.486	0.537	0.744
96	0.769		0.545	0.744
112	0.764			0.744

The in-situ reaction kinetics (three different conditions inside NMR tube) is also compared with the conventional reaction (reaction with CF_3PH reagent for 48 h and lignin recovery through precipitation) followed by the ^{19}F NMR analysis. The value obtained from Equation 3 is 0.744 mmol of C=O per gram of starting non-derivatized lignin.

The conventional method values were in good agreement with the **condition 1** (our work). Based on the results, we found that in order to get the complete carbonyl group conversion reaction at room temperature in the acidic medium is adequate (condition 1), not necessary to increase the temperature up to 40˚C (condition 3). Comparing (condition 2 and 3), heating the reaction mixture without acidic condition significantly improves the reaction conversion in condition 3 than without heating (condition 2).

Three different reaction condition (in-situ) were investigated for the PB1000 lignin and the resulting ^{19}F NMR spectra are shown in Figure 13 (Spectra A) and compared to the spectrum of conventional derivatization, in which lignin was recovered through precipitation method (Spectra B).

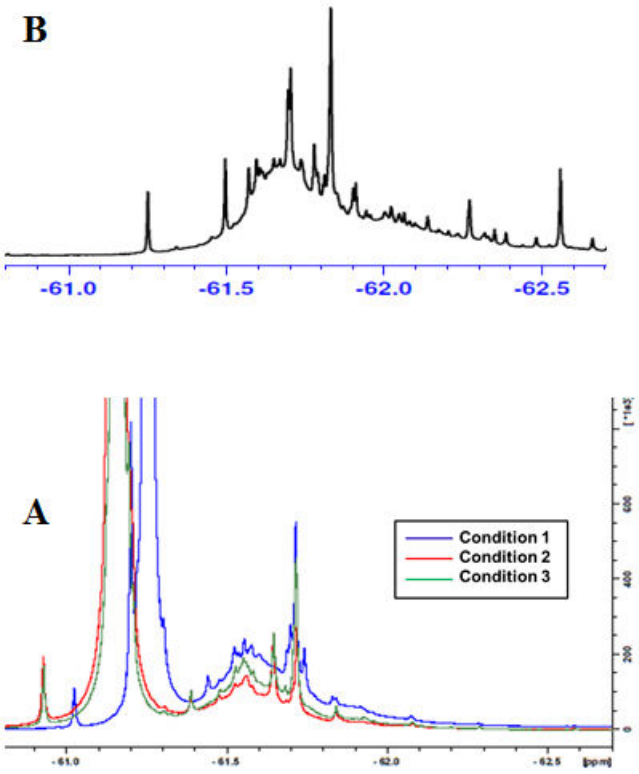

Figure 13. ^{19}F NMR spectra of PB1000 lignin ethylacetate washed. (A) in-situ derivatization (B) derivatization with the conventional method

From the spectra issued, the slight shift in the in-situ kinetics observed on the residual signal of the reagent (CF_3PH) around -61.0 to -61.5 ppm is due to the effect of the pH of the reactional mixture (acidic for condition 1 and neutral for condition 2 and 3). The pH was controlled it by drawing the chemical shift variation of trifluoromethyl phenylhydrazine in function of pH in Figure 14. The NH-NH_2 function of this reagent was responsive to the pH, and this effect is noticeable on ^{19}F NMR chemical shifts. After formation, the hydrazones were not pH sensitive. This explains the small shifting detected only for CF_3PH reagent residual signal.

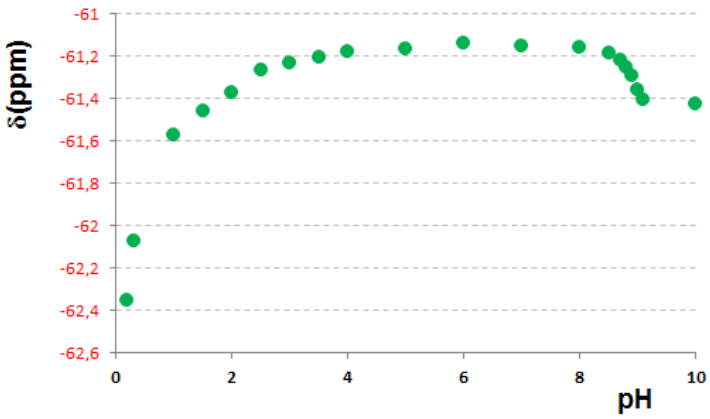

Figure 14. ^{19}F NMR chemical shift of CF_3PH in function of pH

f) Conclusion

In this chapter, various types of carbonyl lignin model compounds at positions α, β, γ and other typical compounds have been investigated. Trifluoromethylphenyl hydrazine derivatization of model compounds were performed inside the NMR tube (in-situ) and its reaction kinetics were observed at neutral and acidic condition. The derivatization of model compounds containing carbonyl groups at β-position was faster compared to α carbonyls. Compounds bearing phenyl group at γ – position, show poor reactivity with the CF_3PH reagent in neutral condition and their corresponding conversion rate is significantly low. Few model compounds bearing α carbonyls showed poor reactivity in neutral medium even after 72 hours of reaction time. In this case, the fluorination reaction was studied in acidic medium because it is known that acidic conditions increase the polarity of the starting carbonyl bond thus leading to the catalysis of the reaction. The results confirmed that the acidic condition significantly improved the carbonyl conversion. The same method has been used to quantify the carbonyl groups in lignin specifically.

Based on the model compounds results different technical lignins derivatization were studied using in-situ reaction kinetics in acidic condition and the results were compared with other conditions applied by Sévillano et al. and Constant et al. Our results show that CF_3PH derivatization method is a better choice for aldehyde and ketone compounds and the resulting hydrazone product was quantified by ^{19}F NMR analysis. The ^{19}F NMR results revealed that higher amount of carbonyl group conversion was achieved in both in-situ and conventional method in acidic medium. Whereas, other employed conditions (2 and 3) exhibited lower carbonyl conversion.

References

Brogdon, D.B.N., Mancosky, D.G., and Lucia, L.A. (2005). New Insights into Lignin Modification During Chlorine Dioxide Bleaching Sequences (I): Chlorine Dioxide Delignification. J. Wood Chem. Technol. *24*, 201–219.

Constant, S., Lancefield, C.S., Weckhuysen, B.M., and Bruijnincx, P.C.A. (2017). Quantification and Classification of Carbonyls in Industrial Humins and Lignins by 19F NMR. ACS Sustain. Chem. Eng. *5*, 965–972.

Deng, D., Deng, P., Wang, X., and Hou, X. (2009). Direct Determination of Sodium Fluoride and Sodium Monofluorophosphate in Toothpaste by Quantitative 19F-NMR: A Green Analytical Method. Spectrosc. Lett. *42*, 334–340.

El Mansouri, N.-E., and Salvadó, J. (2007). Analytical methods for determining functional groups in various technical lignins. Ind. Crops Prod. *26*, 116–124.

Hao, N., Ben, H., Yoo, C.G., Adhikari, S., and Ragauskas, A.J. (2016). Review of NMR Characterization of Pyrolysis Oils. Energy Fuels *30*, 6863–6880.

He, W., Du, F., Wu, Y., Wang, Y., Liu, X., Liu, H., and Zhao, X. (2006). Quantitative 19F NMR method validation and application to the quantitative analysis of a fluoro-polyphosphates mixture. J. Fluor. Chem. *127*, 809–815.

Holzgrabe, U., Deubner, R., Schollmayer, C., and Waibel, B. (2005). Quantitative NMR spectroscopy—Applications in drug analysis. J. Pharm. Biomed. Anal. *38*, 806–812.

Huang, F., Pan, S., Pu, Y., Ben, H., and J. Ragauskas, A. (2014). 19 F NMR spectroscopy for the quantitative analysis of carbonyl groups in bio-oils. RSC Adv. *4*, 17743–17747.

Krolikowski, P. (2004). The Use of 19F NMR to Monitor Organic Reactions on Solid Supports.

Lachenal, D., Benattar, N., Allix, M., Marlin, N., and Chirat, C. (2005). Bleachability of Alkaline Pulps: Effect of Quinones Present in Residual Lignin. In 59th Appita Annual Conference and Exhibition: Incorporating the 13th ISWFPC (International Symposium on Wood, Fibre and Pulping Chemistry), Auckland, New Zealand, 16-19 May 2005: Proceedings, (Appita Inc.), p. 23.

Martino, R., Gilard, V., Desmoulin, F., and Malet-Martino, M. (2005). Fluorine-19 or phosphorus-31 NMR spectroscopy: A suitable analytical technique for quantitative in vitro metabolic studies of fluorinated or phosphorylated drugs. J. Pharm. Biomed. Anal. *38*, 871–891.

Matera, R., Gabbanini, S., Valvassori, A., Triquigneaux, M., and Valgimigli, L. (2012). Reactivity of (E)-4-Hydroxy-2-nonenal with Fluorinated Phenylhydrazines: Towards the Efficient Derivatization of an Elusive Key Biomarker of Lipid Peroxidation. Eur. J. Org. Chem. *2012*, 3841–3851.

Sévillano, R.M. (1999). Structures des lignines résiduelles des pâtes chimiques: influence des méthodes d'extraction, des procédés de délignification et des essences de bois. Thesis.

Sevillano, R.M., Mortha, G., Barrelle, M., and Lachenal, D. (2001). 19F NMR Spectroscopy for the Quantitative Analysis of Carbonyl Groups in Lignins. Holzforschung *55*, 286–295.

Stankovikj, F., McDonald, A.G., Helms, G.L., and Garcia-Perez, M. (2016). Quantification of Bio-Oil Functional Groups and Evidences of the Presence of Pyrolytic Humins. Energy Fuels *30*, 6505–6524.

Zakis, G.F. (1994). Functional analysis of lignins and their derivatives (TAPPI Press).

Zawadzki, M. Quantitative Determination of Quinone Chromophore Changes during ECF Bleaching of Kraft Pulp; Institute of Paper Science and Technology: Atlanta, August 1999. PhD Thesis. Ph. D. Dissertation.

Zawadzki, M.A., and Ragauskas, A.J. (1999). Pulp properties influencing oxygen delignification bleachability.

Appendix B: Fluorobenzylation: Number of mole hydroxyls calculations

This section presented to calculate the number of hydroxyl group present in the lignin which can be obtained from fluorobenzylation derivatization of lignin.

The molar mass of initial lignin is M_L = 200 g

x = Phenolic hydroxyl functions (φ-OH)

y = aliphatic hydroxyl functions (1°)

} mole of original lignin

After fluorobenzylation,

The molar mass of flurorobenzylated lignin is M_{Li}

1 mole {
- $(1 - x - y)$ mole lignin non derivatized
- "x" mole of lignin φ-OH fluoro derivatized
- "y" mole of lignin aliphatic-OH fluoro derivatized

In the case of fluorobenzylation, lignin hydroxyl groups $R^{|} - OH$ ($R^{|}$ represents lignin), especially phenolic hydroxyls are undergone fluorobenzylation using 4-Fluorobenzylchloride (F_1) and form fluorobenzylated lignin (lignin – ORF_1).

$R^{|} - OH \rightarrow R^{|} - ORF + HCl$

IS = Internal standard, Molar mass, M_{IS} = 138.14 g

F = 4-Fluorobenzylchloride (FBC), Molar mass M_F = 144.5 g

HCl, Molar mass M_{HCl} = 36.47 g

Based on the fluorobenzylation, the molar mass of derivatized lignin is calculated from the following relation. M_{Li} – molar mass of derivatized lignin, M_L – molar mass of initial or underivatized lignin.

$$M_{Li} = M_L + x\,M_{HCl} + y\,M_F - y\,M_{HCl}$$

Molar mass of fluoro derivatized lignin introduced

$$M_{Li} = M_L + (x + y) \times (M_F - M_{HCl}) \qquad \textit{Equation 5}$$

After substitution, $M_F - M_{HCl} = 108.03\ g$ *Equation 6*

Therefore, $M_{Li} = M_L + (x + y) \times 108.03$ *Equation 7*

From GPC analysis, the area of internal standard (A_{IS}), integrated area of fluorobenzylated aromatic A_{Lix} (φ-OH) and aliphatic A_{Liy} (aliphatic-OH) hydroxyls lignin, mass of internal standard (m_{IS}) and mass of derivatized lignin (m_{Li}).

$$A_{IS} = k \times \frac{m_{IS}}{M_{IS}} \Rightarrow k = \frac{A_{IS} \times M_{IS}}{m_{IS}} \qquad \textit{Equation 8}$$

$$A_{Lix} = k \times x\,\frac{m_{Li}}{M_{Li}} \Rightarrow k = \frac{A_{Lix} \times M_{Li}}{x \times m_{Li}} \qquad \textit{Equation 9}$$

$$A_{Liy} = k \times y\,\frac{m_{Li}}{M_{Li}} \Rightarrow k = \frac{A_{Liy} \times M_{Li}}{y \times m_{Li}} \qquad \textit{Equation 10}$$

From the above *Equation 8*, *Equation 9*, *Equation 10*, the following relations are derived,

$$A_{IS} \times M_{IS} \times m_{Li} \times x = A_{Lix} \times M_{Li} \times m_{IS} \qquad \textit{Equation 11}$$

$$A_{IS} \times M_{IS} \times m_{Li} \times y = A_{Liy} \times M_{Li} \times m_{IS} \qquad \textit{Equation 12}$$

Since, $A_{IS} = 1$

The *Equation 11* can be written as

$$x = A_{Lix} \times \frac{M_{Li}}{M_{IS}} \times \frac{m_{IS}}{m_{Li}} \qquad \textit{Equation 13}$$

Similarly, *Equation 12* becomes

$$y = A_{Liy} \times \frac{M_{Li}}{M_{IS}} \times \frac{m_{IS}}{m_{Li}} \qquad \textit{Equation 14}$$

Since, *Equation 9* equals to *Equation 10*

$$k = \frac{A_{Lix} \times M_{Li}}{x \times m_{Li}} = \frac{A_{Liy} \times M_{Li}}{y \times m_{Li}} \qquad \textit{Equation 15}$$

Rearranging the *Equation 15*,

$$y \times A_{Lix} \times M_{Li} \times m_{Li} = y \times A_{Lix} \times M_{Li} \times m_{Li}$$

$$y = x \times \frac{A_{Liy}}{A_{Lix}} \qquad \textit{Equation 16}$$

Substitute the *Equation 16* to *Equation 6*,

$$M_{Li} = M_L + \left(x + x \times \frac{A_{Liy}}{A_{Lix}}\right) \times 108.03$$

$$M_{Li} = M_L + x \times \left(1 + \frac{A_{Liy}}{A_{Lix}}\right) \times 108.03 \qquad \textit{Equation 17}$$

The *Equation 13* can be modified by substituting *Equation 17*,

$$x = A_{Lix} \times \frac{m_{IS}}{m_{Li}} \times \left[\frac{M_{Li}}{M_{IS}} + \frac{108.03}{M_{IS}} \times x \times \left(1 + \frac{A_{Liy}}{A_{Lix}}\right)\right] \qquad \textit{Equation 18}$$

However, $\frac{M_{Li}}{M_{IS}} = 1{,}447$ g

The *Equation 18* becomes,

$$x = 1.447 \times A_{Lix} \times \frac{m_{IS}}{m_{Li}} + x \times \frac{A_{Lix}}{M_{IS}} \times 108.03 \times \frac{m_{IS}}{m_{Li}} \times \left(1 + \frac{A_{Liy}}{A_{Lix}}\right) \qquad \textit{Equation 19}$$

$$x\left[1 - 108.03 \times \frac{A_{Lix}}{M_{IS}} \times \frac{m_{IS}}{m_{Li}} \times \left(1 + \frac{A_{Liy}}{A_{Lix}}\right)\right] = 1.447 \times A_{Lix} \times \frac{m_{IS}}{m_{Li}}$$

$$x = \frac{1.447 \times A_{Lix} \times \frac{m_{IS}}{m_{Li}}}{\left[1 - 108.03 \times \frac{A_{Lix}}{M_{IS}} \times \frac{m_{IS}}{m_{Li}} \times \left(1 + \frac{A_{Liy}}{A_{Lix}}\right)\right]} \qquad \textit{Equation 20}$$

Since, M_{IS} 138.14 and therefore $= \frac{108.03}{138.14} = 0.782$

After substituting the value, the *Equation 20* turned into

$$x = \frac{1.447 \times A_{Lix} \times \frac{m_{IS}}{m_{Li}}}{\left[1 - 0.782 \times A_{Lix} \times \frac{m_{IS}}{m_{Li}} \times \left(1 + \frac{A_{Liy}}{A_{Lix}}\right)\right]} \qquad \textit{Equation 21}$$

Similarly, for "*y*"

$$y = \frac{1.447 \times A_{Liy} \times \frac{m_{IS}}{m_{Li}}}{\left[1 - 0.782 \times A_{Lix} \times \frac{m_{IS}}{m_{Li}} \times \left(1 + \frac{A_{Liy}}{A_{Lix}}\right)\right]}$$

Equation 22

From the above *Equation 21*and *Equation 22*, the *x* and *y* values are calculated. The obtained values correspond to the mole-OH present per mole of original lignin. “x” and “y” values represent aromatic and aliphatic hydroxyl groups in lignin molecule.

Appendix C: Fluorobenzoylation: Number of mole hydroxyls calculations

This section devoted to calculating the number of moles of lignin is being derivatized using fluorobenzoylation. In this case,

Initial lignin = M_L = 200 g

u = Phenolic hydroxyl functions (φ-OH)

v = Phenolic hydroxyl functions (φ-OH)

y = Primary hydroxyl functions (1°)

} mole of original lignin

z = Secondary hydroxyl functions (2°)

After fluorobenzoylation,

Fluroro derivatized lignin, M_{Li} = molar mass

1 mole

- (1 – u – v – y – z) mole lignin
- "u" mole lignin derivatized (φ-OH: Fluorobenzylated)
- "v" mole lignin derivatized (φ-OH: Fluorobenzoylated)
- "y" mole lignin derivatized (aliphatic 1°-OH: Fluorobenzylated)
- "z" mole lignin derivatized (aliphatic 2°-OH: Fluorobenzoylated)

In the case of fluorobenzylation, lignin hydroxyl groups $R^{|}$ – OH ($R^{|}$ represents lignin), especially phenolic hydroxyls are undergone fluorobenzylation using 4-Fluorobenzylchloride (F_1) and form fluorobenzylated lignin (lignin – ORF_1).

$R^{|}$ – OH → $R^{|}$ – ORF_1 + HCl

IS = Internal standard, Molar mass M_{IS} = 138.14 g

F_1 = 4-Fluorobenzylchloride (FBC), Molar mass M_{F1} = 144.5 g

HCl, Molar mass M_{HCl} = 36.47 g

After fluorobenzylation, the reaction is forwarded to fluorobenzoylation, treating fluorobenzylated lignin ($R^{|}$ – ORF_1) with 4-Fluorobenzoic Anhydride to give fluorobenzoylated lignin (lignin – $O(C{=}O)R^{\|}F_1$). In this reaction, remaining hydroxyls, mostly aliphatic hydroxyl groups are fluorobenzoylated.

$OH - R^{|} - ORF_1 \rightarrow F_2R^{\|}C(=O)O - ORF_1 + FBA$

F_2 = 4-Fluorobenzoic anhydride (FBAA), Molar mass M_{F2} = 262.2 g

FBA, 4-Fluorobenzoicacid, Molar mass M_{FBA} = 140.1 g

From the above reactions, molar mass of derivatized lignin (M_{Li}) is thus calculated,

$$M_{Li} = M_L + u\,M_{F1} - u\,M_{HCl} + y\,M_{F1} - y\,M_{HCl} + v\,M_{F2} - v\,M_{FBA} + z\,M_{F2} - z\,M_{FBA} \quad \text{Equation 1}$$

$$M_{Li} = M_L + (u+y) \times (M_{F1} - M_{HCl}) + (v+z) \times (M_{F2} - M_{FBA}) \quad \text{Equation 2}$$

Substituting all molar mass values, the molar mass of derivatized lignin

$$M_{Li} = M_L + (u+y) \times 108.03 + (v+z) \times 122.1 \quad \text{Equation 3}$$

The following relations can be obtained from GPC results. A_{IS} – area of internal standard, M_{IS} – molar mass of internal standard, m_{Li} – mole of lignin, A_{Liu} – area of lignin fluorobenzylated (phenolic hydroxyl group), M_{Li} – molar mass of lignin, m_{IS} – mole of internal standard, A_{Liv} – area of lignin fluorobenzoylated (phenolic hydroxyl group), A_{Liy} – area of lignin fluorobenzylated (aliphatic 1° hydroxyl group), A_{Liz} – area of lignin fluorobenzoylated (aliphatic 2° hydroxyl group)

$$A_{IS} \times M_{IS} \times m_{Li} \times u = A_{Liu} \times M_{Li} \times m_{IS} \quad \textit{Equation 4}$$

$$A_{IS} \times M_{IS} \times m_{Li} \times v = A_{Liv} \times M_{Li} \times m_{IS} \quad \textit{Equation 5}$$

$$A_{IS} \times M_{IS} \times m_{Li} \times y = A_{Liy} \times M_{Li} \times m_{IS} \quad \textit{Equation 6}$$

$$A_{IS} \times M_{IS} \times m_{Li} \times z = A_{Liz} \times M_{Li} \times m_{IS} \qquad \textit{Equation 7}$$

After rearranging the above equations *Equation 4*, *Equation 5*, *Equation 6* and *Equation 7*,

$$v = u \times \frac{A_{Liv}}{A_{Liu}} \qquad y = u \times \frac{A_{Liy}}{A_{Liu}} \qquad z = u \times \frac{A_{Liz}}{A_{Liu}}$$

Substituting the *v, y* and *z* to the *Equation 3*,

$$M_{Li} = M_L + \left(u + u \times \frac{A_{Liy}}{A_{Liu}}\right) \times 108.03 + \left(u \times \frac{A_{Liv}}{A_{Liu}} + u \times \frac{A_{Liz}}{A_{Liu}}\right) \times 122.1 \qquad \textit{Equation 8}$$

$$M_{Li} = M_L + u\left[108.03 \times \left(1 + \frac{A_{Liy}}{A_{Liu}}\right) + 122.1 \times \left(\frac{A_{Liv} + A_{Liz}}{A_{Liu}}\right)\right] \qquad \textit{Equation 9}$$

The *Equation 4* can be written as,

$$u = \frac{A_{Liu} \times m_{IS} \times M_{Li}}{A_{IS} \times m_{Li} \times M_{IS}} \qquad \textit{Equation 10}$$

Since $A_{IS} = 1$, therefore

$$u = \frac{A_{Liu} \times m_{IS} \times M_{Li}}{m_{Li} \times M_{IS}} \qquad \textit{Equation 11}$$

Substitute *Equation 11* to the *Equation 9*,

$$u = \frac{A_{Liu}}{M_{IS}} \times \frac{m_{IS}}{m_{Li}} \times \left[M_L + u\left[108.03 \times \left(1 + \frac{A_{Liy}}{A_{Liu}}\right) + 122.1 \times \left(\frac{A_{Liv} + A_{Liz}}{A_{Liu}}\right)\right]\right] \qquad \textit{Equation 12}$$

$$u = A_{Liu} \times \frac{m_{IS}}{m_{Li}} \times \frac{M_L}{M_{IS}} + u \times \frac{A_{Liu}}{M_{IS}} \times \frac{m_{IS}}{m_{Li}}\left[108.03 \times \left(1 + \frac{A_{Liy}}{A_{Liu}}\right) + 122.1 \times \left(\frac{A_{Liv} + A_{Liz}}{A_{Liu}}\right)\right] \qquad \textit{Equation 13}$$

And $\frac{M_L}{M_{IS}} = 1.447$

$$\times \left[1 - \frac{A_{Liu}}{M_{IS}} \times \frac{m_{IS}}{m_{Li}} \left[108.03 \times \left(1 + \frac{A_{Liy}}{A_{Liu}}\right) + 122.1 \times \left(\frac{A_{Liv} + A_{Liz}}{A_{Liu}}\right)\right]\right] \quad \textit{Equation 14}$$

$$= 1.447 \times A_{Liu} \times \frac{m_{IS}}{m_{Li}}$$

u *Equation 15*

$$= 1.447 \times A_{Liu} \times \frac{m_{IS}}{m_{Li}}$$

$$\times \frac{1}{\left[1 - \frac{A_{Liu}}{138.14} \times \frac{m_{IS}}{m_{Li}} \left[108.03 \times \left(1 + \frac{A_{Liy}}{A_{Liu}}\right) + 122.1 \times \left(\frac{A_{Liv} + A_{Liz}}{A_{Liu}}\right)\right]\right]}$$

$$u = \frac{1.447 \times A_{Liu} \times \frac{m_{IS}}{m_{Li}}}{\left[1 - \frac{A_{Liu}}{138.14} \times \frac{m_{IS}}{m_{Li}} \left[108.03 \times \left(1 + \frac{A_{Liy}}{A_{Liu}}\right) + 122.1 \times \left(\frac{A_{Liv} + A_{Liz}}{A_{Liu}}\right)\right]\right]} \quad \textit{Equation 16}$$

Similarly, for the case of "*v*" calculation

$$v = \frac{1.447 \times A_{Liv} \times \frac{m_{IS}}{m_{Li}}}{\left[1 - \frac{A_{Liu}}{138.14} \times \frac{m_{IS}}{m_{Li}} \left[108.03 \times \left(1 + \frac{A_{Liy}}{A_{Liu}}\right) + 122.1 \times \left(\frac{A_{Liv} + A_{Liz}}{A_{Liu}}\right)\right]\right]} \quad \textit{Equation 17}$$

and "*y*" calculation

$$y = \frac{1.447 \times A_{Liy} \times \frac{m_{IS}}{m_{Li}}}{\left[1 - \frac{A_{Liu}}{138.14} \times \frac{m_{IS}}{m_{Li}} \left[108.03 \times \left(1 + \frac{A_{Liy}}{A_{Liu}}\right) + 122.1 \times \left(\frac{A_{Liv} + A_{Liz}}{A_{Liu}}\right)\right]\right]} \quad \textit{Equation 18}$$

and "*z*" calculation

$$z = \frac{1.447 \times A_{Liz} \times \frac{m_{IS}}{m_{Li}}}{\left[1 - \frac{A_{Liu}}{138.14} \times \frac{m_{IS}}{m_{Li}} \left[108.03 \times \left(1 + \frac{A_{Liy}}{A_{Liu}}\right) + 122.1 \times \left(\frac{A_{Liv} + A_{Liz}}{A_{Liu}}\right)\right]\right]} \quad \textit{Equation 19}$$

The final values of "*u, v, y, z*" are in mole OH / mole of original lignin – non derivatized

Summary

Lignin is the second most abundant biopolymer on earth after cellulose and it consists of highly-branched, three dimensional aromatic structures with variety of functional groups. This research work was to establish lignin derivatization methods for lignin analysis, to quantify functional groups and to determine lignin molar mass distribution (MMD) by size exclusion chromatography. Five different technical lignin samples are considered: Protobind 1000 lignin, Organosolv lignin, Pine Kraft lignin, Eucalyptus Kraft lignin and Indulin lignin. Lignin samples are derivatized through classical acetylation method and new methods such as fluorobenzylation and fluorobenzoylation. The number of hydroxyl present in the lignin samples are quantified through GC and NMR (^{1}H, ^{13}C, ^{19}F and ^{31}P) techniques. The molar mass distribution of derivatized lignin samples are calculated using different SEC columns with different solvents (DMAc and THF). Conventional and universal calibration methods are used for MMD calculations. With this approach, new derivatization methods significantly enhance the solubility in THF column system, and the universal calibration method detects the three times higher molar mass than conventional calibration method.

Résumé

La lignine est le deuxième biopolymère et le plus abondant sur la planète après la cellulose. Elle se compose de structures aromatiques tridimensionnelles hautement ramifiées, comportant divers groupes fonctionnels. Ce travail de recherche visait à établir des méthodes de dérivatisation de la lignine pour l'analyse de la lignine, à quantifier les groupes fonctionnels et à déterminer la distribution de la masse molaire de la lignine (DMM) par chromatographie par exclusion de taille. Cinq échantillons techniques de lignine sont pris en compte: la lignine Protobind 1000, la lignine Organosolv, la lignine Pine Kraft, la lignine Eucalyptus Kraft et la lignine Induline. Les échantillons de lignine sont transformés en dérivés par une méthode classique d'acétylation et de nouvelles méthodes telles que la fluorobenzylation et la fluorobenzoylation. Le nombre d'hydroxyles présents dans les échantillons de lignine est quantifié par des techniques GC et RMN (^{1}H, ^{13}C, ^{19}F and ^{31}P). La distribution en masse molaire des échantillons de lignine dérivatisés est calculée en utilisant différentes colonnes SEC avec différents solvants (DMAc et THF). Des méthodes d'étalonnage conventionnelles et universelles sont utilisées pour les calculs MMD. Avec cette approche, les nouvelles méthodes de dérivatisation améliorent de manière significative la solubilité dans le système de colonne THF, et la méthode d'étalonnage universelle détecte la masse molaire trois fois supérieure à la méthode d'étalonnage conventionnelle.

Résumé en Français

1. INTRODUCTION

La biomasse lignocellulosique est considérée aujourd'hui comme une alternative aux ressources fossiles pour la production de matériaux biosourcés et cela dans de nombreuses applications de haute valeur ajoutée. Cette ressource naturelle est composée de cellulose, hémicelluloses et lignine. La lignine est le deuxième biopolymère le plus abondant sur Terre après la cellulose. Elle est constituée de structures aromatiques tridimensionnelles fortement ramifiées, comprenant une grande variété de groupements fonctionnels. En particulier, la lignine contient différentes unités phénylpropanes, portant des fonctions hydroxyles, méthoxyles, carbonyles, et carboxyles. La lignine est utilisée comme précurseur pour différentes applications comme dans les résines phénoliques, les polyuréthanes, les époxydes et les acryliques. La caractérisation de la lignine et de ses groupements fonctionnels est primordiale pour évaluer les applications possibles.

Au cours de ces dernières années, les chercheurs ont travaillé sur la caractérisation de la lignine pour développer de nouveaux matériaux. De nombreuses méthodes et techniques analytiques ont été utilisées pour étudier la structure et la réactivité de la lignine. Parmi elles, la quantification des groupements fonctionnels (-OH, -C=O, -COOH) par dérivation et l'analyse de la **d**istribution des **m**asse **m**olaires (MMD) par chromatographie d'exclusion stérique (SEC) restent les plus largement employées. Pourtant, l'analyse MMD de la lignine est complexe de par la structure irrégulière de ce polymère, de par sa polarité et sa structure partiellement ramifiée, ce qui conduit à une faible solubilité et des phénomènes d'agrégats dans la plupart des solvant de chromatographie. Ainsi, l'analyse SEC donne des résultats quantitatifs insuffisants et peu fiables, ce qui limite les potentielles voies de valorisation de la lignine dans de nouvelles applications. La plupart des études se focalisent sur la modification des groupements hydroxyles de la lignine pour diminuer sa polarité et améliorer sa dissolution dans les solvants. Les principales méthodes de dérivation sont l'acétylation, la fluorobenzylation, la fluorobenzoylation et l'oximation. Par ailleurs, ces méthodes de dérivation améliorent aussi la stabilité des lignines dissoutes dans les solvants de chromatographie de type THF et DMAC-LiCl.

A ce jour, l'acétylation reste la méthode la plus utilisée pour dériver les fonctions hydroxyles avant l'analyse SEC. Mais cette méthode présente de nombreux inconvénients : une solubilité de la lignine dérivée incomplète, des associations entre molécules et la formation d'agrégats dans la colonne, etc.

De nombreuses études se sont concentrées sur l'analyse de la MMD de la lignine par chromatographie SEC en utilisant le polystyrène comme calibrant (étalon) and des détecteurs UV et RI (réfractomètre) dans la ligne. Avec ce type de détecteurs, il est impossible de distinguer des polymères par volume d'élution. La MMD résultante n'est donc pas fiable. Un autre inconvénient est l'utilisation du polystyrène comme calibrant, un polymère linéaire très différent de la lignine, polymère tridimensionnel. Le comportement de la lignine dans les colonnes de chromatographie est donc très éloigné de celui du polystyrène ce qui rajoute un doute sur la fiabilité de l'analyse.

L'objectif de la thèse est d'améliorer la solubilité de la lignine dans les solvants classiques de chromatographie afin d'analyser plus justement la MMD de la lignine, ce qui permettra de développer de nouvelles applications pour la lignine. Ce travail a conduit à utiliser différentes méthodes de dérivation de la lignine comme l'acétylation, la fluorobenzylation et la fluorobenzoylation afin de modifier la réactivité et la polarité de la lignine. En utilisant différentes méthodes analytiques (UV, IR, GC, RMN ^{1}H, RMN ^{13}C NMR, RMN ^{19}F), le nombre de groupes hydroxyles dans la lignine peut être déterminé. De plus, l'utilisation d'un détecteur viscosimétrique dans la ligne de chromatographie SEC permet aussi d'améliorer l'analyse. Enfin, différents calibrants (polystyrène, polyméthylmétacrylate et acétate de cellulose) sont utilisés pour réaliser une calibration universelle des colonnes afin de conduire à la MMD de la lignine la plus proche de la réalité. A notre connaissance, cette méthodologie (calibration universelle et dérivation de la lignine par différentes méthodes) est nouvelle, en particulier la comparaison de l'acétylation classique aux méthodes de fluorobenzylation et fluorobenzoylation dans le système SEC-THF.

Le chapitre 1 présente la biomasse lignocellulosique, sa structure et ses applications potentielles, ainsi que les méthodes usuelles permettant sa caractérisation, groupements fonctionnels et masse molaire. Les limites de ces méthodes seront présentées.

Le chapitre 2 recense le matériel et les méthodes, en particulier les différents types de lignine étudiées (Protobind 1000, Indulin, Organosolv, Kraft et Kraft Eucalyptus), et utilisées pour déterminer et comparer les MMD à partir d'une calibration classique ou conventionnelle. Les méthodes de dérivation de la lignine et les analyses SEC réalisées sont présentées en détails.

La réactivité de la lignine est liée à la présence de groupements hydroxyles phénoliques libres. Ainsi dans le chapitre 3, les groupements hydroxyles de différentes lignines sélectionnées sont quantifiés via une méthode éprouvée l'aminolyse, qui nécessite l'acétylation préalable de la lignine. Cette méthode est comparée à d'autres techniques analytiques reconnues, directes ou indirectes (après dérivation de la lignine) telles que la spectroscopie UV, la RMN ^{1}H, ^{13}C et ^{31}P, la conductimétrie ou la potentiométrie.

Les fluorodérivations sont des réactions intéressantes qui permettent de réduire la polarité de la lignine, ce qui pourrait améliorer la solubilité de celle-ci dans les solvants de chromatographie utilisés pour l'analyse de la distribution de masse. Par ailleurs, ces réactions permettent aussi la quantification, par RMN du ^{19}F, des hydroxyles dérivés, Le chapitre 4 s'intéresse donc à la fluorobenzylation et à la fluorobenzoylation de la lignine. Ainsi la réactivité de différents composés modèles de lignine contenant des hydroxyles phénoliques et/ou aliphatiques, lors de fluorodérivations est étudiée par spectroscopie RMN du ^{19}F et du ^{13}C. Les résultats obtenus sont appliqués à la quantification par RMN du ^{19}F des fonctions hydroxyles de différentes lignines techniques.

A la suite de ce chapitre, la flurobenzylation est employée pour améliorer la solubilisation de la lignine dans les solvants de chromatographie pour l'analyse de la distribution des masses molaires. En 2.425078 parallèle, une nouvelle méthode de calibration universelle est proposée grâce à l'utilisation d'un détecteur viscosimétrique dans la ligne de chromatographie SEC. Les lignines techniques sont acétylées et fluorobenzylées puis analysées dans deux systèmes de chromatographie : (1) système avec le solvant DMAc/LiCl et calibration conventionnelle et (2) système avec THF et calibration universelle. Ces deux systèmes sont comparés.

Enfin, ce manuscrit s'achève par une conclusion générale qui présente les principales avancées dans le domaine de la caractérisation de la lignine, notamment l'analyse des groupements hydroxyles et la distribution des masses molaires, améliorées grâce à la fluorobenzylation de la lignine.

Les paragraphes suivants présentent un résumé en français des différents chapitres.

2. CHAPITRE 1 – revue bibliographique

2.1. La structure de la lignine

La quantité de lignine varie selon la nature de la biomasse lignocellulosique. Les bois de résineux contiennent 25 à 30% de lignine en poids alors que dans les feuillus, la teneur est de 9 à 23%. Dans les plantes herbacées, on compte 10 à 30% de lignine. Par ailleurs, la composition de la lignine elle-même est très variable selon la biomasse végétale considérée. La lignine est un hétéropolymère constitué d'unités phényl-propane : p-hydroxyphényle (**H**), guaiacyle (4-hydroxy-3-méthoxyphényle) (**G**) et syringyle (4-hydroxy-3,5-diméthoxyphényle) (**S**). Ces unités proviennent des principaux précurseurs de la lignine dans la nature, les alcools aromatiques coumarylique, coniférylique et sinapylique (Figure 15). Les plantes grasses et de type paille contiennent les trois unités **H**, **G** et **S**. Dans les bois de résineux en revanche, l'unité **G** est majoritaire, et dans les feuillus, on trouve principalement les unités **G** et **S**. Du fait de la grande diversité de la lignine (on devrait parler « de lignines au pluriel… »), la structure exacte des lignines extraites ne peut pas être pleinement élucidée.

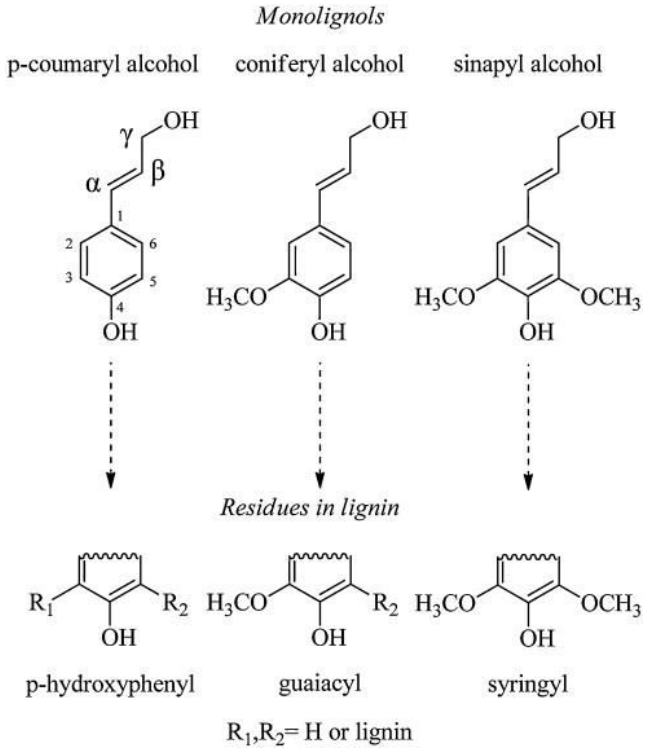

Figure 15. Les trois précurseurs de la lignine (monolignols) et les structures de lignine

2.2. Les liaisons dans la lignine

La lignine présente un grand nombre de liaisons. Les unités phényl propanes sont liées principalement par des liaisons β-O-4, β-5, α-O-4, 4-O-5, 5-5, β- β et β-1. La proportion de ces différentes liaisons est donnée dans le tableau 1.

Tableau 13. Proportion des liaisons inter-unité dans la lignine de résineux et de feuillus

Type de liaison	Poucentage (%)	
	Résineux	Feuillus
β-O-4	45-55	60
5-5	19-22	9
β-5	9-12	6
4-O-5	4-7	6,5
β-1	7-9	1
β- β	2-4	3

La lignine présente de nombreux groupes fonctionnels ; les plus abondants sont listés dans le tableau 2. Les groupes caractéristiques sont les méthoxyles, les hydroxyles phénoliques et aliphatiques, et les groupes carbonyles. Ils sont à l'origine de la réactivité de la lignine. Leur proportion varie selon la nature de la biomasse lignocellulosique.

Tableau 14. Groupes fonctionnels dans les lignines de résineux et de feuillus (abondance pour 100 unités C-9)

Groupes fonctionnels	Lignine de résineux	Lignine de feuillus
Méthoxyle	90 – 95	139 –158
Hydroxyle Phénolique	20 – 30	10 – 15
Alcool benzylique	30 – 45	40 – 50
Carbonyle	10 – 15	17 – 24
Hydroxy aliphatique	115 – 120	88 – 166

2.3. L'extraction de la lignine de la biomasse végétale

Il existe de nombreux procédés permettant d'extraire la lignine de la biomasse végétale. Ils altèrent malheureusement la structure de la lignine, en particulier les groupements fonctionnels et les propriétés physiques et chimiques de sorte que les lignines extraites sont très hétérogènes. Dans l'industrie papetière, les méthodes d'extraction les plus répandues sont les procédés Kraft, sulfite, soude et organosolv. L'objectif premier de ces procédés est d'isoler les fibres de cellulose de la biomasse lignocellulosique pour des applications papetières. Ceci est réalisé en dépolymérisant la lignine, ciment des fibres cellulosique dans la biomasse végétale, ce qui la rend soluble dans le milieu. Ainsi, chaque année, c'est environ 40 à 50 millions de tonnes de lignine qui sont extraites dans le monde, principalement à partir du procédé Kraft puisque c'est le procédé papetier dominant. Aujourd'hui, la lignine extraite est majoritairement brulée dans la chaudière de l'usine de pâte pour produire l'énergie nécessaire à son fonctionnement, seule une faible fraction, environ 2%, est commercialisée pour des applications de haute valeur ajoutée.

La structure de la lignine dépend aussi fortement du procédé d'extraction dont elle est issue.

Le procédé Kraft, procédé papetier dominant dans le monde, produit environ 85% (environ $43x10^6$ tonnes par an) de la lignine dans le monde. Ce procédé permet de produire des pâtes papetières de qualité avec un rendement matière de 45 à 50% à partir de différentes essences de bois. Dans ce procédé, les copeaux de bois sont placés dans une liqueur blanche composée d'une solution aqueuse d'hydroxyde de sodium (NaOH) et de sulfure de sodium (Na_2S), dans un réacteur pressurisé. Le bois est « cuit » dans la liqueur blanche à des températures voisines de 150 à 170°C pendant au moins 2 heures. Pendant la réaction, la lignine est très fortement dégradée et dissoute dans la phase aqueuse suite à la rupture de nombreuses liaisons entre différentes unités lignine.

.

Globalement le procédé sulfite produit 4% de la lignine extraite. Ce procédé est dédié à la production des pâtes de spécialité, très réactives et utilisées pour des applications chimiques. Ce procédé utilise une solution aqueuse contenant des ions sulfite (SO_3^{2-}) ou bisulfite (HSO_3^-). Là encore les copeaux sont cuits à haute température avec cette liqueur blanche. Il existe deux procédés en fonction des conditions de pH, le procédé sulfite ou le procédé bisulfite. Les lignines extraites sont soufrées et sont appelées lignosulfonates. Elles sont contaminées par des sucres, restes de polysaccharides (cellulose, hémicelluloses) liés à la lignine extraite.

Le procédé soude produit environ 5% des lignines extraites dans le monde. Il est particulièrement bien adapté aux plantes annuelles car cette biomasse végétale requiert des conditions de cuisson moins sévères que le bois. La biomasse lignocellulosique est cuite dans une solution aqueuse d'hydroxyde de sodium ou un mélange soude et anthraquinone. Les lignines ainsi extraites ne contiennent pas de soufre, elles sont appelées lignine soude et elles sont récupérées de la phase aqueuse par précipitation acide et séparation liquide/solide. Les lignines soude contiennent moins de cendres et de sucres que les lignosulfonates.

Le procédé organosolv a été développé comme une alternative « verte » aux procédés Kraft et sulfite plus polluants. La cuisson est réalisée à des températures comprises entre 180 et 200°C, avec des solvants organiques en association avec de l'eau et de l'acide pour catalyser la délignification de la biomasse végétale. Plusieurs procédés existent selon la nature du solvant utilisé : le procédé Organocell (méthanol), Alcell (éthanol), Avidel (acides formique et acétique), Acétosolv (acide acétique) et Milox (acide peroxyformique). Les lignines extraites sont très différentes des lignines extraites uniquement en milieu aqueux.

2.4. Les modifications chimiques de la lignine

La lignine contient de nombreux groupes fonctionnels : hydroxyles (aliphatiques et phénoliques), méthoxyles, carbonyles et carboxyles (en minorité pour ces derniers). La richesse de la lignine en groupements fonctionnels variés a favorisé la valorisation de cette dernière dans des applications de haute valeur ajoutée. Ainsi, ces groupements peuvent être modifiés pour améliorer la réactivité chimique de la lignine et sa solubilité dans les solvants organiques et pour réduire la fragilité des polymères dérivés de la lignine. De nombreuses modifications peuvent être réalisées : méthylation, éthérification, amination, halogénation, nitration, sulfonation, estérification, silylation et allylation.

2.5. Les applications lignine

- La lignine est une source potentielle de composés phénoliques pour des applications matériaux renouvelables. Les dérivés de lignine sont largement employés dans de nombreuses applications

comme dans les liants, les adhésifs, les antioxydants, les désinfectants, les résines, les fibres, les médicaments et les protections du bois.

- Les lignines de type amine sont employées comme additifs, émulsifiants, floculants, dispersants, et pour la synthèse de certains polymères synthétiques comme les polyuréthanes, les résines phénoliques et époxy.
- Les panneaux de fibres de haute densité sont fabriqués à partir de lignine Kraft de résineux, de lignine soude de paille de blé et de lignine de paille hydrolysée.
- Les propriétés antioxydantes de la lignine dans les polymères de type polypropylène ont été étudiées avec différentes lignines extraites de plusieurs origines botaniques (addition de 1% de lignine en masse). La conclusion est que la solubilité de la lignine dans le polypropylène est un paramètre clé, plus important que la teneur en groupements phénoliques ou la viscosité intrinsèque de la lignine. La lignine de faible masse molaire et contenant peu de phénol est plus soluble dans la matrice et conduit à de meilleures propriétés antioxydantes.
- Les lignines Kraft et soude activées sont utilisées comme liants et adhésifs pour le bois. Les lignines peuvent être activées par une oxydation au périodate afin d'améliorer leur réactivité. Des chercheurs ont développé des liants 100% renouvelables à partir de lignine avec un alcool polyfurfural et partiellement renouvelable avec un phénol formaldéhyde.
- Les lignines organosolv sont utilisées comme charges dans les encres, vernis, peintures et aussi pour augmenter la viscosité de polyol polyéther et pour améliorer leurs propriétés rhéologiques.
- La lignine peut être source de macromonomères dans la synthèse de résine de type phénol formaldéhyde et, elle peut, après oxypropylation, être employée dans la formulation de polyuréthanes (adhésifs et mousses).

2.6. L'analyse de la lignine

L'analyse de la lignine est cruciale pour le développement de nouvelles applications de haute valeur ajoutée. Les groupements fonctionnels peuvent être analysés par spectroscopie UV, FT-IR, par chromatographie gaz (GC) ou par des techniques de RMN (^{1}H, ^{13}C, ^{19}F, ^{31}P). La caractérisation de la distribution des masses molaires de la lignine est également fondamentale pour mieux comprendre les propriétés de la lignine, que ce soient des propriétés de structure, des propriétés physico-chimiques ou même la réactivité de la lignine. La chromatographie d'exclusion stérique (SEC – aussi appelée GPC pour Gel Permeation Chromatography) est l'outils d'analyse le plus employé pour caractériser la distribution des masses molaires des polymères et en particulier de la lignine. La SEC sépare les macromolécules par taille dans une colonne remplie d'un gel nanoporeux. Les molécules de différentes tailles sont éluées à différents temps de rétention. Le choix du solvant est très important, il doit permettre le gonflement puis la dissolution totale du polymère sans le dégrader. De plus les interactions entre les molécules conduisant souvent à des agrégats dans les colonnes et à des

interactions également avec la phase stationnaire du gel, doivent absolument être évitées. La présence de groupes hydroxyles sur la lignine malheureusement limite sa solubilité dans les solvants de chromatographie non polaires comme le THF et le polystyrène généralement employé comme calibrant est loin de présenter une structure tridimensionnelle aussi complexe que la lignine de sorte que les mesures de masses molaires ne sont pas des valeurs intrinsèques/absolues mais peuvent uniquement être comparées entre différentes lignines. Pour surmonter ces difficultés analytiques, deux méthodologies peuvent être utilisées : 1) l'addition d'électrolytes dans les solvants polaires et 2) la dérivation de la lignine avant sa dissolution dans les solvants non polaires (exemple : acétylation de la lignine). Le travail de thèse présenté a pour objectif de déterminer les masses molaires de différentes lignines en utilisant de nouvelles méthodes de dérivation de la lignine et en appliquant le principe de calibration universelle lors de l'exploitation des analyses SEC.

Avant de présenter les résultats, un bref descriptif des matériels et des méthodes utilisés est donné dans le paragraphe qui suit.

3. CHAPITRE 2 – Matériels et méthodes

3.1. Les composés modèles de lignine

Cinq composés modèles de lignine commerciaux ont été utilisés : la vanilline (CAS: 121-33-5), l'acétovanillone (CAS: 498-02-2), le guaiacol (CAS: 90-05-1), l'alcool vanillique (CAS: 498-00-0) et l'alcool de vératryle (CAS: 93-03-8), ainsi qu'un modèle de cellulose, le cellobiose (CAS: 528-50-7). Ces composés ont été achetés chez Sigma-Aldrich.

3.2. Les échantillons de lignine

Quatre lignines industrielles ont été utilisées : (i) Lignine soude de paille de blé (Protobind 1000) (PB) achetée chez Green Value Enterprises LLC, (ii) Lignine Kraft de pin (KL) fournie par le Centre Technique du Papier (CTP) (Grenoble, France), (iii) Lignine Organosolv (ORG) (BioLignin® CIMV-procédé utilisant un mélange acide formique/ acide acétique/eau à 185-210ºC) issue de paille de blé et achetée chez CIMV Company, et (iv) Lignine Kraft Indulin AT (IND) achetée chez DKSH Switzerland Ltd. Enfin, de la lignine Kraft de feuillus a été obtenue au laboratoire via une cuisson Kraft d'eucalyptus.

3.3. Les produits chimiques utilisés

Dans les réactions de dérivation :

Hydroxyde de tétrabutylammonium (1M dans le méthanol), *noté* ***NBu*** *dans la discussion*, $(CH_3CH_2CH_2CH_2)_4N(OH)$ (CAS: 2052-49-5) et le chlorure de 4-fluorobenzyl, *noté* ***FBC*** *dans la discussion*, $FC_6H_4CH_2Cl$, (CAS: 352-11-4), LiCl (CAS: 7447-41-8), de chez Sigma-Aldrich. Acétonitrile CH_3CN 99,95% (CAS: 75-05-8), acétate d'éthyl *noté* ***EtOA***c *dans la discussion,* $CH_3COOC_2H_5$ 99,5%, (CAS: 141-78-6), sulfate de sodium Na_2SO_4, 99%, (CAS: 7757-82-6) et éther éthylique $(CH_3CH_2)_2O$, 99,5%, (CAS: 60-29-7), méthanol (CAS: 67-56-1), Pyridine (CAS: 110-86-1), anhydride acétique (CAS: 108-24-7) de chez Roth et chlorure de sodium NaCl (CAS: 7647-14-5) et tétrahydrofuran de grade HPLC, *noté* ***THF*** *dans la discussion*, $(CH_2)_4O$ (CAS: 109-99-9) de chez Acros. Toluène (CAS: 108-88-3) de chez Chimie-plus. 4-diméthyl –aminopyridine (1122-58-3) de chez Lancaster et l'acide anhydride 4-fluorobenzoique (CAS: 25569-77-1) de chez Alfa-Aesar. DMAc- de grade HPLC (CAS: 129-19-5) de chez Roth.

Pour la calibration SEC, des polymères standards/étalons sont utilisés : polyméthyl méthacrylates (PMMA: 1520, 6840, 13200, 31380, 73850, 135300, 342700, 525K, 1026K, 2095K) de chez Agilent, polystyrènes (PS: 1670, 4970, 10030, 28400, 64200) de chez Polymer Laboratories Ltd. De l'acétate de cellulose de faible distribution de masse molaire de chez Aldrich est aussi utilisé.

3.4. Les méthodes utilisées

Composition chimique

La composition chimique des lignines est analysée, de même que leur teneur en matière sèche et en cendres (calcination à 525°C pendant 4 heures).

Lavage des lignines avec des solvants

Les lignines sont lavées avec des solvants pour éliminer les impuretés. Une étude sur le lavage des lignines est conduite sur la lignine PB1000. 1g de lignine PB1000 (équivalent masse sèche) est lavée avec environ 60 mL de solvant (éthanol, acétate d'éthyl et hexane) (16.5g/L). Le lavage est réalisé en deux temps : initialement, 30 mL de solvant est versé sur l'échantillon de lignine et le mélange est agité pendant 1 heure environ, suivi par une filtration sous vide à l'aide d'une membrane en PTFE de 0,45µm. La lignine récupérée est de nouveau mélangée à 30 mL de solvant et agitée pendant 24 avant filtration. La lignine filtrée est séchée sous vide à 40°C. A la suite de cette étude, l'acétate d'éthyle a été sélectionné comme étant le solvant le plus intéressant pour laver les lignines à analyser.

Quantification des groupements hydroxyles de la lignine : acétylation

100 mg de lignine (équivalent masse sèche) sont acétylés (Figure 16) avec 5 ml de pyridine en mélange avec de l'anhydride acétique (1/1: V/V) à température ambiante pendant 15 h dans un ballon à fond rond sous agitation continue. Après ce temps de réaction, la réaction est stoppée par ajout de 40

ml d'un mélange méthanol/eau à 50% en volume puis le mélange est séché sous vide. Après évaporation du méthanol, le produit est lavé trois fois avec du toluène (3 x 40ml) pour éliminer les résidus de pyridine, puis à nouveau avec 40 ml de méthanol à 99,5%. Enfin, l'échantillon est lyophilisé pour s'assurer de l'évaporation total des solvants. La lignine acétylée est utilisée pour étudier la réaction d'aminolyse et pour des analyses RMN du ^{13}C quantitatives.

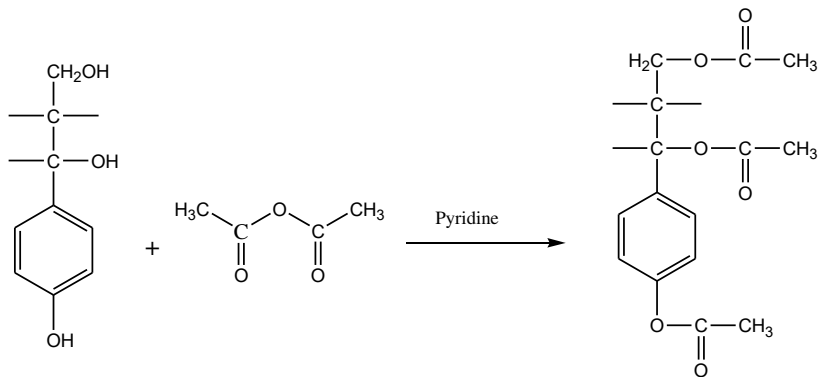

Figure 16. Acétylation de la lignine

Fluorobenzylation des composés modèles

100 mg de composés modèles sont dissous dans 1 mL de NBu (hydroxyde de tétra N-butylammonium dans le méthanol 1M) et mis à agiter pendant 1h à 50°C. Puis 10 mL d'acétonitrile sont ajoutés suivis de 300 mg de chlorure de 4-fluorobenzyl (FBC), l'agent dérivant. La réaction est mise sous agitation pendant une nuit à 50°C. Puis de l'eau distillée (30 mL) et EtOAc (30 mL) sont finalement ajoutés dans le mélange réactionnel. La phase aqueuse est séparée et extraite par un lavage avec EtOAc (2×30mL). La phase dans EtOAc est lavée avec de l'eau distillée (2×30 mL) et une solution saturée de chlorure de sodium (30 mL). La phase extraite avec EtOAc est séchée avec du sulfate de sodium puis filtrée et analysée sans autre purification.

Fluorobenzylation de la lignine

La fluorobenzylation de la lignine est réalisée dans les mêmes conditions expérimentales que celles employées pour la dérivation des composés modèles. La réaction est présentée dans la Figure 17. Puis la lignine dérivée est récupérée par précipitation dans l'éther diéthylique. Cette phase organique forme un précipité visqueux, précipité à nouveau dans des glaçons d'eau distillée. Le précipité est filtré via un filtre PTFE, 0,45 µm, lavé dans l'eau distillée plusieurs fois et séché à 50°C en étuve.

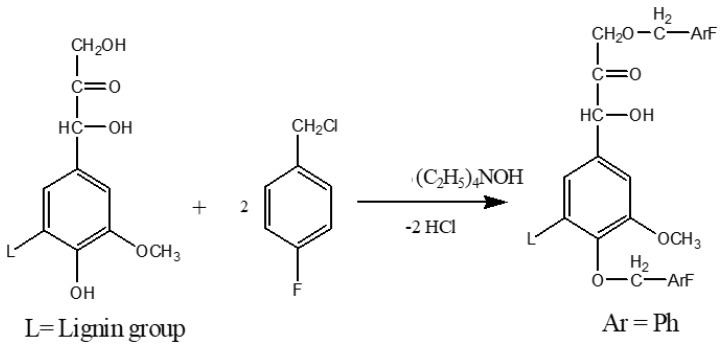

Figure 17. Fluorobenzylation de la lignine

Fluorobenzoylation de la lignine

Les lignines fluorobenzylées (100 mg) sont mises à dissoudre dans 2,5 mL de pyridine. Sont ajoutés progressivement 2,5 mg de 4-diméthyl-aminopyridine (DMAP) et 150 mg d'acide anhydride 4-fluorobenzoique. Le mélange est agité pendant 48 h à 60˚C. Puis les lignines dérivées sont transférées dans de l'eau distillée glacée. Le précipité obtenu est lavé à l'eau distillée plusieurs fois et filtré via un filtre en PTFE de 0,45µm puis séché à 40°C dans une étuve. Il est ensuite analysé par FT-IR, SEC et RMN du ^{19}F. La réaction de fluorobenzylation est présentée dans la Figure 18.

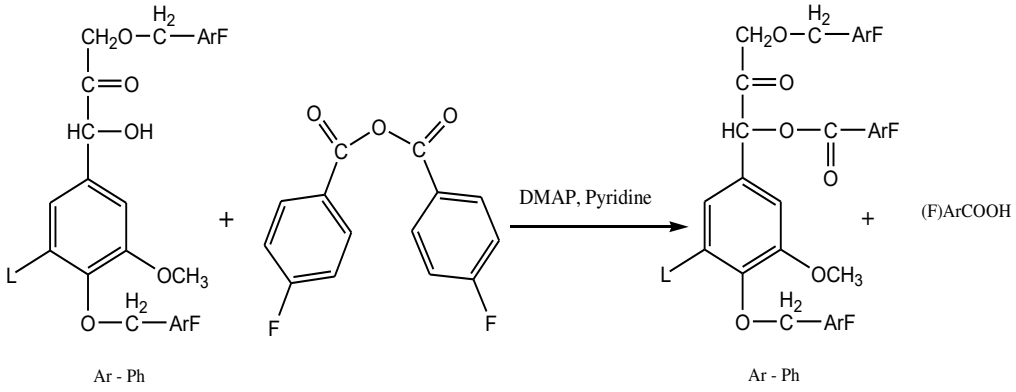

Figure 18. Fluorobenzoylation de la lignine

Quantification des groupes hydroxyles phénoliques de la lignine par spectroscopie UV

Cette méthode est bien connue de la littérature, elle ne sera pas décrite dans ce résumé.

Quantification des groupes hydroxyles phénolique de la lignine par aminolyse et GC

Pour initier la réaction d'aminolyse, 5mL d'un mélange dioxane-pyrrolidine (1/1: v/v) sont ajoutés sur la lignine acétylée à température ambiante. La réaction est donnée dans la Figure 19.

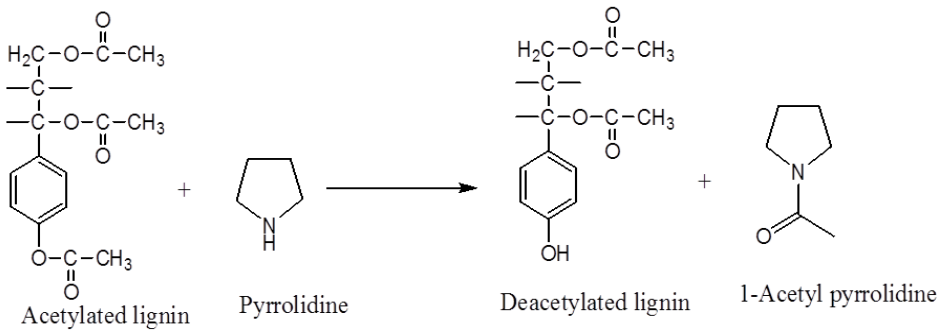

Figure 19. Déacétylation de la lignine par la pyrrolidine (aminolyse)

La vitesse de formation de la 1-acétyl pyrrolidine est suivie dans le temps (après 5, 10, 20, jusqu'à 60 minutes) par injection de 0,5 µL du mélange réactionnel dans une chromatographie gazeuse. La formation de la 1-acétyl pyrrolidine est équivalente à la quantité de OH phénoliques présents sur la lignine. La quantité formée est calculée ainsi :

$$\text{Formation de l'acétylpyrrolidine } (mmol/g \text{ lignine}) = \frac{A \times W_s \times 1000}{A_s \times W_L \times k \times 113}$$

avec, A = surface du signal de chromatographie attribué à la 1-acétyl pyrrolidine, As = surface du signal de chromatographie attribué à l'étalon interne, W_L = masse de lignine (matière sèche), W_S = masse de l'étalon interne (1-méthyl naphthalène) et k = constante de calibration (obtenue par la courbe de calibration).

Analyse de la distribution des masses molaires de la lignine par chromatographie d'exclusion stérique (SEC)

L'analyse SEC est indispensable pour estimer la masse molaire d'une lignine à valoriser. La grande variété des groupes fonctionnels de la lignine augmente sa polarité ce qui la rend difficilement soluble dans les solvants de chromatographie. Deux systèmes sont utilisés.

Système DMAc/LiCl

L'analyse SEC dans le DMAc est réalisée sur une ligne chromatographique OMNISEC équipée de 2 colonnes polargel M (30 cm x 7 mm) et d'une pré-colonne (de chez Agilent). Un mélange à 0,5% de LiCl dans le DMAc (5g de LiCl dessous dans 1 L de DMAc) est utilisé comme éluant à un débit de 1 mL/min dans les colonnes chauffées à 70°C. Un réfractomètre (RI) est utilisé pour la détection. 100 µL de composés à analyser (lignine ou polymères calibrants) sont injectés à une concentration de 2 mg dans 1mL de DMAc/LiCl à 0,5%. Les solutions sont obtenues ainsi : 20 mg de lignine non dérivée sont dissous dans 10 mL de DMAc/LiCl à 0,5% pendant 3 semaines sous agitation continue. Dans le cas des lignines dérivées, 10 mg de lignine sont dissous dans 5 mL de DMAc/LiCl à 0,5% pendant 5

jours sous agitation continue. Toutes les lignines sont ensuite filtrées (0,45 µm filtre seringue en PTFE) avant analyse.

Système THF

L'analyse SEC dans le THF est réalisée sur une ligne chromatographique Malvern TDA 302 équipée de 3 colonnes 300×7,5mm Agilent PLGel mixed B (10 µm mixed B LS) et une pré-colonne. Une triple détection RALS-LALS avec un viscosimètre en ligne à 35°C est utilisée. Pour la calibration des colonnes, des solutions de polymères standards sont préparées (0,4 mg/L à 1,6 mg/mL dans le THF). La lignine à analyser est dissoute à 10 mg/mL dans le THF pendant 1 heure. 100µL de solution (lignine ou polymère standard) sont injectés dans le système SEC à un débit de 1 mL/min. La solution est filtrée sur un filtre seringue en PTFE de 0,45 µm. Une calibration universelle est réalisée avec des polymères standards de polystyrène (PS), de polyméthylméthacrylate (PMMA) et d'acétate de cellulose.

Une calibration universelle est réalisée selon le concept de Mark-Houwink. Il affirme que les polymères sont élués selon leur volume hydrodynamique V_h, qui détermine alors le volume d'élution.

Relation de Mark- Houwink

$$[\eta] = K'M^a$$

$[\eta]$, viscosité intrinsèque du polymère en dL/g

K' et *a* sont les constantes de Mark-Houwink, elles dépendent du couple polymère/solvant

M est la masse molaire du polymère en g/mol

Sur la base de l'équation précédente, les échantillons de même $[\eta]$ et même masse molaire (M) possèdent des volumes hydrodynamiques identiques. Ainsi les échantillons sont élués au même temps de rétention. Les résultats obtenus sont utilisés pour construire une courbe de calibration universelle en traçant log ([η].M) en fonction du temps de rétention.

4. CHAPITRE 3 – Quantification des groups phénoliques de la lignine par aminolyse et comparaison avec d'autres méthodes éprouvées

La quantification des hydroxyles phénoliques peut être réalisées avec différentes méthodes, directement sur la lignine ou après dérivation de celle-ci. Ce chapitre propose d'étudier la méthode d'aminolyse : les hydroxyles de la lignine sont acétylés puis une aminolyse est réalisée. Elle est suivie par analyse GC.

4.1. Aminolyse suivie par GC

La réaction d'aminolyse est donnée dans la Figure 5. La quantité d'hydroxyles phénoliques est déduite de la formation et de la quantification de la 1-acétylpyrrolidine par GC. Pendant l'aminolyse, la vitesse de déacétylation des groupes hydroxyles phénoliques est significativement plus rapide que celle des hydroxyles aliphatiques. Ainsi, la formation d'acétyl-pyrrolidine correspond à la quantité de groupes acétyles aromatiques initialement présents sur la lignine. Attention il est aussi possible que certains groupements acétyles aliphatiques subissent la réaction de déacétylation aux temps de réaction prolongés, ce qui conduit à une surestimation de la teneur en groupements hydroxyles.

Pendant l'aminolyse, les échantillons sont collectés au cours du temps et analysés par GC. Au temps zéro, la formation d'acétyl pyrrolidine est nulle. Au cours du temps, la quantité d'acétyl pyrrolidine augmente. La Figure 20 présente l'évolution de la formation d'acétyl pyrrolidine au cours du temps pour les différents échantillons de lignine étudiés. Il apparait clairement que pendant les 5 premières minutes de réaction, la formation d'acétyl pyrrolidine augmente rapidement puis plus progressivement jusqu'à 20 minutes et au-delà de 20 minutes, elle se stabilise. La lignine Kraft présente une formation en acétyl pyrrolidine supérieure à celles des lignines PB, Indulin et ORG. La plupart des lignines, après 20 min commence à présenter un plateau qui montre que les acétyles phénoliques ont été déacétylés par la réaction d'aminolyse. La teneur en 1-acétyl pyrrolidine formée est calculée en extrapolant la région linéaire entre 20 et 60 minutes au temps zéro. La valeur correspondante est directement proportionnelle à la teneur en hydroxyles phénoliques présents dans les lignines étudiées.

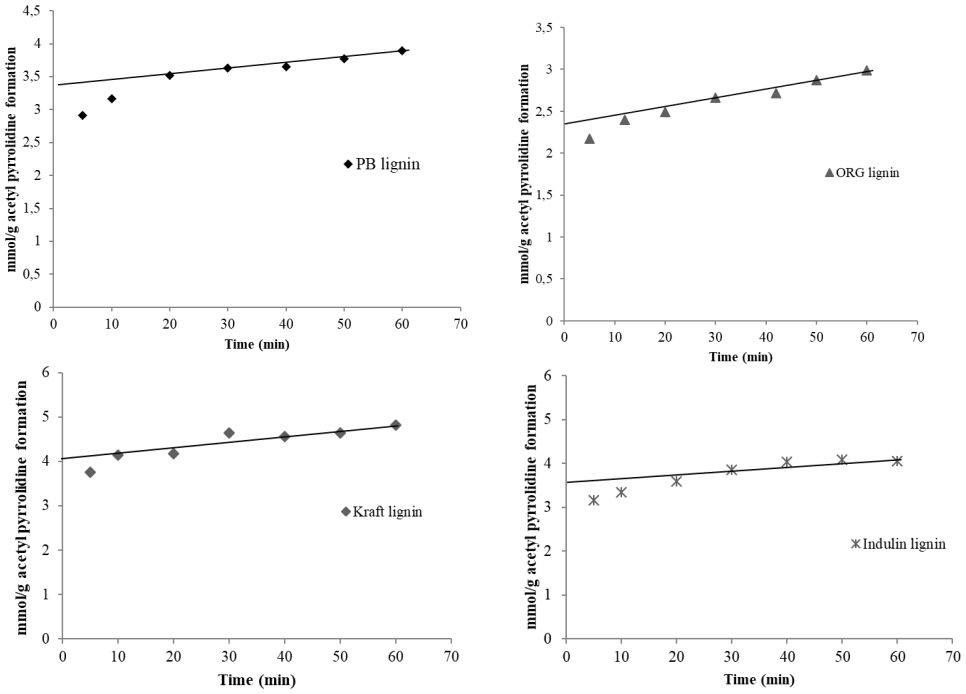

Figure 20. Aminolyse des lignines acétylées, PB-lignine, ORG lignine, Kraft lignine et Indulin lignine

Les teneurs en hydroxyles phénoliques dans les lignines sont comparées dans le Tableau 15. Les réactions ont été répétées trois fois et les écarts type sont présentés.

Tableau 15. Comparaison des teneurs en hydroxyles phénoliques des lignines analysées par la méthode d'aminolyse

Type de lignine	Hydroxyles phénoliques mmol/g lignine
PB - Protobind 1000 lignine	3,4 ± 0,18
ORG - Organosolv lignine	2,4 ± 0,12
KF - Kraft lignine	4,0 ± 0,07
IND – Indulin lignine	3,6 ± 0,05

Parmi les lignines étudiées, la lignin Kraft est celle qui contient la plus grande quantité d'hydroxyles phénoliques, environ 4,0 mmol/g, suivi des lignines Indulin (3,6 mmol/g) et PB (3,4 mmol/g). La lignine Organosolv présente les plus faibles teneurs, i.e. 2,4 mmol/g. Il faut souligner que les lignines de résineux (Kraft et Indulin) sont connues pour contenir davantage de groupements hydroxyles phénoliques que celles issues de plantes annuelles (PB et ORG). Les résultats obtenus par aminolyse sont donc logiques.

4.2. Comparaison entre l'aminolyse et d'autres méthodes analytiques

Les résultats de l'aminolyse sont comparés à ceux issus d'autres techniques analytiques éprouvées comme les spectroscopies FT-IR, UV, RMN ou des méthodes de titration. Les résultats sont présentés dans le Tableau 4.

Tableau 16. Quantification des hydroxyles phénoliques (mmol/g) – comparaison entre l'aminolyse et d'autres méthodes analytiques.

Méthode	Lignine			
	PB-Protobind	ORG-Organosolv	KF-Kraft	IND-Indulin
Aminolyse	**3,4 ± 0,18**	**2,4 ± 0,12**	**4,0 ± 0,07**	**3,6 ± 0,10**
UV	2,6 ± 0,02	1,7 ± 0,01	2,8 ± 0,01	3,4 ± 0,01
^{1}H-RMN	1,8 ± 0,13	0,9 ± 0,07	2,7 ± 0,04	3,1 ± 0,23
^{13}C-RMN	2,4 ± 0,04	2,0 ± 0,03	4,2 ± 0,06	3,6 ± 0,05
^{31}P-RMN	2,7 ± 0,1	1,3 ± 0,06	3,2 ± 0,16	3,2 ± 0,10
Titration rapide	2,4 ± 0,03	1,5 ± 0,03	2,4 ± 0,03	2,7 ± 0,05

Les différentes méthodes conduisent à des teneurs variables en hydroxyles phénoliques (en mmol/g) : 2,4 (ORG) à 4,0 (KF) (aminolyse), 1,7 (ORG) à 3,4 (IND) (UV), 0,9 (ORG) à 3,1 (IND) (^{1}H RMN), 2,0 (ORG) à 4,2 (KF) (^{13}C RMN), 1,3 (ORG) à 3,2 (KF et IND) (^{31}P RMN) et 1,5 (ORG) à 2,7 (IND) (titration rapide). A noter que toutes les méthodes analytiques révèlent que la lignine Organosolv contient la plus faible teneur en hydroxyles phénoliques et que les lignines de résineux Indulin et Kraft au contraire présentent les teneurs les plus importantes. Globalement l'aminolyse prédit des teneurs en hydroxyles phénoliques légèrement plus élevées que les autres méthodes et la RMN ^{1}H conduit aux estimations les plus faibles.

La méthode rapide de titration acido-basique en milieu aqueux, mise au point récemment au LGP2, est intéressante car elle renseigne sur la teneur en carboxyles des lignines. Le Tableau 17 présente les teneurs en carboxyles obtenues via différentes méthodes analytiques comme la méthode rapide, une titration potentiométrique en milieu non aqueux par l'hydroxyde de tétra-n-butylammonium - TnBAH et la RMN du ^{31}P.

Tableau 17. Comparaison des différentes méthodes de quantification des groupes carboxyles de la lignine (mmol/g)

Méthode	Lignine			
	PB-Protobind	ORG-Organosolv	KF-Kraft	IND-Indulin
Titration rapide	1,6 ± 0,02	2,3 ± 0,05	1,2 ± 0,04	1,4 ± 0,02
TnBAH	1,6 ± 0,04	1,3 ± 0,01	1,2 ± 0,03	1,1 ± 0,01
^{31}P RMN	1,4 ± 0,07	1,1 ± 0,05	0,9 ± 0,04	0,9 ± 0,04

Les plus faibles teneurs en carboxyles sont issues de l'analyse RMN ^{31}P alors que les deux autres méthodes conduisent à des valeurs similaires sauf dans le cas de la lignine Organosolv. De plus, les teneurs en carboxyles des toutes les lignines sont inférieures aux teneurs en hydroxyles phénoliques, encore une fois excepté pour la lignine Organosolv. Une teneur en carboxyles plus élevée qu'en hydroxyles phénoliques dans la lignine Organosolv est possible car le procédé utilise des conditions très oxydantes.

Les principales conclusions de ce chapitre sont les suivantes :

1. La méthode d'aminolyse révèle que la lignine Kraft contient une teneur en hydroxyles phénoliques supérieure à celle de la lignine Indulin suivie par la lignine Protobind et enfin Organosolv.

2. Les résultats de l'aminolyse sont comparables à ceux de la RMN ^{13}C. Ceci est logique car les deux méthodes utilisent de la lignine acétylée pour l'analyse.
3. La RMN du ^{1}H, la spectroscopie UV et la méthode rapide sous-estiment la teneur en groupements hydroxyles phénoliques : à cause notamment de recouvrements de signaux dans le cas de la RMN du ^{1}H ; à cause de la présence d'unités lignine présentant plus d'un groupement phénol dans le cas de la méthode UV, et enfin en ce qui concerne la méthode rapide, de grandes quantités de lignine sont nécessaires pour l'analyse et les résultats donnent accès à une teneur globale d'hydroxyles sans information sur leur structure.
4. Enfin, l'aminolyse classique présente aussi des inconvénients comme une dérivation des hydroxyles phénoliques incomplète et une surestimation de ces groupements due à la présence d'impuretés de type sucres dans les lignines.

5. CHAPITRE 4 – Etude de la réactivité de composés modèles de lignine lors de la fluorobenzylation par analyses RMN ^{13}C et ^{19}F : Application à la quantification des hydroxyles phénoliques de la lignine par RMN du ^{19}F

Il y a une vingtaine d'année, Barrelle et al. ont développé une méthode analytique utilisant la spectroscopie RMN du ^{19}F après dérivation de la lignine par des composés fluorés afin de quantifier les groupes hydroxyles aliphatiques et phénoliques et les groupes carbonyles. La fluorobenzylation est utilisée pour quantifier les hydroxyles phénoliques et les hydroxyles aliphatiques primaires, la fluorobenzoylation pour quantifier les hydroxyles aliphatiques secondaires, alors que la dérivation par la trifluorométhylphénylhydrazine permet la quantification des carbonyles. Ainsi le travail présent est un complément des études de Barelle et a pour objectif de montrer que l'analyse de la lignine par RMN du ^{19}F est une méthode robuste pour la quantification des hydroxyles phénoliques.

5.1. Dérivation de composés modèles par fluorobenzylation

Cinq composés modèles de lignine (Figure 21) ont été sélectionnés selon la nature des hydroxyles liés aux différents sites de l'unité phényl-propane, comme les hydroxyles aromatiques ou aliphatiques. Les lignines étant souvent contaminées par des sucres, contenant eux même des hydroxyles, un composé modèle de cellulose a aussi été sélectionné. Tous les composés modèles sont dérivés par fluorobenzylation et les produits sont analysés par spectroscopie RMN ^{13}C and ^{19}F.

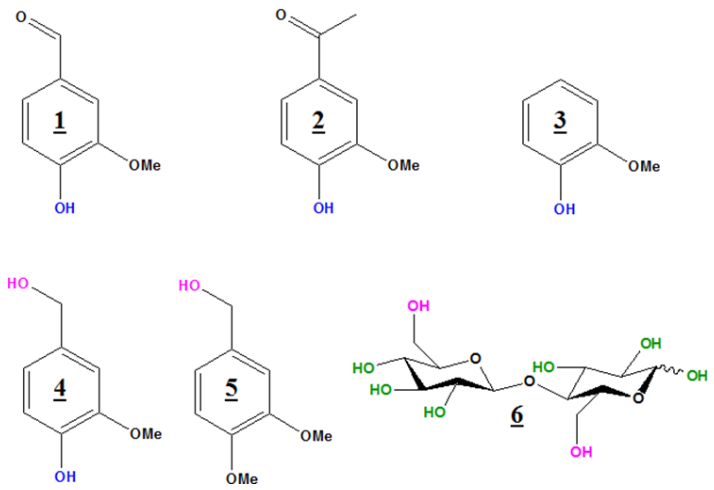

Figure 21. Composés modèles étudiés : Vanilline (1), Acétovanillone (2), Guaiacol (3), Alcool vanillique (4), Alcool de vératryle (5) et D(+) Cellobiose(6)

La Figure 22 présente la réaction de fluorobenzylation des groupes hydroxyles de la lignine et leur conversion en dérivés fluorobenzylés. Les groupes hydroxyles aliphatiques et aromatiques sont supposés être dérivés.

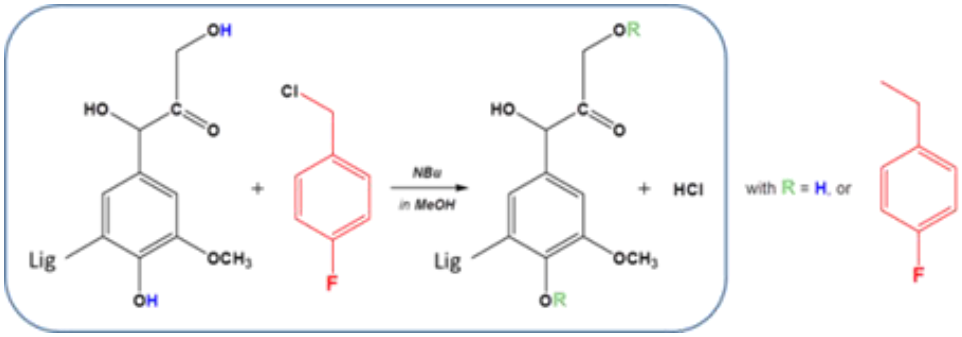

Figure 22. Réaction de fluorobenzylation de la lignine (Cl-R-F: chlorure de 4-fluorobenzyl, Lig=Lignine)

Les déplacements chimiques et la structure hyperfine due aux couplages $^{n}J_{CF}$ sont utilisés pour déterminer la présence ou non de structures aromatiques fluorées (originaires du FBC). Une séquence complémentaire DEPT permet de distinguer les carbones de type $\underline{C}H_2$ (présents dans différents environnements) (Figure 23), et l'examen des déplacements chimiques permet aussi d'analyser la présence ou non de dérivés fluorés.

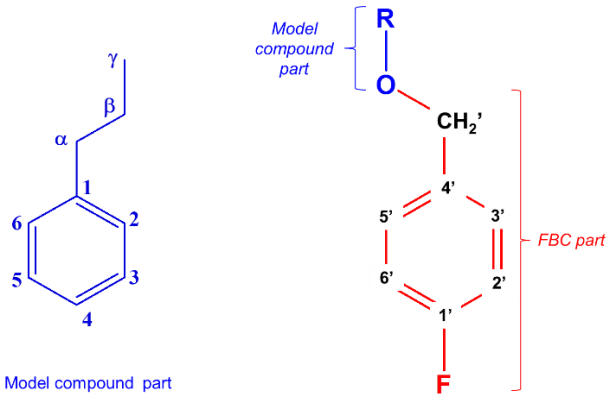

Figure 23. Structure et numérotation des C des composés modèles de lignine et des modèles dérivés

Le Table 4.1 présente l'attribution des déplacements chimiques en RMN ^{13}C des groupes de type méthylène localisés entre le FBC et le composé modèle (Figure 23), pour différents produits récupérés après la dérivation des composés modèles.

Tableau 18. Attribution des déplacements chimiques des $\underline{C}H_2$' en RMN ^{13}C.

δc (en ppm)	45,3	57,54	62-63	69-71	72,81
Groupe méthylène	**-$\underline{C}H_2$Cl**	**-$\underline{C}H_2$N**	**-$\underline{C}H_2$OH**	**-$\underline{C}H_2$OR**	**-$\underline{C}H_2$OMe**
Composé	FBC	NBu	OH FBOH [(a)] Aliphatique	F-composé dérivé	FBOMe [(b)]

(a) FBOH : Produit résultant de la réaction de FBC avec l'eau.
(b) FBOMe : Produisant resultant de la réaction de FBC avec MeOH (solvant de NBu)

Les groupes méthylène du FBC, (**$\underline{C}H_2$Cl**), et ceux de N-Bu (**$\underline{C}H_2$N**) sont détectés à 45,3 ppm et 57,54 ppm respectivement grâce à de la nature de l'hétéroatome (Cl ou N). Le réactif FBC peut réagir avec l'eau (qui provient de l'humidité des réactifs) et/ou avec le méthanol (présent dans le réactif N-Bu) pour former FBOH et/ou FBOMe. Les signaux correspondants apparaissent dans la région de 62-63 ppm et 72,81 ppm respectivement. Enfin les signaux **$\underline{C}H_2$OR** attribués aux composés modèles sont dans la région de 69-71 ppm.

Le rendement de fluorobenzylation est calculé à partir de la quantification de chaque composé présent après réaction de dérivation (Table 5.1) : le composé modèle fluoré (F-modèle) mais aussi le composé modèle initial (qui n'a pas réagi), le FBC restant et les deux sous-produits FBOH et FBOMe. En considérant que la composition totale est égale à 100%, le rendement de dérivation est calculé comme la quantité de F-model divisé par la somme des quantités de F-modèle et du modèle n'ayant pas réagi (en %). L'attribution des déplacements chimiques en RMN du ^{13}C des dérivés fluorés est donnée dans le Table 4.3 .

Tableau 19. Quantités de produits obtenus après fluorobenzylation des composés modèles, calculées à partir des donnée RMN du ^{13}C (analyse de la partie organique)

Composé	Fluorobenzylation	Composition du mélange					
	rendement, %	**Modèle restant %**	**F-Modèle %**	**FBC %**	**FBOH %**	**FBOMe %**	**NBu %**
1	100	-	93,6	6,4	-	-	-
2	100	-	81,3	5,2	-	8,3	5,2
3	100	-	67,6	24,5	-	4,1	3,8
4	100	-	34,0	53,9	Traces	10,1	-
5	9	71,5	7,1	-	Traces	-	21,4
6	-	-	-	-	74,0	-	26
FBC blanc		94,1	-	-	5,9	-	-
FBC réagi		-	-	-	7,9	-	92,1

Tableau 20. Déplacements chimiques RMN ^{13}C (en ppm) des composés modèles fluorobenzylés (C numérotés selon la Figure 23)

Composés		1	2	3	4	5
Partie composés modèles	**C1**	129,8	130,14	120,59	135,75	130,61
	C2	109,9	110,4	112,22	110,76	110,51
	C3	149,4	151,88	149,23	149,05	148,65
	C4	153	148,79	147,66	146,38	148,30
	C5	112,6	112,27	113,88	113,66	111,51
	C6	125,8	122,92	121,25	118,45	120,04
	OCH_3	55,53	55,51	55,44	55,39	55,38 55,46
	C=O	-	196,2	-	-	-
	HC=O	191,34	-	-	-	-
	CH_2 (α)	-	-	-	62,76	71,36
	CH_3	-	26,31	-	-	-
Partie FBC	**C'H_2**	69,28	69,15	69,15	69,33	70,33
	C'4	132,5	132,74	133,44	133,54	134,71
	$^4J_{CF}$ (Hz)			*2,84*		
	C'3,C'5	130,2	130,14	129,92	129,85	129,57
	$^3J_{CF}$ (Hz)			*9,2*		
	C'2,C'6	115,3	115,29	115,15	115,15	115,40
	$^2J_{CF}$ (Hz)			*21,45*		
	C'1	161,98	161,88	161,7	161,72	161,56
	$^1J_{CF}$ (Hz)			*243*		

Le Table 5.1 montre que les composés modèles de lignine **1**, **2**, **3**, contenant uniquement des hydroxyles phénoliques, et **4**, contenant à la fois des hydroxyles phénoliques et aliphatiques, réagissent totalement. Le rendement de dérivation des modèles **1**, **2** et **3** est de 100%. Par ailleurs pour le modèle **4**, le signal restant à 62,76 ppm correspondant au carbone de type méthylène –**C**H_2OH, lié de façon covalente à un groupe hydroxyle aliphatique ; et l'absence du signal à 71 ppm correspondant au carbone –**C**H_2OR du dérivé fluoré aliphatique montre que la conversion est due uniquement aux groupes hydroxyles phénoliques ; les hydroxyles aliphatiques sont peu réactifs.

L'alcool de vératryle modèle **5**, avec un hydroxyle aliphatique et aucun hydroxyle phénolique est très peu converti (9%). Le principal produit de réaction est le composé modèle initial bien que le FBC, l'agent dérivant, soit totalement consommé. Tous ces résultats suggèrent que les hydroxyles phénoliques sont facilement dérivés alors que la fluorobenzylation des hydroxyles aliphatiques est lente et seulement partielle.

Comme les lignines commerciales sont généralement contaminées par des sucres et que ces sucres contiennent des fonctions hydroxyles, un modèle de sucre, le D(+) cellobiose (**6**) est aussi étudié. Après fluorobenzylation, l'analyse de la phase organique de la réaction ne présente aucun signal correspondant à un produit fluoré ni même au produit de départ (Table 4.2). Les sucres étant solubles dans l'eau, la phase aqueuse est aussi analysée. Dans ce cas, aucun dérivé n'a été détecté, le seul produit identifié est le sucre initial non modifié et le réactif NBu. Ainsi les hydroxyles des sucres ne sont pas fluorobenzylés. La contamination en sucres des lignines ne devrait pas interférer avec l'analyse des lignines dérivées par RMN du ^{19}F.

Le mélange réactionnel obtenu après fluorobenzylation des composés modèles et contenant un mélange de différents produits est aussi analysé par RMN du ^{19}F. Etant donné que seuls les composés fluorés sont détectés en RMN du ^{19}F aucun signal correspondant au produit de départ ou au NBu ne peut être enregistré. Ainsi, les compositions du mélange, exprimées en %, issues des analyses RMN du ^{13}C et RMN du ^{19}F NMR sont différentes. Les résultats de RMN du ^{19}F sont présentés dans les Table 4.6 et Table 4. 7.

Tableau 21. Taux de conversion et quantités de produits obtenus après fluorobenzylation des composés modèles, calculés à partir des donnée RMN du ^{19}F

Composés	F-**Composé** *Conversion Rate, %*	**Composition du mélange**			
		F-composé dérivé, %	**FBC** récatif, %	**FBOH**, %	**FBOMe**, %
1	**100**	94,5	5,5	-	-
2	**100**	86,3	6,3	-	7,4
3	**100**	72,3	23,3	-	4,4
4	**98**	38,8	55,9	1,1	10,2
5	**16**	89,7	-	10,3	-
6	**0**	-	-	100	-
FBC	**-**	99,9	-	0,1	-
FBC reacted	**-**	-	-	100	-

Tableau 22. Déplacements chimiques en RMN du^{19}F (en ppm) des composés modèles fluorobenzylés

Composés	δ_F **(ppm)**	**Nature**
1	**-116,36**	**Φ**-OH + Aldehyde (α)
2	**-116,49**	**Φ**-OH + cétone (α)
3	**-116,89**	**Φ**-OH
4	**-116,99**	**Φ**-OH
5	**-117,50**	**CH_2**OH
6	**-**	**CH_2**OH
MeOH	**-117,49**	**CH_3**OH
FBC (blanc)	**-115,85**	**CH_2**Cl
FBOH	**-118,7**	**CH_2**OH

A partir des résultats RMN du ^{19}F, on observe que les groupes hydroxyles phénoliques des composés **1**, **2**, **3** sont quantitativement fluorobenzylés et ils donnent des signaux à -116,36 ppm, -116,49 ppm et -116,89 ppm respectivement. En ce qui concerne le modèle **4**, contenant à la fois des OH aliphatiques et phénoliques, la RMN du ^{19}F confirme que la conversion a lieu uniquement dans la région des phénols (-116,99 ppm) puisqu'aucun signal n'est détecté dans la région des aliphatiques. Le taux de conversion de 98% provient de la dérivation des hydroxyles phénoliques uniquement. La phase aqueuse a été aussi analysée mais aucun signal de ^{19}F n'a pu être détecté ce qui confirme que seuls les phénols peuvent être dérivés dans les conditions étudiées.

5.2. Analyse des hydroxyles phénoliques d'une lignine par RMN ^{19}F

Suite à ces analyses sur composés modèles, des lignines industrielles sont analysées par RMN du ^{19}F. En particulier la lignine organosolv (ORG) de la compagnie CIMV Corporation (France) est étudiée

par RMN du ^{19}F après fluorobenzylation. Le spectre de RMN du ^{19}F est donné dans la Figure 24. L'attribution des signaux est réalisée sur la base des déplacements chimiques déterminés pour les composés modèles. Le signal le plus fin à -118,7 ppm est attribué à FBOH, produit de réaction de l'agent dérivant FBC avec des traces d'eau. Comme vu précédemment, le signal entre -117,3 et -118,5 ppm est associé aux hydroxyles aliphatiques de la lignine. Les hydroxyles aromatiques sortent quant à eux entre -115 et -117,3 ppm et la partie du signal entre -116,2 et -116,5 ppm est attribuée à l'existence de composés contenant un groupe α C=O, alors que le signal à -115,8 ppm est dû au réactif FBC.

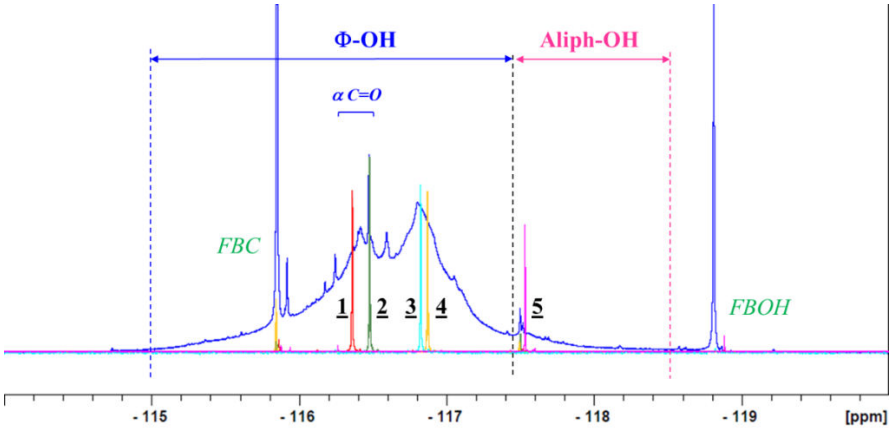

Figure 24. Comparaison des spectres RMN du ^{19}F de la lignine ORG fluorobenzylée (en bleu) et des composés modèles de lignine dérivés (*Note : Seuls les phénols sont dérivés dans le composés modèles* ***4***)

L'analyse conduit aux résultats suivants : 1,71 mmole d'hydroxyles phénoliques et 0,120 mmole d'hydroxyles aliphatiques par g de lignine ORG.

5.3. Amélioration de la solubilité de la lignine par fluorobenzylation

La fluorobenzylation est une réaction intéressante car elle améliore aussi la solubilité de la lignine dans les solvants de chromatographie SEC pour la détermination de sa distribution des masses molaires. La solubilité dans le THF a été étudiée sur la lignine ORG fluorobenzylée par spectroscopies UV-visible et comparée avec celle de la lignine non dérivée ou acétylée. Ces trois lignines ont été solubilisées dans les mêmes conditions, à même concentration dans le THF et analysées par spectroscopie UV à 280nm, dans la région où la lignine absorbe la lumière (Figure 4.10).

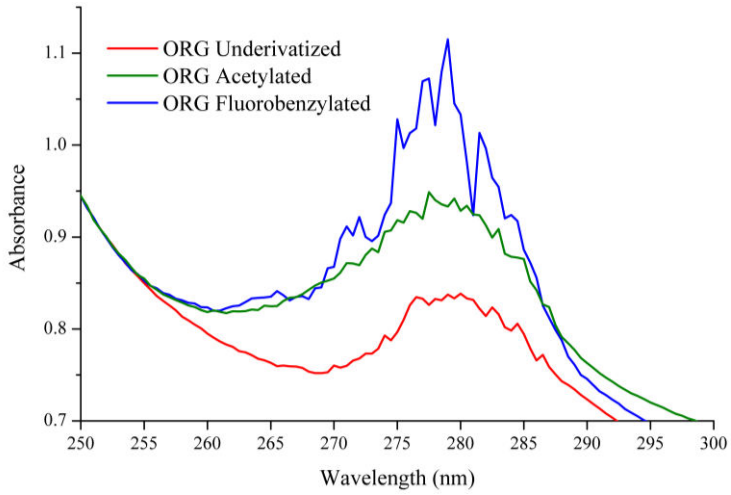

Figure 25. Spectres d'absorbance UV des lignines ORG fluorobenzylée, acétylée et non dérivée dans le THF

La comparaison des spectres montre clairement que la lignine fluorobenzylée présente l'absorbance la plus importante. La fluorobenzylation augmente notablement la solubilité de la lignine dans le THF, davantage que l'acétylation, ce qui est très intéressant pour les analyses SEC.

6. CHAPITRE 5 – Méthode de calibration universelle pour l'analyse de la lignine par chromatographie d'exclusion stérique – utilisation d'une nouvelle méthode de dérivation

L'analyse de la distribution des masses molaires (MMD) est cruciale pour comprendre la réactivité et les propriétés physico-chimiques de la lignine. Bien que cette analyse existe déjà, il existe de nombreux doutes sur la masse molaire de la lignine liés à la méthode choisie.

Le chapitre 5 est dédié à l'analyse des lignines par chromatographie d'exclusion stérique (SEC) dans des solvants organiques (DMAc/LiCl et THF). Toutes les lignines commerciales sont dérivées (acétylation, fluorobenzylation et fluorobenzoylation). La masse molaire des lignines dérivées et non dérivées est ensuite calculée en utilisant une calibration standard dans le cas des analyses réalisées dans le DMAc/LiCl ; et une calibration universelle dans le THF pour les lignines dérivées.

6.1. Conditions d'analyse SEC

Le Table 5.1 présente les conditions d'analyse SEC utilisant différentes colonnes et différents systèmes organiques DMAc/LiCl et THF.

Tableau 23. Conditions d'analyse SEC utilisées pour l'analyse de la lignine, systèmes DMAc/LiCl et THF

	DMAc/LiCl	**THF**
Système	OMNISEC	Malvern TDA 302
Colonne	2 polargel M (30 cm x 7 mm) + 1 Pré-colonne	3 (300 cm x 7,5 mm) Agilent PLGel mixed B (10 µm mixed B LS) + 1 pré-colonne
Eluant	0,5% de DMAc/LiCl (5g de LiCl dissous dans 1L de DMAc)	THF (grade HPLC)
Débit	1 mL/min	1 mL/min
Température de colonne	70°C	35°C
Détecteur	RI (Réfractomètre)	RI, RALS-LALS et détecteur viscosimétrique en ligne
Calibrants	Polystyrène (PS) 1660, 10050, 65500,426600	PS : 1670, 4970, 10030, 28400, 64200 Polyméthylméthacrylate (PMMA) : 1520, 6840, 13200, 31380, 73850, 135300, 342700, 525K, 1026K, 2095K Acétate de cellulose (CA) – polymère standard polydispersé
Volume d'injection	100 µL de lignine ou de calibrant	100 µL de lignine ou de calibrant
Concentration en lignine	2mg/mL	10 mg/mL
Dérivation	Acétylation, Fluorobenzylation, Fluorobenzoylation	Acétylation, Fluorobenzylation, Fluorobenzoylation

6.2. Courbes de calibration SEC

Système SEC-DMAC/LiCl – calibration conventionnelle

Généralement, la distribution des masses molaires est réalisée par calibration conventionnelle en utilisant des polystyrènes (PS) de différentes masses molaires comme calibrants. Le logarithme de chaque masse molaire est tracé en fonction du volume de rétention. La courbe de calibration est donnée dans la Figure 5.2.

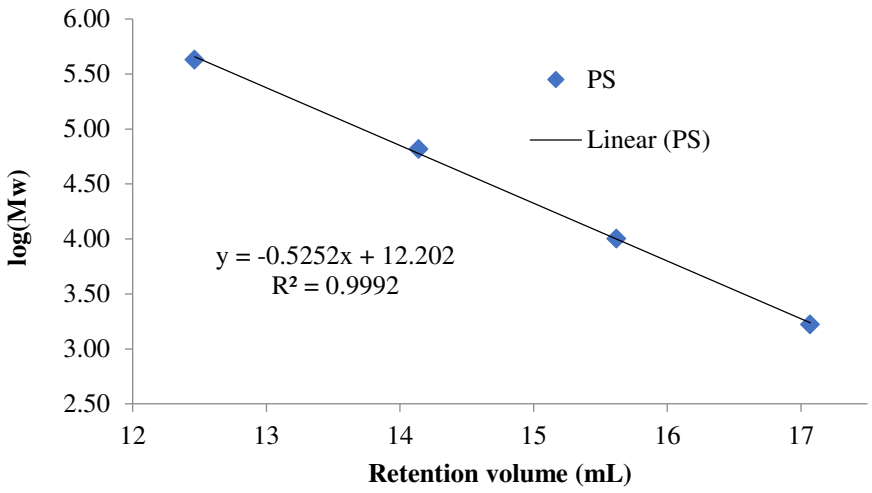

Figure 26. Courbe de calibration avec des PS pour le système DMAc/LiCl

Système THF – calibration conventionnelle

Pour le système THF, trois polymères standards ont été sélectionnés en fonction de leur structure moléculaire. Des polymères monodisperses et polydisperses ont été choisis : PS (polystyrène), PMMA (polyméthylméthacrylate) et l'acétate de cellulose, tous de masse molaire (Mw) connue. Puis log (Mw) est tracé en fonction du volume de rétention des différents polymères en utilisant une détection RI (Figure 5.3). On observe clairement que cette méthode de calibration conventionnelle ne donne pas de courbe unique pour les 3 classes de polymères (Figure 5.3) car les valeurs de log (Mw) ne sont pas alignées. Ainsi les valeurs de Mw calculées pour un échantillon de lignine seront différentes selon le calibrant choisi.

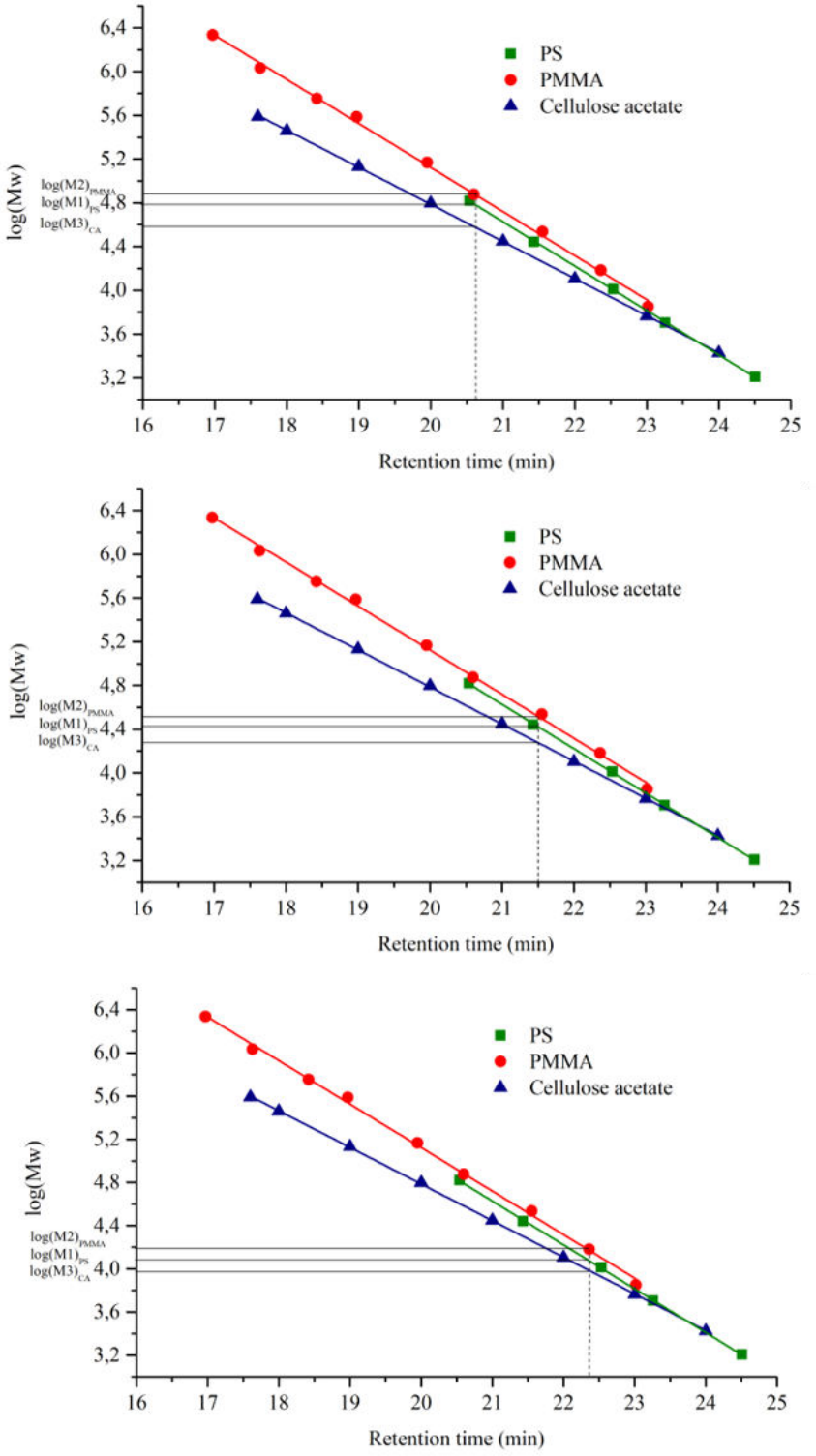

Figure 27. Courbe de calibration conventionnelle réalisée avec du PS, PMMA et de l'acétate de cellulose. Différents temps de rétention sont choisis pour calculer et comparer les log (Mw) correspondant aux différentes courbes de calibration.

Système THF – calibration universelle

Une courbe de calibration universelle a été construire en utilisant le concept de Mark-Houwink qui stipule que les polymères sont élués sur la base de leur volume hydrodynamique V_h, qui détermine à son tour le volume d'élution (voir chapitre 1).

Les résultats obtenus sont utilisés pour construire une courbe de calibration universelle en traçant, à partir des différents polymères calibrants sélectionnés, log ([η].M) en fonction du temps de rétention. Le principal avantage de cette méthode est que la masse molaire d'un polymère inconnu peut être calculée à partir de la mesure de sa viscosité intrinsèque et du volume de rétention, reportés sur la courbe de calibration universelle, ce qui conduit à la masse molaire absolue (ou intrinsèque) du polymère.

Les différentes courbes de calibration réalisées avec les 3 polymères standards, PS, PMMA et acétate de cellulose se superposent parfaitement, validant le concept de Mark-Houwink (Figure 5.4). Ainsi, on obtient une calibration universelle.

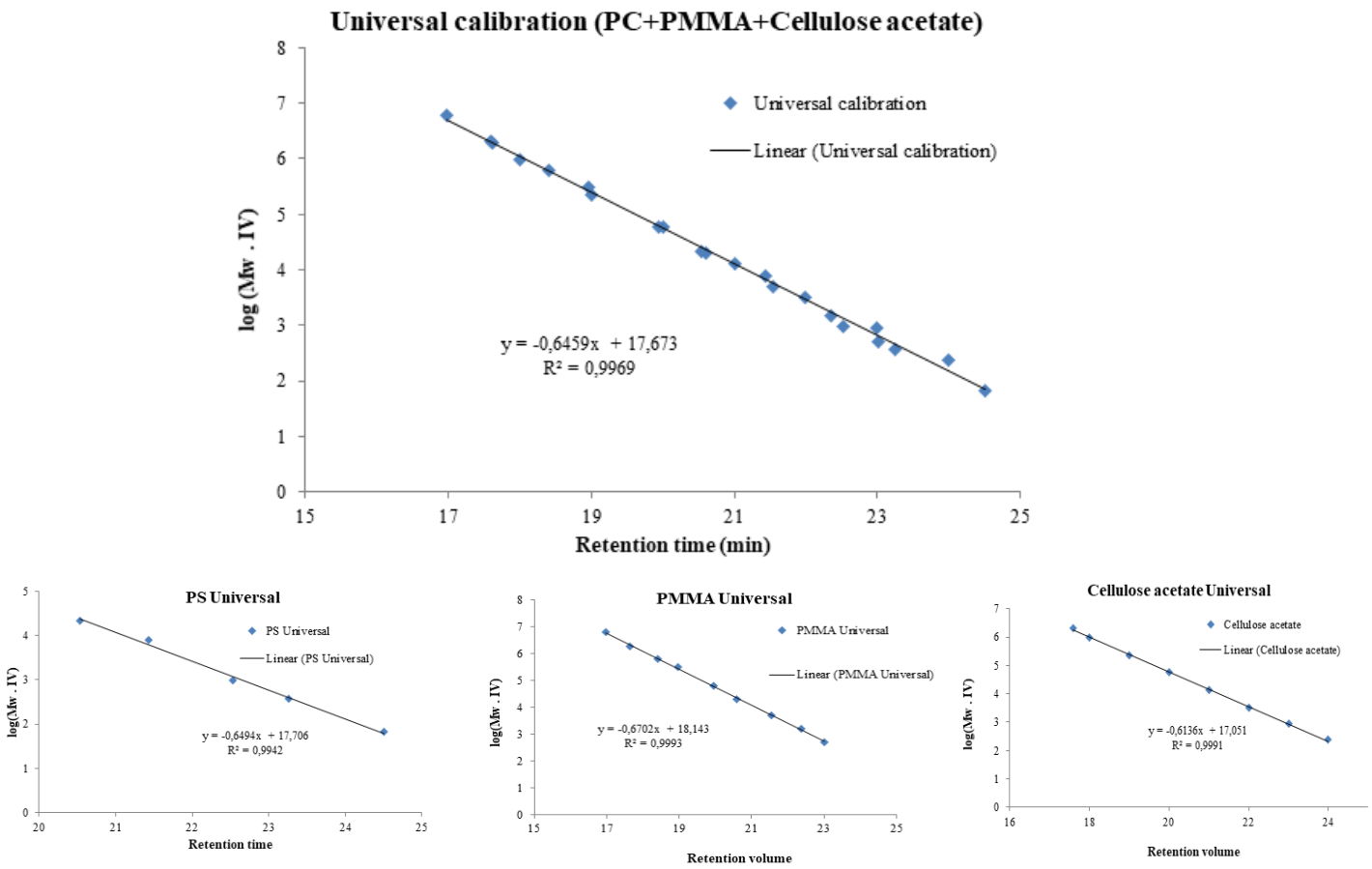

Figure 28. *En haut :* Courbe de calibration universelle incluant tous les points des polymères PS, PMMA et acétate de cellulose ; *en bas :* Courbes de calibration universelle des polymères standards monodispersés (PS et PMMA) et polydispersé (acétate de cellulose), prises individuellement.

6.3. Intégration des chromatogrammes SEC

Dans cette étude deux types de colonnes (Polar et PL gel) et deux types de systèmes solvatant (DMAc/LiCl et THF) sont utilisés. Dans le cas du sytème DMAc/LiCl – polar gel, les lignines, notamment les lignines Indulin et Kraft eucalyptus, présentent des profils d'élution bimodales ou trimodales (Figure 5.5). Dans le système THF – colonne PL, la lignine ORG présente un profil d'élution bimodal qui "traine" aux masses molaires élevées. Dans ces cas particuliers, l'intégration des signaux SEC en incluant tout le profil d'élution conduit à des valeurs de Mw surprenantes. Pour corriger ces valeurs, les signaux qui trainent au niveau des fortes masses et ceux observés aux petites masses sont excluent de l'intégration et du calcul des masses molaires. Nous avons choisi par ailleurs de définir la ligne de base entre V_0 (début des signaux intégrés) et V_t (fin de ces signaux). Ainsi pour la lignine Indulin, présentée ici, le profil SEC (Figure 5.5) présente une distribution uniforme.

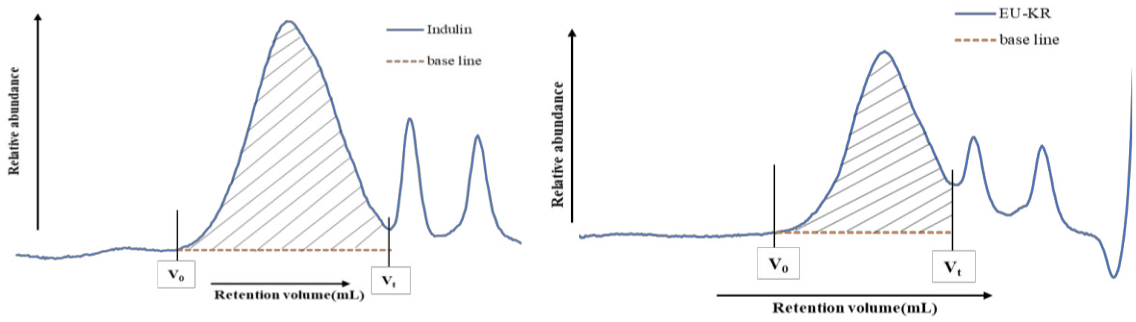

Figure 29. Chromatogrammes SEC des lignines Indulin (*gauche*) and Eucalyptus-Kraft, EU-KR (*droite*), dans le DMAc/LiCl. V_0 et V_t représentent les volumes de rétention de début et fin d'intégration des signaux pour le calcul des masses molaires.

6.4. Distribution des masses molaires des lignines non dérivées dans le DMAc/LiCl

Les lignines non dérivées ont été analysées par SEC dans le système DMAc/LiCl. Les résultats sont présentés dans la Figure 5.6. Les masses molaires moyennes et les degrés de polymérisation correspondant sont donnés dans le Table 5.4.

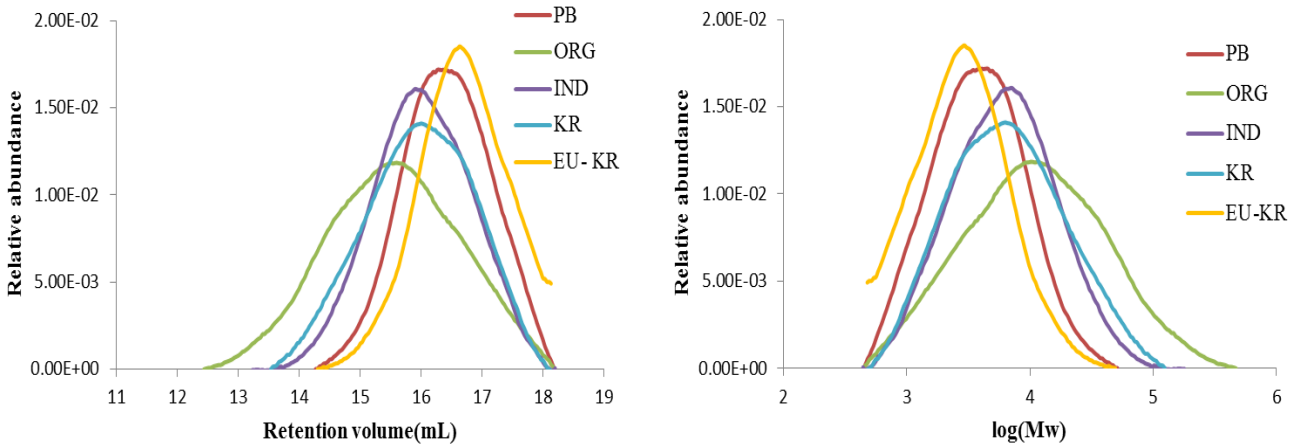

Figure 30. Chromatogrammes SEC des lignines non dérivées analysées dans le système DMAc/LiCl, *gauche :* Abondance relative en fonction du volume de rétention (mL), *droite :* Abondance relative en fonction de log Mw

Tableau 24. Masses molaires moyennes (*M*n, *M*w) en g mol^{-1}, polydispersité (*M*w/*M*n) et degrés de polymérisation moyens (*DPn, DPw*) des lignines non dérivées, après analyse dans le système SEC-DMAc/LiCl

Lignine	Mn	Mw	Mw/Mn	DPn	DPw
PB1000 (plante annuelle)	2,650	5,470	2,1	13	27
Organosolv (plante annuelle)	4,970	25,270	5,1	25	126
Indulin (résineux)	3,430	9,620	2,8	17	48
Kraft (résineux, pin)	4,090	11,500	2,8	20	57
Eucalyptus – Kraft (feuillus)	2,030	4,080	2,0	10	20

6.5. Avantages et inconvénients de l'analyse directe des lignines non dérivées dans le DMAc/LiCl

Avantages : (1) l'analyse est réalisée sur l'échantillon tel quel, ainsi aucun lavage n'est nécessaire ce qui réduit les risques de perte de certaines fractions de molécules (les plus petites) et (2) aucune réaction de dérivation n'est requise, ce qui permet aussi d'éviter la dégradation de l'échantillon pendant la dérivation.

Inconvénients : (1) la dissolution de l'échantillon est très longue, entre 4 à 5 semaines, (2) la probabilité de former des agrégats dans la colonne de chromatographies est plus importante et cela conduirait à obtenir des Mw plus élevées que la réalité, (3) la présence de sucres résiduels ou de cendres peut interférer dans le calcul de la MMD et donc les masses des lignines impures pourraient être mal évaluées.

6.6. Etude du lavage des lignines

L'extraction de la lignine de la biomasse lignocellulosiques utilise des procédés complexes et difficiles à mettre en œuvre. Par ailleurs les lignines ainsi obtenues sont impures, elles contiennent des sucres, des cendres, des minéraux. Pour éviter des interférences lors de leur analyse, les lignines sont donc lavées pour éliminer au mieux ces impuretés. Trois solvants ont été sélectionnés en fonction de leur polarité : l'éthanol, fortement polaire ; l'éthyl acétate moyennement polaire ; et l'hexane apolaire. Les résultats ont montré que l'éthyl acétate est le solvant le plus adapté au lavage de la lignine.

6.7. Analyse des lignines fluorobenzylées

Les fonctions hydroxyles aliphatiques et phénoliques de la lignine sont dérivées par le chlorure de 4-fluorobenzyle. Les dérivés fluorobenzylés de lignine sont soumis à la réaction de fluorobenzoylation avec l'acide anhydride 4-fluorobenzoique. Après ces réactions, les hydroxyles secondaires et les groupes phénoliques restant même après la fluorobenzylation sont convertis en dérivés de type esters. Toutes les lignines dérivées sont analysées par RMN du ^{19}F. La Figure 17 présente le spectre RMN ^{19}F des lignines PB dérivées. Après fluorobenzylation, le signal spectral compris entre 115 et -117,48 ppm (/C_6F_6) correspond à la lignine fluorobenzylée et les hydroxyles phénoliques, alors que le signal compris entre -117,48 et -118,5 ppm est attribué au hydroxyles aliphatiques primaires. Dans le cas des lignines fluorobenzoylées, le signal de droite est dû à la lignine fluorobenzylée alors que le signal de gauche correspond aux groupes fluorobenzoylés. Dans la région spectrale attribuée aux fonctions fluorobenzoylées, les hydroxyles phénoliques sortent entre 104,6 et -107,24 ppm et les hydroxyles aliphatiques secondaires entre -107,24 et -108,64 ppm. Le nombre de groupements hydroxyles phénoliques et aliphatiques est proportionnel à l'aire sous les signaux, et est calculé en utilisant un étalon interne dans le milieu. Il est ainsi possible de déterminer la quantité totale de groupes hydroxyles, en mmol par gramme de lignine dérivée (mmol/g).

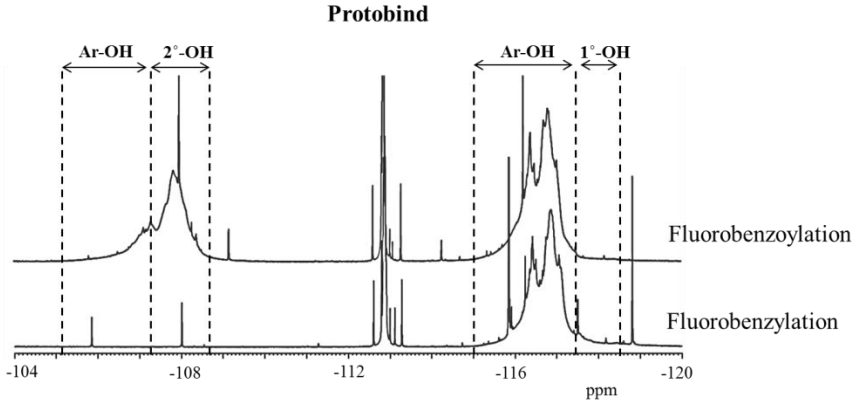

Figure 31. Spectres RMN du ^{19}F de la lignine Protobind (PB) après fluorobenzylation et fluorobenzoylation.

A noter que la fluorobenzylation de la lignine est employée pour améliorer la solubilité du polymère mais aussi pour des analyses RMN du ^{19}F NMR. A partir de cette réaction, les groupes hydroxyles phénoliques et aliphatiques primaires peuvent être quantifiés (Table 5.8). On peut remarquer que la lignine Indulin Kraft présente la teneur en hydroxyles phénoliques la plus importante par rapport aux autres lignines Kraft. Parmi les lignines étudiées, la lignine ORG de plante annuelle contient, quant à elle, la plus faible quantité de groupes hydroxyles.

Tableau 25. Quantité totale de groupes OH (en mmol/g) calculée à partir du spectre RMN du ^{19}F des lignines fluorobenzylées

Lignine	**Lignine fluorobenzylée**		**Quantité totale de $OH_{Calculée}$ mmol/g lignine dérivée**
	Ph-OH	*l˚-OH*	
PB	1,785	0,106	1,891
ORG	1,708	0,120	1,828
IND	2,451	0,078	2,529
KR	2,252	0,089	2,341
EU-KR	2,322	0,059	2,381

A partir de ces analyses RMN du ^{19}F, la masse molaire moyenne d'une unité monomère de chaque lignine testée a été calculée. Théoriquement, la masse molaire de la lignine acétylée est fixée à 220 g/mole. Pour les lignines fluorobenzylées et fluorobenzoylées, les résultats sont présentés dans le Table 5.12. Pour les lignines fluorobenzylées, ce sont les lignines Kraft (IND, KR et EU-KR) qui présentent les unités monomères de plus haute masse molaire, suivies par la lignine PB et la lignine ORG. Dans le cas des lignines fluorobenzoylées, la tendance évolue ainsi : IND > KR > PB > EU-KR > ORG. Ces résultats peuvent être comparés avec les nombres de groupements hydroxyles présents dans chaque lignine (Table 5.8).

Tableau 26. Masse molaire du monomère de lignine fluorobenzylée (FB) et de lignine fluorobenzoylée (FBO) en g mol^{-1}, calculée d'après les analyses RMN du ^{19}F

Lignine	**Masse molaire du monomère**	
	FB	FBO
PB	251	308
ORG	249	275
IND	275	328
KR	268	310
EU-KR	269	291

6.8. Analyse des lignines dérivées par SEC dans le système DMAc/LiCL

Toutes les lignines sont dérivées (acétylation, fluorobenzylation et fluorobenzoylation) et les chromatogrammes SEC – DMAc/LiCl sont présentés dans la Figure 5.10. Les masses molaires obtenues sont comparées dans le Table 5.13. Une distribution étroite des masses molaires est obtenue dans le cas des lignines PB, Indulin et Eucalyptus Kraft, dérivées et non dérivées. Le calcul des valeurs de Mn et Mw apparentes (Table 5.13) ne montre aucun changement significatif de polydispersité.

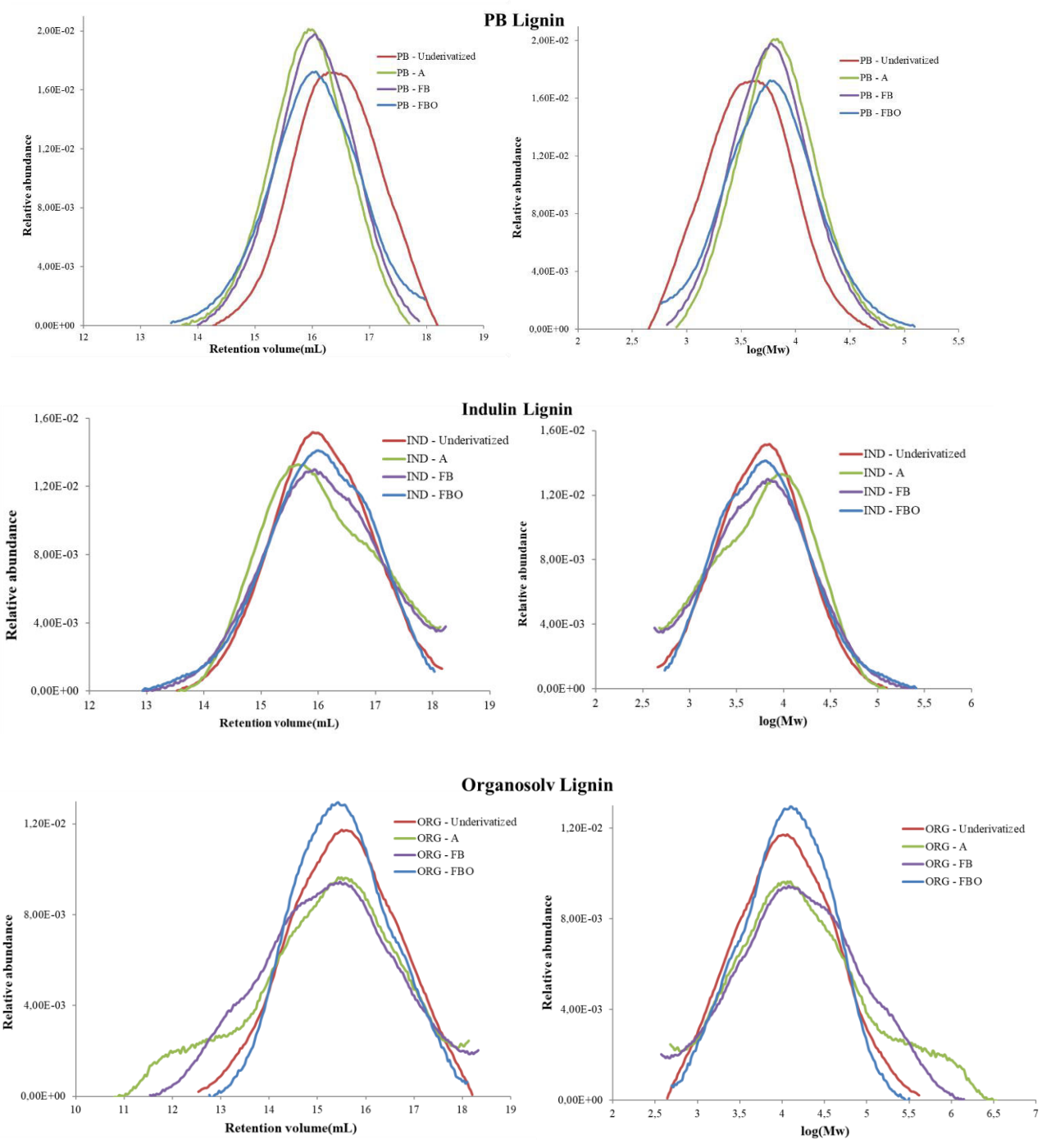

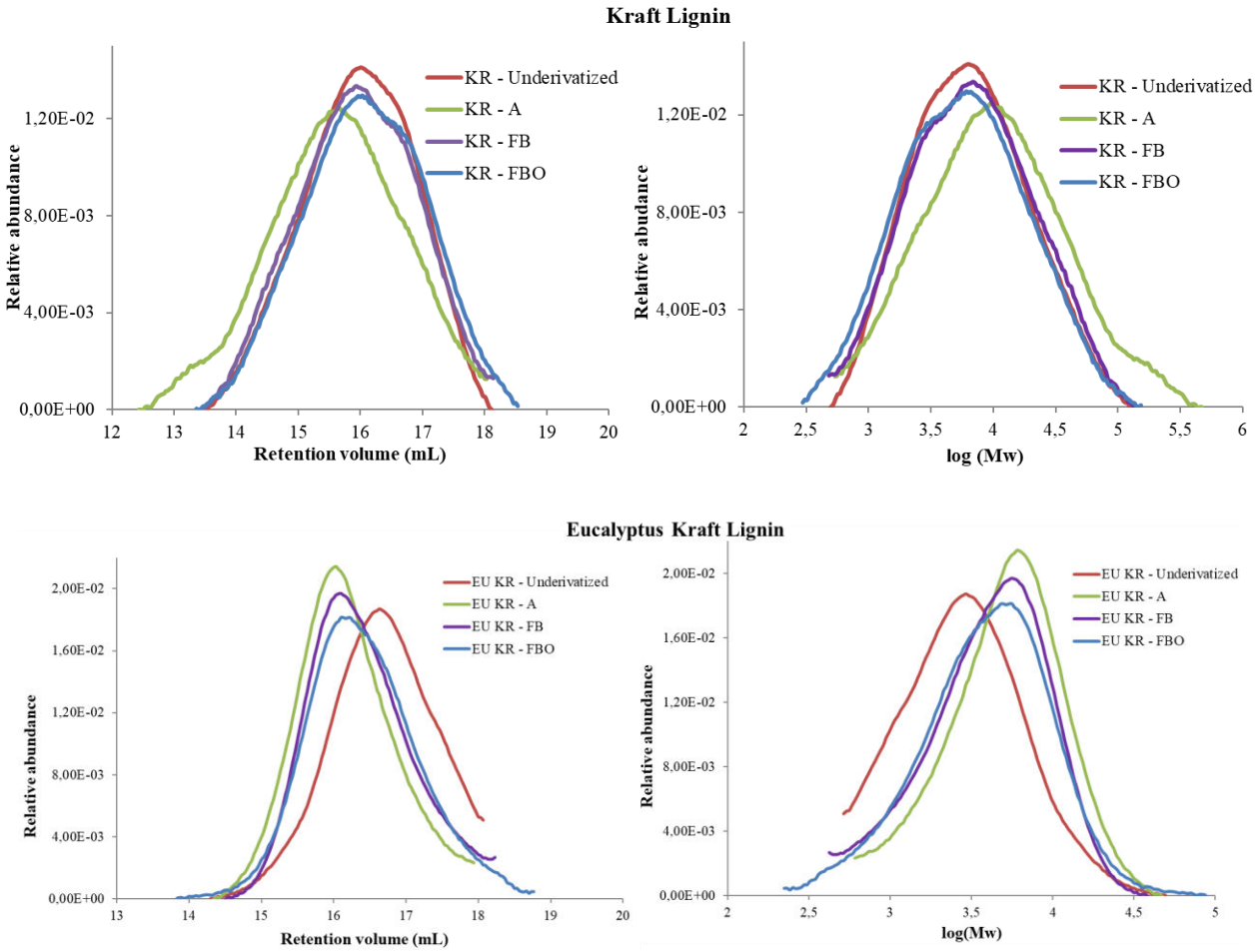

Figure 32. Profils d'élution SEC des lignines non dérivées et dérivées (acétylation, fluorobenzylation et fluorobenzoylation), abondance relative en fonction du volume de rétention (gauche) et abondance relative en fonction de log (Mw) (droite)

Tableau 27. Masses molaires moyennes (*M*n, *M*w en g mol^{-1}), polydispersité (*M*w/*M*n) et degrés de polymérisation moyens (*DPn, DPw*) des lignines non dérivées et dérivées, après analyse SEC-DMAc/LiCl

	Mn	Mw	Mw/Mn	DPn	DPw
PB					
Non dérivée	2650	5470	2,1	13	27
Acétylée	4967	9378	1,9	23	43
Fluorobenzylée	3400	6580	1,9	17	33
Fluorobenzoylée	2490	6200	2,5	12	31
IND					
Non dérivée	3430	9610	2,8	17	48
Acétylée	2774	9790	3,5	14	49
Fluorobenzylée	2070	8210	4,0	10	41
Fluorobenzoylée	2190	7300	3,3	11	36
ORG					
Non dérivée	4970	25270	5,1	25	126
Acétylée	4560	86840	19,1	23	434
Fluorobenzylée	3670	43200	11,8	18	216
Fluorobenzoylée	4040	15560	3,9	20	78
KR					
Non dérivée	3890	11340	2,9	19	57
Acétylée	4390	21480	4,9	22	107
Fluorobenzylée	2750	9150	3,3	14	46
Fluorobenzoylée	1970	7050	3,6	10	35
EU-KR					
Non dérivée	2030	4080	2,01	10	20
Acétylée	3280	6200	1,9	16	31
Fluorobenzylée	1990	4060	2,0	10	20
Fluorobenzoylée	1680	3910	2,3	8	20

6.9. Analyse des lignines dérivées par SEC dans le système THF

Analyse SEC-THF de différentes lignines dérivées – calibration conventionnelle et universelle

La fluoro dérivation améliore la solubilité des lignines dans le THF. En particulier la lignine PB fluoro dérivée présente une meilleure solubilité que toutes les autres lignines dérivées. On observe

également, dans la Figure 33, que les lignines acétylées présentent des profils d'élution qui trainent aux masses molaires élevées ; ceci montre que l'acétylation n'est pas adaptée pour une analyse de lignine dans le système SEC-THF.

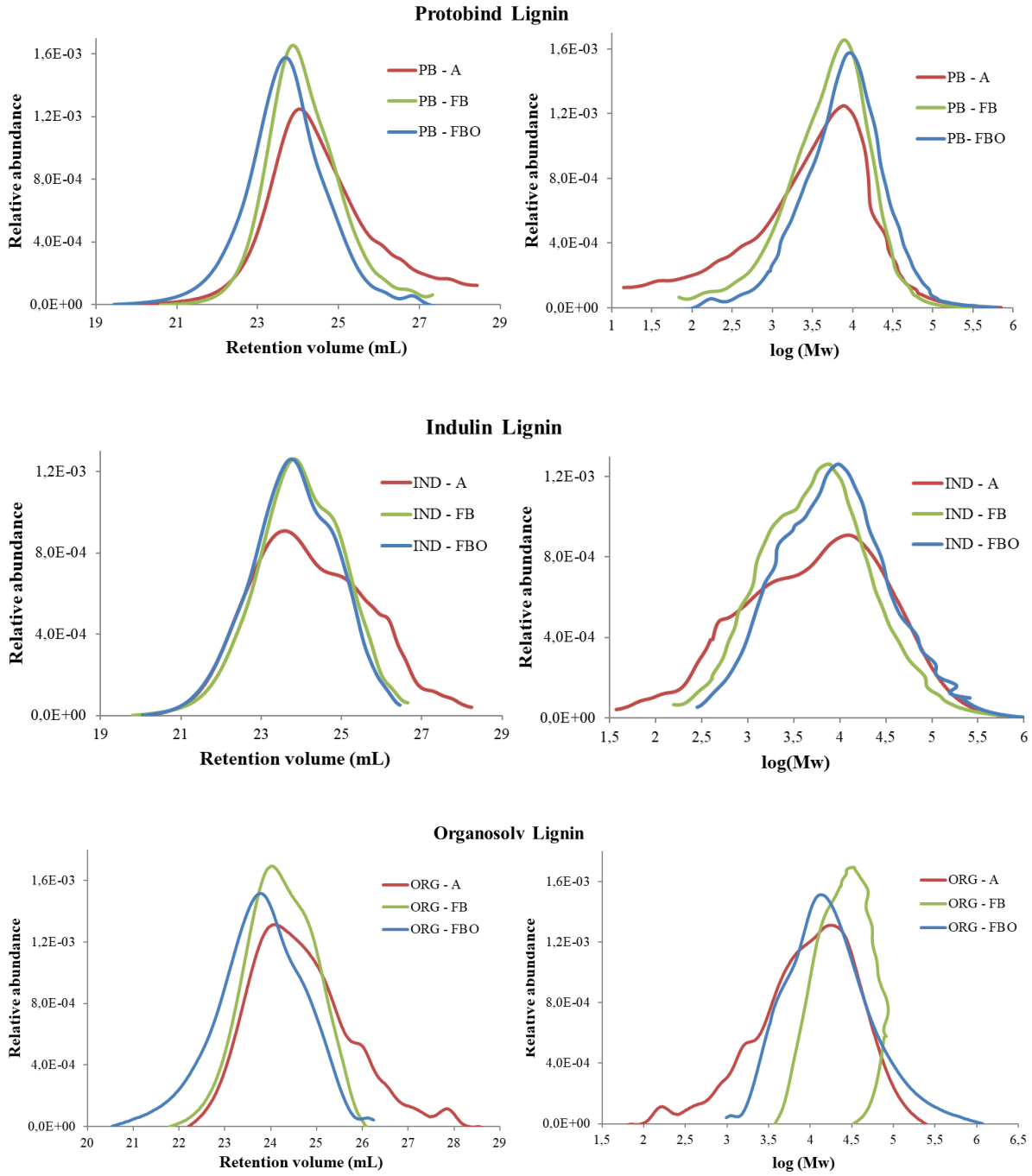

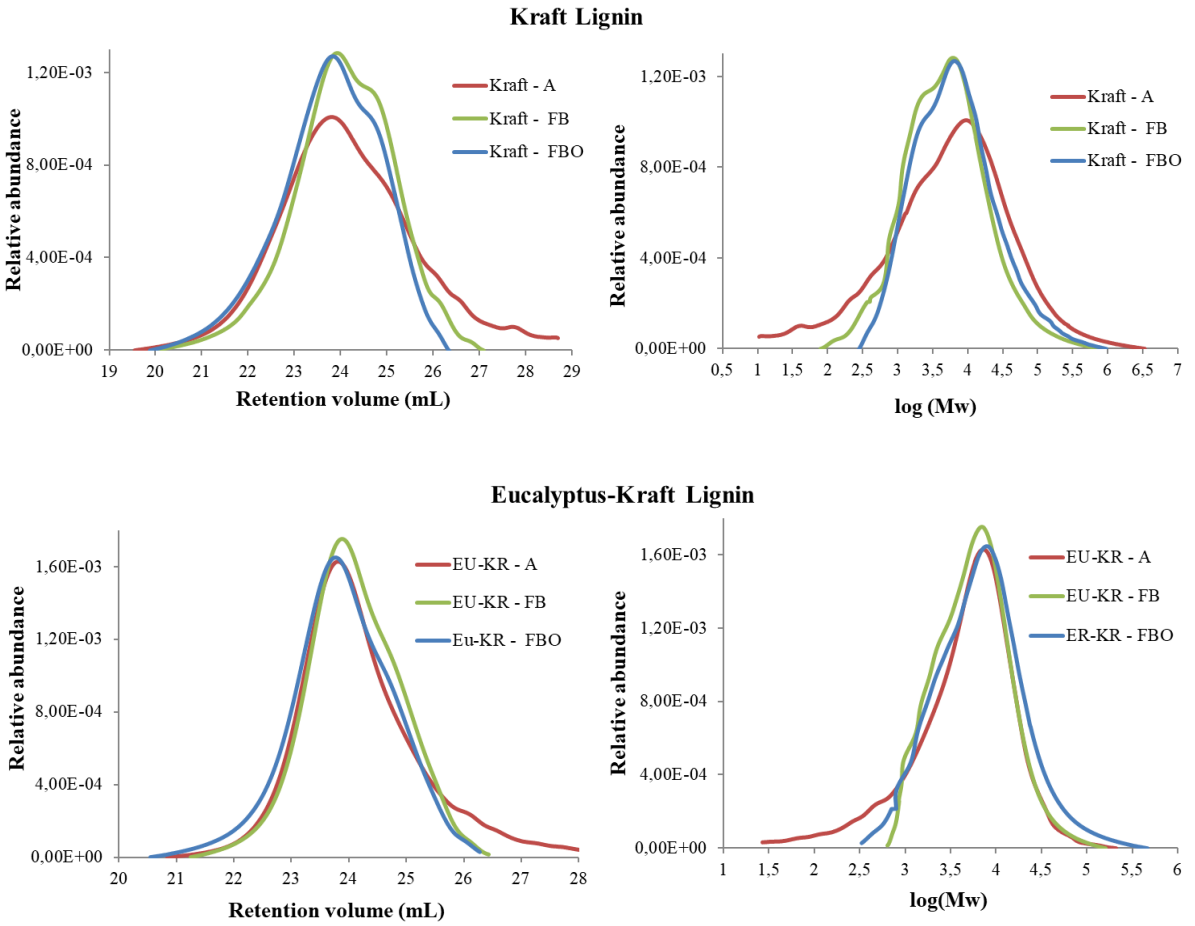

Figure 33. Profils d'élution SEC des différentes lignines dérivées – dans le système THF et calibration universelle : Abondance relative en fonction du volume de rétention (*gauche*) et abondance relative en fonction de log (Mw) (*droite*) (A - acétylée, FB - fluorobenzylée et FBO - fluorobenzoylée)

L'abondance relative est tracée en fonction du logarithme de Mw pour toutes les lignines dérivées, dans le cas de la calibration conventionnelle ou universelle (Figure 34). Avec la calibration universelle, les masses molaires sont systématiquement supérieures par rapport à l'utilisation de la calibration conventionnelle. En revanche les distributions présentent des profils similaires entre les différentes lignines dérivées.

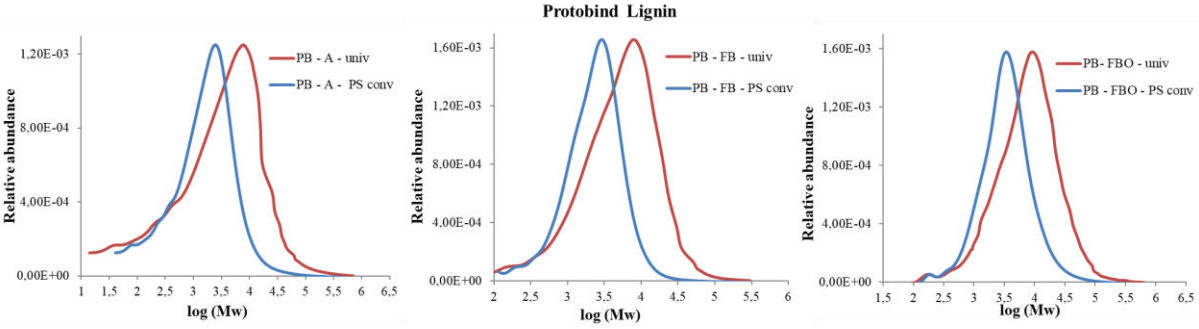

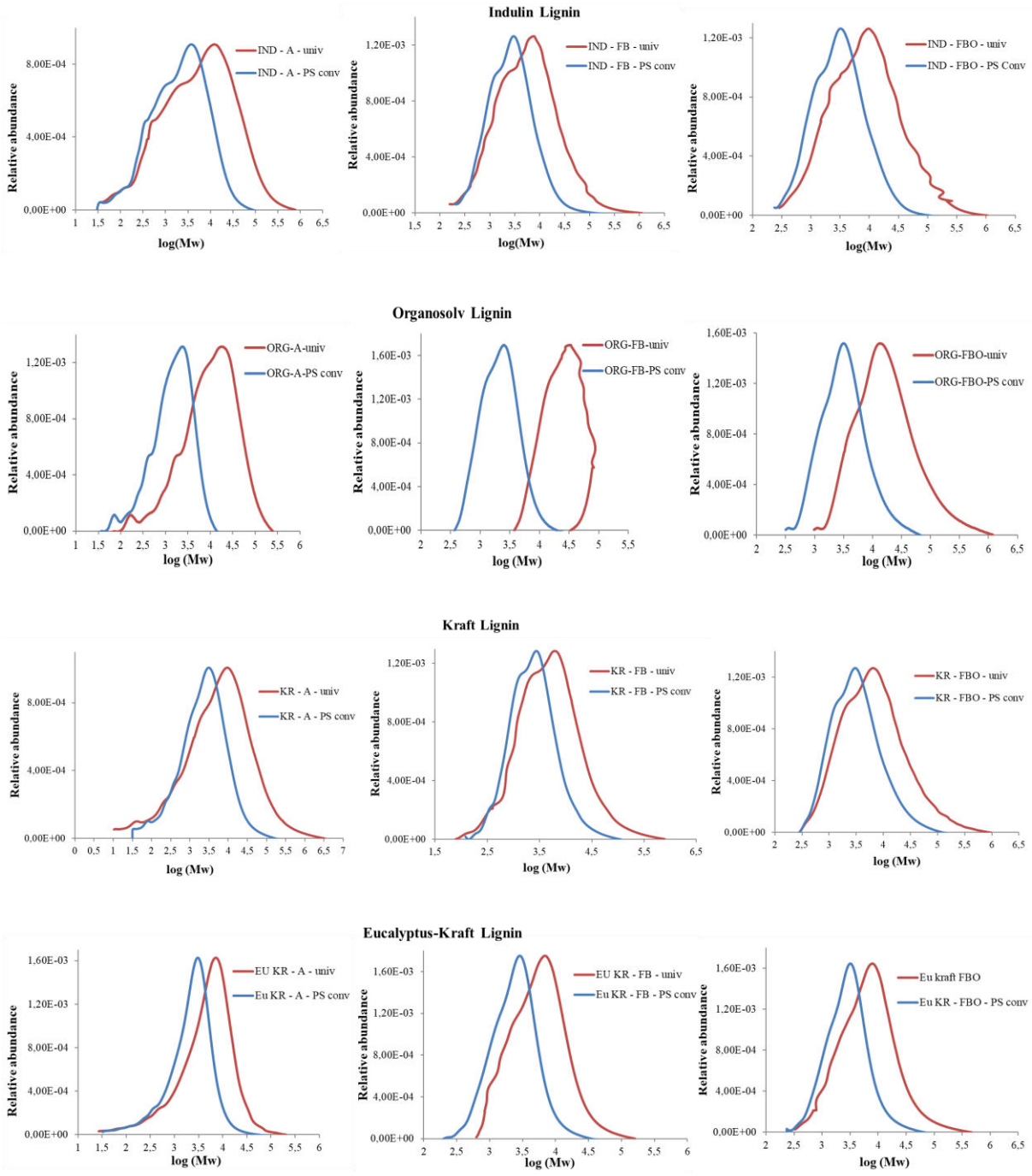

Figure 34. Comparaison entre la calibration conventionnelle et universelle – Profils d'élution SEC de lignines dérivées – Abondance relative en fonction de log(Mw) (A - acetylatée, FB – fluorobenzylée et FBO – fluorobenzoylée)

Les valeurs de Mn, Mw et de polydispersité des lignines acétylées, fluorobenzylées et fluorobenzoylées obtenues par calibration universelle sont comparées à celles obtenues par calibration conventionnelle (Tableau 28 à Tableau 32). Dans le cas de la calibration universelle, les valeurs de Mn et Mw obtenues à partir des étalons PS et PMMA sont proches alors que lorsque l'on utilise l'acétate de cellulose (polymère polydispersé) comme polymère calibrant, les valeurs de Mn et Mw

sont plus élevées et la polydispersité plus faible. Enfin, la calibration conventionnelle conduit à des valeurs de Mw et de polydispersité 3 à 5 fois inférieures à celles obtenues à partir de la calibration universelle.

Tableau 28. MMD de la lignine PB dérivée – analyse par calibration universelle avec la courbe de calibration globale et les courbes individuelles (pour chaque polymère calibrant) – comparaison avec la calibration conventionnelle. Mn et Mw en g/mole.

	Calibration universelle (Détecteur viscosimétrique)				**Calibration conventionnelle (Détecteur RI)**			
PB-Acétylée	Mn	Mw	Mw/Mn	Mp	Mn	Mw	Mw/Mn	Mp
Fit avec courbe globale[a]	380	10060	26,5	7780	-	-	-	-
PS	330	9030	27,4	6910	560	2890	5,2	2500
PMMA	240	8260	34,4	5981	725	3640	5,0	3150
Acétate de cellulose	700	13260	18,9	11090	856	2720	3,2	2620
PB-Fluorobenzylée								
Fit avec courbe globale[a]	2000	9560	4,8	7980	-	-	-	-
PS	1760	8570	4,9	7110	1450	3180	2,2	2930
PMMA	1400	7700	5,5	6200	1840	4000	2,2	3690
Acétate de cellulose	3220	12890	4,0	11230	1770	3060	1,7	2990
PB-Fluorobenzoylée								
Fit avec courbe globale[a]	3690	16140	4,4	9240	-	-	-	-
PS	3230	14550	4,5	8250	2140	5390	2,5	3430
PMMA	2640	13510	5,1	7250	2710	6740	2,5	4320
Acétate de cellulose	5640	20680	3,7	12850	2450	4660	1,9	3420

a = Fit courbe globale (PS, PMMA, acétate de cellulose)

Tableau 29. MMD de la lignine IND dérivée – analyse par calibration universelle avec la courbe de calibration globale et les courbes individuelles (pour chaque polymère calibrant) – comparaison avec la calibration conventionnelle. Mn et Mw en g/mole.

	Calibration universelle (Détecteur viscosimétrique)				**Calibration conventionnelle (Détecteur RI)**			
IND-Acétylée	Mn	Mw	Mw/Mn	Mp	Mn	Mw	Mw/Mn	Mp
Fit avec courbe globale[a]	1090	19920	18,3	12300	-	-	-	-
PS	950	17980	18,9	10990	820	4530	5,5	3770
PMMA	720	16860	23,4	9690	1040	5680	5,5	4750
Acétate de cellulose	1880	25150	13,4	16970	1160	3940	3,4	3700
IND-Fluorobenzylée								
Fit avec courbe globale[a]	2440	15390	6,3	7600	-	-	-	-
PS	2150	13890	6,5	6780	1660	4490	2,7	3040
PMMA	1750	13020	7,4	5920	2110	5630	2,7	3830
Acétate de cellulose	3790	19480	5,1	10670	1970	3980	2,0	3090
IND-Fluorobenzoylée								
Fit avec courbe globale[a]	3760	22270	5,9	9700	-	-	-	-
PS	3320	20100	6,1	8650	1910	5040	2,6	3210
PMMA	2730	18870	6,9	7570	2420	6310	2,6	4050
Acétate de cellulose	5780	28080	4,9	13550	2210	4400	2,0	3230

a=Fit courbe globale (PS, PMMA, acétate de cellulose)

Tableau 30. MMD de la lignine ORG dérivée – analyse par calibration universelle avec la courbe de calibration globale et les courbes individuelles (pour chaque polymère calibrant) – comparaison avec la calibration conventionnelle. Mn et Mw en g/mole.

	Calibration universelle (Détecteur viscosimétrique)				**Calibration conventionnelle (Détecteur RI)**			
ORG-Acétylée	Mn	Mw	Mw/Mn	Mp	Mn	Mw	Mw/Mn	Mp
Fit avec courbe globale[a]	2900	18950	6,5	17810	-	-	-	-
PS	2530	16930	6,7	15850	770	2100	2,7	2380
PMMA	1940	14920	7,7	13660	980	2650	2,7	3010
Acétate de cellulose	4950	26270	5,3	25500	1070	2160	2,0	2520
ORG-Fluorobenzylée								
Fit avec courbe globale[a]	19750	32700	1,7	32630	-	-	-	-
PS	17480	29170	1,7	29050	1680	2690	1,6	2500

PMMA	14610	25550	1,7	25100	2130	3390	1,6	3150
Acétate de cellulose	29610	45760	1,5	46540	1930	2700	1,4	2620
ORG-Fluorobenzoylée								
Fit avec courbe globale[a]	8600	34410	4,0	13540	-	-	-	-
PS	7620	31030	4,1	12080	2240	4800	2,1	3180
PMMA	6400	28970	4,5	10570	2850	6020	2,1	4015
Acétate de cellulose	12800	43720	3,4	18940	2500	4270	1,7	3210

a=Fit courbe globale (PS, PMMA, acétate de cellulose)

Tableau 31. MMD de la lignine KR dérivée – analyse par calibration universelle avec la courbe de calibration globale et les courbes individuelles (pour chaque polymère calibrant) – comparaison avec la calibration conventionnelle. Mn et Mw en g/mole.

	Calibration universelle (Détecteur viscosimétrique)				**Calibration conventionnelle (Détecteur RI)**			
KR-Acétylée	Mn	Mw	Mw/Mn	Mp	Mn	Mw	Mw/Mn	Mp
Fit avec courbe globale[a]	540	31060	57,5	9520	-	-	-	-
PS	470	28190	60,0	8490	750	5110	6,8	3100
PMMA	350	27270	77,9	7420	960	6380	6,6	3910
Acétate de cellulose	990	37450	37,8	13340	1110	4290	3,9	3130
KR-Fluorobenzylée								
Fit avec courbe globale[a]	2190	13670	6,2	6250	-	-	-	-
PS	1930	12340	6,4	5570	1510	4170	2,8	2770
PMMA	1560	11550	7,4	4840	1920	5230	2,7	3490
Acétate de cellulose	3430	17340	5,1	8840	1820	3710	2,0	2850
EU-KR-Fluorobenzoylée								
Fit avec courbe globale[a]	3210	18190	5,7	6530	-	-	-	-
PS	2840	16450	5,8	5830	2020	5580	2,8	3040
PMMA	2350	15630	6,7	5090	2570	6980	2,7	3830
Acétate de cellulose	4860	22540	4,6	9170	2310	4730	2,0	3090

a=Fit courbe globale (PS, PMMA, acétate de cellulose)

Tableau 32. MMD de la lignine EU-KR dérivée – analyse par calibration universelle avec la courbe de calibration globale et les courbes individuelles (pour chaque polymère calibrant) – comparaison avec la calibration conventionnelle. Mn et Mw en g/mole.

	Calibration universelle (Détecteur viscosimétrique)				Calibration conventionnelle (Détecteur RI)			
EU-KR-Acétylée	Mn	Mw	Mw/Mn	Mp	Mn	Mw	Mw/Mn	Mp
Fit avec courbe globale[a]	1260	8460	6,7	7270	-	-	-	-
PS	1100	7580	6,9	6480	1010	3210	3,2	3070
PMMA	840	6820	8,1	5660	1300	4040	3,1	3870
Acétate de cellulose	2150	11370	5,3	10200	1390	3080	2,2	3110
EU-KR-Fluorobenzylée								
Fit avec courbe globale[a]	3390	8580	2,5	7000	-	-	-	-
PS	3000	7680	2,6	6240	1780	3130	1,8	2870
PMMA	2500	6880	2,8	5430	2260	3940	1,7	3630
Acétate de cellulose	5120	11610	2,3	9870	2040	3050	1,5	2940
EU-KR-Fluorobenzoylée								
Fit avec courbe globale[a]	3630	13210	3,6	7990	-	-	-	-
PS	3210	11890	3,7	7130	2040	4060	2,0	3200
PMMA	2670	10930	4,1	6240	2580	5100	2,0	4040
Acétate de cellulose	5470	17200	3,1	11170	2300	3740	1,6	3230

a=Fit courbe globale (PS, PMMA, acétate de cellulose)

Analyse SEC-THF de différentes lignines dérivées – Calcul des degrés de polymérisation (DP)

Le degré de polymérisation est calculé à partir des masses molaires des monomères, ces dernières étant déterminées par l'analyse RMN du ^{19}F NMR. Le degré de polymérisation en nombre est donné par (DPn = Mn / masse molaire du monomère) et celui en poids par (DPw = Mw / masse molaire du monomère). La polydispersité Q est égale à Q = DPw/DPn. Les valeurs de Mn et Mw sont issues de l'analyse SEC dans le système THF avec la calibration universelle (courbe globale). Les valeurs de DPn, DPw et Q (DPw / DPn) sont données dans le

Table **5.20**. Dans le cas de la lignine acétylée, la masse molaire du monomère a été prise égale à 220 g/mol.

Tableau 33. DP calculés à partir de la calibration universelle (courbe globale) dans le système SEC-THF

		Masse molaire du monomère (g/mol)	DPn	DPw	Q=DPw/DPn
PB	Acétylée	220	2	46	26,2
	FB	251*	8	38	4,8
	FBO	308*	12	52	4,4
IND	Acétylée	220	5	91	18,3
	FB	275*	9	56	6,3
	FBO	328*	11	68	5,9
ORG	Acétylée	220	13	86	6,5
	FB	249*	79	131	1,7
	FBO	275*	31	125	4
KR	Acétylée	220	2	141	57,5
	FB	268*	8	51	6,2
	FBO	310*	10	59	5,7
EU-KR	Acétylée	220	6	38	6,7
	FB	269*	13	32	2,5
	FBO	291*	12	45	3,6

*Masse molaire des monomères des lignines FB-fluorobenzylées et FBO- fluorobenzoylées calculée à partir de l'analyse RMN du ^{19}F.

Les conclusions de ce chapitre sont les suivantes :

1. L'acétate d'éthyle est utilisé pour laver les lignines de leurs impuretés.
2. Différentes réactions de dérivation (acétylation, fluorobenzylation et fluorobenzoylation) ont été réalisées sur la lignine afin de dissoudre la lignine dans le THF, la lignine étant difficilement dissoute dans le DMAc/LiCl.
3. Les résultats SEC montrent que les fluoro-dérivations améliorent la dissolution de la lignine et que cette dernière présente alors une distribution de masses plus uniforme que les lignines acétylées (dans le système THF).
4. Comme l'analyse SEC dans le DMAc/LiCl avec calibration conventionnelle donne des résultats imparfaits, une méthode de calibration universelle dans le système THF a été développée. Elle utilise un viscosimètre en ligne dans la ligne de chromatographie afin d'avoir accès à la MMD absolue du polymère.
5. L'analyse par calibration universelle prédit des masses molaires 3 à 5 fois supérieures à celles obtenues par calibration standard. Les lignines acétylées présentent aussi des Mn plus faibles et des polydispersités plus élevées, probablement car les fractions de lignine acétylée de hautes masses sont plus difficiles à solubiliser.
6. Globalement la fluorobenzylation et la fluorobenzoylation de la lignine suivies de l'analyse SEC dans le THF restent encore imparfaites à cause du solvant utilisé. En effet, la qualité des

courbes SEC est moindre par rapport aux courbes obtenues dans le système DMAc/LiCl. Seules les lignines EU-KR et PB présentent des profils d'élution réguliers, conduisant à des valeurs de Mw et Mn fiables. Dans le cas des autres lignines, les valeurs obtenues sont fortement affectées par les signaux aux hautes masses qui ont tendance à trainer, probablement suite à des problèmes de rétention dans les colonnes (la phase PLgel dans le système THF n'est peut-être pas adaptée aux dérivés fluorés de lignine).

7. Enfin, il faut noter que les différentes méthodes de dérivation testées peuvent aussi conduire à la dégradation de la lignine, ainsi il est impératif d'optimiser ces réactions.

7. CONCLUSIONS

Ce travail de recherche a permis d'établir des méthodes de dérivation de la lignine pour l'analyse de la lignine, de quantifier les groupes fonctionnels et de déterminer la distribution des masses molaires de la lignine (MMD) par chromatographie par exclusion de taille. Cinq échantillons techniques de lignine ont été étudiés : la lignine Protobind 1000, la lignine Organosolv, la lignine Pine Kraft, la lignine Eucalyptus Kraft et la lignine Indulin. Les échantillons de lignine ont été transformés en dérivés par une méthode classique d'acétylation et de nouvelles méthodes telles que la fluorobenzylation et la fluorobenzoylation. Le nombre d'hydroxyles présents dans les échantillons de lignine a été quantifié par des techniques GC et RMN (^{1}H, ^{13}C, ^{19}F and ^{31}P). La distribution en masse molaire des échantillons de lignine dérivées a été calculée en utilisant différentes colonnes SEC avec différents solvants (DMAc et THF). Des méthodes d'étalonnage conventionnelles et universelles ont été utilisées pour les calculs et MMD. Avec cette approche, les nouvelles méthodes de dérivation de la lignine améliorent de manière significative la solubilité dans le système de colonne THF, et la méthode d'étalonnage universelle conduit à des masses molaires trois fois supérieures à celles issues de la méthode d'étalonnage conventionnelle.